The natural history of human atherosclerosis : a histopathological approach

Dijk, R.A. van

THE NATURAL HISTORY OF HUMAN ATHEROSCLEROSIS

A HISTOPATHOLOGICAL APPROACH

Rogier A. van Dijk

Cover design: Mark Limburg, Amstelveen
Printed by: Ipskamp Printing

The Natural History of Human Atherosclerosis; A Histopathological Approach
The Netherlands 2017.

ISBN: 978-94-028-0620-5

THE NATURAL HISTORY OF HUMAN ATHEROSCLEROSIS

A HISTOPATHOLOGICAL APPROACH

Proefschrift

Ter verkrijging van
de graad van Doctor aan de Universiteit Leiden
op gezag van de Rector Magnificus Prof. Mr. C.J.J.M. Stolker,
volgens besluit van het College voor Promoties
te verdedigen op donderdag 18 mei 2017 klokke 15.00 uur

door

Rogier Alexander van Dijk

Geboren te Alphen a/d Rijn in 1979

PROMOTOR:
Prof. Dr. J.F. Hamming

COPROMOTORES:
Dr. J.H.N. Lindeman
Dr. A.F.M. Schaapherder

Leden van de promotiecommissie:
Prof. Dr. J.W. Jukema
Prof. Dr. M. van Eck (LACDR, Leiden)
Prof. Dr. A.C. van der Wal (Academisch Medisch Centrum, Amsterdam)
Dr. R. Kleemann (TNO, Leiden)

Primary Funding Source: N/A.

Financial support by the Dutch Heart Foundation for the publication of this thesis is gratefully acknowledged.

Printing of this thesis is further financially supported by Guerbet Nederland B.V., Bayer B.V., Chipsoft and Sai Registeraccountants.

CONTENTS

CHAPTER 1

General Introduction and outline of the thesis

GENERAL INTRODUCTION

Atherosclerosis is a complex pathology of large and medium-sized arteries that constitutes the principle cause of cardiovascular disease[1,2]. Despite major clinical successes, complications of atherosclerosis remain the most common cause of death in Westernized societies[3]. Consequently there is a persistent need for better pharmaceutical strategies and improved risk stratification.

The atherosclerotic process reflects a complex interplay of metabolic, environmental, inflammatory and physical factors[1]; aspects that are extensively reviewed and continuously updated in state-of-the art reviews[4,5,6.] It is becoming more and more apparent that the clinical manifestations of atherosclerosis (*i.e.* myocardial infarction, stroke and peripheral arterial disease) relate to qualitative changes in plaque structure (*i.e.* plaque rupture) rather than to a mass (quantitative) effect. As such insight in the qualitative changes is crucial for understanding the chain of events underlying the clinical manifestations of this disease.

The qualitative changes in atherosclerotic process proceed through distinct, histological stages. These consecutive stages were first outlined by an American Heart Association (AHA) working group. This initial classification scheme from the mid-1990s was later updated in 2000[7,8,9,10] (figure 1). This AHA consensus scheme has been criticized for ignoring aspects of plaque destabilization (*viz.* vulnerable lesions) that predispose to clinical events[11]. Based on the morphology of coronary atherosclerotic lesions, Virmani *et al.*[11] proposed a more comprehensive classification scheme that incorporates both the various aspects of vulnerable lesion development as well as plaque destabilization (Table 1). An open question remains whether and how this classification based on observations from coronary arteries, translates to other vascular beds with different risk factor profiles[12,13].

Current mechanistic insight into the atherosclerotic process is largely based on static information from epidemiological studies and on (histological) evaluation of surgical specimens (*viz.* late stage and sudden coronary death victims). Dynamic insight in the disease processes essentially relies on animal (murine) studies. Although mice are indispensable tools for atherosclerosis research, mice are naturally protected from atherosclerosis by their atheroprotective lipoprotein profile[14]. As such atherosclerosis development in mice critically depends on interference with the lipoprotein metabolism along with specific dietary interventions. Consequently, atherosclerosis in these models is essentially lipid (cholesterol) driven.

The ideal animal model of atherosclerosis will mimic the pathophysiological chain of events leading to human disease, and will develop lesions and complications similar to those found in humans[15]. Available data indicate overlap

between disease development in murine atherosclerosis models and human disease[16]. However, it is acknowledged that full translation is hampered by fundamental physiologic, anatomical, inflammatory, immunologic and metabolic differences between men and mice, as well as differences between mice strains[17,18]. A further major limitation is the fact that atherosclerotic lesions in mice fail to progress to advanced unstable culprit lesions that give rise to the clinical manifestations of atherosclerosis (Figure 2). As such specific information on the sequence of events leading to plaque destabilization is missing from these models.

Experimental atherosclerosis in murine models of atherosclerosis provides an important research tool. However, the leap from experimental animal findings to human atherosclerosis and clinical application yet still presents many challenges.

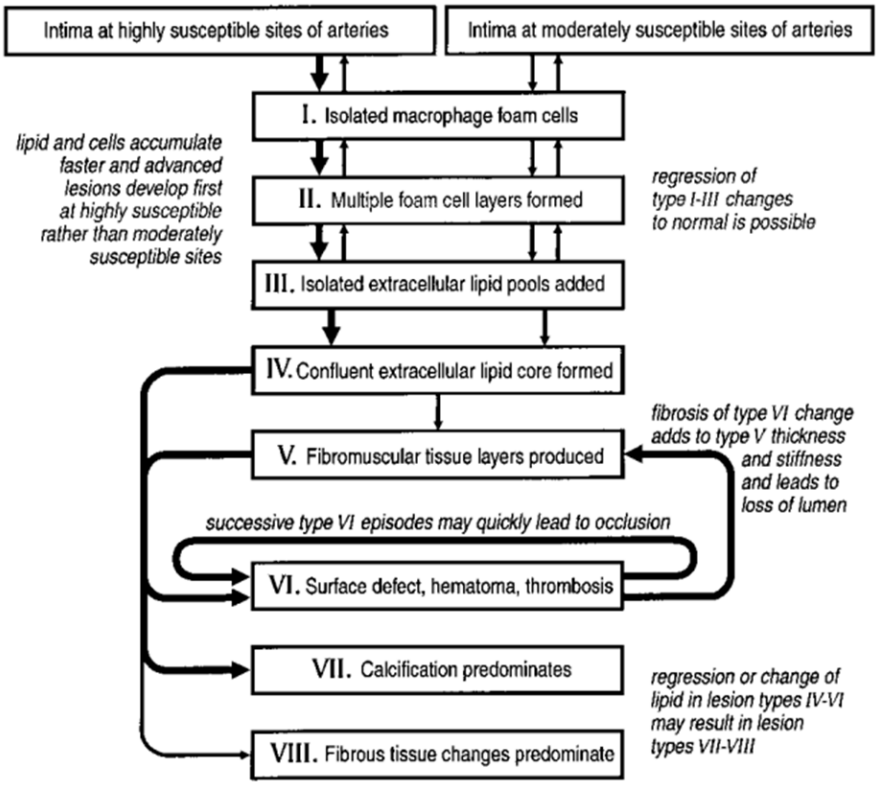

Figure 1. Outline of the sequence in the evolution of atherosclerotic lesions from type I to type IV and of the various possible subsequent pathways of progression to lesion types beyond type IV. The diagram lists the main histological characteristics of each sequential step (lesion type). Adapted from reference 10.

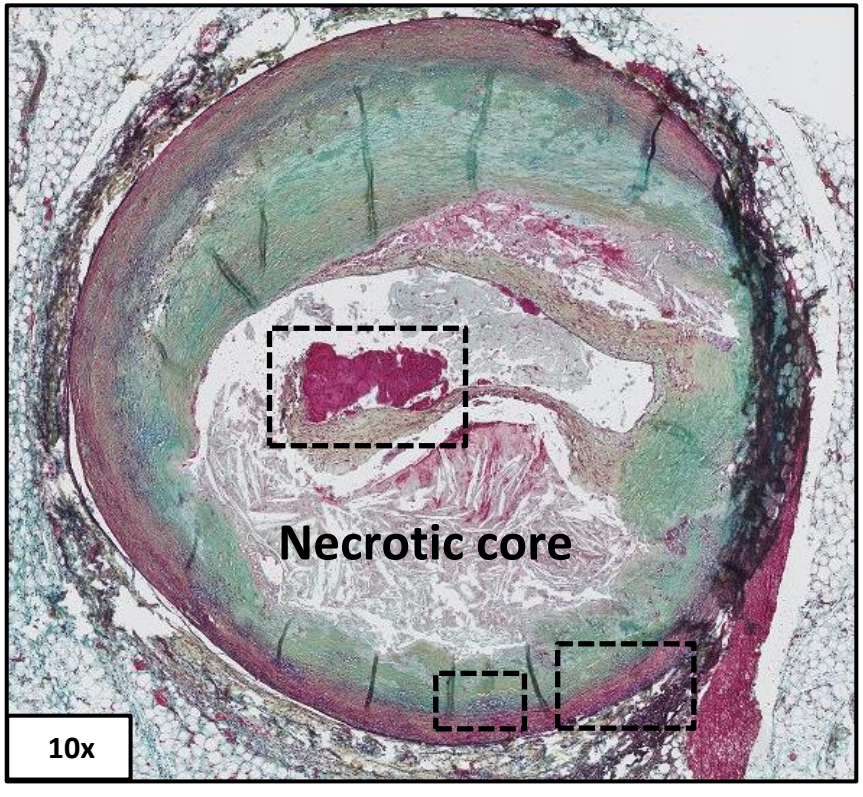

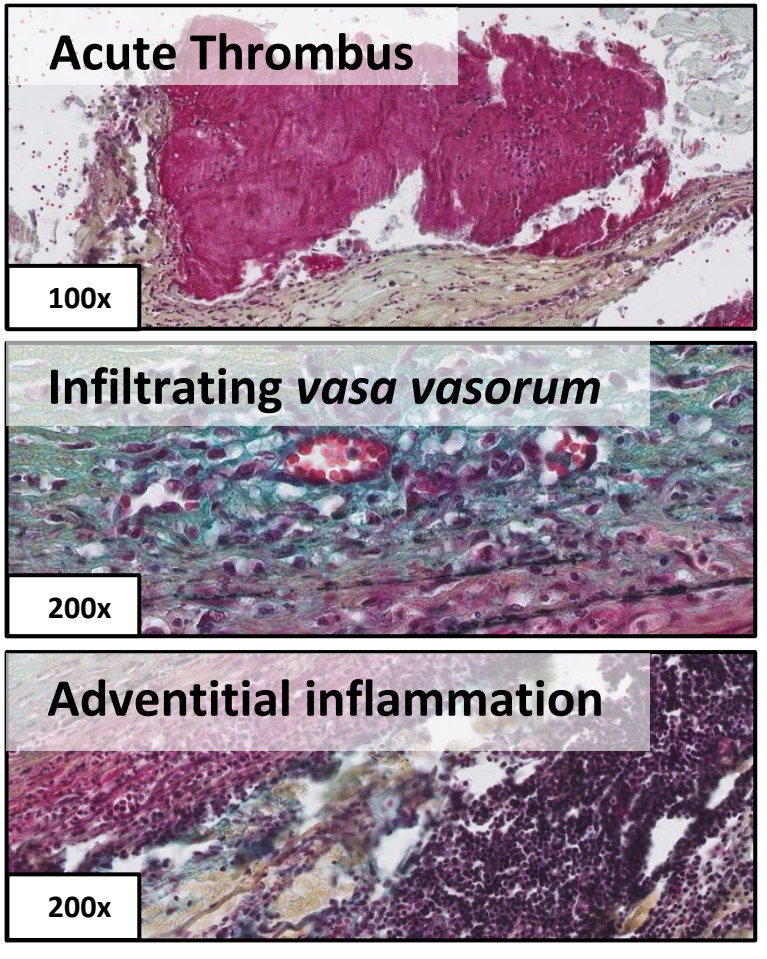

Figure 2. A typical example of an unstable culprit coronary lesion that gives rise to the clinical manifestations of atherosclerosis due to cap rupture hence exposing the large thromboembolic necrotic core.

Table 1 Modified AHA Classification Based on Morphological Description. Adapted from reference 11.

	Description	Thrombosis
Nonatherosclerotic intimal lesions		
Intimal thickening	The normal accumulation of smooth muscle cells (SMCs) in the intima in the absence of lipid or macrophage foam cells	Absent
Intimal xanthoma, or "fatty streak"	Luminal accumulation of foam cells without a necrotic core or fibrous cap. Based on animal and human data, such lesions usually regress.	Absent
Progressive atherosclerotic lesions		
Pathological intimal thickening	SMCs in a proteoglycan-rich matrix with areas of extracellular lipid accumulation without necrosis	Absent
Erosion	Luminal thrombosis; plaque same as above	Thrombus mostly mural and infrequently occlusive
Fibrous cap atheroma	Well-formed necrotic core with an overlying fibrous cap	Absent
Erosion	Luminal thrombosis; plaque same as above; no communication of thrombus with necrotic core	Thrombus mostly mural and infrequently occlusive
Thin fibrous cap atheroma	A thin fibrous cap infiltrated by macrophages and lymphocytes with rare SMCs and an underlying necrotic core	Absent; may contain intraplaque hemorrhage/fibrin
Plaque rupture	Fibroatheroma with cap disruption; luminal thrombus communicates with the underlying necrotic core	Thrombus usually occlusive
Calcified nodule	Eruptive nodular calcification with underlying fibrocalcific plaque	Thrombus usually non-occlusive
Fibrocalcific plaque	Collagen-rich plaque with significant stenosis usually contains large areas of calcification with few inflammatory cells; a necrotic core may be present.	Absent

Despite all the progress we still lack definitive evidence to show that processes such as lipoprotein oxidation, inflammation and immunity have a crucial involvement in human atherosclerosis and its complications. A systematic evaluation of the human atherosclerotic process, especially regarding plaque vulnerability is highly relevant.

This thesis systematically evaluates the critical morphological, pathophysiological and immunological aspects of the human atherosclerotic process using a unique biobank containing over 500 individual peri-renal abdominal aortic wall patches and over 600 coronary artery segments of the left coronary artery. The aortic patches were obtained during liver, kidney or pancreas transplantation and the coronary artery segments were collected from healthy human hearts that were retrieved from Dutch post-mortem donors within 24 hours after circulatory stop and brought to the National Heart Valve for heart valve donation. Contrary to other histological studies investigating mechanistic insight into the atherosclerotic process, we used tissue from a group of apparently healthy individuals with an equal age and sex distribution, thereby avoiding potential bias introduced by the use of autopsy material from coronary death victims (mostly either young or old patients) or by the use of material from patients undergoing vascular surgery (generally end-stage atherosclerotic disease).

AIM AND OUTLINE OF THIS THESIS

Of the primary locations, *i.e.* coronaries, carotids and aorta, surprisingly little is known about how atherosclerosis in the aorta, the second largest manifestation of atherosclerosis, progresses from early to more advanced, complicated lesions [19,20,21]. This lack of information is remarkable, especially considering the fact that the aorta is the reference vessel in mouse atherosclerosis models.
The primary aim of this thesis was to explore the natural history of human aortic atherosclerosis in order to gain more insight in the pathophysiology of plaque development and unstable culprit lesion formation that potentially gives rise to the clinical manifestations of atherosclerosis.

The first part of this thesis focusses on the general morphology of aortic atherosclerosis. **Chapter 2** evaluates the comprehensive morphological classification scheme as proposed by Virmani[11] using a well-documented large tissue bank of human peri-renal aortic tissue that covers the whole spectrum of atherosclerotic disease. Aortic atherosclerotic lesions follow a similar pattern of progression as seen in coronaries but grow far beyond the size of coronary

atherosclerotic lesions. Yet presumably owing to the aortic diameter plaque rupture, remains clinically silent[22].

In order to improve atherosclerosis risk prediction and to detect clinically relevant lesions, the intimal media thickness (IMT) along with coronary calcium scores (CCS) have been brought forward as epidemiological measures of atherosclerosis burden[23,24]. In **Chapter 3** we look into IMT and the coronary calcium scores and their relation to disease progression in order to assess their value as individual risk prediction tools. There is a moderate correlation between age and IMT but the influence is minimal and hardly affects the estimates.

As mentioned above, the aorta is the reference vessel in mouse atherosclerosis models. However, to what extend the available mouse models of atherosclerosis mimic the spectrum of lesions present in humans is unclear and a direct translation from the findings in mice models to the situation seen in humans is still missing. **Chapter 4** presents a morphological overview and a 1 to 1 comparison of the human coronary and aortic atherosclerotic lesions and their murine counterpart. By doing so, we aim at a detailed classification scheme for atherosclerosis in mice based on the Virmani classification that parallels the human situation since a uniform classification system for mouse lesions is missing[25,26,27].

The second part of this thesis focusses on key players in the process of human atherosclerosis. A primordial event in atherogenesis is LDL accumulation in intimal layer of the vessel wall and extensive experimental data exists defining the role of oxidation of LDL cholesterol in both progression and regression of atherosclerosis[1]. **Chapter 5** systematically describes the relationship of several oxidation specific neoepitopes and human atherosclerosis and their relationship to early atherosclerotic lesions and clinically relevant advanced, unstable, or ruptured plaques. Understanding this relationship may have significant clinical implications with the emergence in the clinical and translational arenas of oxidative biomarkers, molecular imaging, and therapeutic approaches including immune modulation.

Information on the immune response in initiation, progression and complications of atherosclerotic disease is largely based on experimental studies. It is unclear how these observations translate to the human situation. **Chapter 6** systematically evaluates the cellular components of the innate immune system (macrophages and their subtypes, dendritic cells, mast cells, natural killer cells, neutrophils and eosinophils) throughout the process of human atherosclerosis.

Chapter 7 further explores the inflammatory component that drives atherosclerosis by evaluating the adaptive immune response within the process of atherosclerotic lesion formation, progression, destabilization and stabilization. These explorative studies confirm extensive and dynamic presence of cellular

components of the innate and adaptive immunity in the human atherosclerotic process, and reveal profound changes in the inflammatory foot print immediately prior to and during the process of plaque destabilization.

Since inflammation is a canonical factor in the progression and complications of atherosclerotic disease, strategies aimed at the 'central hub' of inflammation have been brought forward as a target in limiting vascular inflammation. In **Chapter 8** we first of all histologically evaluate and acknowledge abundant activation of the proinflammatory transcription factor AP-1 (activator protein-1) in early and advanced atherosclerotic disease. This is followed by an interventional study to test whether quenching AP-1 activation improves vascular function in high-risk patients (*viz.* patients with peripheral artery disease).

The regulation of plaque and matrix homeostasis is evaluated in **Chapter 9**. Members of the TGF-β superfamily have been proposed as critical regulators of the atherosclerotic process but their role in human disease remains controversial[28,29]. By using Smad phosphorylation as a read out for TGF-β and BMP signaling and immunostaining against T-cells, monocytes and macrophages (CD68) we explore the putative association between TGF-β and BMP signaling and vascular inflammation during the initiation, progression and (de)stabilization of human atherosclerotic disease.

Finally, this thesis is completed with a summary and future perspectives in **Chapter 10**, samenvatting (Dutch summary) **Chapter 11**, list of publications and a *Curriculum Vitae* of the author.

REFERENCES

1 Ross R. Atherosclerosis—an inflammatory disease. The New England Journal of Medicine. 1999;340(2):115–126.

2 Glass CK,Witztum JL. Atherosclerosis the road ahead. Cell. 2001;104:503–516.

3 http://www.who.int/mediacentre/factsheets/fs310/en/index1.html.

4 Hansson, G. K., Libby, P., Schönbeck, U., & Yan, Z. Q. Innate and adaptive immunity in the pathogenesis of atherosclerosis. Circulation research. 2002; 91(4), 281-291.

5 Libby, P., Ridker, P. M., & Hansson, G. K. Progress and challenges in translating the biology of atherosclerosis. Nature. 2011; 317-325.

6 Hansson, G. K., & Libby, P. The immune response in atherosclerosis: a double-edged sword. Nature Reviews Immunology, 2006; 508-519.

7 STARY, H. C., *et al*. A definition of the intima of human arteries and of its atherosclerosis-prone regions. A report from the Committee on Vascular Lesions of the Council on Arteriosclerosis, American Heart Association. Circulation. 1992; 391-405.

8 Stary, Herbert C., *et al*. A definition of initial, fatty streak, and intermediate lesions of atherosclerosis. A report from the Committee on Vascular Lesions of the Council on Arteriosclerosis, American Heart Association. Arteriosclerosis, Thrombosis, and Vascular Biology, 1994, 14.5: 840-856.

9 Stary, Herbert C., *et al*. A definition of advanced types of atherosclerotic lesions and a histological classification of atherosclerosis A report from the Committee on Vascular Lesions of the Council on Arteriosclerosis, American Heart Association. Circulation, 1995, 92.5: 1355-1374.

10 Stary, Herbert C. Natural history and histological classification of atherosclerotic lesions an update. Arteriosclerosis, thrombosis, and vascular biology, 2000, 20.5: 1177-1178.

11 Virmani, R., Kolodgie, F. D., Burke, A. P., Farb, A. & Schwartz, S. M. Lessons from sudden coronary death: a comprehensive morphological classification scheme for atherosclerotic lesions. Arteriosclerosis, Thrombosis, and Vascular Biology. 2000, 1262–1275.

12 Chambless LE, Folsom AR, Davis V, *et al*. Risk factors for progression of common carotid atherosclerosis: the Atherosclerosis Risk in Communities Study, 1987–1998. American Journal of Epidemiology 2002;155:38–47.

13 Bauer M, Möhlenkamp S, Lehmann N, *et al*. The effect of age and risk factors on coronary and carotid artery atherosclerotic burden in males—Results of the Heinz Nixdorf Recall Study. Atherosclerosis. 2009;205:595–602.

14 Kleemann, R., Zadelaar, S., & Kooistra, T. Editor's Choice: Cytokines and atherosclerosis: a comprehensive review of studies in mice. Cardiovascular Research 2008. 79(3), 360.

15 Zadelaar, S., Kleemann, R., Verschuren, L., de Vries-Van der Weij, J., van der Hoorn, J., Princen, H. M., & Kooistra, T. Mouse models for atherosclerosis and pharmaceutical modifiers. Arteriosclerosis, thrombosis, and vascular biology. 2007, 27(8), 1706-1721.

16 Hansson GK, Libby P, Schönbeck U, Yan ZQ. Innate and adaptive immunity in the pathogenesis of atherosclerosis. Circulation Research. 2002;91(4):281-291.

17 Haley, P. J. Species differences in the structure and function of the immune system. Toxicology. 2003. 188:49-71.

18 Seok J, Warren HS, Cuenca AG, Mindrinos MN, Baker HV, Xu W, Richards DR, McDonald-Smith GP, Gao H, Hennessy L, Finnerty CC, López CM, Honari S, Moore EE, Minei JP, Cuschieri J, Bankey PE, Johnson JL, Sperry J, Nathens AB, Billiar TR, West MA, Jeschke MG, Klein MB, Gamelli RL, Gibran NS, Brownstein BH, Miller-Graziano C, Calvano SE, Mason PH, Cobb JP, Rahme LG, Lowry SF, Maier RV, Moldawer LL, Herndon DN, Davis RW, Xiao W, Tompkins RG. Genomic responses in mouse models poorly mimic human inflammatory diseases. Proceedings of the National Academy of Sciences U S A. 2013;110(9):3507-3512.

19 Virmani R, Avolio AP,MergnerWJ, *et al*. Effect of aging on aortic morphology in populations with high and low prevalence of hypertension and atherosclerosis. Comparison between occidental and Chinese communities. American Journal of Pathology 1991;139:1119–1129.

20 Natural history of aortic and coronary atherosclerotic lesions in youth. Findings from the PDAY Study. Pathobiological Determinants of Atherosclerosis in Youth (PDAY) Research Group. Arteriosclerosis, Thrombosis, and Vascular Biology 1993;13:1291–1298.

21 Kolodgie FD, Burke AP, Farb A, *et al*. Differential accumulation of proteoglycans and hyaluronan in culprit lesions insights into plaque erosion. Arteriosclerosis, Thrombosis, and Vascular Biology. 2002;22:1642–1648.

22 Burke AP, Kolodgie FD, Farb A, *et al*. Healed plaque ruptures and sudden coronary death evidence that subclinical rupture has a role in plaque progression. Circulation, 2001;103:934–940.

23 Greenland P, Alpert JS, Beller GA, *et al*. American College of Cardiology Foundation; American Heart Association. 2010 ACCF/AHA guideline for assessment of cardiovascular risk in asymptomatic adults: a report of the American College of Cardiology Foundation/American Heart Association Task Force on Practice Guidelines. Journal of American College of Cardiology. 2010; 56 :e50-103.

24 Greenland P, Bonow RO, Brundage BH, *et al*. American College of Cardiology Foundation Clinical Expert Consensus Task Force (ACCF/AHA Writing Committee to Update the 2000 Expert Consensus Document on Electron Beam Computed Tomography); Society of Atherosclerosis Imaging and Prevention; Society of Cardiovascular Computed Tomography. ACCF/AHA 2007 clinical expert consensus document on coronary artery calcium scoring by computed tomography in global cardiovascular risk assessment and in evaluation of patients with chest pain: a report of the American College of Cardiology Foundation Clinical Expert Consensus Task Force (ACCF/AHA Writing Committee to Update the 2000 Expert Consensus Document on Electron Beam Computed Tomography) developed in collaboration with the Society of Atherosclerosis Imaging and Prevention and the Society of Cardiovascular Computed Tomography. Journal of American College of Cardiology. 2007; 49: 378-402.

25 Hartwig, H., Silvestre-Roig, C., Hendrikse, J., Beckers, L., Paulin, N., Van der Heiden, K.,... & Soehnlein, O. Atherosclerotic Plaque Destabilization in Mice: A Comparative Study. PloS one. 2015. 10(10), e0141019.

26 Lutgens, E., Daemen, M., Kockx, M., Doevendans, P., Hofker, M., Havekes L, Wellens H, de Muinck ED. Atherosclerosis in APOE* 3-Leiden transgenic mice: from proliferative to atheromatous stage. Circulation. 1999; 99(2), 276-283.

27 van der Hoorn, J. W., Kleemann, R., Havekes, L. M., Kooistra, T., Princen, H. M., & Jukema, J. W. Olmesartan and pravastatin additively reduce development of atherosclerosis in APOE* 3Leiden transgenic mice. Journal of hypertension, 2007. 25(12), 2454-2462.

28 Mallat Z., Gojova A., Marchiol-Fournigault C., Esposito B., Kamate C., Merval R., Fradelizi D. and Tedgui A. Inhibition of transforming growth factor-β signaling accelerates atherosclerosis and induces an unstable plaque phenotype in mice. Circulation Research. 2001. 89, 930-934.

29 Lutgens E., Gijbels M., Smook M., Heeringa P., Gotwals P., Koteliansky V.E. and Daemen E.J. Transforming growth factor-β mediates balance between inflammation and fibrosis during plaque progression. Arteriosclerosis, Thrombosis, and Vascular Biology. 2002. 22, 975-982.

CHAPTER 2

The natural history of aortic atherosclerosis: A systematic histopathological evaluation of the peri-renal region

R.A. van Dijk
R. Virmani
J.H. von der Thüsen
A.F. Schaapherder
J.H.N. Lindeman

Atherosclerosis 2010

ABSTRACT

Background: Risk factor profiles for the different vascular beds (*i.e.* coronary, carotid, peripheral and aortic) are remarkably different, suggesting that atherosclerosis is a heterogeneous disorder. Little is known about the morphologic progression of atherosclerosis in the peri-renal aorta, one of the primary predilection sites of atherosclerosis.

Methods: A systematic analysis was performed in 260 consecutive peri-renal aortic patches (stained with Movat Pentachrome and H&E) collected during organ transplantation (mean donor age 46. 5 (range 5–76) years; 54% ♂;mean BMI 24. 9; 40% smokers; 20% hypertensive). Plaque morphology was classified according to the modified AHA classification scheme proposed by Virmani *et al*. (Arteriosclerosis, Thrombosis, and Vascular Biology; 2000). Immunostaining against CD68 was used to identify the distribution of intimal macrophages and monocytes in several predefined locations among various plaque types and fibrous cap thickness.

Results: There was significant intimal thickening ($p < 0.013$) and medial thinning ($p < 0.032$) with advancing age. The incidence of atherosclerotic plaques in the abdominal aorta correlated with age ($r = 0.640$, $p = 0.01$). During the first three decades of life adaptive intimal thickening and intimal xanthomas were the predominant lesions. In contrast, the fourth, fifth and sixth decades hallmarked more complicated plaques of pathological intimal thickening, early and late fibroatheromas (EFAs and LFAs), thin-cap FAs (TCFAs; cap thickness <155m), ruptured plaques (PRs), healed rupture and fibrotic calcified plaques. The mean percentage of lesional macrophages increased significantly from LFAs to TCFAs (5–17%; $p < 0.001$). Macrophage infiltration of the fibrous cap was negatively correlated with fibrous cap thickness ($p < 0.0004$); TCFAs and PRs (caps < 100μm) contained significantly more macrophages (19%) compared with caps 101–300μm (6%) and >300μm (2%). Macrophages in shoulder regions were highest in early and late FAs (~45%) followed by TCFAs (27%) and PR (20%). Further, intimal *vasa vasorum* were mostly seen adjacent to the necrotic core of advanced atherosclerotic plaques and remained confined to the intimo-medial border despite marked thickening of the intima.

Conclusion: This study shows that peri-renal aortic atherosclerosis starts early in life. Gross plaque morphologies of the peri-renal abdominal aorta are similar to coronary atherosclerosis yet indications were found for site specific differences in macrophage content and neovascularization.

INTRODUCTION

Atherosclerosis is a complex pathology of large and medium sized arteries that leads to cardiovascular disease. Although elevated LDL-cholesterol is generally accepted as the dominant and universal risk factor for atherosclerotic disease, risk factor profiles for the various predilection places are remarkable distinct[1,2]. Consequently it has been suggested that atherosclerosis is a heterogeneous disease that may proceed through different pathophysiological pathways[3].

Of the primary locations, *i.e.* coronaries, carotids and aorta, surprisingly little is known about how atherosclerosis in the aorta, the second largest manifestation of atherosclerosis, progresses from early to more advanced, complicated lesions [4,5,6,7,8]. This lack of information is remarkable, especially considering the fact that the aorta is generally used in rodent studies of atherosclerotic disease.

In order to establish the natural course of human aortic atherosclerotic disease we here systematically evaluate the histological progression aortic atherosclerosis in a well-documented, large tissue bank of human peri-renal aortic tissue from apparently healthy individuals (organ donors) that covers all age groups and the whole spectrum of atherosclerotic disease. Atherosclerotic lesions were classified according to adapted AHA classification[9] as proposed by Virmani *et al.*[4]. Particular attention is paid to the lesional macrophages as well as to the morphology of the fibrous cap, the critical determinant of plaque stability.

MATERIAL & METHODS

Patients and tissue sampling

Two hundred and sixty consecutive aortic patches were studied. The patches were obtained during clinical organ transplantation with grafts derived from cadaveric donors. All the aortic samples were harvested by the same surgeon at the time of transplantation or organ harvest. Two centimetres of excessive aorta proximal and distal from the ostium of the renal artery was removed and used for this study. Aneurysmal aortas (circumference > 2. 5 cm, n = 2) were excluded from the study. Demographic data concerning the causes of death are summarized in supplemental Tables I–II (data available online at http://www.atherosclerosis-journal.com). All donors met the criteria set by The Eurotransplant Foundation. Due to national regulations, only for transplantation relevant data from donors is available for research. Sample collection and handling was performed in accordance with the guidelines of the Medical and Ethical Committee in Leiden, Netherlands and the code of conduct of the Dutch Federation of Biomedical Scientific Societies (http://www.federa.org/?s=1&m=82&p=0&v=4#827).

Histological classification of lesions

All patches were divided in parallel sections of approximately 5mm width. Movat pentachrome staining was performed for the histological evaluation of each individual section. Each section was individually classified according to the modified classification of the AHA as proposed by Virmani *et al*.[4] (Table 1, Fig. 1) by two independent observers with no knowledge of the characteristics of the aortic patch. The section showing the highest degree of atherosclerosis was used as the reference section for further studies.

In progressive atherosclerotic lesions the fibrous cap and shoulder regions were assessed for the presence of macrophages. A TCFA was defined as a fibrous cap less than 155μm thick. The 155μm thickness in cases without rupture was chosen as a criterion for thin cap because in arteries with ruptured plaque, the mean (±SEM) cap thickness was 99±27μm (95 percent of the caps measured less than154μm). Note that independent of dominant plaque type there may be several plaque components in a single section. For detailed descriptions concerning histological components of the aortic sections we refer to the online supplements.

Immunohistochemistry

The paraffin embedded sections were stained for the identification of intimal macrophages and monocytes (CD68; clone KP-1; 1:400 overnight; Dako, Denmark) as previously described and evaluated at predefined locations[8]. Smooth muscle actin (clone 1A4, 1:400; overnight; Dako, Denmark) and smooth muscle heavy chain myosin (clone 3F8, 1:1000; overnight; ABCAM, Cambridge, UK) staining were used to determine the lesional VSMC phenotype in the dominant lesion.

Morphological analysis

Morphometric and histological analyses were performed with calibrated software (IPLab, Scanalytics Inc., Rockville, MD) on all sections stained with Movat pentachrome. All measurements were performed on the dominant plaque in the tissue section showing the most advanced grade of atherosclerosis. For detailed descriptions concerning the morphological measurements of the various components of the aortic sections we refer to the online supplements.

Statistical analysis

Data in figures are presented as mean ± SEM. Mean variables between the various lesions were compared with the one-way analysis of variance (ANOVA; SPSS 16. 0; Chicago, IL) Differences between the groups were assessed by Fisher's LSD. Spearman's correlation was used to demonstrate the relationship between the age of the aortic patch and the severity of atherosclerosis and intimal thickness. Pearson 2-test was used to compare the presence of *vasa vasorum* in the intima in the various lesions. A value of $p < 0.05$ was considered statistically significant.

RESULTS

Studied population

Data were obtained from 260 consecutive peri-renal aortic samples from organ donors in age from5 to 76 years (Supplemental Table 1, available online at http://www.atherosclerosis-journal.com). Males and females were evenly distributed as was the mean age of both genders. Within the studied population 81 subjects were considered obese (BMI > 25). One hundred and four individuals had a known history of smoking at time of death with an average of 21 and 22 pack-years (1 package of cigarettes/day/year) for males and females, respectively. One-fifth of the population had a history of hypertension (antihypertensive medication or systolic blood pressure >140mmHg and diastolic >90mmHg in the period preceding death). Only 4 patients were on statin therapy. Further details on the donor characteristics are provided in the online supplement.

Morphometric measurements

Effect of age on aortic intimal thickness (supplemental Fig. Ia)

The intimal thickness increases significantly with advancing age ($R= 0.601$, $p < 0.01$). In the third decade of life the intima of the abdominal aorta is about 0.5mm thick and almost triples in size in the upcoming years. In comparison to non-smokers, intima thickness is significantly increased in the younger smokers (31–45 years, $p < 0.003$), but no differences are found for the other age groups (46–60 and >60 years, $p < 0.203$ and $p < 0.232$ respectively; data not shown). No significant difference in intimal thickness was observed between the sexes or in the presence of (a history of) hypertension.

Effect of age on aortic medial thickness (supplemental Fig. Ib)

The medial thickness increases during the first 45 years of life but significant thinning was observed from the fifth decade and onwards ($p < 0.0001$). Smoking was associated with increased medial thinning in the age group >60 years ($p < 0.030$; data not shown). Medial thickness was not influenced by gender or by a history of hypertension.

Table 1 Histological classification of the aortic tissue according to the modified classification of the AHA proposed by Virmani *et al*. [4].

Morphological description	Associated AHA classification	Male		Female	
		N	Mean age (range)	N	Mean age (range)
Normal aorta	-	5	22.4 (6–55)	4	10.3 (4–17)
Nonprogressive intimal lesions					
Adaptive intimal thickening	I	26	31.4 (16–53)	25	40.0 (12–67)*
Intimal xanthoma	II	18	34.5 (13–62)	16	35.3 (11–57)
Progressive atherosclerotic lesions					
Pathological intimal thickening	III	19	48.7 (17–66)	17	52.2 (35–68)
Early fibroatheroma	IV	12	51.1 (36–62)	11	45.6 (36–56)
Late fibroatheroma	IV/Va	16	61.8 (50–75)	16	50.6 (37–74)**
Thin-cap fibroatheroma	-	19	56.7 (48–71)	15	53.3 (35–67)
Plaque rupture	VI	7	56.8 (48–60)	5	52.5 (43–62)
Healing rupture	VI	6	64.0 (57–73)	3	55.3 (42–67)
Fibrotic calcified plaque	Vb,c, VII	12	63.2 (47–76)	8	56.6 (48–72)

* $p < 0.023$ in AIT between mean age among gender.

**$p < 0.013$ in LFA between mean age among gender.

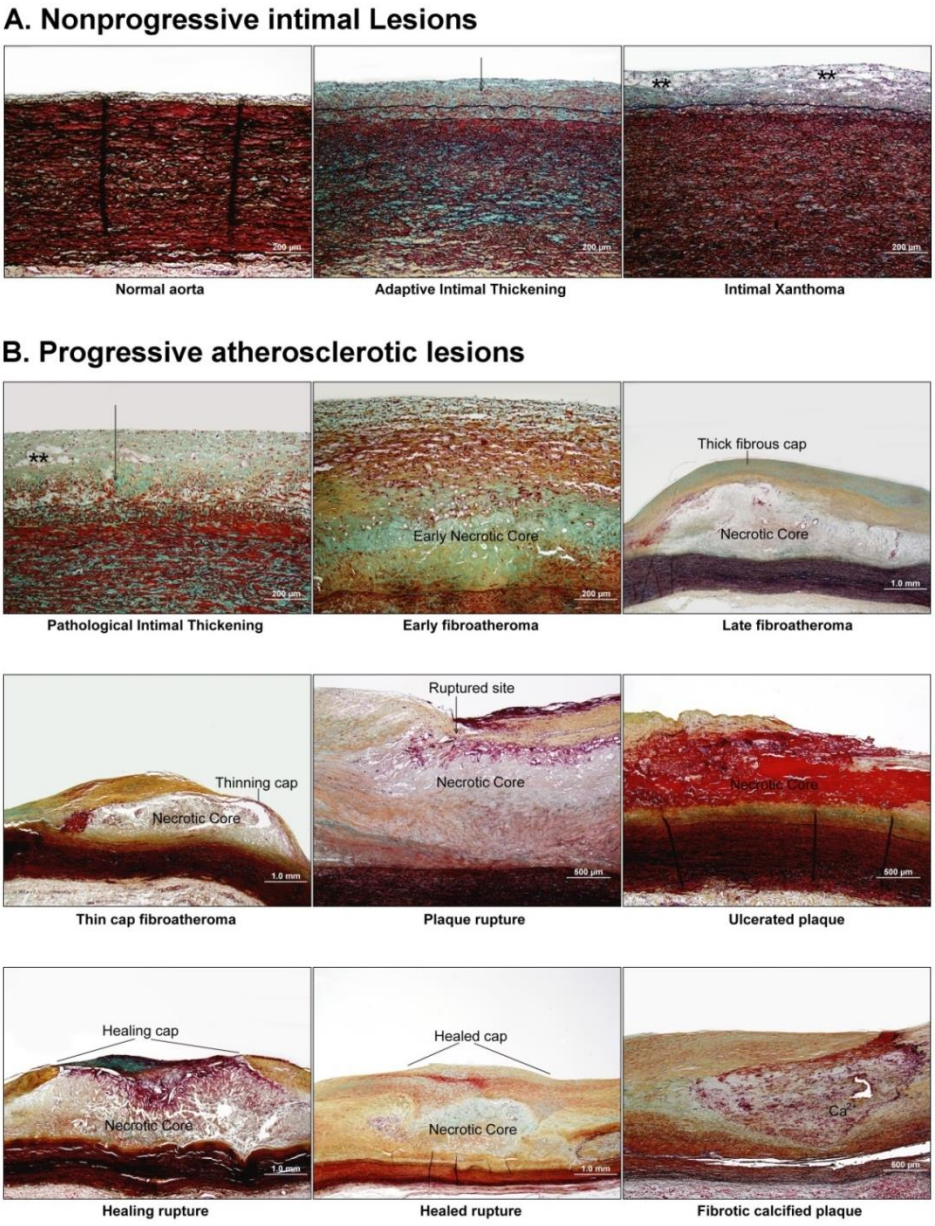

Figure 1. *Nonatherosclerotic intimal lesions (Normal, AIT and IX) and progression prone atherosclerotic lesions (PIT, early- and late-FA, TCFA, PR, ulcerated plaque and HR).* (**A**) Adaptive intimal thickening consists mainly of smooth muscle cells in a proteoglycan-rich matrix (black arrow). Intimal xanthomas were characterized by infiltrating macrophage-derived foam cells (*) in the intima. (Movat pentachrome stain). (**B**) Pathological intimal thickening is characterized by the presence of lipid pools deep within the intima near the intimal medial border with overlying SMCs (black arrow) in a proteoglycan matrix with or without macrophage infiltration (*). The early FA shows macrophage in the early necrotic core. After a rupture the plaque can become ulcerated and of the 260 studied aortas, only one lesion met that criterion. (Movat pentachrome stain).

Effect of age on lesion progression

Pre-atherosclerotic lesions (nonprogressive intimal lesions) (Figs. 1a, 2 and Table 1)

Age and gender distribution of the 260 histologically classified lesions of the aortic samples are shown in Table 1 and Fig. 2. Nine specimens were classified as normal aortic tissue as no signs of thickening of the intima were detected. Aortic tissue with intimal thickening consisting mainly of SMCs with an increase in proteoglycan-rich matrix and are referred to as AIT. As soon as macrophage-derived foam cells become evident in the intima the lesion are referred to as IX which are known as "fatty streaks". These lesions are seen within all age groups but were most predominant during the first three decades of life.

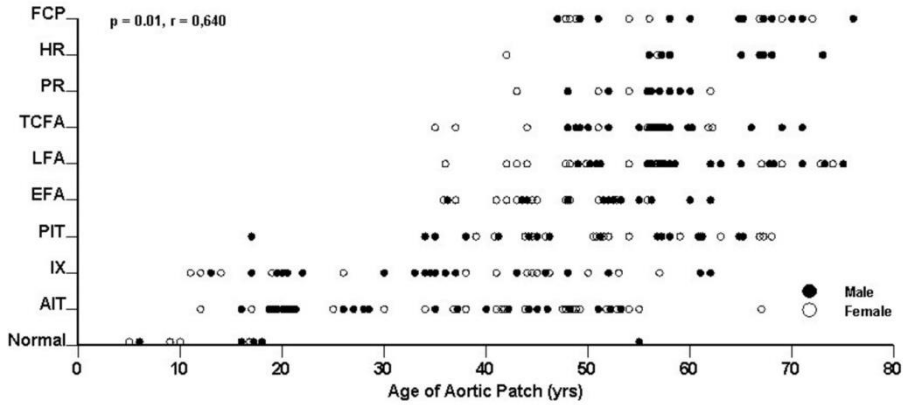

Figure 2. *Histological classification of human aortic atherosclerotic lesion type and the relationship to age.* Two hundred sixty aortic patches were characterized for the type of atherosclerosis according to Virmani *et al*.4 and plotted in relation to the age of the donor. There is a significant correlation of lesion type with age (R = 0.640, p = 0.01). For abbreviations see histological classification in Material and Methods section.

Progressive atherosclerotic lesions (Figs. 1b and 2 and Table 1)

A strong positive correlation (R = 0.640, $p < 0.01$) was found between the age of the donors and the degree of atherosclerosis when classified according to pathologic subtypes (Table 1 and Fig. 2). The fourth, fifth and sixth decade of life showed progressive advancement of the atherosclerotic lesions.

Lesions are evenly distributed among both genders. Pathological intimal thickening was frequently observed in young individuals and in the male population. However, females tend to have more advanced lesions at a younger age (from EFA to more advanced plaques) with the mean age for FA being significantly lower in comparison to men ($p < 0.013$).

Despite the noticeable thinning of the media during the evolution of the atherosclerotic plaque the internal elastic lamina remained grossly intact.

Advancing atherosclerotic lesions were associated with a significant increase in intimal *vasa vasorum* ($p < 0.001$; Fig. 3) at the intimo-medial border. The same phenomenon was seen within the inner third of the media with the presence of *vasa vasorum* correlating with advancing plaques (data not shown).

With 34 cases of TCFAs, 12 PRs and 9HRs the incidence of vicious lesions is remarkably high in this apparently healthy population. In PR the area of the fibrous cap disruption with an overlying thrombus showed continuity with the underlying necrotic core and was located near the centre of the plaque in the majority of cases. The remnants of the fibrous cap and the large necrotic core are rich in macrophages.

The nine cases of healing or healed ruptures show a remarkable proteoglycan and SMC rich cap between the remnants of the ruptured cap (Fig. 1b). The necrotic core is separated from the lumen and still consists of macrophages and lymphocytes. The healed cap however shows a reduction in the amount of infiltrated macrophages and an increase of SMCs when compared to TCFAs and PRs.

The FCP partly matches the criteria of a HR, but the necrotic core is largely 'missing'. If present at all it was usually small and contained extensive amounts of calcium.

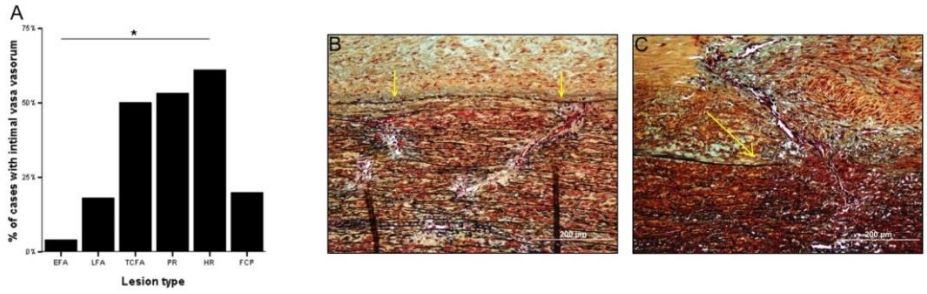

Figure 3. Percentage of cases with intimal *vasa vasorum* in relation to type of atherosclerotic plaque. (**A**) The number of cases with intimal *vasa vasorum* increased significantly with advancing atherosclerotic lesion (*$p < 0.001$). (**B**) High power magnification (200×) of *vasa vasorum* in the inner third of the media with intact internal elastic lamina (yellow arrows) in a case of early fibroatheroma. (**C**) High power magnification (200×) of *vasa vasorum* in the intima in the intimo-medial border showing disrupted internal elastic lamina (yellow arrow) in a case of plaque rupture. Bars represent 200m. For abbreviations see histological classification in Material and Methods section.

SMC phenotype, intimal and medial thickness in the atherosclerotic lesions (supplemental Figs. II–IV)

The intima thickens during lesion progression (PIT to early FA) but decreases during development of TCFAs and PRs. There is a trend towards increased intima thickness during healing of the ruptured plaque but thickness decreases again in FCPs with deposition of large amounts dense collagen.

A decrease in medial thickness was found when the lesion progresses into a late fibroatheroma and beyond. (supplemental Fig. IIb).

Alpha-SMC-actin was abundantly expressed in the intimal and medial layers. No relation was found between plaque progression and α-SMC-actin expression. Progression of atherosclerotic lesions was associated with reduced intimal SMC myosin heavy chain (SMC-MHC) expression in the shoulder and cap regions. SMC-MHC in the medial layers decreased with advancing lesions and was confined to the medio-adventitial border in the more advanced lesions (supplemental Figs. III and IV).

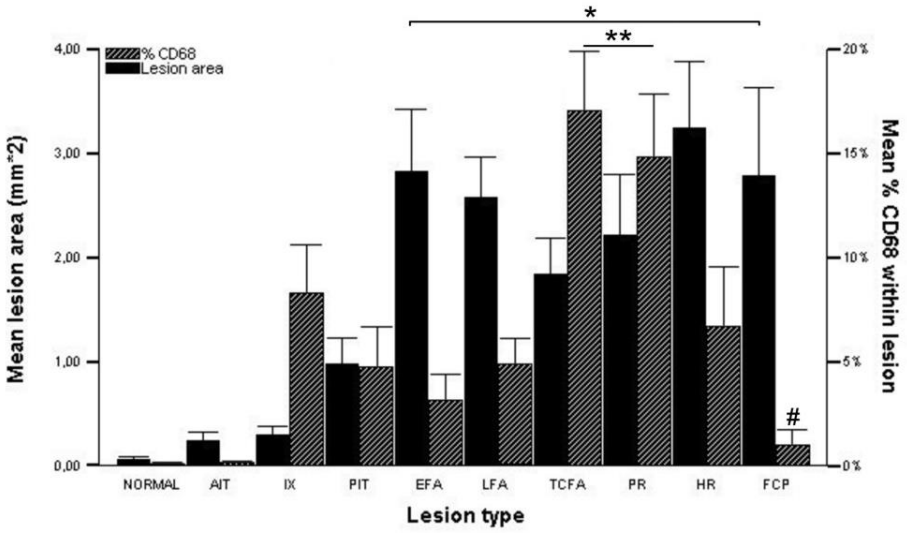

Figure 4. Total lesion area in relation to the atherosclerotic lesion type plotted with adjoining mean percent of CD68 within the total lesion type. The total lesion area (solid bars) show significant increase in lesion size in the early fibroatheroma and more advanced lesions (*$p < 0.027$). From the fatty streak to progression of advanced lesion types, the amount of macrophages in the lesions (striped bars) is significantly increased ($p < 0.023$). The mean percent of macrophages were maximum in the TCFA and PR (**$p < 0.003$) and thereafter decreasing in HR and FCP (#$p < 0.030$). Solid bars represent mean values (±SEM), striped bars represent mean percent values (±SEM). For abbreviations see histological classification in Material and Methods section.

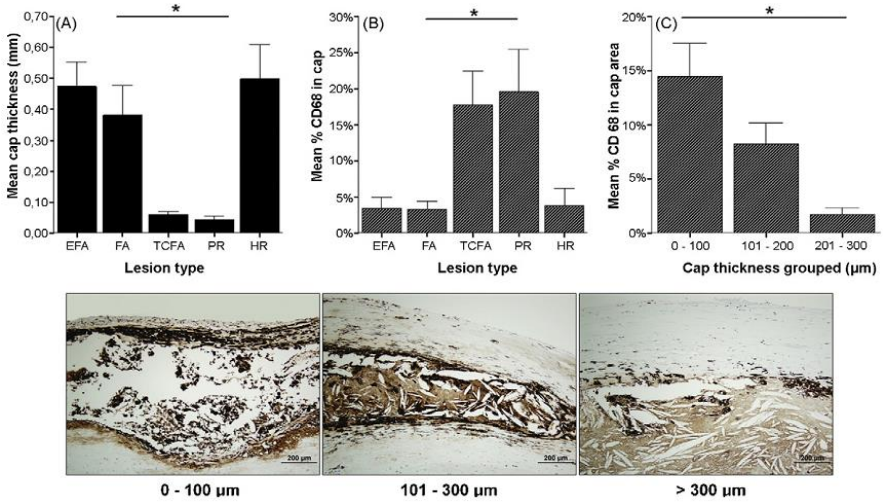

Figure 5. Fibrous cap thickness in relation to the atherosclerotic lesion type and macrophage distribution. (**A**) There is significant thinning of the fibrous cap in the thin cap fibroatheroma and ruptured plaque (*p < 0.003). (**B**) A significant increase in macrophages infiltration was observed in thin-cap fibroatheroma and ruptured plaques (*p < 0.003). Note that the fibrous cap in the healed ruptures shows a remarkable increase in thickness and decrease in macrophages infiltration. (**C**) The amount of macrophages in cap areas >300µm is significantly lower when compared to thickness <100µm (*p < 0.0004). Solid bars represent mean values (±SEM), striped bars represent mean percent values. Bars represent 200µm. For abbreviations see histological classification in Material and Methods section.

Macrophage infiltration with plaque progression

Lesional macrophages (Fig. 4)

Aortic IX are small (average size 0.3mm2) and are characterized by profuse macrophage infiltration. With advancing atherosclerotic lesions, lesion size increases and the relative percentage of macrophages decreases. The mean percent of macrophages however increases significantly in the TCFA and PR ($p < 0.003$) and thereafter decreasing in HR and FCP ($p < 0.03$).

Relationship of cap thickness to plaque type and CD68 infiltration (Fig. 5)

There is a significant thinning of the cap with advancing fibroatheromas and remarkable thickening of the fibrous cap in HRs. Only 3–5% of the area in the EFA and LFA consists of macrophages, but 45% of those macrophages reside in the shoulder, 45-49% is core related and <5% is located in the cap. In the TCFA 20% of the total amount of macrophages are located in the shoulder regions and 18% in the cap ($p < 0.003$). In PRs the percentage of macrophages related to capsize is similar (20%). In HRs only 4% of macrophages are located in the cap ($p < 0.003$). A negative correlation is found between cap thickness and macrophage infiltration, with greater density of macrophage seen in caps <100µm and significantly less as the cap thickens ($p < 0.0004$) (Fig. 5c).

DISCUSSION

In the present study we evaluated the natural history of human aortic atherosclerosis at a fixed, lesion prone location[10,11]. Unlike previous histological studies, we used tissue from a group of apparently healthy individuals with an equal age and sex distribution, thereby avoiding potential bias introduced by the use of autopsy material from coronary death victims (mostly either young or old patients[4,12]) or by the use of material from patients undergoing vascular surgery (generally end-stage atherosclerotic disease[13]).

Age is an important factor in the atherosclerotic process and is related with the significant change in the physiological properties of the afflicted vessel[14,15]. Our study demonstrates that advancing age is associated with pronounced intimal thickening and medial thinning of the peri-renal aorta. These findings are consistent with the autopsy-based studies of perfusion-fixed human aortas that have shown that wall thickening is mostly confined to the intima and is a well-known effect of atherosclerosis[6,16]. It has also been shown that the increase in intimal thickness with age is maximal in the abdominal region compared with other locations and is the predominant factor for the well-known age related increase in total wall thickness of the aorta[6,17]. Our study extends these findings and shows a clear relationship between intimal thickness and plaque characteristics in aortic atherosclerosis. This observation indicates that intimo-medial thickness measurements in conjunction with the used classification scheme provide a useful method for the overall evaluation of the presence of atherosclerosis[6].

Proliferation and migration of SMCs is an integral part of atherosclerotic plaque progression[18]. We observed stable α- actin but reduced intimal SM-MHC expression with progression of atherosclerosis. This observation may indicate a phenotypical change in SMC during the progression of atherosclerosis, or alternatively that advanced atherosclerotic lesions are dominated by myofibroblasts rather than by SMCs[19].

Our findings indicate rapid progression of peri-renal aortic atherosclerosis as early as the fourth decade of life. This observation is remarkable and, if also valid for the other predilection places, suggests that preventive conservative measures and pharmaceutical interventions should be initiated at a much younger age than commonly thought[6,7,13].

This study shows that advanced atherosclerotic disease is common in people over 45. Our data suggests that aortic atherosclerosis advancement occurs at a younger age in women than in men, an observation that concurs with clinical observations showing that peripheral artery disease develops earlier and at a relatively high rate in women[20,21,22]. Although this observation may appear

counterintuitive, it is important to realize that the male dominance in atherosclerotic disease is limited to the coronary bed[1,2,4].

Our data show that aortic atherosclerotic lesions follow a similar pattern of progression as in coronary tissue but grow far beyond the size of coronary atherosclerotic lesions in our apparently healthy population. Owing to the size of the aorta all plaques remained clinically silent. We observed numerous ruptured and healed plaques (21 (8%) in total) in this apparently healthy population, suggesting that plaque rupture is more common than generally thought and at least for the aorta does not necessary result in clinical events. A similar phenomenon has also been reported in coronary atherosclerosis[23].

Intraplaque haemorrhage and plaque neovascularization are considered key factors in atherosclerotic plaque growth and destabilization in coronary and carotid arteries[24,25,26]. Similar to the other vascular beds we found an increasing number of *vasa vasorum* with advanced atherosclerotic lesions. Yet, unlike the coronaries and carotids, the *vasa vasorum* in the aorta atherosclerotic lesions remain confined to the disrupted intimo-medial border and plaque neovascularization remains minimal despite to prominent intimal thicknesses and necrotic core sizes. These observations are remarkable and suggest that plaque neovascularization plays a less prominent role in aortic atherosclerotic plaque destabilization than reported for the other vascular beds[16].

Monocytes are key players in the atherosclerotic process. Monocyte accumulation in intimal layer of the vessel wall is a primordial event in atherogenesis[27] and is thought to be primarily driven by presence of high amounts of oxidized LDL[28,29]. Apart from their role in foam cell formation, it is generally assumed that macrophages, through release of matrix metalloproteinases directly contributed to destabilization. This process is well studied in the coronary and carotid tissue[4,30,31,32], but remains underreported and appreciated in the aortic vascular bed[32,33]. Analysis of the fibrous cap in this study reveals significant increase in macrophage infiltration in the thinned cap and a significant decrease in healing ruptures.

Conclusion

This study demonstrates that plaque morphologies of the perirenal abdominal aorta are similar to coronary atherosclerosis with macrophage and foam cells seemingly playing a larger role than plaque neovascularization in the evolution of the necrotic core, plaque progression and destabilization in our relatively young and healthy population.

REFERENCES

1 Chambless LE, Folsom AR, Davis V, *et al*. Risk factors for progression of common carotid atherosclerosis: the Atherosclerosis Risk in Communities Study, 1987–1998. American Journal of Epidemiology 2002;155:38–47.

2 Bauer M, Möhlenkamp S, Lehmann N, *et al*. The effect of age and risk factors on coronary and carotid artery atherosclerotic burden in males—Results of the Heinz Nixdorf Recall Study. Atherosclerosis 2009;205:595–602.

3 Hansson GK. Immunemechanisms in atherosclerosis. arteriosclerosis, Thrombosis, and Vascular Biology 2001;21:1876–1890.

4 Virmani R, Kolodgie FD, Burke AP, Farb A, Schwartz SM. Lessons from sudden coronary death: a comprehensive morphological classification scheme for atherosclerotic lesions. Arteriosclerosis, Thrombosis, and Vascular Biology 2000;20:1262–1275.

5 Naghavi M, Libby P, Falk E, *et al*. From vulnerable plaque to vulnerable patient: a call for new definitions and risk assessment strategies. Part I. Circulation 2003;108:1664–1672.

6 Virmani R, Avolio AP, Mergner WJ, *et al*. Effect of aging on aortic morphology in populations with high and low prevalence of hypertension and atherosclerosis. Comparison between occidental and Chinese communities. American Journal of Pathology 1991;139:1119–1129.

7 Natural history of aortic and coronary atherosclerotic lesions in youth. Findings from the PDAY Study. Pathobiological Determinants of Atherosclerosis in Youth (PDAY) Research Group. Arteriosclerosis, Thrombosis, and Vascular Biology 1993;13:1291–1298.

8 Kolodgie FD, Burke AP, Farb A, *et al*. Differential accumulation of proteoglycans and hyaluronan in culprit lesions insights into plaque erosion. Arteriosclerosis, Thrombosis, and Vascular Biology 2002;22:1642–1648.

9 Stary HC. Natural history and histological classification of atherosclerotic lesions an update. Arteriosclerosis, Thrombosis, and Vascular Biology 2000;20:1177–1178.

10 Lusis AJ. Atherosclerosis. Nature 2000;407:233–241.

11 Wissler RW. USA multicenter study of the pathobiology of atherosclerosis in youth. Annals of the New York Academy of Sciences 1991;623:26–39.

12 McGill Jr HC. Fatty streaks in the coronary arteries and aorta. Laboratory Investigations 1968;18:560–564.

13 Diehm N, Shang A, Silvestro A, *et al*. Association of cardiovascular risk factors with pattern of lower limb atherosclerosis in 2659 patients undergoing angioplasty. European Journal of Vascular and Endovascular Surgery 2006;31:59–63.

14 O'Rourke MF. Arterial aging: pathophysiological principles. Vascular Medicine 2007;12:329-341.

15 Stein JH, Korcarz CE, Post WS. Use of carotid ultrasound to identify subclinical vascular disease and evaluate cardiovascular disease risk: summary and discussion of the American Society of Echocardiography Consensus Statement. Preventive Cardiology 2009;12:34–38.

16 Moreno PR, Purushothaman KR, Fuster V, O'Connor WN. Intimomedial interface damage and adventitial inflammation is increased beneath disrupted atherosclerosis in the aorta implications for plaque vulnerability. Circulation 2002;105:2504–2511.

17 Movat HZ, More RH, Haust MD. The diffuse intimal thickening of the human aorta with aging. The American Journal of Pathology 1958;34:1023–1031.

18 Aikawa M, Sakomura Y, Ueda M, *et al*. Redifferentiation of smooth muscle cells after coronary angioplasty determined via myosin heavy chain expression. Circulation 1997;96:82–90.

19 Hinz B. Formation and function of the myofibroblast during tissue repair. Journal of Investigational Dermatology 2007;127:526–537.

20 Leng GC, Papacosta O, Whincup P, *et al*. Femoral atherosclerosis in an older British population: prevalence and risk factors. Atherosclerosis 2000;152:167–174.

21 Diehm C, Schuster A, Allenberg JR, *et al*. High prevalence of peripheral arterial disease and co-morbidity in 6880 primary care patients: cross-sectional study. Atherosclerosis 2004;172:95–105.

22 Resnick HE, Lindsay RS, McDermott MM, *et al*. Relationship of high and low ankle brachial index to all-cause and cardiovascular disease mortality the strong heart study. Circulation 2004;109:733–739.

23 Burke AP, Kolodgie FD, Farb A, *et al*. Healed plaque ruptures and sudden coronary death evidence that subclinical rupture has a role in plaque progression. Circulation 2001;103:934–940.

24 Kolodgie FD, Gold HK, Burke AP, *et al*. Intraplaque hemorrhage and progression of coronary atheroma. New England Journal of Medicine 2003;349:2316–2325.

25 Virmani R, Kolodgie FD, Burke AP, *et al*. Atherosclerotic plaque progression and vulnerability to rupture angiogenesis as a source of intraplaque hemorrhage. Arteriosclerosis, Thrombosis, and Vascular Biology 2005;25:2054–2061.

26 Yuan C, Mitsumori LM, Ferguson MS, *et al*. In vivo accuracy of multispectral magnetic resonance imaging for identifying lipid-rich necrotic cores and intraplaque hemorrhage in advanced human carotid plaques. Circulation 2001;104:2051–2056.

27 Ross R. Atherosclerosis—an inflammatory disease. The New England Journal of Medicine 1999;340(2):115–126.

28 Glass CK,Witztum JL. Atherosclerosis the road ahead. Cell 2001;104:503–16.29 Stary HC. Lipid and macrophage accumulations in arteries of children and the development of atherosclerosis. American Journal of Clinical Nutrition 2000;72:1297S–306S.

30 Schrijvers DM, De Meyer GRY, Herman AG, Martinet W. Phagocytosis in atherosclerosis: molecular mechanisms and implications for plaque progression and stability. Cardiovascular Research 2007;73:470–480.

31 Peeters W, Hellings WE, de Kleijn DP, *et al*. Carotid atherosclerotic plaques stabilize after stroke. Insights into the natural process of atherosclerotic plaque stabilization. Arteriosclerosis, Thrombosis, and Vascular Biology 2009;29:128–133.

32 Kolodgie FD, Burke AP, Farb A, *et al*. The thin-cap fibroatheroma: a type of vulnerable plaque: the major precursor lesion to acute coronary syndromes. Current Opinion in Cardiology 2001;16:285–292.

33 Virmani R, Burke AP, Farb A, Kolodgie FD. Pathology of the vulnerable plaque. Journal of the American College of Cardiology 2006;47:13–18.

SUPPLEMENTARY DATA

Methods

Plaque Processing

All specimens were collected at the origin of the renal artery and fixed in formalin for 24 hrs and subsequently decalcified in Kristensen fluid during 5 days. Depending on their size, the aortic patches were divided into 2 or more sections prior to paraffin embedding. The sections were cut into 5 μm thick slices and mounted on aminopropylethoxysilane (APES)-coated slides and dried overnight at 37 degrees Celcius. All aortic sections were stained with hematoxylin and eosin (H&E) and Movat pentachrome method as previously described[1]. The section displaying the highest grade of atherosclerosis was used for further evaluation.

Histological Definitions

The dominant plaque type per section were defined as adaptive intimal thickening (AIT), intimal xanthoma (IX), pathological intimal thickening (PIT), early fibroatheroma (EFA), late fibroatheroma (LFA), thin cap fibroatheroma (TCFA), acute plaque rupture (PR), healed plaque rupture (HR) and fibrotic calcified plaque (FCP) (table 1, figure 1).

Intimal xanthomas were defined as areas of foam cell macrophages in the absence of significant extracellular lipid[2]. Those lesions prone to lipid accumulation were further classified as lipid pool and necrotic core. Lipid pools within PIT denoted localized areas of loss of smooth muscle cells (SMC) within the fibrous plaque usually adjacent to the media, with absence of macrophage cell death, fibrin, and hemorrhage. These lipid pools were often surrounded by macrophage foam cells, especially towards the lumen, or SMC rich areas. The distinction between early and late fibroatheroma was made as previously defined[3] namely, the complete loss of matrix with extensive cellular breakdown in the latter. Necrotic core denoted central areas of necrosis, often infiltrating the lipid pool, with apoptotic macrophage debris, prominent cholesterol crystals, presence of fibrin, and partial or complete loss of matrix.

Morphological Analysis

The intimal thickness was defined as the greatest distance between the internal elastic lamina and the lumen. The medial thickness was measured at the thinnest portion between the external and internal elastic lamina at the location of the lesion. The media adjacent to the plaque was visually divided into an outer, middle and inner third and together with the intimo-medial border each area was observed for the presence of *vasa vasorum*. The fibrous cap thickness was measured at the thinnest portion of the early and late fibroatheroma and at the

remnant site of the ruptured plaque. The lesions were measured over a distance of 1mm and grouped by cap thickness as followed: 0-100μm, 101-300μm and >300μm. The lesion area was defined as the area between the endothelium and internal elastic lamina over a distance of 1mm. In the presence of a necrotic core the distance was expanded another 500μm on both sides of the necrotic core to include the adjacent shoulder region.

Table I. Demographic data of the 260 studied aortic samples

	Male	**Female**
Distribution	140 (53.8%)	120 (46.2%)
Mean age in years	47.3 (6 – 76)	45.4 (5 – 74)
Mean BMI (kg/m^2)	24.3 (8.3 – 32.9)	23.9 (13.1 – 37.2)
Number of patients with known history of nicotine abuse	59	55
Number of patients with known history of hypertension	31	22
Number of patients with known diabetes	0	1
Cause of Death:		
Severe head trauma	31	17
CVA / SAB	26 / 24	19 / 35
Basilar artery thrombosis	0	3
Myocardial infarction	1	0
Cardiac arrest	7	0
Suicide	4	0
Other	47	47
Medication		
Anti-hypertensives	19	12
Statins	3	1
Anti-coagulants	6	6

* CVA; Cerebral vascular accident, SAB; Subarachnoid bleeding

Threshold imaging

The percentage of area occupied by macrophages in the cap, core, shoulders and total lesion was quantified by digital color threshold imaging (IPLab). The regions of interest were selected from each lesion in the Movat Pentachrome stained section and matched with the immunohistochemically stained section. The percent CD68 positive cells within the lesion or cap were calculated byCD68 positive staining area in lesion or cap / total plaque or cap area*100.

Additional information concerning the studied population

The majority of patients died from a severe head trauma (18.5%), cerebral vascular accidents (*i.e.* hemorrhage (17.3%) or subarachnoid bleeding (22.7%)). Only one patient died as a result of myocardial infarction. The four cases that committed suicide were strangulations. The remaining causes of death (n=94) were non-traumatic and not cardiovascular related and include meningitis and respiratory insufficiency. Patients who received anti-coagulants were known to have either coronary stents, an artificial aortic valve or cardiac arrhythmias. Only four patients in our database received lipid lowering agents and only one was known to have hypercholesteremia (total cholesterol >240 mg/dL).

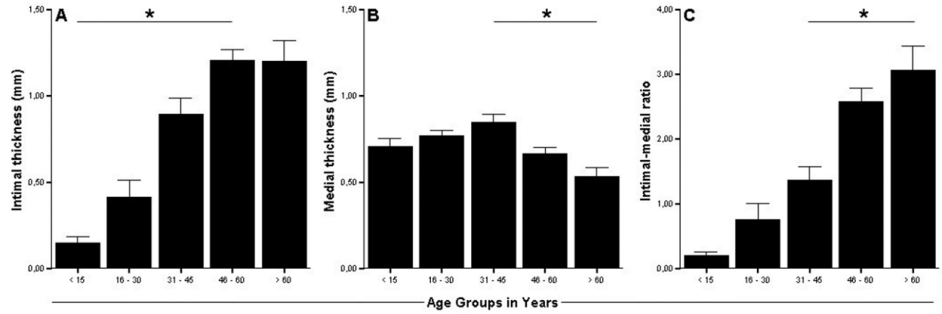

Figure I. Aortic intimal and medial wall thickness and intimal-medial ratio in the abdominal aorta in five age groups at 15 years interval. **A.** Significant difference in intimal thickening were observed between < 15 years, 16 to 30, 31 to 45 years and 46 to 60 years (*p<0,013). **B.** Medial thinning occurred between the age group 31 to 45 years vs. 46 to 60 years (* p<0,0001) and between age group 45 to 60 years and > 60 years (* p<0,032). **C.** The intimal-medial ratio showed significant increase from the age group 31 to 45 years in relation to the 46 to 60 years and > 60 years age groups (* p<0,005). Bars represent mean values (±SEM). (ANOVA across all age groups in all figures p<0.0001).

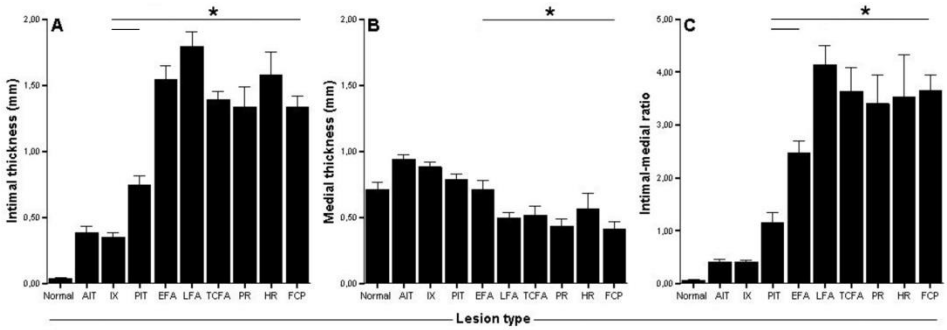

Figure II. Aortic intimal and medial wall thickness and intimal-medial ratio in the abdominal aorta in relation to characteristics of the atherosclerotic plaque type. **A.** The intimal thickness increased significantly with pathological intimal thickening, early fibroatheroma and with progression to advanced lesion types (*p<0,0001). **B.** There is significant medial thinning of the abdominal aorta in plaques which are more advanced than early fibroatheroma (*p<0,03). There is no significant difference in medial thickness between the healed ruptures and the atherosclerotic lesions preceding the late fibroatheroma. **C.** The intimal-medial ratio increased significantly from pathological intimal thickening, early fibroatheroma and with progression to advanced lesion types (* p<0,019). Bars represent mean values (±SEM). (ANOVA across all lesion types in all figures p<0.0001). For abbreviations see histological classification in methods section.

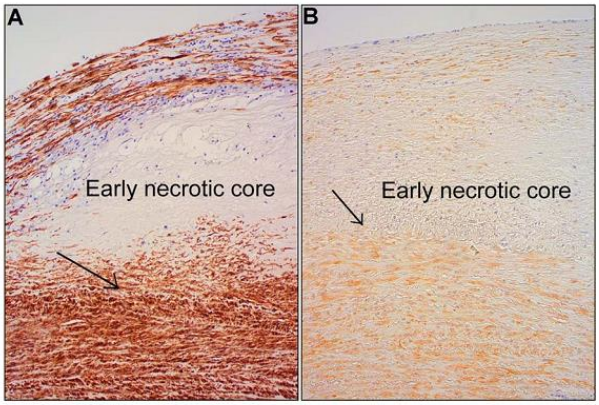

Figure III. Alpha-Smooth muscle cell (α-SMC) actin and myosin heavy chain (SMC-MCH) expression in early fibroatheroma (in adjacent sections). **A.** α-SMC-actin is abundantly expressed in the cap and shoulder region in the early fibroatheroma. Note the SMC infiltration towards the necrotic core adjacent to the internal elastic lamina (black arrow). **B.** SMC-MCH staining in the adjacent section. In comparison to α-SMC –actin, reduced number of SMC-MHC positive cells is found in the shoulder and cap regions. (100X).

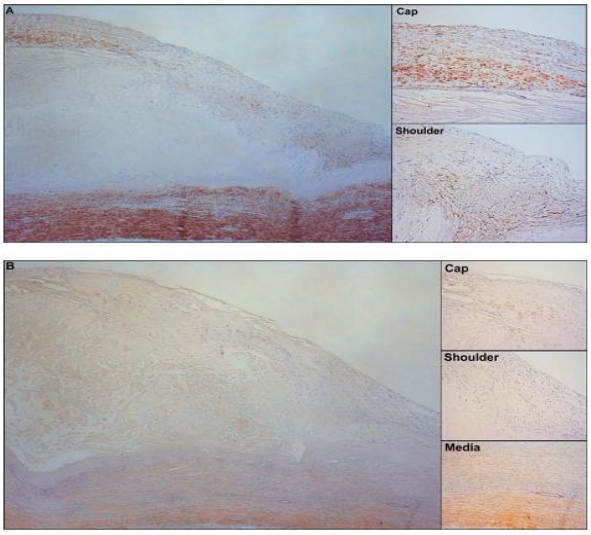

Figure IV. Alpha-Smooth muscle cell (α-SMC) actin and myosin heavy chain (SMC-MCH) expression in the healed ruptures (in adjacent sections). **A.** α-SMC -actin expression regresses in the shoulder and cap region of the more advanced plaques but not in the medial layer. **B.** Progression of atherosclerotic lesions was associated with a further reduction in intimal SMC-MHC positive cells the shoulder and cap regions. SMC-MHC positive cells in the medial layers decreased with advancing lesions and was confined to the medio-adventitial border in the more advanced lesions. (Overview shown at 40x; cap, shoulder and media regions at 100x).

Table II. The cause of death related to the histopathology of the 260 studied aortic samples.

	Cause of Death (N)						
	Severe head trauma	CVA/SAB*	Basilar artery thrombosis	Myocardial infarction	Cardiac arrest	Suicide	Other
Morphological descriptions							
Normal	5	0/2	-	-	-	-	2
Adaptive intimal thickening	22	6/10	-	-	1	1	11
Intimal xanthoma	12	6/4	1	-	-	-	11
Pathological intimal thickening	1	8/19	1	1	-	1	15
Early fibroatheroma	1	4/6	-	-	-	-	12
Late fibroatheroma	3	8/5	1	-	2	-	13
Thin cap fibroatheroma	1	7/9	-	-	1	2	15
Plaque rupture	1	0/2	-	-	1	-	8
Healing rupture	1	2/0	-	-	-	-	6
Fibrotic calcified plaque	1	4/2	-	-	2	-	11
Total:	**48**	**45/59**	**3**	**1**	**7**	**4**	**104**

REFERENCES

1 Farb A, Weber DK, Kolodgie FD, Burke AP, Virmani R. Morphological Predictors of Restenosis After Coronary Stenting in Humans. Circulation. 105:2974-2980.

2 Kolodgie FD, Narula J, Burke AP, Haider N, Farb A, Hui-Liang Y, Smialek J, Virmani R. Localization of Apoptotic Macrophages at the Site of Plaque Rupture in Sudden Coronary Death. American Journal of Pathology. 2000;157:1259-1268.

3 Virmani R, Kolodgie FD, Burke AP, Farb A, Schwartz SM. Lessons from sudden coronary death: a comprehensive morphological classification scheme for atherosclerotic lesions. Arteriosclerosis, Thrombosis, and Vascular Biology. 2000;20:1262-1275.

CHAPTER 3

Histological evaluation disqualifies IMT and calcification scores as surrogates for grading coronary and aortic atherosclerosis

A. Meershoek
R.A. van Dijk
S. Verhage
J.F. Hamming
A.J. van den Bogaerdt
A.J.J.C. Bogers
A.F. Schaapherder
J.H.N. Lindeman

International Journal of Cardiology 2016

ABSTRACT

Background: Carotid intimal media thickness (IMT) and coronary calcium scores (CCS) are thought to reflect atherosclerotic burden. The validity of this assumption for IMT is challenged by recent meta-analyses; for CCS by absence of a relationship between negative scores, and freedom of future events. As such, we considered evaluation of the relationship between tissue IMT and CCS, and extend of atherosclerotic disease relevant.

Methods: Analyses were performed on donor aortas obtained during renal graft procurement, and on coronary arteries collected during heart valve procurement for tissue donation. Movat pentachrome and Haematoxylin staining was performed, and the degree of atherosclerosis histologically graded. IMT and presence of calcium deposits were quantified on graded tissue sections.

Results: 304 aortas and 185 coronary arteries covering the full atherosclerotic spectrum were evaluated. Aortas and coronaries showed similar relationships between tissue IMT and degree of atherosclerosis, with gradual increase in tissue IMT during earlier phases of atherosclerosis ($r = 0.68$ and $r = 0.30$, $P < 0.00001$ for aorta and coronaries respectively), followed by plateauing of the curve in intermediate and advanced stages. Results for tissue IMT reveal high variability, resulting in wide confidence intervals. Results for CCS are similar for aorta and coronaries, with calcium depositions limited to advanced lesions.

Conclusion: Histological IMT measurements for the aorta and coronaries show large variations around the trend and plateauing of, and possibly reductions in IMT in late stage atherosclerotic disease. These observations for the aorta and coronaries may (partly) explain the limited benefit of including carotid IMT in risk prediction algorithms.

Abbreviations:
IMT (intimal media thickness), CCS (coronary calcium scores), AHA (American Heart Association), H&E (hematoxylin and eosin stain), AIT (Adaptive Intimal Thickening), IX (Intimal Xanthoma), PIT (Pathological Intimal Thickening), EFA (early fibroatheroma), LFA (late fibroatheroma), TCFA (thin cap fibroatheroma), PR (plaque rupture), HR (healed rupture), FCP (fibrous calcified plaque).

INTRODUCTION

Although the value of conventional cardiovascular risk factors for individual risk assessment has been firmly established, most cardiovascular events occur in patients not classified at increased risk by using current risk algorithms. As a consequence, there is a strong need for complementary individual risk prediction tools.

Carotid intimal media thickness (IMT) and coronary calcium scores (CCS) emerged as epidemiological measures of atherosclerotic burden[1,2]. Yet, these measures are also progressively advocated as individual risk prediction tools[3,4] and changes in carotid IMT are now used as surrogate endpoints in clinical trials aimed at stabilizing or reversing the atherosclerotic disease[5,6].

Paradoxically, a number of prominent meta-analyses fail to demonstrate an additional benefit of including carotid IMT in existing risk algorithms, thereby challenging the value of carotid IMT as an individual risk marker[6,7,8,9]. Studies on the validity of CCS as a personalized risk stratification tool point to a low predictive value of a negative CCS;[10] a limitation thought to reflect absence of an association between calcification and plaque characteristics[11].

In this context, it is important to note that manifestations of atherosclerotic disease (*i.e.* myocardial infarction and stroke) are caused by qualitative changes in the plaque structure (plaque rupture)[12,13], rather than by quantitative changes in plaque volume. In fact, it has long been established that the degree of stenosis poorly relates to future events[14,15]. As such the value of the quantitative imaging tool IMT and the presumably late qualitative marker CCS critically depend on their ability to flag the dynamic aspects of the atherosclerotic process[13,16].

Given the emerging limitations of carotid IMT and CCS for individual risk prediction, we considered a direct validation of an association between IMT and CCS, and qualitative aspects of atherosclerotic disease progression relevant. Such an evaluation is obviously not feasible in the clinical setting in which there is no access to the actual tissue. In order to test a putative association between the grade of atherosclerosis, and IMT and calcium scores we directly assessed IMT and CCS on arterial wall sections from two unique vascular tissue banks that cover the full spectrum of aortic and coronary atherosclerosis.

MATERIAL & METHODS

Patients and tissue sampling

Sample collection and handling was performed in accordance with the guidelines of the Medical and Ethical Committee of the Leiden University Medical Center, the

Netherlands, and the code of conduct of the Dutch Federation of Biomedical Scientific Societies. Due to national regulations, only for transplantation relevant data from donors was available for research (http://www.federa.org/codes-conduct).

This study includes data from 304 consecutive aorta samples from as many donors collected during kidney transplantation, and from 185 consecutive left coronary artery samples from as many donors collected during aortic valve harvesting for tissue donation. Due to the implied age restrictions maximum age of the aortic valve donors was 65 years. No formal age restrictions apply to kidney donations, as such this group also includes older patients.

Aortic patches (from the level of the renal artery) were obtained during kidney transplantation procedures. During the donation procedure the donor kidney including the renal artery is removed along with a large part of the adjoining aorta. Prior to transplantation the aorta is removed and the renal artery trimmed to the required length. The donor-derived aortic segments are not required for transplantation and used for further studies. Aneurysmal aortas (circumference > 2.5 cm, n = 2) were excluded from the study. All donors met the Eurotransplant criteria[17].

The left coronary artery segments were collected from healthy human hearts that were retrieved from Dutch postmortem donors within 24 h after circulation stop and brought to the Heart Valve Bank Rotterdam for heart valve donation. All donors gave permission for research, and met the criteria maintained by the Dutch Transplantation Foundation.

In the donation procedure the aortic valve is removed from the donated heart. During further aortic valve preparation the adjacent left coronary artery is trimmed according to standard procedures. Small segments of the left coronary artery were collected especially for this study, without hampering the pathological analysis of the heart necessary for release of the harvested valves.

Histological classification of lesions

All material was formaldehyde fixed and decalcified (Kristensen's solution). All aorta patches and coronary arteries were divided in consecutive 5mm segments, paraffin embedded, and 4µm sections were prepared from each segment. Sections were Movat pentachrome and H&E stained and classified according to the revised classification of the American Heart Association (AHA) as proposed by Virmani *et al*.[16,17] by two independent observers with no knowledge of the donor characteristics. Although all samples were decalcified in order to allow processing of the samples. Decalcification does not interfere with CCS scoring as footprints of earlier calcium deposits can easily be recognized in H&E staining (dark purple deposits) or Movat staining (brown and dark purple deposits) (Fig. 1). For each

individual the tissue section showing the most advanced degree of atherosclerosis was used as reference section for further studies, *viz.* each sample in the study is from a different individual.

A thin cap fibroatheroma (TCFA) was defined as a fibrous cap less than 155μm thick (aorta)[17] or less than 65μm thick (coronary)[18]. Note that multiple lesions and lesion types may be present in a single section. Because of the low number of TCFAs, Plaque Ruptures (PR) and Healed Ruptures (HR) in the coronaries, we also included readings from these stages from sections in which more advanced stages were also present.

Morphological and histological analysis

Morphometric and histological analysis were performed on Movat pentachrome stained sections with Image J calibrated software (http://imagej.nih.gov/ij/) 17. Tissue IMT was measured perpendicular to the lumen on 4 locations in the area showing the maximum IMT. A positive CCS (H&E staining) was defined by presence of a calcified area of minimal 200μm. This lower cut-off value was chosen as it reflects the resolution of high-end CT scanning.

Statistical analysis

Statistical analysis was performed using SPSS 20 (IBM, Amsterdam, the Netherlands). Data in figures is presented as medians with IQR. Spearman's rho test was used to demonstrate the relation between IMT and the atherosclerotic stage. To that end the lesion type was reclassified in a numeric score (normal = 0…, FCP = 9). ANOVA and Kruskal-Wallis followed by post-hoc analysis (LSD and Mann-Whitney respectively) were used to test potential differences in respectively IMT and Calcium Scores, and the individual stages of atherosclerosis. ANOVA and co-variance analysis was performed to test the influence of age and sex on the IMT readings. P values < 0.05 were considered significant.

RESULTS

Studied population

Details on the study populations are provided in Table 1 (donor characteristics of the kidney donor (aortic patch)) and Table 2 (aortic valve donor (left coronary artery)).

Classification of atherosclerotic disease

Representative images illustrating the atherosclerosis grading system are shown in Fig. 1. The distribution of most advanced lesion types, and the relationships with

donor age and sex are shown in Fig. 2 (aorta) and Fig. 3 (coronary artery). Clear differences were found between aortic and coronary segments with respect to the distribution pattern of the dominant lesion type (Fig. 2, Fig. 3), with regard to a low prevalence of so-called (pre)vulnerable lesions (*viz.* Late Fibro Atheroma, TCFA and PRs) and a high prevalence of so called stabilized lesions (*i.e.* Fibrous Calcified Plaque, FCP) in the coronary artery group.

Table 1. Donor characteristics (aorta, mean (sd)).

	Male N = 156	Female N = 145
Age	45.2 (17.5)	44.6 (15.7)
BMI (kg/m2)	24.8 (3.6)	23.5 (4.4)
Cause of death (n)		
Cerebrovascular accident	34	29
Subarachnoid hemorrhage	32	56
Head trauma	47	21
Cardiac arrest	7	4
Myocardial infarction	1	0
Suffocation	5	3
Pulmonary embolism	0	1
Other/not specified	30	31
Antihypertensive use (n)	20	18
Statin use (n)	6	1

Table 2. Donor characteristics (left coronary artery, mean (sd)).

	Male N = 99	Female N = 87
Age	48.8 (12.4)	53.4 (9.6)
BMI (kg/m2)	25.9 (3.3)	25.5 (4.3)
Cause of death (n)		
Cerebrovascular accident	18	11
Subarachnoid hemorrhage	8	22
Head trauma	16	11
Cardiac arrest	12	4
Myocardial infarction	27	19
Suffocation	7	9
Pulmonary embolism	4	5
Other/not specified	9	6
Antihypertensive use (n)	29	40
Statin use (n)	19	15

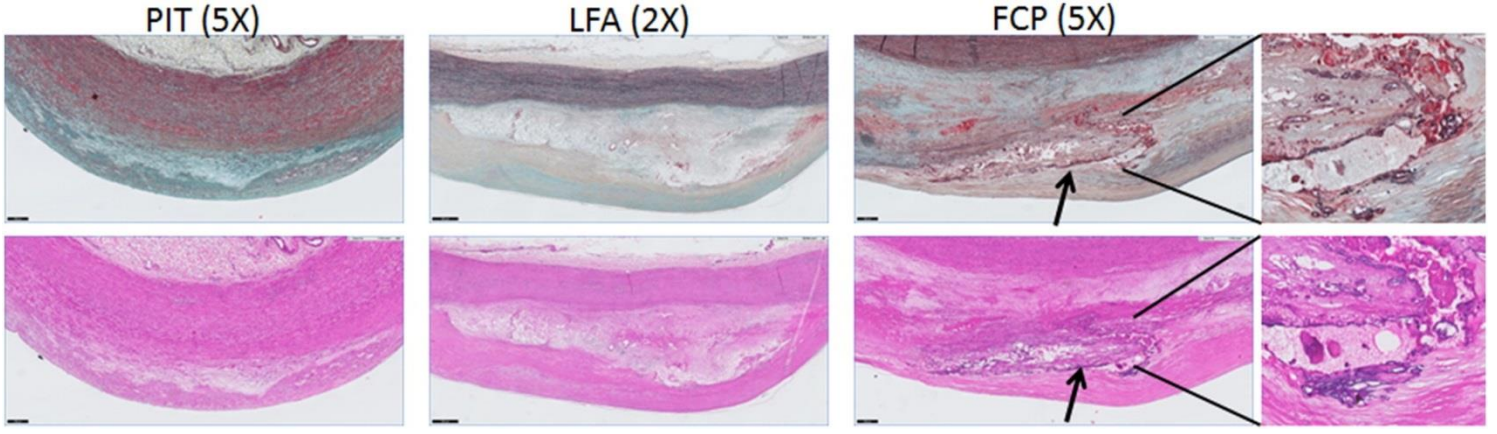

Figure. 1. Movat Pentachrome (top) and Hematoxylin Eosin (H&E) staining (bottom) of atherosclerotic lesions in different aortic lesions. Representative images illustrating aspects of the Virmani classification system for atherosclerosis. Pathological Intimal Thickening (PIT) is characterized by presence of a an acellular lipid pool in the outer intima. Late Fibroatheroma (LFA) presents with a large necrotic containing multiple cholesterol crystals and that is covered by a fibrous cap.A FibrousCalcified Plaque (FCP) represent represents a fibrotic lesion with a single, condensed calcified area [16].Decalcification does not interfere with CCS scoring as footprints of earlier calcium deposits can easily be recognized in H&E staining (dark purple deposits) or Movat staining (brown and dark purple deposits in the detail (20-fold, right)).

Table 3A. P-values for a comparing of aortic IMT between the different stages (LSD post-hoc test).

	Normal	AIT	IX	PIT	EFA	LFA	TCFA	RP	HR
AIT	0,051462								
IX	0,013681	0,450608							
PIT	7,43E−06	9E−05	0,000966						
EFA	2,18E−09	1,74E−09	2,71E−08	0,004753					
LFA	2,9E−12	3,98E−13	6,24E−12	6,59E−06	0,0658				
TCFA	2,51E−15	2,65E−17	4,17E−16	2,64E−09	0,000907	0,14849			
RP	5,48E−15	1,96E−16	2,91E−15	6,81E−09	0,000975	0,132691	0,912142		
HR	1,49E−15	3,2E−17	4,76E−16	1,55E−09	0,000403	0,082835	0,735055	0,825458	
FCP	3,63E−12	1,5E−12	2,06E−11	6,9E−06	0,042112	0,767626	0,281548	0,251151	0,171564

Table 3B. P-values for a comparing of coronary IMT between the different stages (LSD post-hoc test).

	Normal	AIT	IX	PIT	EFA	LFA	TCFA/RP	HR
AIT	0,529884							
IX	0,34549	0,622489						
PIT	0,030391	0,016838	0,11385					
EFA	0,010435	0,004541	0,034858	0,39813				
LFA	1,68E−06	4,6E−09	6,15E−07	1,33E−05	0,001224			
TCFA/RP	0,00019	4,36E−05	0,000438	0,006783	0,048938	0,524844		
HR	8,67E−06	1,53E−08	3,24E−06	7,48E−05	0,007026	0,392468	0,998496	
FCP	1,75E−06	1,25E−11	8,33E−08	5,52E−07	0,001492	0,302046	0,979117	0,969555

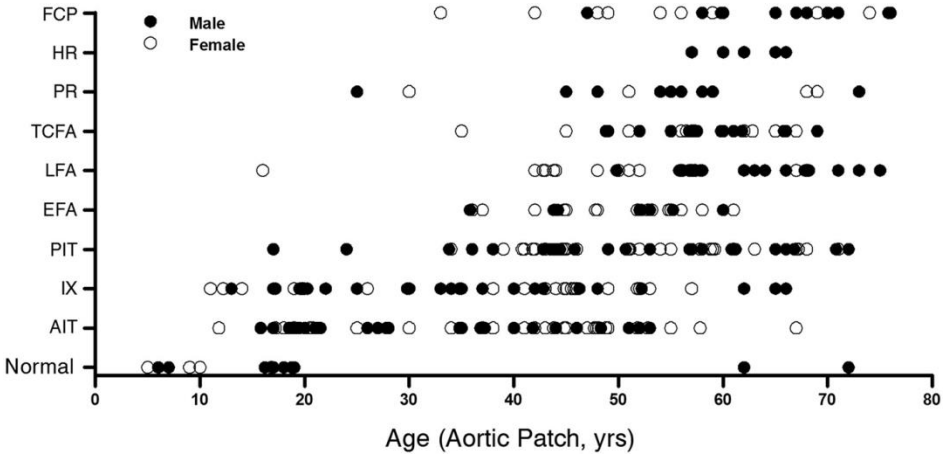

Figure 2. Histological classification of human aortic atherosclerotic lesion type, and the re-lationship to age and sex. Three hundred and four aortic patches were characterized for the type of atherosclerosis according to Virmani *et al*. 16 and classified on basis of the highest degree of atherosclerosis present. The graph shows the highest grade of aortic athero-sclerosis in relation to the age of the donor. There is a significant correlation of lesion type with age (r = 0.640, P = 0.01). Abbreviations; AIT: Adaptive Intimal Thickening, IX: Intimal Xanthoma, PIT: Pathological Intimal Thickening, EFA: Early Fibroatheroma, LFA: Late Fibro-atheroma, TCFA: Thin Cap Fibroatheroma, PR: Plaque Rupture, HR: Healing Rupture, FCP: Fibrotic Calcified Plaque.

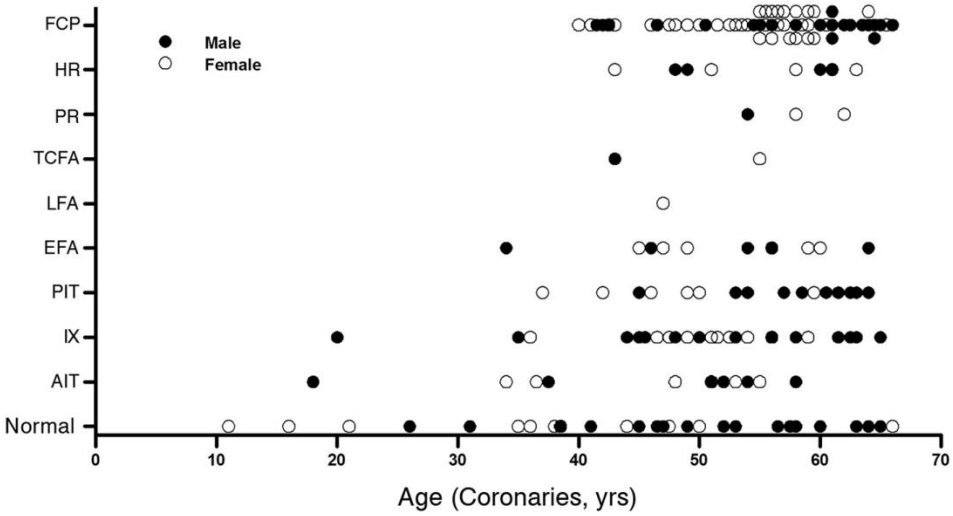

Figure 3. Histological classification of human coronary artery atherosclerotic lesion type and the relationship to age and sex. One hundred eighty five coronary samples were characterized for the type of atherosclerosis according to Virmani *et al*. 16 and classified on basis of the highest degree of atherosclerosis present. The graph shows the highest grade of aortic atherosclerosis in relation to the age of the donor. There is a significant correlation of lesion type with age (r = 0.30, P = 0.00005). Abbreviations are defined in the legend of Fig. 1.

Distribution of tissue IMT and stages of atherosclerosis

Fig. 4 shows the relationship between tissue IMT and the aortic lesion type. A positive relationship is found during lesion initiation and early progression ($r=0.68$, $P<0.00001$), but the curve plateaus in the advanced, vulnerable lesions (TCFA, PR and HR) and the stabilized lesions (HR and FCP). Results for the coronary artery segments (Fig. 5) follow those of the aorta and show an increase in tissue IMT in the early phases ($r=0.30$, $p<0.00005$) of the disease, plateauing of tissue IMT in the advanced and stabilized lesions. Along these lines clear differences were found between the individual stages of atherosclerosis (ANOVA: Aorta: $P<2.1\ 10^{-37}$; Coronary: $P<2.9\ 10^{-16}$, differences between the individual stages are shown in Tables 3A and 3B). The variation around the trend is high, thus resulting in wide confidence intervals (confidence intervals are indicated in Fig. 4, Fig. 5).

Distribution of calcium scores

Calcium deposits are absent in normal arteries and the early phases of atherosclerotic disease. Relevant calcium deposits start to appear in a minority of the LFAs and the prevalence rapidly increases thereafter (Kruskal-Wallis: Aorta: $P<6.5\ 10^{-29}$; Coronary: $P<2.5\ 10^{-16}$), and relevant calcification deposits are found in 75% ($P<0.002$) and 96% ($P<0.00006$) of the aortic and coronary FCPs respectively. Although calcified plaques are often considered stabilized lesions, we observed signs of instability such as penetrating calcified lesions (*i.e.* eroded calcified lesions (Fig. 6A) or newly forming lesions over old calcified lesions, Fig. 6B)

Ageing and IMT

Age is a co-variant of the atherosclerotic disease and has been brought forward as a potential confounder of IMT. We used to two different strategies to test the effect of age on tissue IMT in the aortic samples. In the first approach we sought for an association between tissue IMT and age in adult patients (with non-pathological intimal thickening (*i.e.* normal, adaptive intimal thickening and intima xanthoma) through simple regression analysis. The analysis showed a moderate correlation between age and tissue IMT ($r=0.335$; adjusted $r2=0.083$) and borderline significance in the ANOVA ($P=0.057$). The second analysis was based on co-variant analysis on the full cohort. This approach showed that correction for age and sex minimally influences the estimates (Table 4).

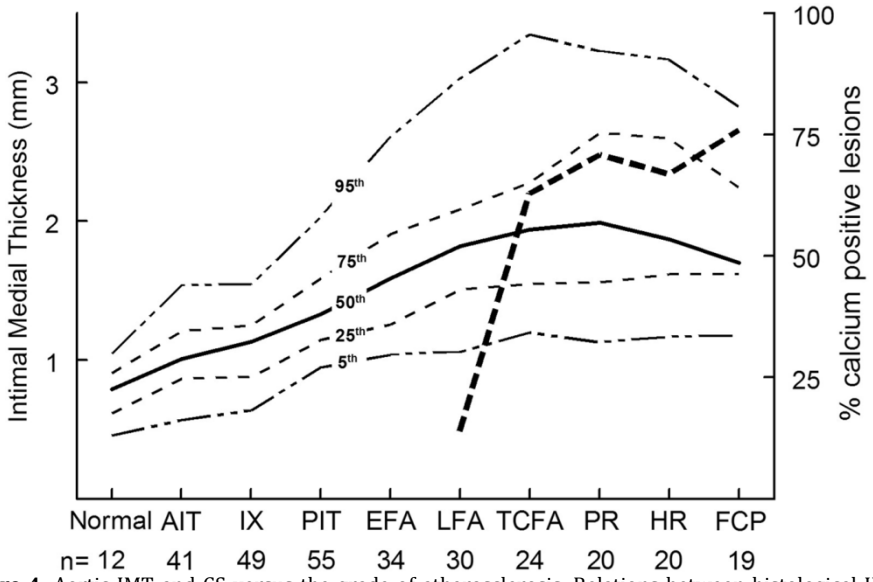

Figure 4. Aortic IMT and CS versus the grade of atherosclerosis. Relations between histological IMT (the thick line represents the median IMT, dispersion around the median is shown by the 5th, 25th, 75th and 95th percentile lines). Presence of detectable (defined by presence of at least one or more calcium aggregates >200 μm) is indicated by the robust dashed line; and the dominant aortic atherosclerotic lesion type). Abbreviations are defined in the legend of Fig. 2.

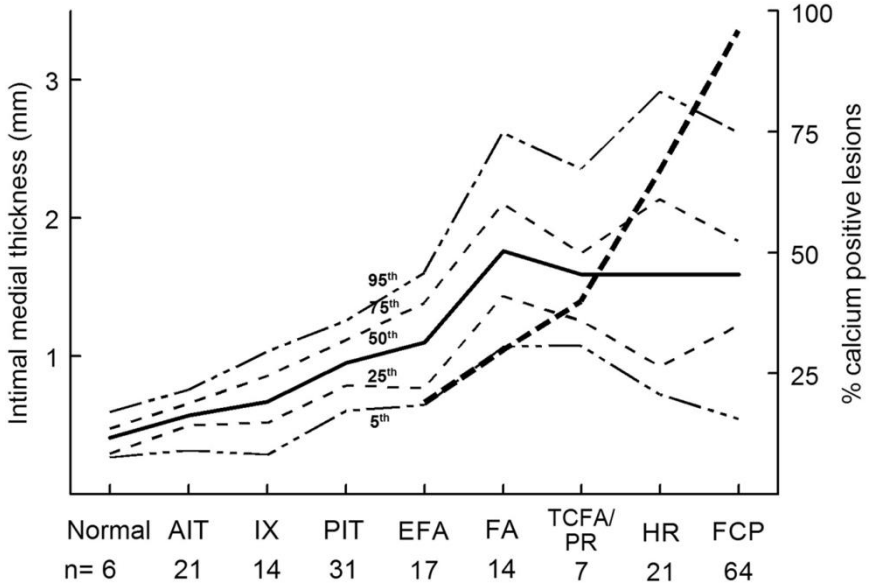

Figure 5. Coronary IMT and CS versus the grade of atherosclerosis. Relations between histological IMT (the thick line represents the median IMT, dispersion around the median is shown by the 5th, 25th, 75th and 95th percentile lines). Presence of detectable (defined by presence of at least one or more calcium aggregates >200 μm in the lesion; indicated by the robust dashed line), and the dominant atherosclerotic lesion type. Abbreviations are defined in the legend of Fig. 2.

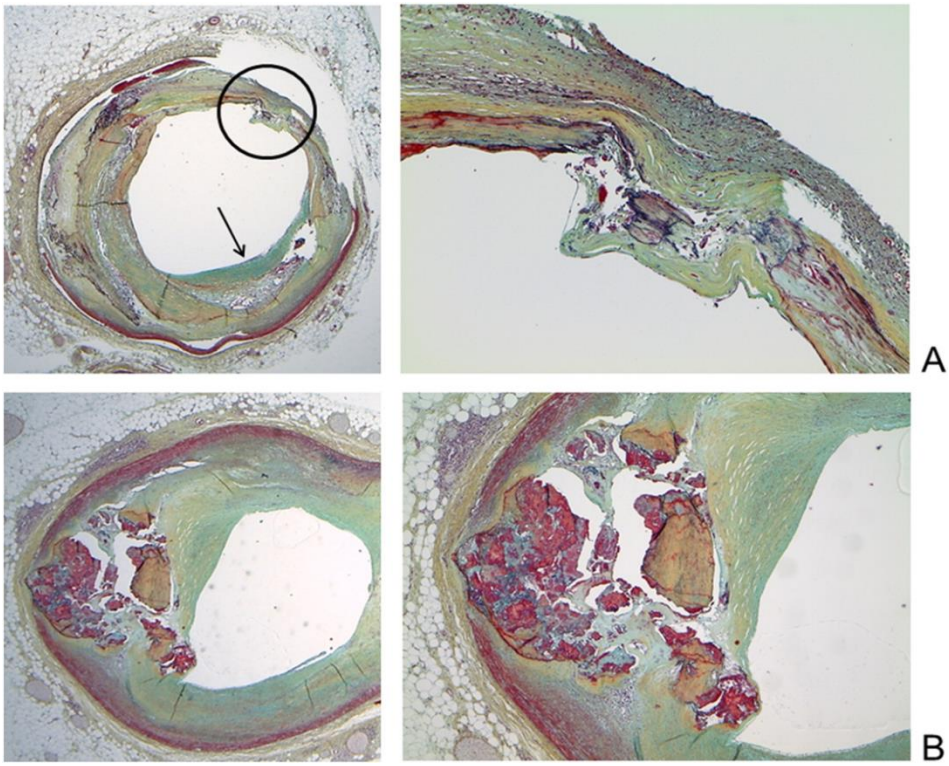

Figure 6. Instable lesions in calcified coronaries. **A:** Movat pentachrome staining showing a ruptured fibrous cap overlying a small calcified nodule (circle). Note presence of multiple lesions in this single cross section and the formation of a new lesion (neo atherosclerosis, greenish proteoglycan/collagen rich area, arrow) (12.5 fold (overview), and 100 times magnification (detail). The defect in the upper right corner reflects a cutting artifact. **B:** Movat Pentachrome staining showing a penetrating calcium nodule. Note the complete loss of media in the underlying area and an extremely thin, a-cellular overlying cap (12.5 fold (overview), and 40-fold magnification (detail)). **Note:** color legend for the Movat staining: blue: proteoglycans, yellow: collagen, black: elastin, red: smooth muscle cells and fibrinogen, purple: nuclei. Green reflects co-localization of proteoglycans and collagen.

Table 4. Plain regression coefficients and corrected (age and sex) regression coefficients in adult donors (age N 20 years) for the association between IMT and the stage of atherosclerosis.

	Uncorrected	Corrected
AIT	0.27 (0.14)	0.24 (0.14)
IX	0.33 (0.13)	0.31 (0.14)
PIT	0.61 (0.13)	0.55 (0.15)
EFA	0.87 (0.14)	0.81 (0.16)
LFA	1.07 (0.15)	1.02 (0.17)
TCFA	1.25 (0.15)	1.22 (0.17)
RP	1.26 (0.15)	1.22 (0.17)
HR	1.29 (0.15)	1.26 (0.18)
FCP	1.11 (0.15)	1.01 (0.18)

DISCUSSION AND CONCLUSIONS

This study evaluates putative associations between IMT and calcium scores, and atherosclerotic disease progression (histological plaque characteristics defined on the modified AHA classification) in vessel material obtained during organ/tissue donation, *viz.* material from the donor. Results confirm an association between tissue IMT and plaque progression, but also show plateauing and even reductions in tissue IMT readings in the advanced stages of the disease. Findings also show a large variability in tissue IMT, thereby resulting in wide confidence intervals around the trend. Results for the CCS confirm data from Mauriello *et al*.[11] and characterize CCS as a marker of advanced and end-stage atherosclerotic disease.

Carotid IMT is now widely accepted as a screening tool to detect atherosclerosis in the early and asymptomatic stages of the disease. Indeed IMT has been adopted by the AHA as a surrogate marker for coronary artery disease[1]. In addition to its use as a screening tool, carotid IMT evolved as a surrogate endpoint in trials monitoring the effectiveness of pharmaceutical interventions aimed at reducing atherosclerotic progression and cardiovascular risk[5,6]. Notwithstanding the broad recognition of carotid IMT as a complementary risk prediction tool, large epidemiological evaluations shed doubt on the validity of carotid IMT as an individual risk prediction tool[7,8,9]. In fact these recent evaluations only indicate a modest or fail to show a benefit of including IMT in risk prediction algorithms. In fact, a large meta-analysis concluded that "The addition of common CIMT (carotid IMT) measurements to the Framingham Risk Score was associated with small improvement in 10-year risk prediction of first-time myocardial infarction or stroke, but this improvement is unlikely to be of clinical importance"[8]. Along similar lines a 2012 AHA position statement denounced the use of CCS and carotid IMT for screening the asymptomatic adult population for CHD[10]. These observations are remarkable and imply that the added value of IMT is less than commonly thought and that individualized use of IMT is challenged.

A possible explanation for the limited additional benefit of including IMT in established risk algorithms is the fact that IMT is a pure quantitative measure, and therefore may not necessarily reflect the atherosclerotic disease process. Moreover, it has been pointed out that increases in IMT are a consequence of the aging process, and thus that increased IMT could simply reflect physiologic, ageing-related thickening of the intimal-medial layers[19]. On the other end of the spectrum, it is well established that the degree of luminal stenosis caused by plaque growth poorly predicts future cardiovascular events[14,15]. In this context it is important to note that atherosclerosis is a multi-stage disease process that evolves through successive stages of intimal lipid accumulation, plaque formation and progression, followed by plaque destabilization and plaque rupture, and finally

plaque stabilization[12,13]. It is now assumed that plaque destabilization is the pivotal factor in the development of insidious manifestations of the disease.

At this point it is unclear how and to what extent IMT readings translate to the process of plaque evolution, destabilization and subsequent stabilization. In order to assess such a relationship, we considered a systematic evaluation of a possible relationship between IMT and plaque characteristics relevant. To that end we performed a systematic evaluation of a putative association between intimal media thickness directly measured on tissue slides (tissue IMT) and histological grading in two large biobanks of human vascular tissue.

In the ideal world situation such a study would be performed on carotid tissue. Yet, available biobanks of carotid tissue are all based on surgical specimens of carotid endarteriectomies; hence representing end-stage atherosclerotic disease and, depending on the depth of the -tomy missing segments of the medial layer. In order to be able to cover the full atherosclerotic spectrum, and the obvious need for an intact media (hence full thickness samples) we decided for a study on material collected during transplantation procedures (*i.e.* intact arterial tissue).

The first series of studies was performed on donor material from a biobank of aortic segments[17]. These donor aortic segments come with the kidney graft and are (partially) removed during transplantation. The peri-renal aorta constitutes a predilection place for atherosclerotic disease; although its large local diameter generally precludes clinical manifestations[17]. An obvious question is whether these observations from an elastic artery such as the aorta are also valid for other arterial beds. We therefore validated the findings for the aorta on material from a second biobank based on donor coronary arteries that were collected during aortic valve procurement for tissue donation. Although this material is from an obviously more relevant arterial bed, material in this bank is more circumscribed due to stricter age restrictions (maximum age for aortic valve donation is 65), and the fact that hearts from younger/healthier donors are more likely to be allocated for whole organ donation. Hence, it's likely that material in this biobank is less representative to the general population than the material in the aorta-based biobank.

We classified all donor material in our study according to the modified AHA classification as proposed by Virmani *et al.*[16]. This classification is thought to better differentiate between the more advanced stages of the atherosclerotic process, and unlike the AHA classification it has a continuous (progressive) association between disease progression and score. Classification was performed on basis of the Movat staining as this staining allows for clear differentiation between the different advanced lesions (in particular late fibroatheroma and fibrous calcified lesion).

A systematic evaluation in the aortic tissue bank shows that atherosclerotic disease is very common among those over 40years of age, and that unstable

plaques and healed plaques (FCP) are present in 7% of the donors. Results for the coronary artery segments roughly followed those for the aorta, although the very limited availability of material from donors under the age of 30 interferes with firm conclusions on a possible age relationship. A remarkable observation is the very low prevalence of classical lesions (early and late fibroatheroma) and instable lesions, and the high prevalence of fibrous calcified lesions in coronary arteries (32% of the specimens were classified as a FCP). Although lack of longitudinal data interferes with firm conclusions, these observations may indicate that plaque destabilizing in the coronary arteries is a relative rapid process and that asymptomatic plaque rupture and subsequent healing, as reflected by the high prevalence of FCPs, is a very common phenomenon, even in individuals as young as 40–50years.

IMT measurements performed on the tissue slices confirm a positive relationship between tissue IMT and the histologic classification of atherosclerosis. Yet, the data also show flattening, and possibly even a decline in tissue IMT in the vulnerable and particularly stabilized lesions. This phenomenon challenges the use of sequential IMT measurements as surrogate end-point in interventional studies as disease regression or progression may occur in the absence of changes in IMT, or alternatively that reductions in IMT can reflect regression or progression. Such a conclusion is supported by clinical evidence failing to characterize IMT as a dynamic marker[20].

The number of tissue samples in our study also allowed for the establishment of confidence intervals, which indicate a marked variation in tissue IMT around the trend. These wide confidence intervals profoundly interfere with the interpretation of individual measurements, thus challenging the use of IMT for personalized care and (partly) explaining the limited value of including IMT in risk algorithms.

Results for histological assessment of CCS herein follow the conclusions of Mauriello *et al.*[11] and show that calcium deposits reflect the later stages of the disease, and are particularly prominent in the so called stabilized lesions. This observation supports the notion that calcium deposits are associated with end stage, stabilized lesions. Yet, we found indications that penetrating ulcers can develop in the fibrous cap overlying a calcium nodule (Fig. 5). Moreover, new lesions can develop on top of extinguished lesions, resulting in a repetitive process of plaque healing, followed by formation and destabilization of a new plaque over the existing pacified lesion (Fig. 5). Formed buried lesions show that calcium deposits persist for extended periods of time, and hence that calcium scores largely reflect the past.

All in all, results for calcium deposits suggest that CCS should be considered a retrospective marker, identifying patients with manifest atherosclerotic disease, whereas a negative calcium score does not rule out presence of atherosclerotic disease. The apparent persistence of calcium implies a very low clearance rate, hence disqualifying calcium scores as a dynamic marker.

Limitations

For practical reasons outlined above we were unable to evaluate a relation between carotid IMT and qualitative measures of carotid atherosclerosis. Yet, given the established relation between carotid IMT and coronary readings we consider our findings from the aorta and coronary arteries relevant for the carotid bed[1]. A second limitation is that measurements are performed on paraffin embedded tissue sections. As such, we were able to use clear anatomical land marks for the tissue IMT. It is unknown how these actual landmarks translated to the contrast-based defined landmarks used in B-mode ultrasound[21]. Another point is that the process of tissue preparation for histology involves tissue shrinkage due to intrinsic tissue contractility as well as due to the dehydration process required for paraffin embedding[22]. As such measures in the study are relative, and do not translate one to one with the real-life situation. Moreover, we cannot exclude that shrinkage may be less in more fibrotic tissues such as the FCP lesion type. As such our data may underestimate the apparent decline in IMT during plaque stabilization. Finally, we observed a low number of vulnerable lesions in our set of coronary arteries; hence conclusions for this stage should be interpreted with caution.

In conclusion, this histological evaluation shows a weak association between histological IMT and the atherosclerotic process. Extremely wide confidence intervals interfere with the interpretation of individual data, whereas flattening or possible even declining IMT values may severely compromise interpretation of sequential IMT in the context of intervention studies. Consequently, on basis of our observations for the aorta and coronaries IMT cannot be recommended as a qualitative measure of atherosclerosis. Findings for the calcium deposits show that calcium deposition occurs late in the process and the calcium deposits are stable. As such, CCS do not qualify as a dynamic marker and largely reflect the past. Consequently, positive CCS identify those patients with manifest advanced atherosclerotic disease.

REFERENCES

1 Greenland P, Alpert JS, Beller GA, *et al*. American College of Cardiology Foundation; American Heart Association. 2010 ACCF/AHA guideline for assessment of cardiovascular risk in asymptomatic adults: a report of the American College of Cardiology Foundation/American Heart Association Task Force on Practice Guidelines. Journal of American College of Cardiology. 2010; 56 :e50-103.

2 Greenland P, Bonow RO, Brundage BH, *et al*. American College of Cardiology Foundation Clinical Expert Consensus Task Force (ACCF/AHA Writing Committee to Update the 2000 Expert Consensus Document on Electron Beam Computed Tomography); Society of Atherosclerosis Imaging and Prevention; Society of Cardiovascular Computed Tomography. ACCF/AHA 2007 clinical expert consensus document on coronary artery calcium scoring by computed tomography in global cardiovascular risk assessment and in evaluation of patients with chest pain: a report of the American College of Cardiology Foundation Clinical Expert Consensus Task Force (ACCF/AHA Writing Committee to Update the 2000 Expert Consensus Document on Electron Beam Computed Tomography) developed in collaboration with the Society of Atherosclerosis Imaging and Prevention and the Society of Cardiovascular Computed Tomography. Journal of American College of Cardiology. 2007; 49: 378-402.

3 http://yourimt.com/diseaseinfo/carotidimtscanning.html (July 5, 2016)

4 http://www.theheartinstituteny.com/calcium-scoring/ (July 5, 2016)

5 Kastelein JJ, Akdim F, Stroes ES, *et al*. Simvastatin with or without ezetimibe in familal hypercholesterolemia. New England Journal of Medicine. 2008; 358: 1431-1443.

6 Costanzo P, Cleland JG, Atkin SL, Vassallo E, Perrone-Filardi P. Use of Carotid Intima-Media Thickness Regression to Guide Therapy and Management of Cardiac Risks. Current Treatment Options in Cardiovascular Medicine. 2012; 14: 50-56.

7 Polak JF, Pencine MJ, Pencina KM, O'Donnell CJ, Wolf PA, D'Agostino RB Sr. Carotid-Wall Intima-Media Thickness and Cardiovascular Events. New England Journal of Medicine. 2011; 365: 213-221

8 Den Ruijter HM, Peters SA, Anderson TJ, *et al*. Common Carotid Intima-Media Thickness Measurements in Cardiovascular Risk Prediction, A Meta-analysis. JAMA 2012; 308: 796-803

9 Robertson CM, Gerry F, Fowkes R, Price JF. Carotid intima-media thickness and the prediction of vascular events. Vascular medicine. 2012; 17: 239-48

10 www.heart.org/idc/groups/heart-Public/@wcm/@adv/documents/downloadable/ucm_437479.pdf (July 5, 2016)

11 Mauriello A, Servadei F, Zoccai GB, *et al*. Coronary calcification identifies the vulnerable patient rather than the vulnerable Plaque. Atherosclerosis. 2013; 229: 124-129

12 Bentzon JF, Otsuka F, Virmani R, Falk E. Mechanisms of plaque formation and rupture. Circulation research. 2014; 114: 1852-1866.

13 Libby P. Mechanisms of Acute Coronary Syndromes and Their Implications for Therapy. New England Journal of Medicine. 2013; 368: 2004-2013.

14 Little WC, Constantinescu M, Applegate RJ, *et al*. Can coronary angiography predict the site of a subsequent myocardial infarction in patients with mild-to-moderate coronary artery disease? Circulation. 1988; 78: 1157-1166.

15 Minana G, Nunez J, Sanchis J. Coronary Angiography, Too Far to be a Gold Standard Technique for Identifying a Vulnerable Plaque. Journal of Clinical & Experimental Cardiology. 2011; 2: 1000132

16 Virmani R, Kolodgie FD, Burke AP, Farb A, Schwartz SM. Lessons from sudden coronary death: a comprehensive morphological classification scheme for atherosclerotic lesions. Arteriosclerosis, thrombosis, and vascular biology. 2000; 20: 1262-75.

17 van Dijk RA, Virmani R, von der Thüsen JH, Schaapherder AF, Lindeman JH. The natural history of aortic atherosclerosis: a systematic histopathological evaluation of the peri-renal region. Atherosclerosis. 2010; 210: 100-106.

18 Virmani R, Burke AP, Kolodgie FD, Farb A. Pathology of the thin-cap fibroatheroma: a type of vulnerable plaque. Journal of Interventional Cardiology. 2003; 16: 267-272.

19 Finn AV, Kolodgie FD, Virmani R. Correlation between carotid intimal/medial thickness and atherosclerosis, a point of view from pathology. Arteriosclerosis, thrombosis, and vascular biology. 2010; 30: 177-181.

20 Zanchetti A, Hennig M, Hollweck R, *et al*. Baseline values but not treatment-induced changes in carotid intima-media thickness predict incident cardiovascular events in treated hypertensive patients: findings in the European Lacidipine Study on Atherosclerosis (ELSA). Circulation. 2009; 120: 1084-1090.

21 Salonen JT, Salonen R. Ultrasound B-mode imaging in observational studies of atherosclerotic progression. Circulation. 1993; 87: 56-65.

22 Kerns MJ, Darst MA, Olsen TG, Fenster M, Hall P, Grevey S. Shrinkage of cutaneous specimens: formalin or other factors involved? Journal of cutaneous pathology. 2008; 35: 1093-1096.

CHAPTER 4

A universal lesion classification for human and murine atherosclerosis

R.A. van Dijk
R. Kleemann
A.F. Schaapherder
J.F. Hamming
J.H.N. Lindeman

In preparation to be submitted.

ABSTRACT

Background: Qualitative characterization of the atherosclerotic process fully relies on histological evaluation and grading of plaque characteristics. An extensive morphological classification scheme exists for human coronary artery atherosclerosis and has been validated for the human aorta. However, it is unclear to what extent this classification scheme can be used to grade human aortic lesions and experimental lesions in murine models of atherosclerotic disease.

Methods: Human coronary artery and human aorta sections were collected from large tissue banks. They were analysed together with histologic sections of the aortic root from mice in accordance with the modified American Heart Association classification as recently proposed by Virmani *et al*. (Nature Reviews Cardiology; 2015).

Results: The overall histological features of (non-)progressive, vulnerable and stabilizing aortic atherosclerotic lesions in mice are remarkably similar to human coronary atherosclerosis. The early stages of atherosclerosis in mice are comparable to adaptive intimal thickening, intimal xanthoma, pathological intimal thickening, and early fibroatheroma. Importantly, the most advanced lesions in mice do not progress to the equivalent of a late fibroatheroma in humans. Therefore mice do not develop the vulnerable lesion phenotype.

Conclusion: The initial and more advanced atherosclerotic lesions in mice follow a more or less similar pattern of progression compared to coronary and aortic atherosclerosis in humans and can be classified accordingly using a uniform, detailed morphological classification scheme based on the Virmani classification. However, vulnerable lesions do not develop in mice, and therefore analysis of plaque stability in mice carries a considerable risk of over interpretation.

INTRODUCTION

Atherosclerosis is a complex pathology of the large and medium-sized arteries[1,2]. It is well accepted that progression of atherosclerosis and its clinical consequences is related to qualitative changes in plaque characteristics. Indeed, the common insidious manifestations of the disease are thought to essentially reflect abrupt plaque destabilization and rupture rather than gradual obstruction due to quantitative changes in plaque volume[3]. It is now conceived that atherosclerotic disease reflects a long-term process that proceeds through well-defined sequential, morphologically distinct stages, up to the point of plaque destabilization and rupture. Plaque rupture is then followed by thrombus formation, a healing process and consolidation (*i.e.* fibrosis). At this point qualitative grading of atherosclerotic lesions fully relies on histological evaluation and classification based on plaque characteristics.

A first consensus classification scheme for grading human atherosclerosis has been introduced by the American Heart Association (AHA) working group[4,5,6,7]. However, this classification fails to capture all clinical aspects of coronary thrombus formation and was therefore refined by Virmani and co-workers[8]. Based on their observations from autopsy material, they extended the AHA classification in order to better reflect the heterogeneity of the advanced stages of atherosclerotic disease. It describes the critical phases of plaque destabilization, rupture and subsequent healing in more detail. Furthermore, this classification better reflects the sequence of events of the disease process.

The insight in the molecular aspects of the atherosclerotic process is mainly based on extrapolation of observations from murine models, but there is no one-to-one morphological comparison of human with murine disease[9,10,11]. It is unclear whether and how the refined human classification system by Virmani can be employed for murine lesions especially regarding the interpretation of lesion vulnerability and stability. Moreover, there is currently no uniform classification system for murine atherosclerosis. As a consequence, comparison of observations from different disease models with different diets and interventions is challenging, and extrapolation and translation of murine findings to the human situation is almost impossible.

We therefore considered a morphological comparison of human to murine atherosclerosis, and an evaluation of the Virmani classification scheme as a universal grading system for atherosclerotic disease relevant. Results of this evaluation show that this classification scheme can be applied to mouse studies, but confirm the notion that murine lesions fail to develop atherosclerotic features unique to the human vulnerable lesions that give rise to clinical symptoms.

MATERIAL AND METHODS

Human aortic tissue sampling

Tissue sections were selected from a large tissue bank containing over 500 individual abdominal aortic wall patches (AAWPs) that were obtained during liver, kidney or pancreas transplantation (*viz.* all material was from cadaveric donors). Details of this bank have been described previously by van Dijk *et al*[9]. All patches were harvested from grafts that were eligible for transplantation (*i.e.* all donors met the criteria set by The Eurotransplant Foundation) and due to national regulations, only transplantation relevant data for donation is available. Sample collection and handling was performed in accordance with the guidelines of the Medical and Ethical Committee in Leiden, Netherlands and the code of conduct of the Dutch Federation of Biomedical Scientific Societies (https://www.federa.org/sites/default/files/digital_version_first_part_code_of_conduct_in_uk_2011_12092012.pdf).

Human coronary tissue sampling

Tissue sections were selected from a large tissue bank containing over 700 individual coronary artery segments (CAS) of the left coronary artery obtained from human hearts. CAS were retrieved from Dutch post-mortem donors within 24 hours after circulatory arrest and brought to the Heart Valve Bank Rotterdam for valve donation. All donors gave permission for research, and met the criteria maintained by the Dutch Transplantation Foundation. In the donation procedure the aortic valve is removed from the donated heart. During further aortic valve preparation the adjacent tissue including the left coronary artery is trimmed according to standard procedures. The removed coronary artery segments are used in this study. This procedure does not interfere with the pathological analysis of the heart necessary for release of the harvested valves.

Characterization of the lesions and histological definitions (Table 1)

Histologic sections of AAWPs and CASs were stained by haematoxylin and eosin (H&E), and Movat pentachrome for classification of the lesions in accordance with the modified AHA classification as proposed by Virmani *et al*[8]. Classification was performed by two independent observers with no knowledge of the patient characteristics of the aortic or coronary tissue. A detailed description of plaque characterization, morphological analysis for AAWPs is provided in reference 9 and for CASs in reference 8. Plaque morphologies included adaptive intimal thickening (AIT), intimal xanthoma (IX), pathological intimal thickening (PIT), early (EFA) and late fibroatheroma (LFA), thin cap fibroatheroma (TCFA), acute plaque rupture (PR), healed rupture (HR) and fibrotic calcific plaque (FCP).

Table I. Morphological classification of aortic and coronary tissue according to the modified AHA classification proposed by Virmani *et al* [8].

Subtype of Lesion	Abbr.	Morphological description	Mouse equivalent morphological description
Normal	N	No signs of intimal thickening and intimal inflammation	No signs of intimal thickening and intimal inflammation
Non-progressive intimal lesions			
Adaptive intimal thickening	AIT	Natural accumulation of SMCs in the absence of lipid and macrophage foam cells	Accumulation of SMCs in the absence of lipid and macrophage foam cells
Intimal xanthoma	IX	Superficial accumulation of foam cells without a necrotic core or fibrous cap	Up to several layers of foam cells without a necrotic core or fibrous cap
Progressive atherosclerotic lesions			
Pathological intimal thickening	PIT	Plaque rich of SMCs and focal accumulation of extracellular lipids with or without the presence of macrophages	Small extracellular lipid pools with overlying or adjacent located macrophages. Intimal SMC can be identified.
Early fibroatheroma	EFA	Focal macrophage infiltration into areas of lipid pools with an overlying fibrous cap	Larger amounts of extracellular lipid with infiltrating macrophages and cholesterol clefts are visible. The core is shielded from the bloodstream by several layers of SMC. No apoptosis or necrosis.
Late fibroatheroma	LFA	Loss of matrix and extensive cellular debris with an overlying fibrous cap with or without calcification.	Macrophage accumulation within the core of extracellular lipid with distinguishable cholesterol clefts. The core is shielded from the bloodstream by several layers of SMC and macrophages.
Vulnerable atherosclerotic lesions			
Thin cap fibroatheroma	TCFA	A thin fibrous cap (<65 μm in coronary artery and <155 μm in the aorta) overlying a large necrotic core. Intraplaque haemorrhage can be present in coronary lesions	N/A
Plaque rupture	PR	Thin cap fibroatheroma with cap disruption with a luminal thrombus communicating with the necrotic core	N/A
Stabilizing lesions			
Healing rupture	HR	Healed lesion composed of SMCs, proteoglycans and collagen with or without an underlying disrupted fibrous cap. With or without calcifications.	N/A
Fibrotic calcified plaque	FCP	A fibrous lesion with large amounts of calcification without an underlying necrotic core.	N/A

Tissue samples from preclinical models of atherosclerosis

Hearts and aortic tissues were obtained from an extensive mouse tissue biobank (TNO, Leiden, The Netherlands) and atherosclerotic lesions of Ldlr-/- mice, ApoE-/- mice and ApoE*3Leiden mice were analysed. Lesion development in these mice was induced as reviewed in reference 10 (and references therein) involving feeding of atherogenic cholesterol-containing diets. The heart and the aortic root were collected at sacrifice, embedded in paraffin and subsequently used for preparation of aortic cross-sections as previously reported[12]. The aortic tissue was stained by Movat pentachrome for classification of the lesions according to the modified AHA classification as proposed by Virmani *et al*[8]. Morphological analysis and classification of the lesions were performed by two independent observers. Plaque morphologies included adaptive intimal thickening (AIT), intimal xanthoma (IX), pathological intimal thickening (PIT) and early fibroatheroma (EFA). The mouse lesions were also analysed for presence of more advanced lesion stages.

RESULTS

The Movat pentachrome staining allows a clear visualization of the different constituents of the vessel wall. More specifically, this staining procedure identifies mucins/proteoglycans (blue), collagen (yellow), elastic fibers (black), smooth muscle cells, erythrocytes and fibrinogen (red) and nuclei (purple). Different shades of turquoise and green reflect co-localization of collagen and proteoglycans.

The obvious size differences between normal human aorta, coronary artery and the murine aortic root (*i.e.* the predilection places of atherosclerotic lesion formation) are illustrated in figure 1.

The morphology of the intima (composed of endothelial cells with sometimes focal thickened segments of extracellular matrix), is essentially similar for these three vessels (Figure 1A-C). The internal and external elastic laminae of the coronary artery and to a lesser extent of the aorta are clearly shown. The Movat stain clearly illustrates the different structures of the muscular coronary artery and the elastic aorta. This is visualized by the large number of collagen and elastin filaments in the tunica media (black elastic fibers). In terms of structure, the adventitia of the coronary artery and aorta are almost similar. Differences were found for the adventitia and the vaso vasorum in these different arteries. The vaso vasorum in the coronary artery remains confined to the adventitia. In the human aorta the vaso vasorum crosses the medial/adventitial border whereas in mice the adventitia lacks vaso vasorum at the level of the aortic root.

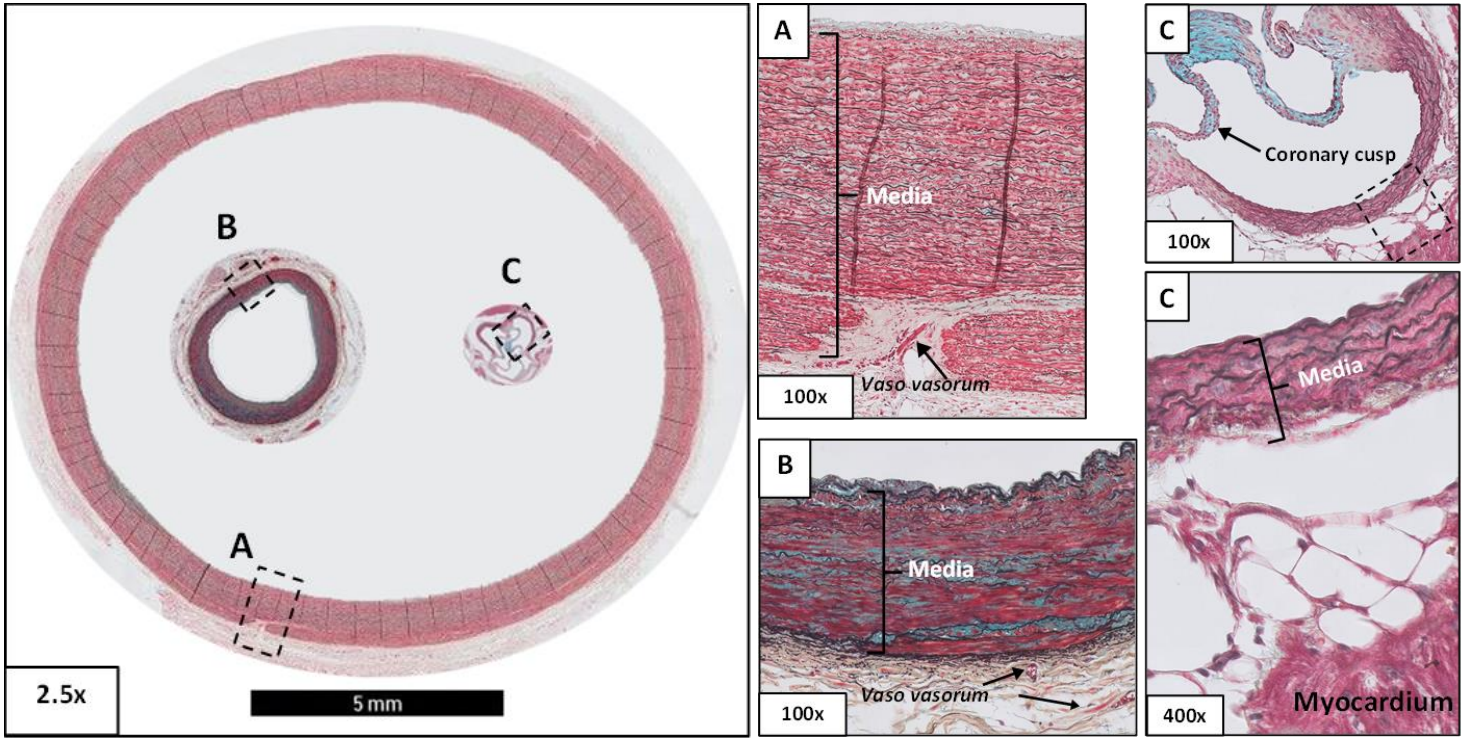

Figure 1. The normal human aorta (A), normal human coronary artery (B) and normal aortic root in mice (C). Images of a normal human peri-renal abdominal aorta, a normal human coronary artery and a sample of a normal aortic root of a mouse all taken at the same 2,5x magnification. This image clearly shows how the various vessels relate to one another. Additional high resolution images of the various vessels clearly show the concentrically arranged fenestrated elastic laminae in the media of the aorta (A) and the coronary artery (B) and to lesser extent in the aortic root (C). The medio-adventitial border of the human aorta and coronary artery consist of vaso vasorum while, by contrast, near the aortic root of mice only myocardium and fatty cells are identified. Note the absence of an intima in the aortic root.

Non-atherosclerotic intimal lesions (Figure 2 and 3)

Adaptive intimal thickening (AIT) and intimal xanthoma (IX)

Thickening of the intima (AIT) through infiltration of smooth muscle cells and deposition of a proteoglycan-rich matrix (Figure 2) is considered the earliest (and reversible) transition in the atherosclerotic process[8]. Lipid deposits, in particular foam cells, and inflammatory cells are absent. The media and adventitia remain normal. As illustrated in figure 2, the histological aspects of this stage are similar for the three vessels studied.

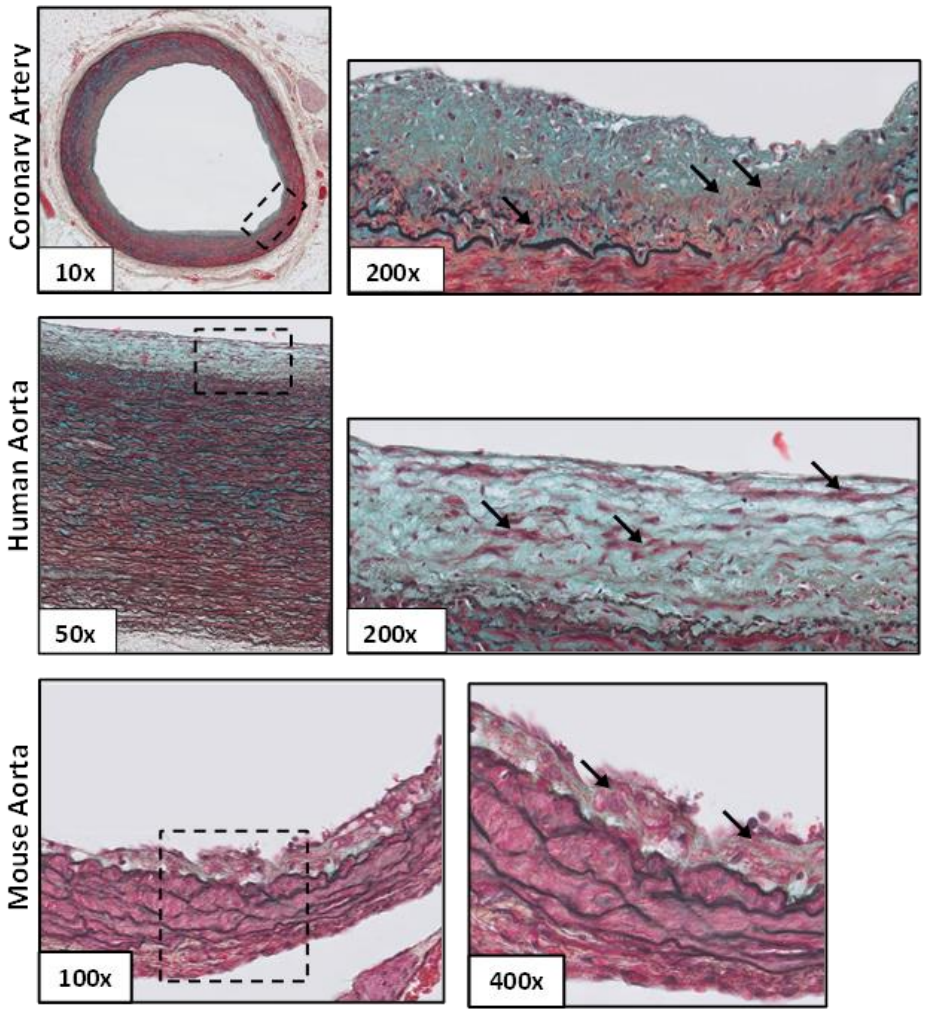

Figure 2. Adaptive intimal thickening in the human coronary artery, the human aorta and the mouse aorta. AIT is characterized by accumulating smooth muscle cells (black arrows) in a proteoglycan-rich matrix (green and turquoise background). Movat pentachrome staining.

Transition from AIT to IX (Figure 3) is hallmarked by the appearance of intimal foam cells. Significant variation is found in the number of foam cells and the size and thickness of foam cell clustering. By definition an (a-cellular) lipid pool is absent. The morphological characteristics of IX in the human arteries and the murine aortic root appear to be identical (Figure 3).

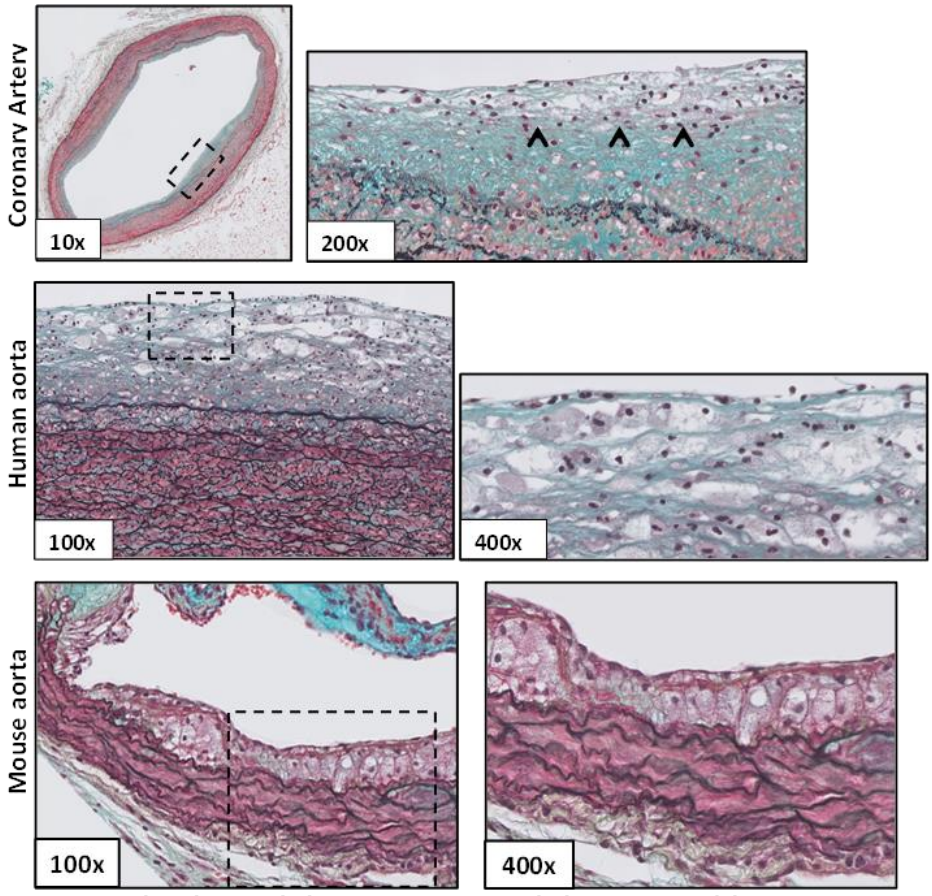

Figure 3. Intimal xanthoma in the human coronary artery, the human aorta and the mouse aorta. IX are characterized by one or several layers of infiltrating macrophage-derived foam cells (^) in the intima. Movat pentachrome staining.

Progressive atherosclerotic lesions (Figure 4 - 6).

Pathological intimal thickening (PIT), early and late fibroatheroma (EFA and LFA)

Focal acellular areas consisting of accumulated extracellular lipid within the intimal extracellular matrix (*i.e.* lipid pools; Figure 4) characterize progressive lesions. The earliest progressive lesion is referred to as PIT[8]. This phase is characterized by a matrix rich lipid pools, but absent cholesterol clefts. Lipid pools are mainly located at the medial border zone of the intima and are covered by smooth muscle cells and clusters of macrophages (Figure 4).

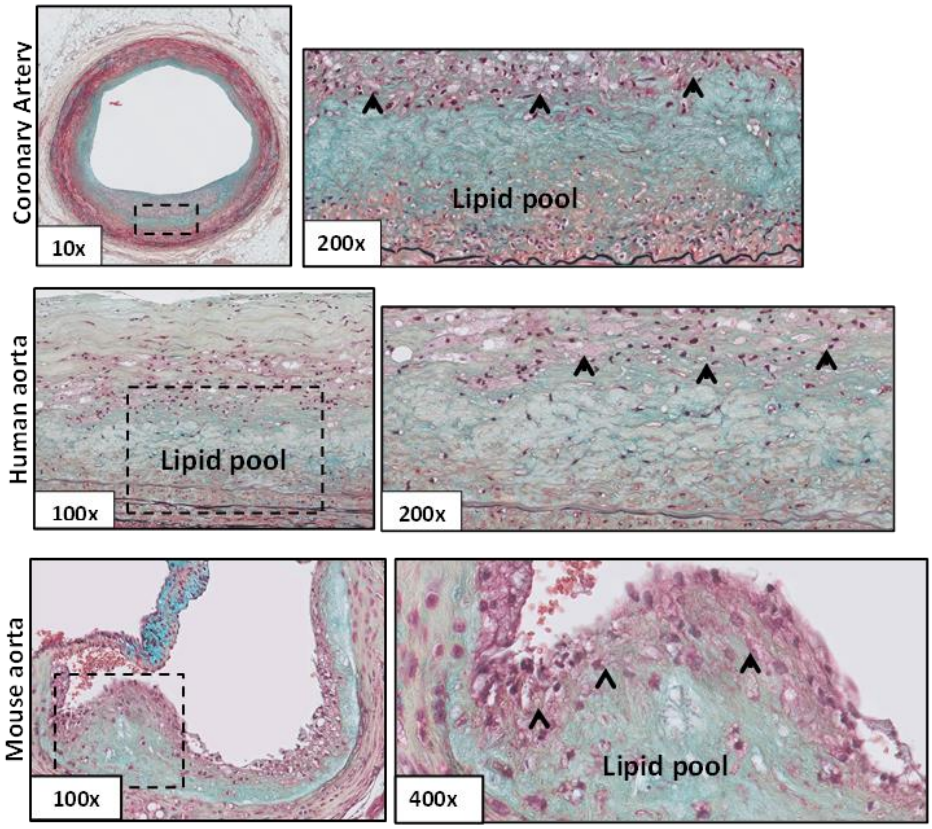

Figure 4. Pathological intimal thickening in the human coronary artery, the human aorta and the mouse aorta. PIT is characterized by the presence of lipid pools deep within the intima near the intimal medial border with overlying and infiltrating SMCs in a proteoglycan matrix with or without macrophage infiltration(^). The morphological appearance is almost identical in all the three vascular beds. Movat pentachrome staining.

A common phenomenon in the coronary artery, but not in the human and murine aorta, is disruption of the adjacent internal elastic lamina by infiltrating vasa vasora and presence of clusters of basal macrophages/foam cells in the vicinity of these infiltrating vasa vasora (illustrated in a high resolution image of the coronary artery; Figure 5). Coherence of these basal foam cells with lipid pools suggests that foam cells may contribute to lesion formation. The morphology of human and murine PIT is essentially similar, yet infiltrating vasa vasora are absent in murine lesions

Transition of PIT to an EFA is characterized by the emergence of cholesterol clefts and development of an acellular necrotic core in the existing lipid pools. Formation of this early necrotic core is thought to reflect consolidation of the existing extracellular components into one or more masses comprising large amounts of extracellular lipid, cholesterol crystals, and necrotic debris[8]. Transition from PIT to EFA in the coronary artery and human aorta is associated with an appreciable decrease in proteoglycans within the lipid pools. This, together with infiltrating macrophages ultimately undergoing necrosis or apoptosis, results in the development of an early necrotic core (Figure 4 and 5). Yet, the structure of the core remains intact. The overall morphological characteristics of the early necrotic core in the human aorta resemble that of the coronary artery with the exception of intraplaque haemorrhage which is, in the case of coronary EFA, frequently associated with infiltrating vasa vasora. Intraplaque haemorrhage is not seen within the aortic lesions.

Figure 5 shows clear gross resembles of the murine and human EFAs: the aspect of the necrotic core of advanced murine lesion bears many similarities with human EFA. However, clear differences are observed with respect to the tissue response. Mice EFA lack vasa vasora and, contrary to human EFA in which the necrotic core is covered by a multi layered fibrous cap, the core of mouse lesions is shielded from the lumen by a thin layer of SMCs (see the 400x high resolution images of the EFA in mice; Figure 5).

Transition towards a LFA is characterized by further maturation of the core that has now become mostly translucent and contains large cholesterol clefts (Figure 6). As with EFA, the necrotic core is covered by a thicker fibrous cap (*i.e.* a distinct layer of connective tissue). The thick, fibrous cap in the human coronary and human aorta consists of smooth muscle cells in a collagenous proteoglycan rich matrix, with varying degrees of infiltration by macrophage and lymphocyte infiltrates.

Importantly, the key characteristics of LFA (late necrotic core with a multi-layer fibrous cap) are absent in the murine models. Although large cholesterol clefts may occur in murine lesions, mice do not develop multi-layer thick fibrous caps.

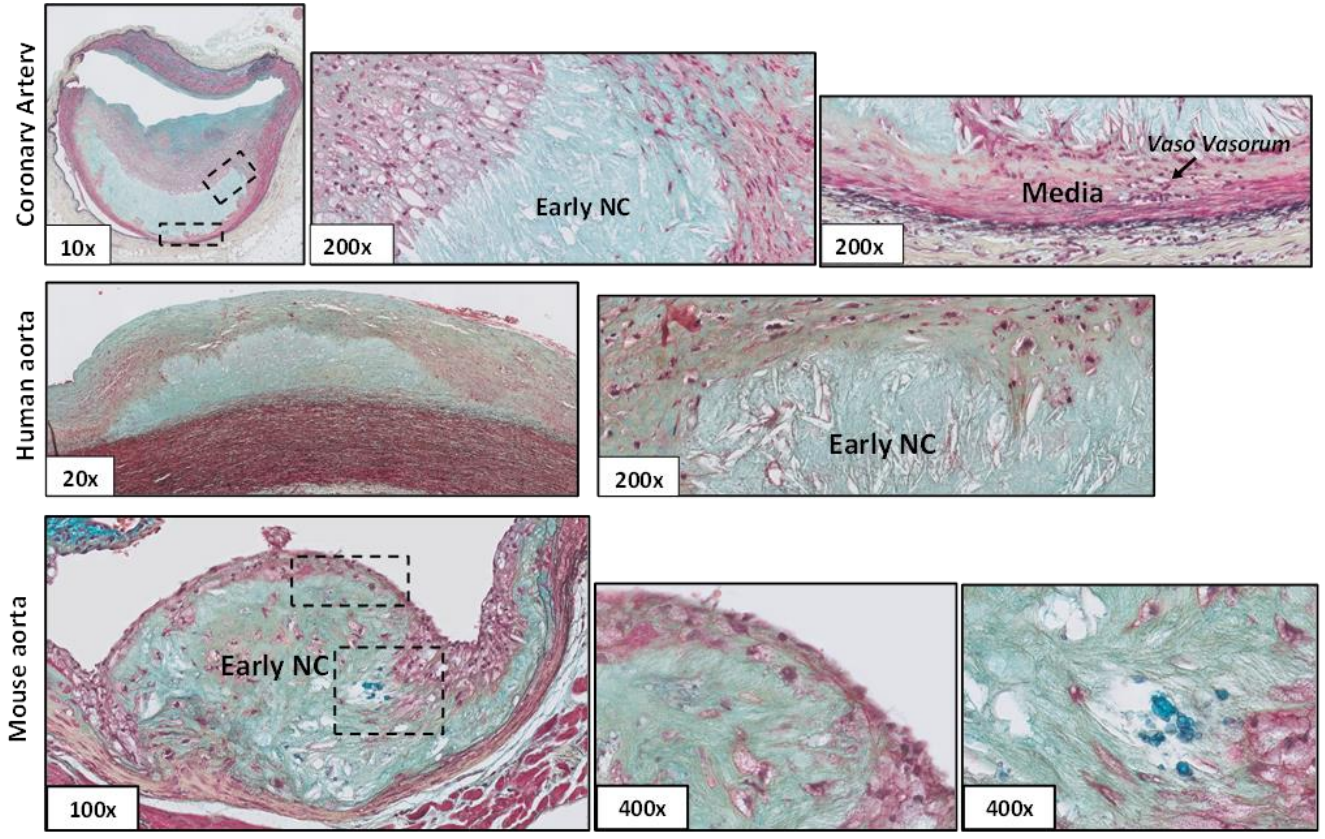

Figure 5. Early fibroatheroma in the human coronary artery, the human aorta and the mouse aorta. The EFA shows macrophage in the early necrotic core.Within the coronary artery the vaso vasorum extends through the media into the intima. This is not observed in the human aorta and in mice. Movat pentachrome staining.

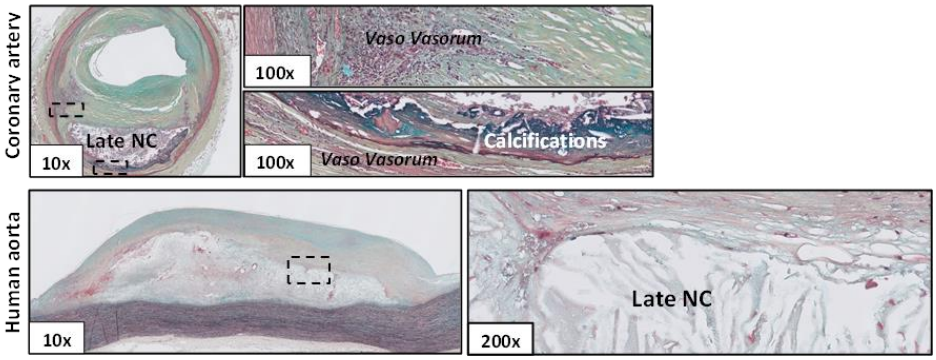

Figure 6. Late fibroatheroma in the human coronary artery and the human aorta. The larger size of the progressive lesions in the aorta compared to those identified in the coronary artery is probably the most obvious difference. The lipid pools lay deep within the intima near the intimal medial border with overlying and infiltrating macrophages (arrowheads) and areas of calcifications can easily be identified. The late necrotic cores are identical to the ones seen in the coronary artery. Unlike the coronary artery, the infiltrating vaso vasorum is limited to the intimo-medial border in the aorta. Movat pentachrome staining.

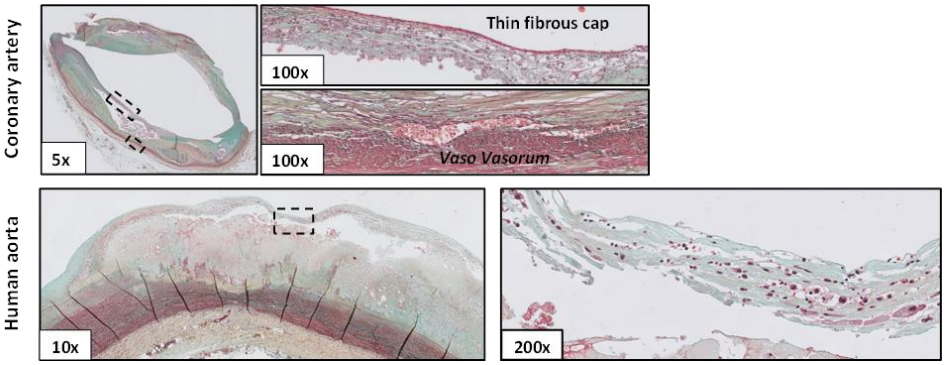

Figure 7. Thin cap fibroatheroma in the human coronary artery and the human aorta. Examples of a TCFA with 100x and 200x high resolution images of the thin fibrous cap with excessive macrophage infiltration, the progressive infiltrating vaso vasorum reaching within the necrotic core, the significant medial thinning and the abundant influx of inflammatory cells in the adventitia. Movat pentachrome staining.

Vulnerable atherosclerotic lesions (Figure 7 and 8).

Thin cap fibroatheroma (TCFA) and plaque rupture (PR)

Transition from a late progressive lesion (LFA) to a vulnerable lesion (TCFA) is defined by significant thinning of the fibrous cap (Figure 7). The necrotic core is usually larger, haemorrhage (in coronary lesions) and intraplaque vasa vasora are abundantly present in both coronary and aortic lesions (Figure 7).

PR is characterized by a disrupted fibrous cap whereby the overlying thrombus or remnants of thrombus is in continuity with the underlying necrotic core. Most

ruptured lesions have a typical large necrotic core and a disrupted fibrous cap infiltrated by macrophages and lymphocytes. The remnants of the luminal thrombus at the site of rupture are essentially composed of platelets and may be obstructive. TCFA and PR were not identified in mice.

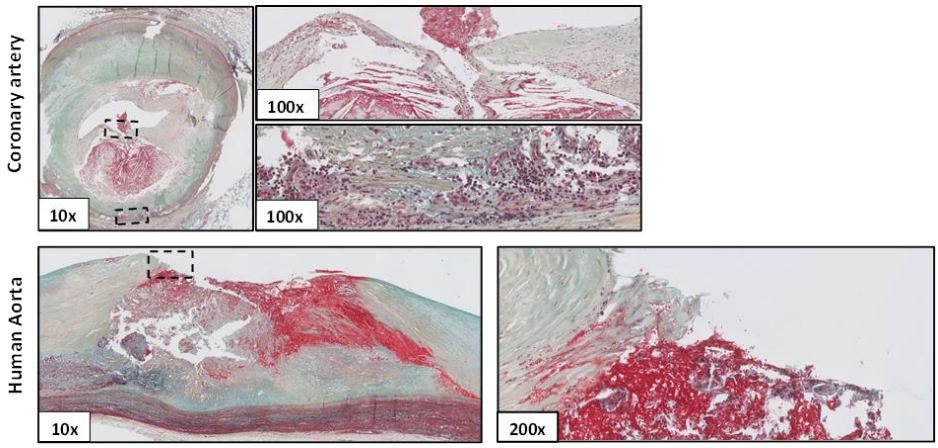

Figure 8. Plaque rupture in the human coronary artery and the human aorta. High resolution images PR with high resolution images of the thin fibrous cap and the rupture site. Movat pentachrome staining.

Stabilizing atherosclerotic lesions (Figure 9 and 10).

Healed ruptures (HR), fibrocalcific plaques (FCP)

Consolidation of a PR is characterized by a wound healing response in which a disrupted fibrous cap is covered by smooth muscle cell and proteoglycan cell-rich tissue (green/blue on Movat). The matrix within the healed fibrous cap consists of a proteoglycan-rich mass adjacent to or covering the fibrotic remnants of original cap. Lesions can contain large consolidated areas of calcification with few inflammatory cells and have a small or no necrotic core.

The FCP reflects consolidation of the healing process is associated with large condensed areas of calcification in an overall fibrotic, acellular remnant of the former necrotic core(s). Inflammatory cells are no longer present in the adventitia and there is regression of the pre-existing vasa vasora. Stacked FCPs illustrate the repetitive and chronic character of the atherosclerotic process.

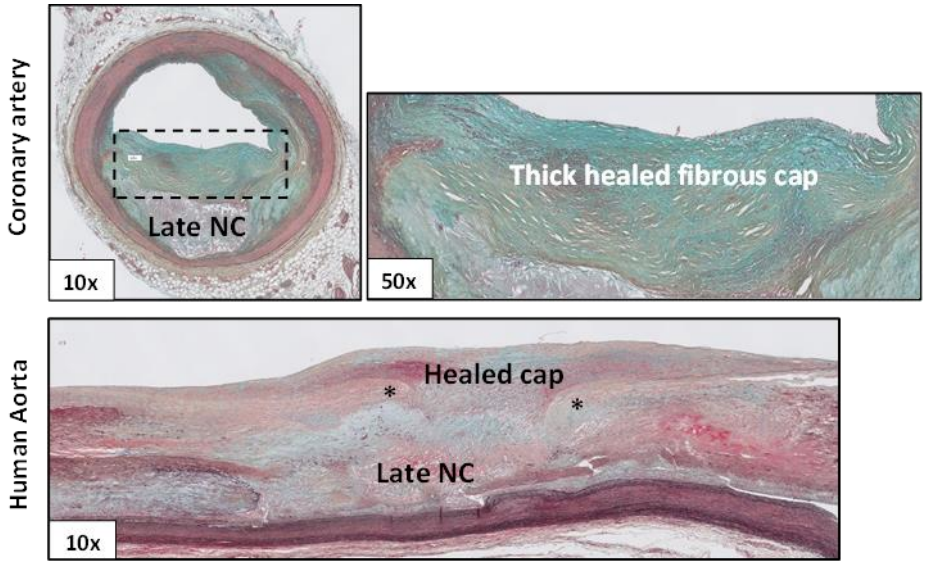

Figure 9. Healed rupture in the human coronary artery and the human aorta. The newly formed thick fibrous cap shields the remnants of the necrotic core from the lumen. The * denotes the edge of the ruptured site. This example of a FCP contains multiple calcified lesions in an almost circumferential appearance. Movat pentachrome staining.

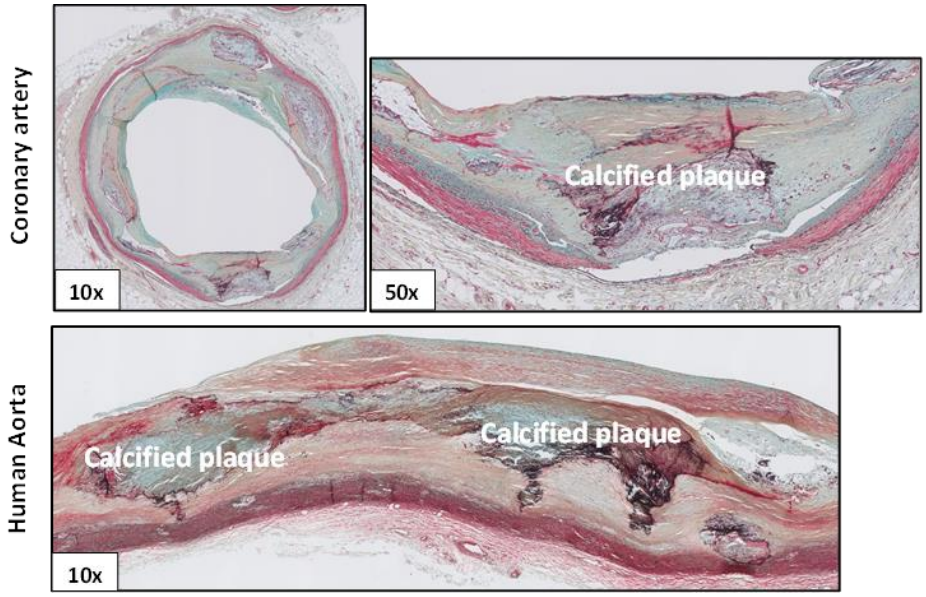

Figure 10. Fibrotic calcified plaque in the human coronary artery and the human aorta. Images of a FCP in coronary artery and the aorta. Note the relative quiescent adventitia when compared to the adventitia in the vulnerable atherosclerotic lesions (Figure7 and 8).Movat pentachrome staining.

DISCUSSION

This systematic histopathologic comparison of human and murine atherosclerosis lesions shows that the established refined Virmani classification system for coronary atherosclerosis can be applied for grading of human aortic and murine atherosclerosis. Based on the histological characteristics the lesions in mice do not progress beyond the stage of EFA. Consequently, specific aspects of advanced and vulnerable lesion formation, and successive healing, are not present in murine experimental models. Therefore, these aspects cannot be studied in translational studies.

Staging the various phases of the atherosclerotic process and assessment of lesion vulnerability exclusively relies on a histopathological evaluation of plaque morphology. The first comprehensive classification scheme provided by the AHA involved an orderly numerical classification embedding six distinct categories[4-7]. Unfortunately this classification fails to capture several important clinical etiologies of coronary thrombus formation that are distinct from plaque rupture like plaque erosions and calcified nodules[3, 8]. It further lacks the recognition of precursor lesions that potentially give rise to clinical events, does not reflect the dynamics of the disease process, and does not acknowledge the process of plaque healing. Based on their observations and experience, Virmani *et al*. refined the AHA classification in order to better reflect the heterogeneity of the late stages of atherosclerotic disease by staging atherosclerosis based on plaque morphology. This descriptive morphological classification incorporates both the various aspects of vulnerable lesion development and plaque destabilization, thereby better mirroring the pathophysiology of the disease[8]. Moreover, the progressive character of the classification system better reflects the natural history of the disease. Over the past years, the Virmani classification scheme has increasingly been employed in clinical research and practise but it is only sporadically employed for the evaluation in experimental models of disease[13,14]. Our study demonstrates that the Virmani classification system allows for the analysis of morphological changes during early lesion development in humans aortic and murine samples, and we therefore advocate the use of the Virmani classification system in mice.

More specifically changes in matrix composition and tissue morphology are key elements in the atherosclerotic process[15]. These changes and co-localizations of proteoglycans, collagen and fibrinogen are insufficiently addressed with conventional stainings such as H&E and Sirius Red (SR). For example changes and co-localizations of proteoglycans, collagen and fibrinogen are missed with H&E staining. The Movat pentachrome staining is technically more challenging but provides a more detailed appreciation of the matrix biology of the plaque and

better distinguishes the more complex, advanced lesions from one another[16]. Hence, a Movat pentachrome staining provides additional information and should be preferred above a H&E and SR standard stainings. Movat staining shows that murine lesions do not develop aspects that characterize vulnerable lesions of humans. This notion contrasts with the progressive use of plaque collagen content (Sirius red (SR)) as a surrogate of plaque stability. Several studies suggest that SR staining can be used to identify the degree of plaque stabilization and destabilization in mice[17]. Sirius red stains ground substance and decreased SR content in mouse lesions reflects displacement of ground substance by foam cells and / or cholesterol clefts. However, the human-like fibrosis and cap formation with multiple layers is not identified in mice using the Movat staining. This reveals an important drawback in the translation of murine models of arteriosclerosis to the human situation. This is an important outcome of our study, the more so because mouse studies are often used to investigate basic molecular mechanisms or new intervention principles involving changes in lesion composition, potentially affecting lesion stability. Our comparisons of lesions in mice to vulnerable lesions in humans clearly demonstrate that there is no murine equivalent to the multi-layered cap in humans and that the morphological changes associated with plaque rupture in humans are not observed in mice. As a consequence, the ongoing discussion whether the absolute area or the lesional percentage of these three components is a good estimate of lesion stability in mice, comes into a different perspective. Furthermore SR staining solely reflects the substitution of the ground substance (*i.e.* matrix) by lipid accumulation and foam cells and does by itself not predict plaque stability. Our present study advocates a more careful interpretation of 'lesion stability data' in murine studies.

We previously validated the coronary artery-based Virmani classification for the human aorta[9]. We now extend this validation and show that this classification scheme can be directly applied to murine aortic atherosclerosis, allowing a one to one comparison of murine and human atherosclerosis at the various stages and positioning preclinical findings in the human context.

Our findings also show that the most advanced lesions identified in mice best match the morphological description of an EFA. This notion is based on the morphology of the lipid core and the fact that the lipid core is shielded from the bloodstream by one or several layers of smooth muscle cells. Compared to humans mice lesions lack an overlying cap, the hallmark of an EFA and LFA. Second, the integrity of the lipid core, with exception of the visible cholesterol clefts, remains intact. In humans the EFA precedes advanced LFA lesions, plaque destabilization, plaque rupture and subsequent plaque healing. These phenomena are all absent in the murine model of atherosclerosis, consequently prohibiting a translational analysis of plaque (de-)stabilisation in mice[18,19].

Our extensive histological analyses provides a number of clues why murine lesions fail to progress towards advanced lesions. In direct comparison with their human counterpart, the advancing lesions in mice are significantly smaller in size, lack ischemia and neovascularization[20,21,22]. The relatively small lesions in mice do not progress beyond the critical 200 μm diffusion distance. As a result, the maximum diffusion distance of oxygen and nutrients in tissue is not reached and the entire atherosclerotic process can still evolve via diffusion, and an ischemic trigger is missing[23]. It is thought that this ischemic trigger in human atherosclerosis is critical and eventually results in plaque neovascularization originating from the infiltrating vasa vasora[24]. These vasa vasora are thought to further contribute to intraplaque haemorrhage due to leaky vessels and is a major contributor to plaque expansion via cholesterol influx with consequently thinning of the fibrous cap resulting in vulnerable rupture prone lesions in the coronary artery[3,8]. Ischemia of the developing cap may also underlie the advanced fibrotic changes in humans.

Fibrosis is a notable phenomenon in advancing lesions. In fact, it is a distinct part of the atherosclerotic process in human that is minimally present in mice[14]. Factors not captured in this study, but need to be kept in mind interpreting the results, are the age related differences of the plaques in humans and mice and the fundamental immunological and inflammatory differences between rodents and humans[25,26,27].

The major contributor to lipid core expansion in mice is the excessive intimal cholesterol influx due to the required hypercholesterolaemia[28] as well a systemic inflammatory component involving inflammatory mediators produced locally in the aorta and in liver or adipose tissue[29, 30]. Lesions with this type of histology lack a pronounced fibrotic component, therefore remain reversible and are rarely clinically significant except in examples of severe experimental hyper-cholesterolaemia, a situation that is quite atypical and does not reflect the chronic multifactorial nature or complexity of the human disease[31,32].

Limitations; This is an observational study with findings merely based on histological Movat Pentachrome staining of human coronary and aortic tissue, and mice tissue. Consequently, findings in this study should be considered in this context.

Conclusion; The initial and more advanced atherosclerotic lesions in mice follow a similar pattern of progression compared to coronary and aortic atherosclerosis in humans and can be classified accordingly using a uniform, detailed morphological classification scheme based on the Virmani classification. Experimental data obtained from murine studies to estimate lesion stability should be interpreted with care since morphological changes associated with instable lesions in humans are not observed in mice.

REFERENCES

1 Ross R. Atherosclerosis—an inflammatory disease. The New England Journal of Medicine. 1999;340(2):115–126.

2 Glass CK,Witztum JL. Atherosclerosis the road ahead. Cell. 2001;104:503–516.

3 Virmani, R., Kolodgie, F. D., Burke, A. P., Farb, A., & Schwartz, S. M. (2000). Lessons from sudden coronary death a comprehensive morphological classification scheme for atherosclerotic lesions. Arteriosclerosis, thrombosis, and vascular biology, 20(5), 1262-1275.

4 Stary, H. C., *et al*. A definition of the intima of human arteries and of its atherosclerosis-prone regions. A report from the Committee on Vascular Lesions of the Council on Arteriosclerosis, American Heart Association. Circulation, 1992, 85.1: 391.

5 Stary, Herbert C., *et al*. A definition of initial, fatty streak, and intermediate lesions of atherosclerosis. A report from the Committee on Vascular Lesions of the Council on Arteriosclerosis, American Heart Association. Arteriosclerosis, Thrombosis, and Vascular Biology, 1994, 14.5: 840-856.

6 Stary, Herbert C., *et al*. A definition of advanced types of atherosclerotic lesions and a histological classification of atherosclerosis A report from the Committee on Vascular Lesions of the Council on Arteriosclerosis, American Heart Association. Circulation, 1995, 92.5: 1355-1374.

7 Stary, Herbert C. Natural history and histological classification of atherosclerotic lesions an update. Arteriosclerosis, thrombosis, and vascular biology, 2000, 20.5: 1177-1178.

8 Yahagi, K., Kolodgie, F. D., Otsuka, F., Finn, A. V., Davis, H. R., Joner, M., & Virmani, R. (2015). Pathophysiology of native coronary, vein graft, and in-stent atherosclerosis. Nature Reviews Cardiology.

9 van Dijk RA, Virmani R, von der Thüsen JH, Schaapherder AF, Lindeman JH. The natural history of aortic atherosclerosis: a systematic histopathological evaluation of the peri-renal region. Atherosclerosis. 2010;210(1):100-106.

10 Zadelaar, S., Kleemann, R., Verschuren, L., de Vries-Van der Weij, J., van der Hoorn, J., Princen, H. M., & Kooistra, T. (2007). Mouse models for atherosclerosis and pharmaceutical modifiers. Arteriosclerosis, thrombosis, and vascular biology, 27(8), 1706-1721.

11 Daugherty, A. Mouse models of atherosclerosis. The American journal of the medical sciences, 2002, 323.1: 3.

12 Morrison M, van der Heijden R, Heeringa P, Kaijzel E, Verschuren L, Blomhoff R, Kooistra T, Kleemann R. Epicatechin attenuates atherosclerosis and exerts anti-inflammatory effects on diet-induced human-CRP and NFκB in vivo. Atherosclerosis. 2014 Mar 31;233(1):149-56.

13 Koppara T, Sakakura K, Pacheco E, Cheng Q, Zhao X, Acampado E, Finn AV, Barakat M, Maillard L, Ren J, Deshpande M. Preclinical evaluation of a novel polyphosphazene surface modified stent. Koppara Preclinical testing of a PzF-coated stent. International Journal of Cardiology. 2016 Nov 1;222:217-25.

14 He C, Medley SC, Hu T, Hinsdale ME, Lupu F, Virmani R, Olson LE. PDGFR [beta] signalling regulates local inflammation and synergizes with hypercholesterolaemia to promote atherosclerosis. Nature communications. 2015 Jul 17;6.

15 Hansson, G. K., & Libby, P. (2006). The immune response in atherosclerosis: a double-edged sword. Nature Reviews Immunology, 6(7), 508-519.

16 Farb A, Weber DK, Kolodgie FD, Burke AP, Virmani R. Morphological Predictors of Restenosis After Coronary Stenting in Humans. Circulation. 105:2974-2980.

17 Mallat, Z., Corbaz, A., Scoazec, A., Graber, P., Alouani, S., Esposito, B., Tedgui, A. (2001). Interleukin-18/interleukin-18 binding protein signaling modulates atherosclerotic lesion development and stability. Circulation research, 89(7), e41-e45.

18 Libby, P., Ridker, P. M., & Hansson, G. K. (2011). Progress and challenges in translating the biology of atherosclerosis. Nature, 473(7347), 317-325.

19 Whitman, S. C. (2004). A practical approach to using mice in atherosclerosis research. The Clinical Biochemist Reviews, 25(1), 81.

20 Hartwig, H., Silvestre-Roig, C., Hendrikse, J., Beckers, L., Paulin, N., Van der Heiden, K. & Soehnlein, O. (2015). Atherosclerotic Plaque Destabilization in Mice: A Comparative Study. PloS one, 10(10).

21 Maganto-Garcia, E., Tarrio, M., & Lichtman, A. H. (2012). Mouse models of atherosclerosis. Current Protocols in Immunology, 15-24.

22 Lutgens, E., Daemen, M., Kockx, M., Doevendans, P., Hofker, M., Havekes L, Wellens H, de Muinck ED. Atherosclerosis in APOE* 3-Leiden transgenic mice: from proliferative to atheromatous stage. Circulation. 1999; 99(2), 276.

23 Chauhan, V. P., Stylianopoulos, T., Boucher, Y., & Jain, R. K. (2011). Delivery of molecular and nanoscale medicine to tumors: transport barriers and strategies. Annual review of chemical and biomolecular engineering, 2, 281-298.

24 Sluimer JC, Gasc JM, van Wanroij JL, Kisters N, Groeneweg M, Sollewijn Gelpke MD, Cleutjens JP, van den Akker LH, Corvol P, Wouters BG, Daemen MJ, Bijnens AP. (2008). Hypoxia, hypoxia-inducible transcription factor, and macrophages in human atherosclerotic plaques are correlated with intraplaque angiogenesis. Journal of the American College of Cardiology, 51(13), 1258-1265.

25 Martinez FO, Helming L, Milde R, Varin A, Melgert BN, Draijer C, Thomas B, Fabbri M, Crawshaw A, Ho LP, Ten Hacken NH, Cobos Jiménez V, Kootstra NA, Hamann J, Greaves DR, Locati M, Mantovani A, Gordon S. Genetic programs expressed in resting and IL-4 alternatively activated mouse and human macrophages: similarities and differences. Blood. 2013;121(9):e57-69.

26 Bryant CE, Monie TP. Mice, men and the relatives: cross-species studies underpin innate immunity. Open Biology. 2012;2(4):120015.

27 Colucci F, Di Santo JP, Leibson PJ. Natural killer cell activation in mice and men: different triggers for similar weapons? Nature Immunology. 2002;3(9):807-813.

28 van der Hoorn, J. W., Kleemann, R., Havekes, L. M., Kooistra, T., Princen, H. M., & Jukema, J. W. (2007). Olmesartan and pravastatin additively reduce development of atherosclerosis in APOE* 3Leiden transgenic mice. Journal of hypertension, 25(12), 2454.

29 Kleemann R, Princen HM, Emeis JJ, Jukema JW, Fontijn RD, Horrevoets AJ, Kooistra T, Havekes LM. Rosuvastatin Reduces Atherosclerosis Development Beyond and Independent of Its Plasma Cholesterol–Lowering Effect in APOE* 3-Leiden Transgenic Mice Evidence for Antiinflammatory Effects of Rosuvastatin. Circulation, 2003, 108.11: 1368-1374.

30 Salic K, Morrison MC, Verschuren L, Wielinga PY, Wu L, Kleemann R, Gjorstrup P, Kooistra T. Resolvin E1 attenuates atherosclerosis in absence of cholesterol-lowering effects and on top of atorvastatin. Atherosclerosis, 2016, 250: 158-165.

31 van Dijk RA, Duinisveld AJ, Schaapherder AF, Mulder-Stapel A, Hamming JF, Kuiper J, de Boer OJ, van der Wal AC, Kolodgie FD, Virmani R, Lindeman JH. A change in inflammatory footprint precedes plaque instability: a systematic evaluation of cellular aspects of the adaptive immune response in human atherosclerosis. Journal of American Heart Association. 2015;4(4).

32 R.A. van Dijk, K. Rijs, A. Wezel, J.F. Hamming, F.D. Kolodgie, R.Virmani, A.F. Schaapherder, J.H.N. A systematic evaluation of the cellular innate immune response during the process of human atherosclerosis. Journal of American Heart Association. 2016.

CHAPTER 5

Differential expression of oxidation-specific epitopes and apolipoprotein(a) in progressing and ruptured human coronary and carotid atherosclerotic lesions

R.A. van Dijk
F. Kolodgie
A. Ravandi
G. Leibundgut
P. P. Hu
A. Prasad
E.Mahmud
E. Dennis
L. K. Curtiss
J. L. Witztum
B. A. Wasserman
F. Otsuka
R. Virmani
S. Tsimikas

Journal of lipid research 2012

ABSTRACT

Background: The relationships between oxidation-specific epitopes (OSE) and lipoprotein (a) (Lp(a)) and progressive atherosclerosis and plaque rupture have not been determined.

Methods: Coronary artery sections from sudden death victims and carotid endarterectomy specimens were immunostained for apoB-100, oxidized phospholipids (OxPL), apo(a), malondialdehyde-lysine (MDA), and MDA-related epitopes detected by antibody IK17 and macrophage markers. The presence of OxPL captured in carotid and saphenous vein graft distal protection devices was determined with LC-MS/MS.

Results: In coronary arteries, OSE and apo(a) were absent in normal coronary arteries and minimally present in early lesions. As lesions progressed, apoB and MDA epitopes did not increase, whereas macrophage, apo(a), OxPL, and IK17 epitopes increased proportionally, but they differed according to plaque type and plaque components. Apo(a) epitopes were present throughout early and late lesions, especially in macrophages and the necrotic core. IK17 and OxPL epitopes were strongest in late lesions in macrophage-rich areas, lipid pools, and the necrotic core, and they were most specifically associated with unstable and ruptured plaques. Specific OxPL were present in distal protection devices.

Conclusion: Human atherosclerotic lesions manifest a differential expression of OSEs and apo(a) as they progress, rupture, and become clinically symptomatic. These findings provide a rationale for targeting OSE for biotheranostic applications in humans.

Abbreviations:

AIT, adaptive intimal thickening; apo(a), apolipoprotein (a); EFA, early fibroatheroma, H and E, hematoxylin and eosin; IX, intimal xanthoma; LFA, late fibroatheroma, Lp(a), lipoprotein (a); MDA, malondialdehyde-lysine; OSE, oxidation-specific epitope; OxPL, oxidized phospholipid; PIT, pathologic intimal thickening; PR, plaque rupture; SMC, smooth muscle cell; SVG, saphenous vein graft; TCFA, thin cap fibroatheroma.

INTRODUCTION

Oxidative pathways in the subendothelial space activate proinflammatory, immunogenic, and atherogenic processes, resulting in endothelial dysfunction, plaque growth and destabilization, platelet activation, and thrombosis, ultimately leading to clinical events[1]. A variety of oxidation-specific epitopes (OSE) are generated during oxidative modification of plaque components. These epitopes are not only expressed on modified lipoproteins but also on apoptotic cells and proteins in the extracellular matrix of atherosclerotic vessels[2]. Extensive experimental data exists defining the role of oxidation in both progression and regression of atherosclerosis. Atherosclerotic lesions of hypercholesterolemic animal models, which represent primarily early and inter-mediate stage atherosclerosis, contain significant amounts of OSE, often in proportion to plaque burden. OSE in the vessel wall of atherosclerotic animals can also be imaged with nuclear and magnetic resonance techniques using murine and human oxidation-specific antibodies, such as MDA2, E06, and IK17[3,4,5]. Dietary interventions in hypercholesterolemic animals that promote regression result in more rapid removal of OSE than apoB, which occurs prior to plaques diminishing significantly in size, and is associated with markers of plaque stabilization, such as increased collagen and smooth muscle cell (SMC) expression, and a decrease in reactive oxygen species and macrophages[6,7,8].

Despite this wealth of animal data on the relationship of OSE and atherosclerosis, relatively little is known about their relationship to clinically relevant advanced, unstable, or ruptured plaques. Furthermore, a systematic analysis of the presence of OSE in human lesions has not been performed to date. Therefore, the purpose of this study was to determine the presence and relative distribution of well-characterized OSE in various stages of human atherosclerotic lesions, including native coronary lesions, carotid endarterectomy samples, and material from carotid and saphenous vein graft (SVG) embolic protection filters. Such knowledge may have significant clinical implications with the emergence in the clinical and translational arenas of oxidative biomarkers, molecular imaging, and therapeutic approaches, including immune modulation and vaccine approaches targeting these moieties[9,10,11,12], broadly characterized as “biotheranostic” (biomarker, therapeutic, diagnostic imaging) applications

METHODS

Human atherosclerotic lesions

Hearts of patients who had died suddenly with coronary artery disease (CAD) were obtained as previously described[13]. Cases were identified prospectively by

the presence and type of CAD and included nonatherosclerotic intimal lesions, pathologic intimal thickening, early and late fibroatheroma, thin cap fibroatheroma (TCFA) and plaque rupture. Eighty-nine representative lesions from 25 consecutive patients (22 men and 3 women, age at death 47 ± 13) were selected prior to staining.

To rule out postmortem oxidation occurring prior to heart harvesting, we also evaluated carotid endarterectomy specimens (n =13) from symptomatic patients undergoing clinically indicated procedures. The specimens were removed en bloc and immediately fixed in formalin. Additionally, we evaluated material derived from distal protection devices (n =10) obtained during percutaneous intervention of stenotic internal carotid arteries and coronary SVGs. The entire filter material was immediately placed in ice-cold phosphate buffered solution of EDTA/BHT (100 μM / 20 μM), and then rapidly lipid extracted and stored at -80°C for analyses as described below.

To further rule out postmortem effects, we additionally evaluated five carotid endarterectomy specimens under various handling conditions as follows: each specimen was manually cut into three equal sections and stored at room temperature for 24 h in PBS (phosphate buffered saline), on ice for 24 h in PBS, or on ice in EDTA/BHT for 24 h, respectively. Each of the specimens was then paraffin embedded, and sections were placed on glass slides and immunostained as above.

Histological preparation

Formalin-fixed, paraffin-embedded coronary segments were cut into 5 μm thick sections, mounted on charged slides, and stained with hematoxylin and eosin (H and E) and the modified Movat pentachrome method as previously described[14].

Histological classification of lesions

Plaque components. In a single section, there may be several plaque components, independent of dominant plaque type. Those lesions that were prone to lipid accumulation, either intracellular or extracellular, were identified. Foam cell lesions were defined as areas of macrophages in the presence or absence of significant extracellular lipid (intimal xanthoma)[15]. Lipid pools within pathologic intimal thickening (PIT) consisted of a proteoglycan-rich matrix with trapped lipid and absence of fibrin and hemorrhage in the deeper intima. These pools were often surrounded by macrophage foam cell or SMC-rich areas toward the lumen. Necrotic core denoted focal areas of necrotic debris with presence of apoptotic macrophage debris, prominent cholesterol crystals, and presence of fibrin with partial or complete loss of proteoglycan matrix[15]. The presence of macrophages within the fibrous cap or shoulder region denoted cases of early and late fibroatheroma, thin fibrous cap atheroma, and ruptured plaques.

Plaque types.

The dominant plaque type per coronary artery section was defined as adaptive intimal thickening (AIT, n =7); intimal xanthoma (IX, n =8); PIT (n =11); early fibroatheroma (EFA, n =25); late fibroatheroma (LFA, n =17); thin-cap fibroatheroma (TCFA, n =13); and acute plaque rupture (PR, n =8). Lesions were classified according to a modification of the current American Heart Association recommendations[16]. The distinction between early and late fibroatheroma was made as previously defined[16], namely, the complete loss of matrix and extensive cellular breakdown defined late fibroatheromas[17].

Antibodies

Five unique monoclonal antibodies were used in this study to assess the presence of apolipoprotein B-100, OSE, and apo(a). MB47 is an IgG murine monoclonal antibody that binds near the LDL-receptor domain of human apoB-100[18]. MB47 binds to all apoB-containing lipoproteins equally, and it also binds to fragments of apoB-100 on OxLDL if it is minimally to even extensively modified during oxidation by expo-sure to copper in vitro. E06 is a natural IgM murine monoclonal antibody cloned from apoE $^{-/-}$ mice that binds the PC head-group of oxidized phospholipids (OxPL) and thus recognizes this whether the OxPL is free or covalently bound to proteins. Covalent binding of OxPL occurs via the reactive oxidized moieties, such as aldehydes, generated on the sn2 side chains when the phospholipids are oxidized. The PC is preserved in this setting and is the moiety recognized by E06. E06 recognizes a variety of OxPL with varying sn2 chain lengths terminated by aldehydes, such as 5, 6, and even 9 carbon lengths. It would not recognize oxovaleryl bound to protein unless it was present as the sn2 side chain of an OxPL[19,20]. MDA2 binds to malondialdehyde (MDA) adducts with lysine residues of proteins, in which MDA acts as a hapten on a protein carrier. It thus recognizes a wide variety of MDA-modified proteins[21]. IK17 is a fully human Fab fragment generated with phage display library technology that also binds to MDA adducts with lysine, but it appears to be more specific for MDA-modified LDL, as it does not bind to MDA-modified BSA or polylysine[22].The chemistry of MDA modification is complex; we believe IK17 detects a more complex MDA adduct, although we have not definitely defined it. Uniquely, IK17 also binds to OxLDL, whereas MDA2 does not. Thus its epitope appears to be an MDA adduct that is present on both MDA-LDL and OxLDL. It does not bind OxPL. LPA4 is a murine monoclonal IgG antibody binding the sequence TRNYCRNPDAEIRP on apolipoprotein(a), and it does not cross-react with plasminogen[23]. All preparations were greater than 99% pure.

Immunohistochemistry

Formalin-fixed paraffin sections (5 μm) were incubated over-night at 4°C with primary antibodies MDA2, MB47, E06, and LPA4 at respective dilutions of 1:400, 1:50, 1:1,200, and 1:400. The detection of primary antibodies bound to their respective antigen was achieved using the biotinylated link antibody LSAB2 System-HRP DAB kit (Dako, Carpenteria, CA) with appropriate secondary antibodies directed to mouse IgG or IgM. Histologic sections for antibody staining against IK17 were initially incubated overnight with nonimmune goat anti-human IgG (GAH, Vector, BA-3000) at a dilution of 1:100 in 2% goat serum to re-duce nonspecific background staining. For IK17 immunostaining, IK17 was diluted 1:600 in 2% goat serum and incubated for 1 h at room temperature (RT). Primary labeling was then visualized using an alkaline phosphatase-labeled goat anti-human secondary antibody (dilution 1:200, Sigma A3813) for 1h at RT and visualized with Vector Red (Vector SK-5100).

For the identification of specific cell types, paraffin sections were immunostained for resident macrophages with anti-CD68 (KP-1) (dilution 1:400, M0814, Dako) and SMC with an anti-SMC α-actin (dilution 1:400, M0851, Dako). Both antibodies were visualized using an Envision+System-HRP (DAB) kit (Dako).

Assessment of immunolocalization of OSE, apo(a), and macrophage markers

The degree of MB47, MDA2, E06, LPA4, and IK17 and macrophage marker positivity was assessed qualitatively and quantitatively. Qualitative assessment within plaque components was performed on a scale of 0–3+: 0 (absent); + <10% of component area; ++ =10–50% of component area; +++ > 51% of component area. Morphometric measurements of coronary sections were performed using image-processing software (IPLabs, Scanalytics, Rockville, MD) on slides stained with Movat Pentachrome. Quantitative planimetry with computer-assisted color image analysis segmentation with background correction quantified immuno-histochemical stains of OSE for each antibody within regions of interest.

Total lipid extraction and LC-MS/MS of material from distal protection devices

All distal protection devices were of the filter variety (Filter-Wire EZ, 110 μm pores, Boston Scientific; Accunet Rx, 100 μm pores, Abbott). Filter material was subjected to a Folch lipid ex-traction with chloroform/methanol (2:1). For total lipid extraction, 500 μl of filter material homogenates was transferred into a glass tube, 2.5 ml of ice-cold chloroform/methanol and 17:1/17:1 PC were added as internal standards, and the tubes were vortexed at a maximum speed for 30 s. After centrifugation, the lower organic phase was transferred into a fresh glass

tube using a Pasteur pipette, and the organic phase was dried under argon to ~200 µl and stored at - 80°C.

Isocratic high performance liquid chromatography (HLPC) was carried out using a Shimadzu (Columbia, MD) LC-10AD high-performance pump interfaced with a Shimadzu SCL-10A controller. Sample was injected onto a 2.1 mm × 250 mm Vydac (Hysperia, CA) C18 column (Vydac catalog number 201TP52) held at 40°C using a Leap Technologies (Carrboro, NC) PAL autosampler. A buffer of isopropyl alcohol/water/tetrahydrofuran (40/40/20, v/v/v) with 0.2% formic acid at a fl ow rate of 300 µl/min was used for sample elution. The eluate was coupled to a mass spectrometer for further analysis. Separation optimization and verification of HPLC retention times were achieved using 16:0–05:0 (ALDO) PC standard.

All of the mass spectral analyses were performed using an Applied Biosystems (Foster City, CA) 4000 QTrap hybrid quadrupole linear ion trap mass spectrometer equipped with a Turbo V ion source, as previously described and validated (24). Protonated adducts of the 1-palmitoyl-2-(5 ′ -oxo-valeroyl) *sn* -glycero-3-phosphocholine (POVPC) were formed using the following settings: CUR, 10 psi; GS1, 40 psi; GS2, 0 psi; IS, 5500V; CAD, high; temperature, 500°C; ihe, ON; DP, 70V; CE, 35V; EP, 15V; and CXP, 15V. The 4000 QTrap is capable of carrying out tandem mass spectrometry, where a specified precursor ion (denoted by its mass-to-charge ratio, m/z) can be isolated in the first sector of the instrument, fragmented in a second sector collision cell, and the fragments produced then identified by their m/z in a third sector. A specialized form of tandem mass spectrometry is multiple reaction monitoring (MRM), in which multiple MRM pairs can be monitored in a single analysis. In (+)ESI mode, the fragment produced by all protonated PC species, regardless of their parent mass or moiety, is the phosphocholine headgroup with m/z 184. Thus, in the same analysis, 16:0–05:0 (ALDO) PC were monitored employing the MRM pairs 650/184 and 664/184, respectively.

Statistical analysis

Mean variables between the various lesions were compared with one-way ANOVA (ANOVA; SPSS) followed by Student t -test for all differences among means. Spearman's correlation was used to demonstrate the relationship between macrophages and OSE. A value of $P \leq 0.05$ was considered statistically significant.

Table 1.
Qualitative staining intensity of plaque components

Plaque Component	Macrophages (KP-1)	ApoB-100 (MB47)	MDA-Lysine (MDA2)	OxPL (E06)	IK17	Apo(a) LPA4)
SMC rich area*	-	+/-	+/-	+	+	+
Foamy macrophages	++/+++	-	+/-	+++	++	++
Lipid pools	+/-	+/++	+/++	+/++	++	++
Necrotic core	+++	+/-	+	++	++	+++
Fibrous cap macrophages	++	-	-	+++	+++	++

* Values represent evaluation in AIT, IX, and PIT only, as SMCs were present only in very limited numbers in more advanced atherosclerotic lesions.

Table 2.
Quantitative immunostaining of macrophages and oxidation markers by plaque composition and cell type

Cell type and plaque component	KP-1	Apo-B100(MB47)	MDA-lysine(MDA2)	OxPL(E06)	IK17	Apo(a)(LPA4)
SMC expression (% of α-Actin)*	-	11.5	9.7	100	59	100
Foamy macrophage expression (% of KP-1 area)	-	25.2	10.4	100	100	100
Fibrous cap macrophages (% of KP-1 area)	-	100	56.6	100	100	100
Lipid pools (% of area)	1.1	6.3	1.0	4.7	5.6	24.8
Shoulder region (% of area)	8.2	1.4	1.0	13.8	9.7	17.5
Fibrous cap (% of area)	11.3	2.0	1.9	17.0	12.9	22.3
Necrotic core (% of area)	38.7	3.0	1.8	15.9	36.1	28.9

Values expressed as percentage of α-actin, KP-1, or plaque component.
* Values represent evaluation in AIT, IX, and PIT only, as SMCs were present only in very limited numbers in the progressive atherosclerotic lesions.

Table 3.

Quantitative immunostaining of macrophages and oxidation markers by plaque type

Morphology	Macrophages (KP-1)	ApoB-100 (MB47)	MDA-Lysine (MDA2)	OxPL (E06)	IK17	Apo(a) LPA4)
Non-progressive intimal lesions						
AIT (n=7)	0.08 ± 0.02	0.05 ± 0.03	0.4 ± 0.2	0.8 ± 0.3	0.02 ± 0.02	1.5 ± 0.3
IX (n=8)	19.4 ± 3.3	0.6± 0.4	0.8 ± 0.30	18.1 ± 5.1	5.4 ± 4.7	11.2 ± 5.9
Early progressive atherosclerotic lesions						
PIT (n=11)	1.4 ± 0.6	3.0 ± 0.9	0.9 ± 0.7	3.6 ± 0.9	2.9 ± 1.5	14.3 ± 3.8
EFA (n=25)	10.6 ± 1.5	1.8 ± 1.1	0.5 ± 0.1	5.3 ± 1.0	8.2 ± 1.6	11.8 ± 1.4
Late progressive atherosclerotic lesions						
LFA (n=17)	11.8 ± 2.1	1.3 ± 0.3	1.0 ± 0.4	7.5 ± 1.9	12.9 ± 3.1	17.1 ± 3.4
TCFA (n=13)	25.5 ± 3.6	3.6 ± 1.6	1.9 ± 0.6	18.0 ± 4.3	24.4 ± 4.8	31.1 ± 8.4
Plaque rupture (n=8)	25.9 ± 6.5	2.0 ± 0.7	2.3 ± 0.7	25.6 ± 5.4	31.9 ± 4.9	30.1 ± 5.9
P value*	< 0.0001	0.45	0.50	< 0.0001	< 0.0001	< 0.0001

Values represent mean percentage (± SEM) positive stained area of macrophage and lipid oxidation marker within each coronary section classified by dominant lesion type. *ANOVA, across all plaque types.

RESULTS

Qualitative and quantitative patterns of coronary artery immunostaining

Qualitative immunostaining patterns of macrophage, OSE, and apo(a) by plaque composition.

The immunostaining patterns and intensity by plaque composition in all plaque types are displayed in Table 1. The macrophage marker KP-1 strongly stained foam cells and the necrotic core, as expected. ApoB-100, detected by MB47, was seen primarily in early lesions in lipid pools and in lesser amounts in SMC-rich areas and the necrotic core. Foamy macrophages did not stain for apoB-100 with MB47. Malondialdehyde (MDA) epitopes, detected by MDA2, demonstrated a similar pattern of staining as apoB-100 but showed some positivity in foamy macrophages. OxPL epitopes, detected by E06, were strongest in macrophage-rich areas, lipid pools, and the necrotic core. IK17 epitopes were strongest within necrotic cores and were mainly present in areas rich in foamy macrophages. Apo(a) epitopes, detected by LPA4, were consistently present throughout early and late lesions, especially in macrophages and the necrotic core.

Quantitative immunostaining patterns of macrophages and oxidation markers by plaque composition and cell type in all plaque types.

Macrophage expression was primarily present in fibrous caps, shoulder areas, and the necrotic core (Table 2). ApoB-100 and MDA epitopes were primarily present in macrophage-rich areas in the fibrous cap and foamy macrophages, but they were almost absent in the necrotic core and shoulder regions. OxPL, IK17, and apo(a) epitopes were nearly uniformly expressed in SMC and macrophage-rich areas. IK17 epitopes were more prevalent in the necrotic core compared with the other epitopes. The fibrous cap expressed minimal apoB-100 and MDA epitopes, but OxPL, IK17, and apo(a) epitopes were present in 13–22% of the fibrous cap area.

Quantitative immunostaining patterns across plaque types and epitopes.
ACROSS PLAQUE TYPES.

The extent of macrophage staining was most prevalent in TCFA and plaque rupture, less so in IX, EFA, and LFA, and minimally in AIT and PIT (Table 3). Macrophages were primarily present in the necrotic core and within the fibrous cap and increased with advancing plaque types. ApoB-100 and MDA staining was minimal in most lesion types, representing only 3–4% at most of total lesion area. Staining for apoB-100 was generally within the extracellular space, most prominent within areas of lipid pools and SMCs. OxPL and IK17 epitopes were strongly present in plaque rupture, TCFA, and IX, less so in PIT, EFA, and LFA, and virtually absent in AIT. The predominant site of OxPL staining was in the necrotic

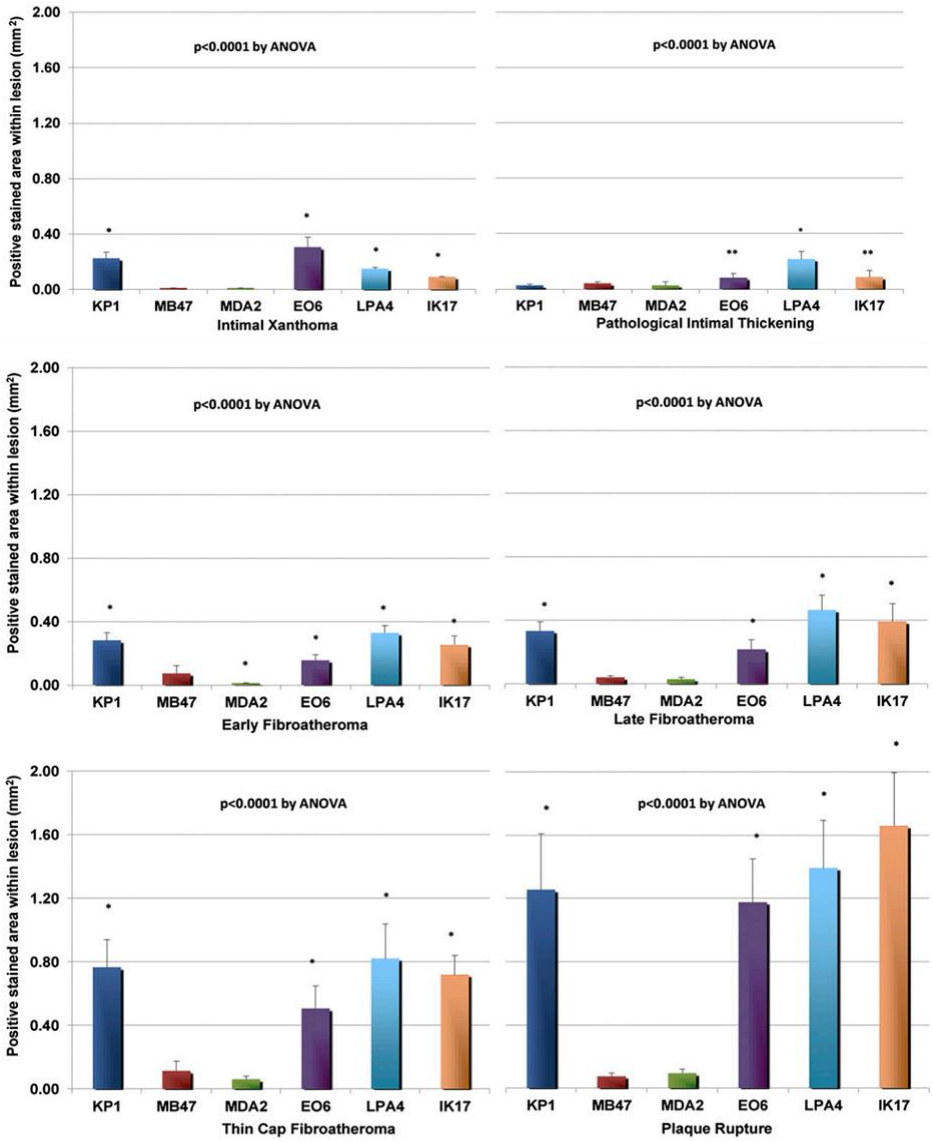

Figure 1. Morphometric analysis of macrophages and OSE between IX and PIT, EFA, LFA, TCFA, and ruptured plaques. Bars represent mean values (± SEM) of positively stained area (mm 2) of macrophages (KP-1) and lipid/oxidation markers. * P < 0.001, ** P < 05 compared with MB47 by posthoc Bonferonni correction of one-way ANOVA.

core and in foam cell macrophages. IK17 staining was most prominent in the necrotic core with strong positive staining also seen in macrophages. Apo(a) epitopes were strongly present in PR and TCFA, and they were modestly present in IX, PIT, EFA, and LFA, suggesting more nonspecific accumulation. Apo(a) staining was intense in the necrotic core, as well as in foam cell and non-foamy

macrophages. There was strong staining for OxPL, apo(a), and IK17 epitopes within the necrotic core of ruptured plaques (mean of total percentage OxPL, apo(a), and IK17 stained area, respectively, 60%, 57%, and 72%). OxPL and apo(a) were strongly expressed in foamy cell macrophages within the fibrous cap, whereas IK17 epitopes were mostly ab-sent within viable macrophages.

ACROSS EPITOPE TYPES. In normal coronary arteries with AIT, staining of macrophages and all OSE and apo(a) was negligible (data not shown). In contrast, IX contained few apoB-100 and MDA epitopes, significantly more macrophage, OxPL, and apo(a) epitopes, and fewer IK17 epitopes (Figure 1). PIT lesions were enriched in apo(a) epitopes. EFA and LFA were strongly positive for macrophages, OxPL, IK17, and apo(a) epitopes, whereas TCFA and plaque ruptures showed enhanced staining for macrophages, OxPL, apo(a), and IK17 epitopes. Significant differences were noted in expression of epitopes in all six lesion types by ANOVA (all $P < 0.0001$). In posttest Bonferonni analysis among paired comparison of epitope types, in general, significant differences were not present between apoB and MDA2 epitopes, but they were present among OxPL, apo(a), and IK17 epitopes (ranging from $P < 0.05$ to $P < 0.001$).

Morphometric patterns of immunostaining

Intimal xanthoma. Immunostaining of normal segments of coronary arteries revealed no staining with any of the oxidation-specific monoclonal antibodies, but there was occasional minimal endothelial cell staining noted with monoclonal antibody LPA4 for apo(a) epitopes. Immunostaining of an intimal xanthoma (Figure 2) shows an early superficial lesion rich in macrophages without evidence of necrosis. There is a relative absence of staining for apoB-100 and MDA epitopes but strong positive staining for OxPL, which are present in areas rich in macrophages and SMCs. IK17 and apo(a) epitopes are expressed in select populations of macrophages in a distribution different from E06.

Pathologic intimal thickening. Immunostaining of pathologic intimal thickening (Figure 3) shows a superficial plaque with an acellular lipid pool in a proteoglycan-rich matrix. SMCs are mostly present in the medial wall and superficial layers outside the lipid pool, whereas macrophages are present above the regions of the lipid pool. There is moderate staining for apoB-100 but intense staining for apo(a) in areas of the lipid pool. Staining for MDA epitopes is essentially negative. OxPL staining is primarily present in areas of superficial macrophages and SMCs above the area of the lipid pool, whereas weak to moderate staining for IK17 epitopes is seen in the lipid pool.

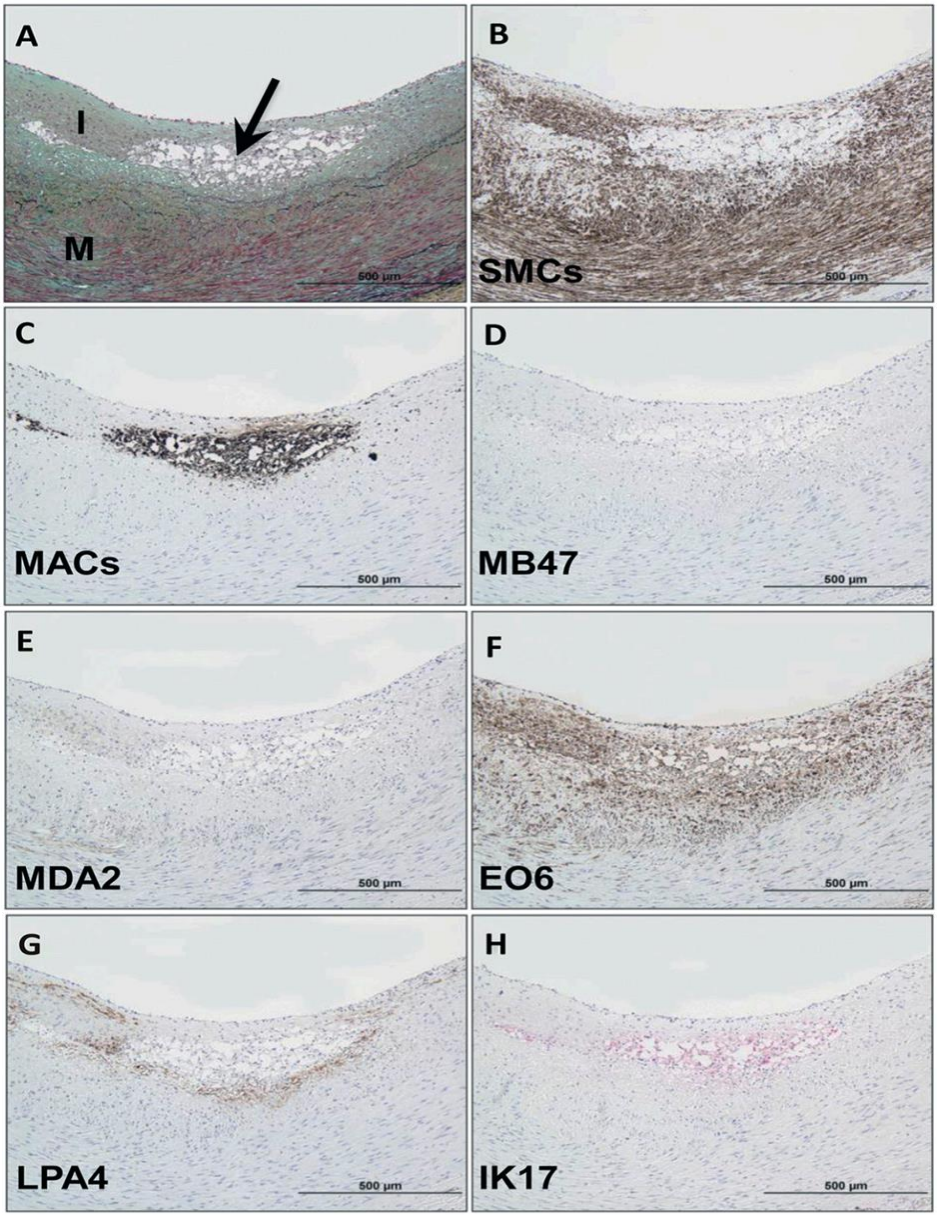

Figure 2. Immunostaining of OSE in a human coronary intimal xanthoma. A: Intimal xanthoma recognized as an early superficial lesion rich in macrophages without evidence of necrosis. Arrow, Movat pentachrome; I, intima; M, media) B: Areas of SMC (anti-SMC α-actin). C: Localization of CD68 staining for macrophages, which do not overlay regions of SMCs. D, E: Relative absence of staining for apoB-100 (MB47) and MDA epitopes (MDA2), respectively. F: Strongly positive OxPL (E06) staining colocalizes with macrophages and nearby SMCs of the neointima. G, H: apo(a) (LPA4) and IK17 epitopes, respectively, are expressed in select populations of macrophages. B–G: Immunoperoxidase (brown reaction product). H: Alkaline phosphatase (red reaction product). Magnification ×200.

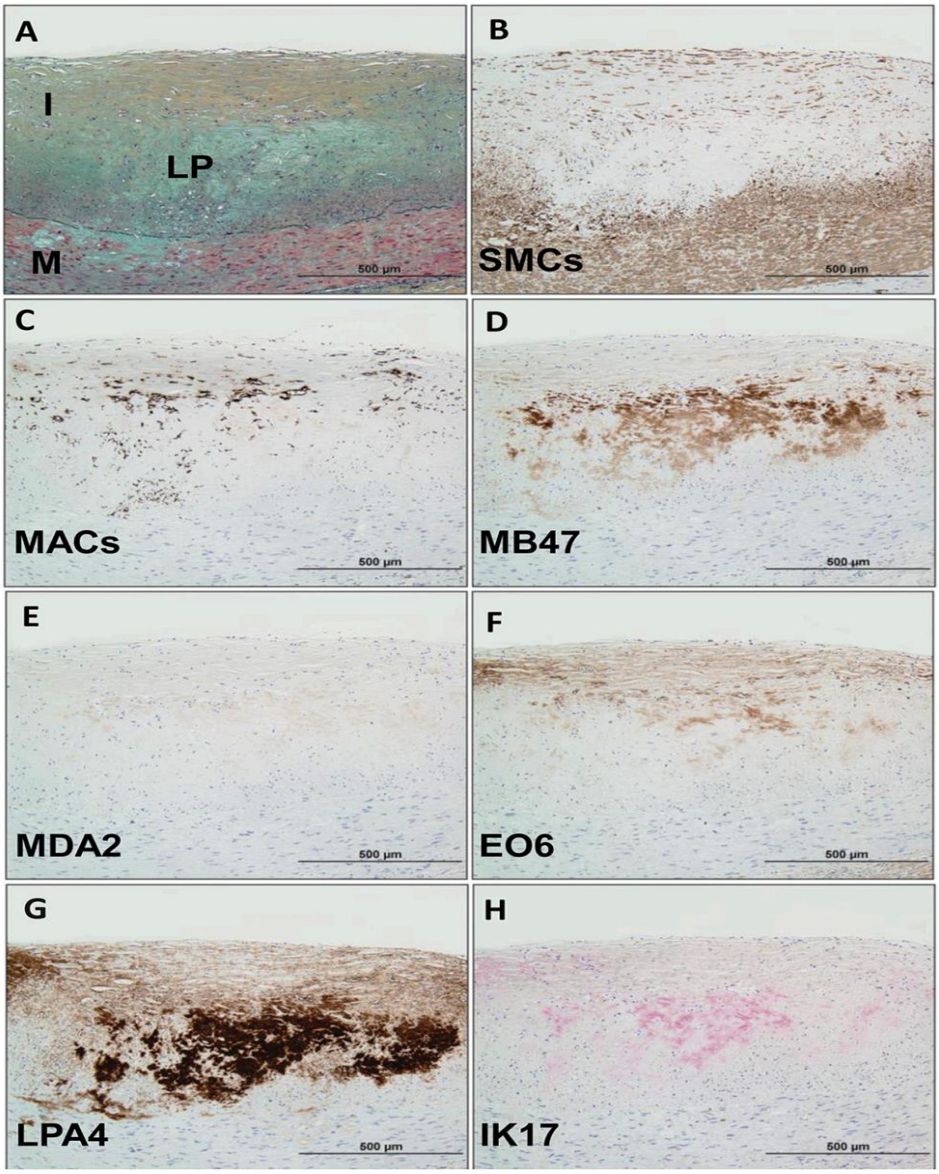

Figure 3. Immunostaining of OSE in a human coronary lesion recognized as pathologic intimal thickening. A: Human coronary lesion shows a superficial plaque with an acellular lipid pool (LP) rich in proteoglycan matrix. Movat pentachrome; I, intima; M, media. B: α-Actin-positive SMCs are mostly localized to the medial wall and superficial layers outside the LP. C: Localization of CD68 staining shows few positive macrophages above the regions of the LP. D: Moderate staining for MD47 is noted for superficial macrophages and deeper areas of the LP. E: MDA2 expression is essentially negative. F: E06 is found primarily localized to superficial macrophages and SMCs above the area of the LP. G: Intense reaction against LPA4 primarily localized to the region of the LP. H: Weak to moderate staining of IK17 is seen in the LP. B–G: Immunoperoxidase (brown reaction product). H: Alkaline phosphatase (red reaction product). Magnification ×200.

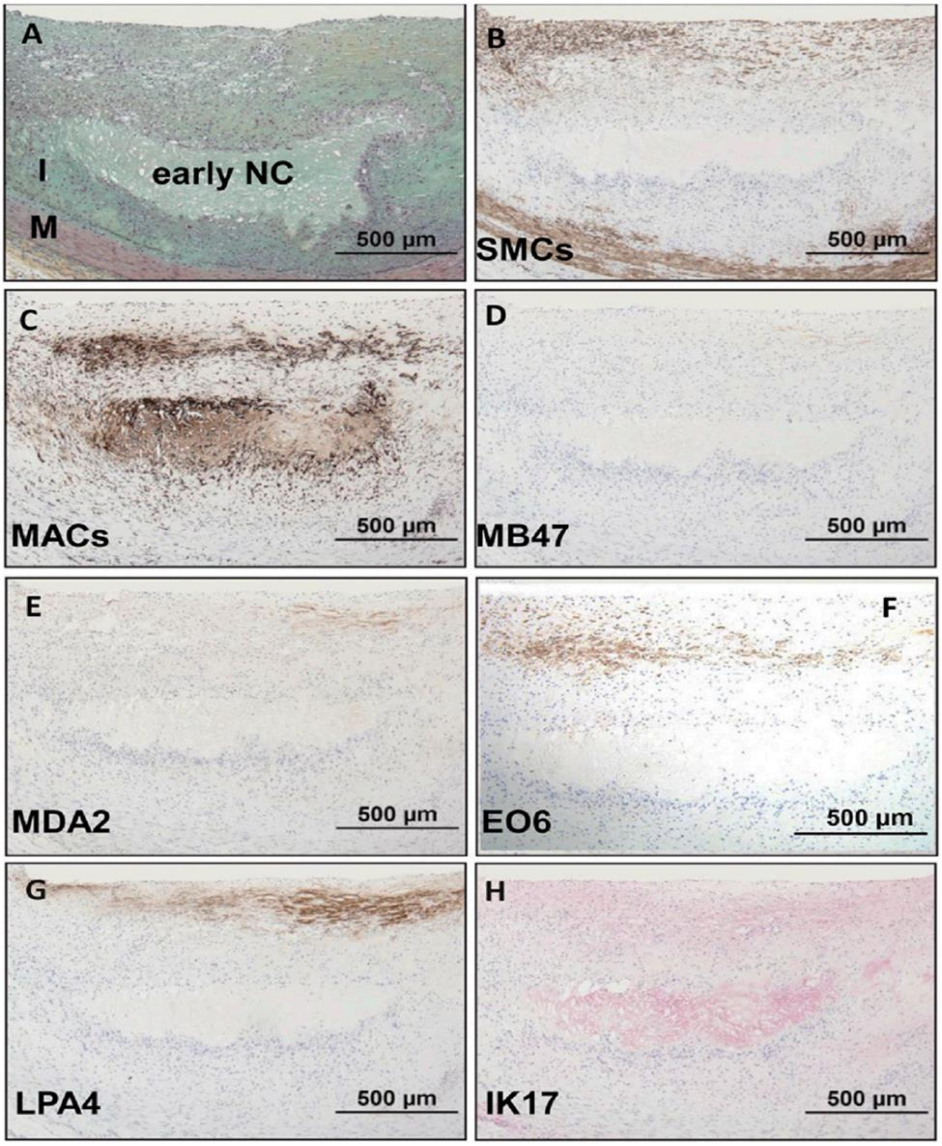

Figure 4. Immunostaining of OSE in a human coronary lesion recognized as early fibroatheroma. A: Human coronary lesion shows a superficial plaque with an early necrotic core (NC) characterized by macrophages, free cholesterol, and extracellular matrix. Movat pentachrome; I, intima; M, media. B: α-Actin-positive SMCs are mostly localized to the medial wall and fibrous cap. C: Localization of CD68 staining shows positive intense macrophage staining of the fibrous cap and necrotic core. D, E: Negative staining for MD47 and MDA2, respectively. F: E06 is found primarily localized to macrophages of the fibrous cap. G: Expression of LPA4 is primarily localized to the extracellular matrix of the fibrous cap. H: Weak to moderate staining of IK17 is seen in the necrotic core. B–G: Immunoperoxidase (brown reaction product). H: Alkaline phosphatase (red reaction product). Magnification ×200.

Early fibroatheroma. Immunostaining of an early fibroatheroma (Figure 4) shows a superficial plaque with an early necrotic core characterized by macrophages, free cholesterol, and extracellular matrix. SMCs are mostly present in the medial wall and fibrous cap, whereas macrophages stain intensely in the fibrous cap and necrotic core. Staining for apoB-100 and MDA epitopes is essentially negative. OxPL are primarily present in areas rich in macrophages in the fibrous cap, whereas weak to moderate staining for IK17 epitopes is seen in the necrotic core. Expression of apo(a) is primarily localized to the extracellular matrix of the fibrous cap.

Late fibroatheroma. Immunostaining of a late fibroatheroma (Figure 5) shows an intact thick fibrous cap overlying a late necrotic core characterized by cell debris, free cholesterol, and relative absence of extracellular matrix. SMCs are present in the media and superficial area of the fibrous cap. Macrophages are mainly present in the necrotic core and pericore regions, with some infiltration in the fibrous cap. There is relatively weak staining for apoB-100 in the region of the necrotic core, and MDA epitopes are essentially absent. OxPL and apo(a) epitopes show a similar distribution and are found primarily in the extracellular matrix of the fibrous cap and necrotic core. IK17 epitopes are strongly positive in the necrotic core and absent elsewhere.

Thin cap fibroatheroma. Immunostaining of a thin cap fibroatheroma (Figure 6) shows an intact thin fibrous cap overlying a late necrotic core. SMCs are conspicuously absent in the fibrous cap but present in the media and intimal/medial interface. There is marked infiltration of macrophages in the thin fibrous cap and underlying necrotic core. ApoB-100 is predominantly localized to the necrotic core and surrounding acellular areas, and MDA epitopes are seen in similar areas, except the intensity of staining is markedly weaker. OxPL are primarily present in the fibrous cap rich in macrophages and in the extracellular matrix, including in the periphery of the necrotic core. There is intense staining for apo(a) in the fibrous cap and regions of the necrotic core, mostly in the extracellular matrix. IK17 is strongly positive in the late necrotic core.

Plaque rupture. Immunostaining of plaque rupture (Figure 7) shows a coronary lesion with fibrous cap disruption and superimposed luminal thrombus. SMCs are present in the medial layer but not in the plaque. In contrast, there is marked infiltration of macrophages in the fibrous cap and underlying necrotic core. Staining for apoB-100 is essentially negative. MDA epitopes are moderately expressed in the fibrous cap within cells and extracellular matrix and necrotic core. OxPL are primarily localized to macrophages in the periphery of the necrotic core. There is intense reaction to apo(a) in the disrupted fibrous cap overlying the necrotic core. IK17 epitopes are present only in the late necrotic core.

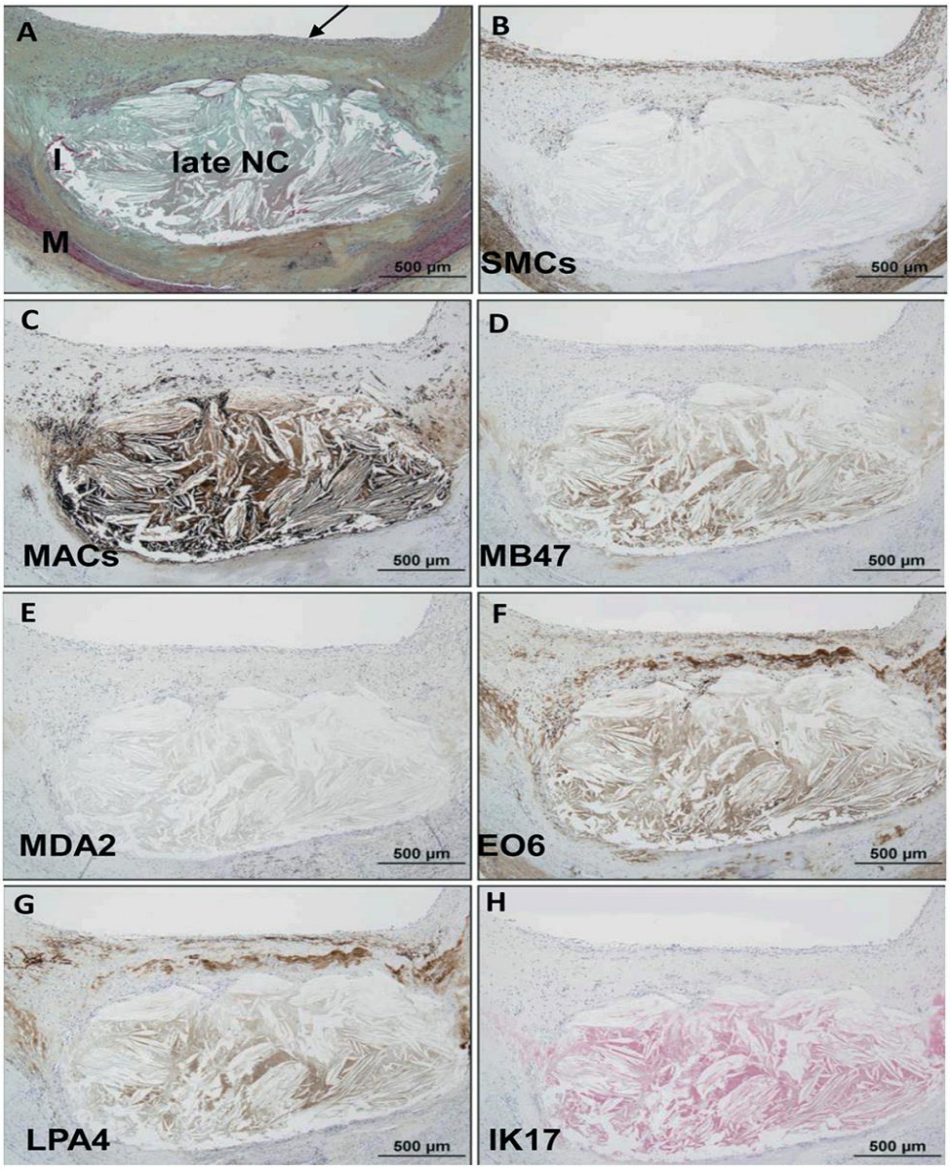

Figure 5. Immunostaining of OSE in human coronary fibroatheroma with late necrosis. A: Human coronary lesion with an intact thick fibrous cap (arrow) overlying a late necrotic core (NC) characterized by cell debris, free cholesterol, and relative absence of extracellular matrix. Movat pentachrome; I, intima; M, media. B: α-Actin staining for SMCs is positive in the media and superficial area of the fibrous cap. C: Localization of CD68 staining shows infiltration of macrophages within the fibrous cap but mostly necrotic core and pericore regions. D: Relatively weak staining for MD47 in the region of the necrotic core. E: MDA2 expression is negative. F: E06 is found primarily localized to the extracellular matrix of the fibrous cap and necrotic core. G: Staining intensity and localization of LPA4 is similar to E06 in (F). H: IK17 is strongly positive in the NC. B–G: Immunoperoxidase (brown reaction product). H: Alkaline phosphatase (red reaction product). Magnification ×200.

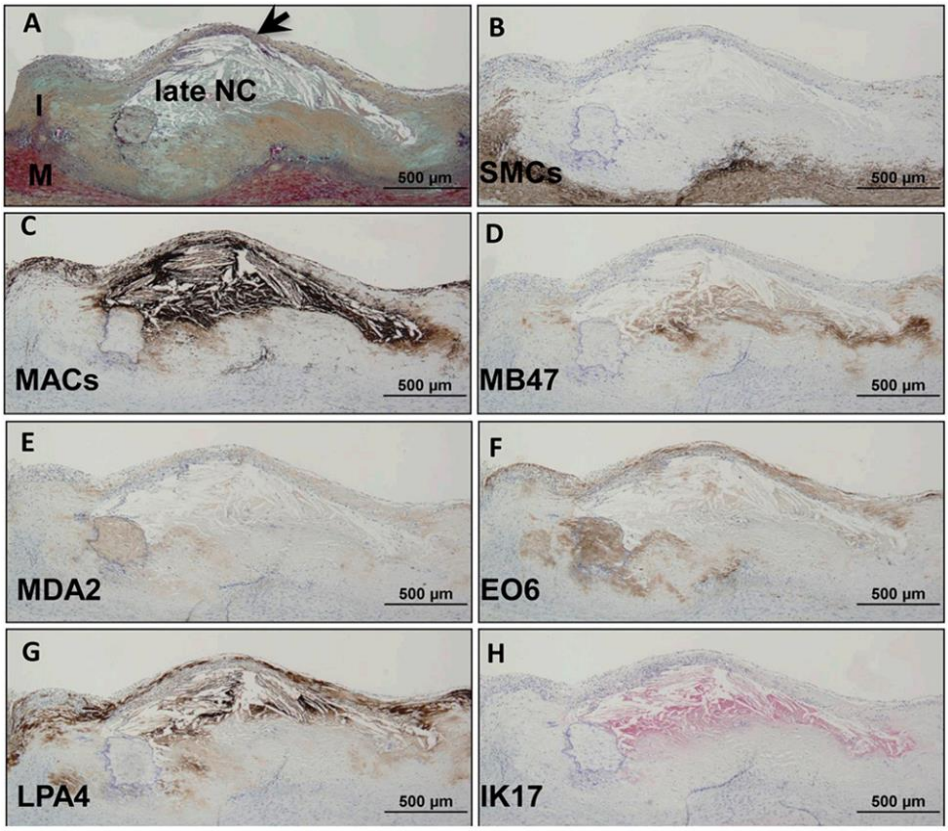

Figure 6. Immunostaining of OSE in human coronary TCFA or high-risk plaque for rupture. A: Human coronary lesion with an thin intact fibrous cap (arrow) overlying a late necrotic core (NC). Movat pentachrome; I, intima; M, media. B: α-Actin staining for SMCs is positive in the media and intimal/medial interface, whereas the majority of plaque, in particular the fibrous cap, is negative. C: Localization of CD68 staining shows marked infiltration of macrophages in the thin fibrous cap and underlying necrotic core. D: Staining for MD47 is predominantly localized to the necrotic core and surrounding acellular areas. E: MDA2 expression is seen in similar areas as in (D), except the intensity of staining is markedly weaker. F: E06 is found primarily localized to fibrous cap macrophages and extracellular matrix including in the periphery of the necrotic core. G: Intense reaction against LPA4 is seen in the fibrous cap and regions of the necrotic core, mostly in the extracellular matrix. H: IK17 is strongly positive in the late NC. B–G: Immunoperoxidase (brown reaction product). H: Alkaline phosphatase (red reaction product). Magnification ×200.

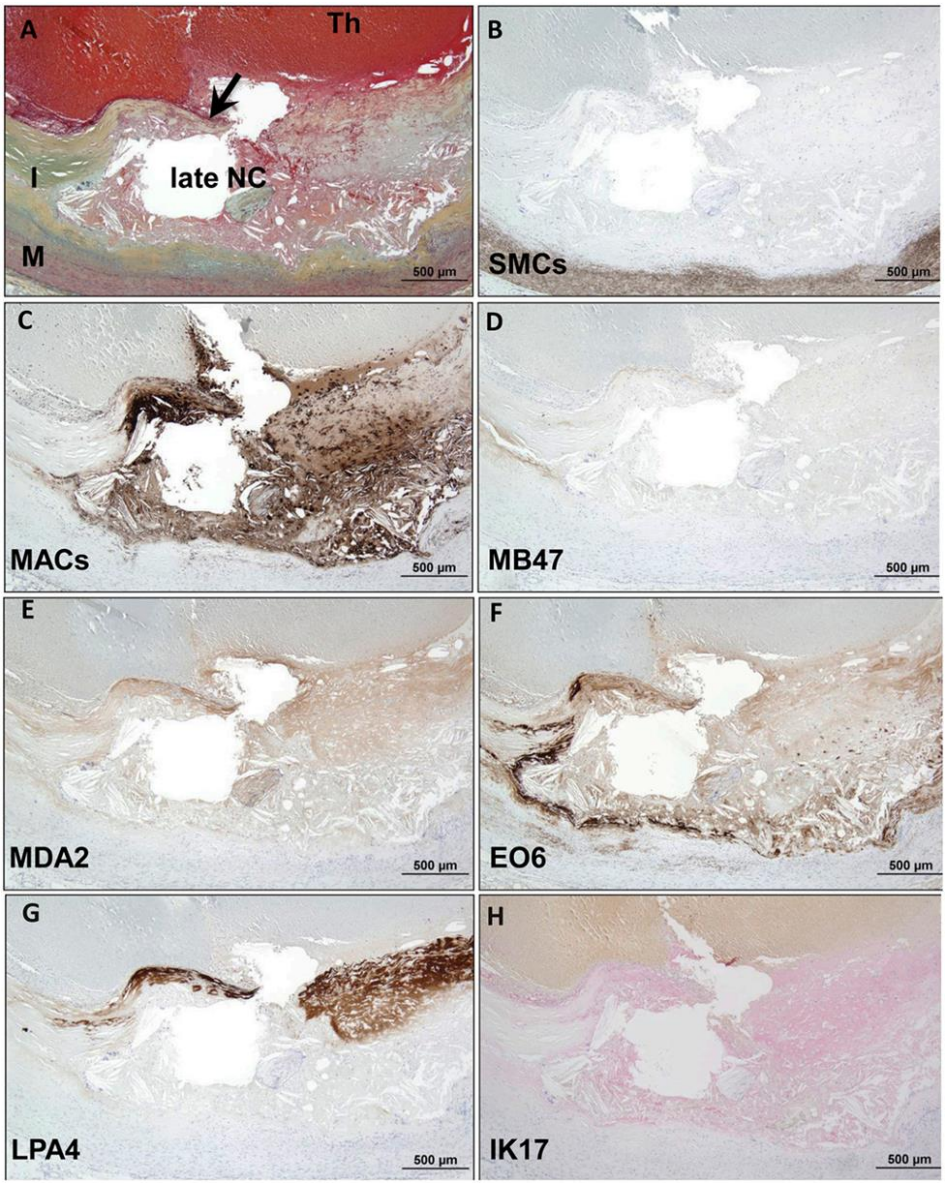

Figure 7. Immunostaining of OSE in human coronary plaque rupture. A: Human coronary lesion with fibrous cap disruption (arrow) and superimposed luminal thrombus (Th, arrow). Movat pentachrome; I, intima; M, media. B: α-Actin staining for SMCs is positive in the medial layer but negative in the plaque. C: Localization of CD68 staining shows marked infiltration of macrophages in the fibrous cap and underlying late necrotic core (NC). D: Staining for MD47 is essentially negative. E: MDA2 expression is moderately expressed in the fibrous cap within cells and extracellular matrix and necrotic core. F: E06 is found primarily localized to macrophages in the periphery of the necrotic core. G: Intense reaction against LPA4 is seen in the disrupted fibrous cap overlying the necrotic core. H: Weak to moderate staining of IK17 is seen in the late NC. B–G: Immunoperoxidase (brown reaction product). H: Alkaline phosphatase (red reaction product). Magnification ×200.

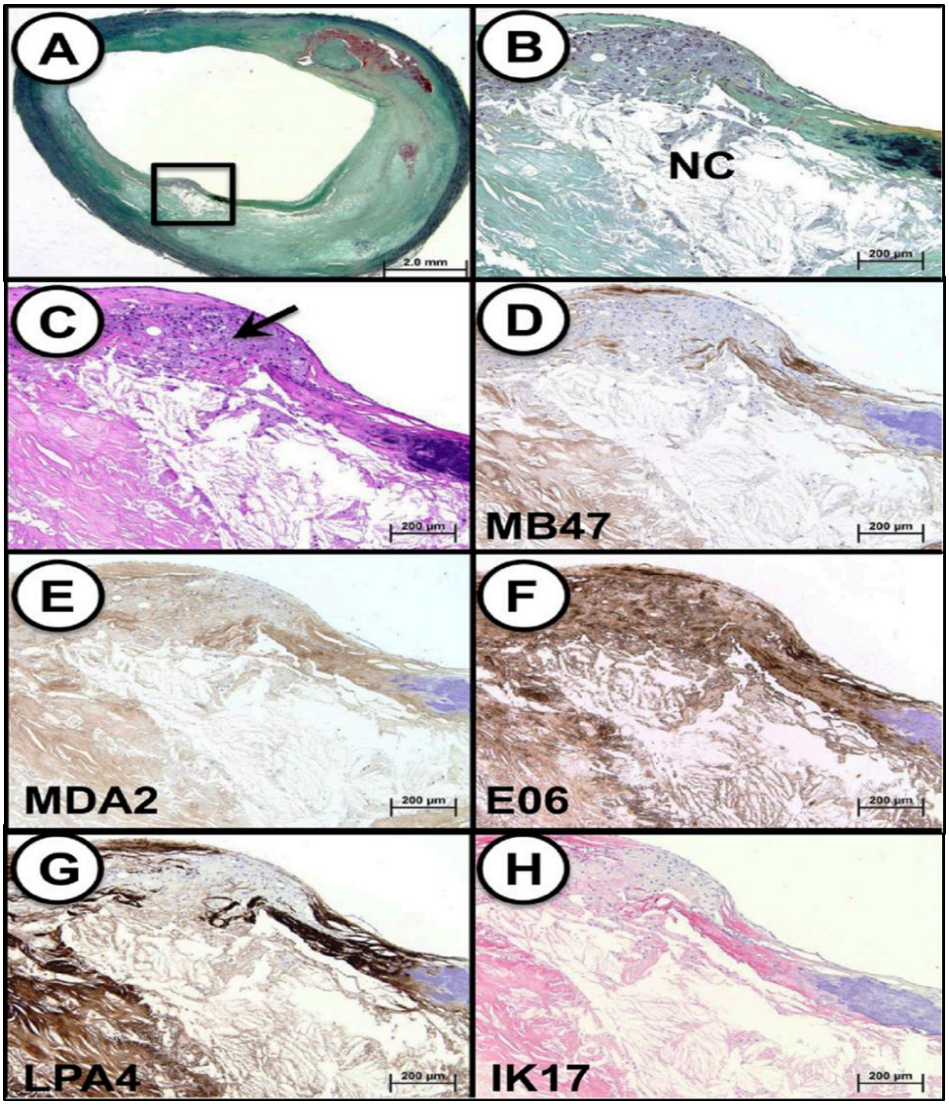

Figure 8. Immunostaining of OSE in human carotid TCFA. A: Low-power view of a TCFA (Movat pentachrome); note the insignificant clinical stenosis. B: Higher power view of the region represented by the black box in (A) showing a necrotic core (NC) with a overlying intact thin fibrous cap, which is partially degraded by infiltrating macrophages. C: Cluster of macrophages within the fibrous cap (arrow; H and E staining). D: Immunostaining for MD47 is predominantly localized to the less lytic areas of necrotic core (lower left) and extracellular matrix of the fibrous cap; there is a relative absence of staining within fibrous cap macrophages. E: MDA2 expression is diffusely present in the fibrous cap, including macrophages and less lytic areas of the necrotic core; the staining intensity is the weakest of the five OSE epitopes. F: EO6 is strongly positive within the fibrous cap, including macrophages, as well as connective tissue and necrotic core. G: Immunostaining against LPA4 is intense in the less lytic areas of the necrotic core and connective tissue matrix. H: Staining pattern for IK17 mirrors that of LPA4 in which a strong signal is noted in the less lytic areas of the necrotic core and connective tissue matrix. D–G: Immunoperoxidase (brown reaction product). H: Alkaline phosphatase (red reaction product). A: Magnification ×10.25. B–H: Magnification ×100.

Presence of OSE in carotid endarterectomy specimens

We also studied carotid endarterectomy specimens that were surgically removed en bloc and then immediately fixed in neutral buffered formalin. Remarkably, these carotid lesions displayed findings very similar to those observed with the coronary lesions. An example of immunostaining of a carotid TCFA with a necrotic core and presence of macrophages signifying the presence of OSE is shown in Figure 8. Similar to the findings in the coronary arteries, apoB and MDA epitopes were predominantly localized to the less lytic areas of necrotic core. However, OxPL, apo(a) and IK17 epitope staining was strongly positive within macrophages and the necrotic core.

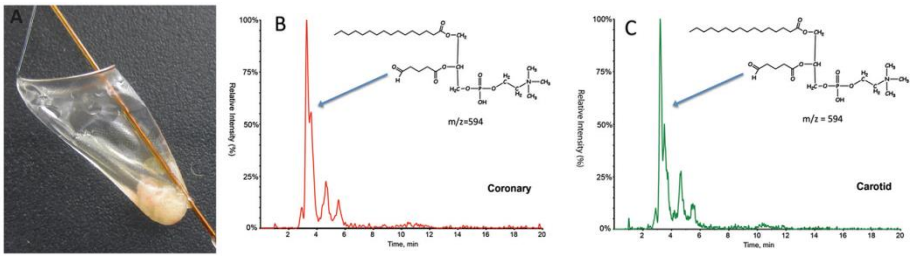

Figure 9. A: Atheroemboli captured in a FilterWire following SVG intervention. B, C: LC-MS/MS multiple reaction monitoring (MRM) analysis of 1-palmitoyl-2-(5 ′-oxo-valeroyl)-sn-glycero-3-phosphocholine (POVPC) (m/z= 594) identified in atherosclerotic debris recovered from distal embolic protection filters following percutaneous angioplasty and stent placement of coronary SVG (B) and internal carotid artery (C). The later eluting, lower intensity peaks are due to stereoisomer effects.

Presence of OxPL in carotid and coronary SVG distal protection devices documented by LC-MS/MS. To obtain physical evidence for the presence of oxidized lipids in these necrotic lesions, we collected plaque material released from such lesions during interventional procedures and trapped by distal protection devices. The filters were placed in potent antioxidants, frozen at -70°C, and then lipid extracted and examined by LC-MS/MS for the presence of OxPL. Protonated adducts of 1-palmitoyl-2-(5 ′-oxo-valeroyl) sn -glycero-3-phospho-choline (POVPC) (m/z 594), a well validated bioactive, pro-inflammatory and pro-atherogenic OxPL (25, 26) that reacts with E06 (27), were detected from both carotid and coronary distal SVG protection devices (Figure 9). This finding demonstrated that the OxPL detected in both the coronary and carotid lesions by E06 immunostaining represented epitopes present *in vivo* and not products of artifactual oxidation that occurred during tissue processing.

Effect of time to harvest and expression of OSE

Immunostaining of freshly procured carotid endarterectomy specimens stored at room temperature for 24 h, on ice for 24 h, or in antioxidants for 24 h demonstrated no appreciable qualitative differences in immunostaining patterns among antibodies with different methods of storage prior to analysis (Figure 10).

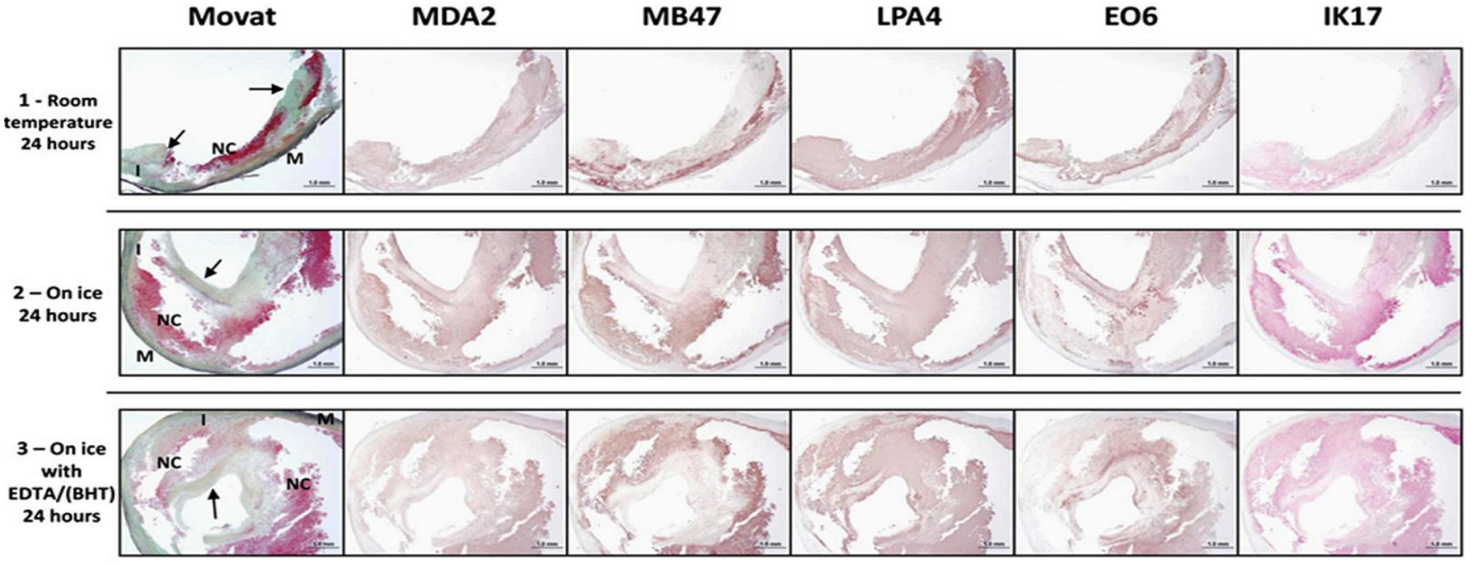

Figure 10. Immunostaining of oxidation-specific epitopes represented by antibodies MDA2, MB47, LPA4, EO6, and IK17 of fresh human carotid endarterectomy specimens. Prior to paraffin embedding, the endarterectomy specimens were manually cut into three sections (proximal, mid, distal) because the specimens were not symmetrical, and due to some fragmentation during removal, the immunostained sections are of different size. Specimens were then handled according to the following procedures: (Row 1) Proximal specimen stored at room temperature for 24 h in PBS (phosphate buffered saline. Staining for MDA2 is weakly present in predominantly the necrotic core. MB47 staining is more intense and seen in similar areas as for MDA2. Expression of LPA4 and EO6 is located in the extracellular matrix regions of the fibrous cap and the necrotic core. IK17 is positive in the late necrotic core. Fibrous cap (arrows) adjacent and partially overlying a late necrotic core (NC). Movat pentachrome; I, intima; M, media. (Row 2) Mid specimen stored on ice for 24 h in PBS. MDA2 expression is present within the necrotic core. MB47 expression is more intense and is located within the areas as seen in the MDA2 staining. The localization of LPA4 and EO6 expression is similar as described for row 1, mostly in the extracellular matrix regions of the fibrous cap and the necrotic core. IK17 is strongly positive in the large late necrotic core. (Row 3) Distal specimen stored on ice in EDTA/BHT antioxidant for 24 h. MDA2 is weakly present in the necrotic core, whereas MB47 expression is more intense. Expression of LPA4 and EO6 is mostly seen in the extracellular matrix regions of the fibrous cap and the necrotic core, and the intensity of the staining is comparable to the staining in row 2. IK17 is strongly present in the late necrotic core. MDA2, MB47, LPA4, EO6: Immunoperoxidase (brown reaction product). IK17: Alkaline phosphatase (red reaction product). Magnification ×100.

DISCUSSION

This is the first comprehensive analysis evaluating several well-characterized OSE and apo(a) in a wide range of human coronary, carotid, and SVG atherosclerotic lesions. The study demonstrates a differential expression of apoB-100, OSE, and apo(a) in the progression of atherosclerosis from early lesions to plaque rupture. Plaques that develop during early atherosclerosis are enriched in apoB-100, apo(a), and all the OSE measured in this study. However, as lesions progress, apo(a), OxPL, and IK17 epitopes become progressively enriched. Specifically, apo(a) epitopes were present in most lesions, whereas OxPL and IK17 epitopes were mainly associated with foamy macrophages of the fibrous cap and the necrotic core. IK17 epitopes were most specifically associated with necrotic cores and plaque rupture. Additionally, a similar distribution was noted in TCFA of freshly procured carotid endarterectomy specimens. Finally, LC-MS/MS documented the presence of OxPL in material trapped by distal protection devices, documenting their presence in vivo in clinically symptomatic plaques. These observations provide a frame-work for understanding the relationship between OSE and Lp(a) and the progression and destabilization of human coronary and carotid atherosclerosis.

This study used unique monoclonal antibodies targeting well-characterized lipoprotein and OSE to study their relationship to human atherosclerosis, as described in Methods. For example, MB47 detects not only the native apoB-100 moiety of unoxidized LDL but also apoB of minimally oxidized LDL and even apoB fragments of extensively oxidized LDL. MDA2 can recognize both MDA-LDL as well as MDA-lysine epitopes on other proteins in the vessel wall, such as apoAI[28,29], and it has also been utilized for noninvasive imaging of experimental atherosclerotic lesions[3,4,5]. E06 is a well-characterized murine IgM natural antibody cloned from apoE $^{-/-}$ mice (20) that has previously been used to stain mouse and rabbit atherosclerotic lesions and to image atherosclerotic lesions in apoE $^{-/-}$ mice using magnetic resonance techniques[3,4,5]. E06 is also used in plasma immunoassays to detect OxPL on circulating apoB-100 particles (OxPL/apoB) in humans[10]. In support of these pathologic findings, plasma levels of the OxPL epitopes on apoB-100 particles (OxPL/apoB) measured by E06 were recently shown to be strongly associated with the presence of angiographically defined coronary artery disease, to predict the presence and progression of carotid and femoral atherosclerosis, and to predict cardiovascular death, myocardial infarction, and stroke in unselected epidemiological populations[30,31]. LPA4 binds to the apolipoprotein(a) portion of Lp(a) and is used in immunoassays to measure plasma Lp(a) levels, but it has not been previously used to immunostain tissues[23]. Apo(a) itself is not an oxidation-specific epitope, but apo(a) and Lp(a) bind OxPL, which may reflect the

key atherogenic component of Lp(a)[32]. IK17 is a human Fab fragment derived from a phage dis-play library, and it binds to a unique MDA-like epitope present on both MDA-LDL and copper-oxidized LDL. IK17 has also been used in detecting and imaging atherosclerosis in LDLR $^{-/-}$ mice and apoE $^{-/-}$ mice[3,4,5,22].

The differences in immunoreactivity patterns present among the different antibodies suggest that specific epitopes are generated and/or enriched during different pathophysiological stages of lesion development, progression, and destabilization. Such epitopes can be generated through peroxidation of unsaturated fatty acids present on lipoproteins, phospholipids, and cell membranes in the vessel wall, as well when cells, such as macrophages, undergo apoptosis. Despite the fact that these epitopes are generated through oxidative modification, expression of specific epitopes appears dependent on the stage of lesion progression. For example, MDA epitopes were more common in early lesions, such as in PIT and early fibroatheromas, whereas OxPL, apo(a), and IK17 epitopes were more prevalent in advanced lesions. Most of the prior data with antibody MDA2 were generated in mouse and rabbit models, with early to intermediate lesions showing diffuse staining patterns both intra and extracellularly[33]. MDA2 has been used to stain early lesions in teenage subjects in the Bogalusa Heart Study[34]. Surprisingly, in the current study, MDA epitopes did not become more prevalent as lesions advanced. It may be postulated that MDA epitopes are generated early in the development of atherosclerosis and may more closely reflect plaque initiation and plaque accumulation rather than plaque destabilization. It is also possible that there is decomposition of these epitopes in more aged tissues. We have recently shown that complement factor H also binds MDA epitopes, both in the eyes of patients with macular degeneration and in human coronary atherectomy specimens[35]. In fact, prior side-by-side staining of such tissues with anti-CFH antibodies and MDA2 has shown partial co-localization but also in-dependent staining. It is possible that CFH may bind and mask some of these epitopes. It is also possible that these epitopes may be bound by autoantibodies to MDA-LDL that have been well characterized[36]. Additionally, some of these epitopes may be transported out of the lesion wall on migrating macrophages or lipoproteins.

In contrast, apo(a), OxPL, and IK17 epitopes were highly prevalent in foamy macrophages in thin fibrous caps, necrotic cores, and ruptured plaques, suggesting that they more closely reflect advancing and unstable plaques. In conjunction with these findings in late lesions, there was also a similarly increased expression of macrophage markers and a lack of SMC, consistent with the pathophysiological findings of plaque vulnerability. Thus, the expression of apo(a), OxPL, and IK17 epitopes may more closely reflect plaque inflammation, destabilization, and rupture. Some variability was noted in the earlier stage coronary lesions in cell-

associated OxPL staining, and some of this may be due to destruction of OxPL epitopes as lesions progress. Alternatively, changes in extracellular matrix components in later stage lesions may allow greater accumulation of noncell-associated epitopes. Similarly, although both the carotid and coronary plaque are considered TCFA, the extent of macrophages, particularly in the cap region, appears much greater for the carotid, and E06 staining is present both in the macrophages of the cap and cap ECM, whereas relatively less in the necrotic core. These data in human lesions that span a broad array from early lesions to plaque rupture can only be tangentially compared with animal data in which most lesions studied are at the fatty-streak level. Nonetheless, the staining patterns for equivalent lesions seem similar, and these epitopes are equally expressed in animals and humans and are not species specific, but specific to the oxidative pathways generating these epitopes.

The origin and generation of the OSE merits some discussion. ApoB-100 is present on VLDL, VLDL remnants (IDL), LDL, and Lp(a). Once such apoB-containing lipoproteins enter the arterial intima, they bind to extracellular matrix[37] and then undergo oxidation mediated by a variety of free radical-mediated mechanisms. This likely explains the presence of apoB and MDA epitopes in relatively early lesions. As plaques progress, macrophage number and activation increase, which among other properties, leads to further oxidation of LDL, resulting in progressive lipid oxidation and accumulation of OxPL and IK17 epitopes. IK17 epitopes, which appear primarily in the necrotic core where macrophage foam cells and necrotic debris have accumulated, may represent a byproduct of very advanced oxidation of MDA-related adducts. Interestingly, prior attempts in our laboratory to detect IK17 epitopes on circulating lipoproteins, which appear to reflect advanced MDA-related epitopes, have been unsuccessful (S. Tsimikas, unpublished observations), suggesting that they may only be present in highly oxidized lipids and modified proteins within advanced lesions. It is important to note that both E06 and IK17 bind to apoptotic cells and apoptotic debris[2,22], which are clearly enriched in late lesions and a major contributor to the unstable plaque. Indeed, Lp(a) and the OxPL it contains are likely to be a major stimulus leading to macrophage apoptosis and cell death[24]. Further studies are needed to define the pathways through which these various OSE are generated *in vivo*.

In the current study, it was clearly demonstrated that Lp(a) is quite ubiquitous in atherosclerotic plaques, even in early lesions, and that it progressively increases as lesions progress to plaque rupture. The fact that apoB, apo(a), and OxPL did not necessarily uniformly co-localize suggests that the apoB and OxPL components of Lp(a) may be degraded and removed but that the apo(a) component continues to be bound to the plaque and have a longer residence time[38]. It also suggests that

additional and quantitatively significant amounts of OxPL are formed in the vessel wall in situ and independently of those OxPL potentially carried by Lp(a). Consistent with the current findings of the enhanced presence of Lp(a) in vulnerable plaques, a correlation was previously noted with plasma Lp(a) levels, apo(a) immunopositivity in atherectomy specimens, and the severity of the clinical presentation in patients with acute coronary syndromes[39]. Indeed, as noted above, Lp(a) may well promote macrophage cell death via a CD36/TLR2-dependent process, thus contributing to plaque rupture[24]. With the confluence of data showing that Lp(a) is an independent and potentially causal risk factor for cardiovascular disease[40,41] and with emerging therapeutic interventions to lower Lp(a)[42,43, 44 and B. C. Kolski and S. Tsimikas, unpublished observations], these data provide a scientific rationale why Lp(a) may contribute to both plaque progression and plaque destabilization, and they validate potential therapeutic targeting approaches.

Limitations

Artifactual oxidation may have occurred during procurement of the coronary specimens due to delay in harvesting after sudden death, and it may have impacted the findings in the later stage lesions. However, this cannot explain the findings with the carotid or SVG, as they were processed immediately in EDTA/BHT and handled optimally subsequently to maximally limit artifactual oxidation. In these specimens, we saw the same pattern of OSE expression. In addition, the fact that MDA epitopes did not increase with lesion size and that the experimental study of various exposures of carotid endarterectomy specimens showed no major differences in immunostaining suggests that if postmortem oxidation did occur in the coronary specimens, it did not significantly impact the findings.

Clinical implications and conclusions

This comprehensive analysis of a range of human plaque types and stages of atherosclerosis demonstrates that OSE, in particular those detected by antibodies E06, IK17, and LPA4, are highly prevalent and progressively enriched in advancing atherosclerotic lesions and ruptured plaques. Several translational "biotheranostic" (biomarker, therapeutic, and diagnostic imaging) approaches targeting OSE, such as in-vitro assays, *in vivo* and noninvasive diagnostic imaging modalities, and therapeutic applications have reached the investigational clinical frontier[9,11,12]. As these studies ultimately make their way to clinical applications, the data generated in this study will provide a foundation for appropriate clinical applications and interpretation of the findings. Furthermore, the presence of vasoactive OxPL within distal protection devices is consistent with our prior data showing increased OxPL in plasma following PCI[23], and it suggests the design of studies with therapies directed to binding and inactivating OxPL or other OSE released during percutaneous coronary, carotid, SVG, or peripheral interventions. For example, this could be achieved by infusing oxidation-specific antibodies or similarly directed therapies at time of presentation of an acute vascular syndrome or prior to intervention, such as with humanized E06-type antibodies or the human antibody IK17, which has been shown to bind OSE, prevent foam cell formation, and reduce atherosclerosis progression when infused in atherosclerotic mice[9]. Because this study is retrospective and cross-sectional, it does not prove causality for the role of OSE in plaque progression and rupture. Future studies using human OSE antibodies therapeutically and showing clinical efficacy will be needed to prove the role of OSE in mediating CVD events.

REFERENCES

1. Miller , Y. I. , S. H. Choi , P. Wiesner , L. Fang , R. Harkewicz , K. Hartvigsen , A. Boullier , A. Gonen , C. J. Diehl , X. Que , *et al*. 2011. Oxidation-specific epitopes are danger-associated molecular patterns recognized by pattern recognition receptors of innate immunity. Circulation Research. 108: 235 – 248.

2. Chang , M. K. , C. J. Binder , Y. I. Miller , G. Subbanagounder , G. J. Silverman , J. A. Berliner , and J. L. Witztum. 2004. Apoptotic cells with oxidation-specific epitopes are immunogenic and proinflammatory. Journal of Experimental Medicine. 200: 1359 – 1370.

3. Briley-Saebo , K. C. , P. X. Shaw , W. J. Mulder , S. H. Choi , E. Vucic , J. G. Aguinaldo , J. L. Witztum , V. Fuster , S. Tsimikas , and Z. A. Fayad. 2008. Targeted molecular probes for imaging atherosclerotic lesions with magnetic resonance using antibodies that recognize oxidation-specific epitopes. Circulation. 117: 3206 – 3215.

4. Briley-Saebo , K. C. , Y. S. Cho , P. X. Shaw , S. K. Ryu , V. Mani , S. Dickson , E. Izadmehr , S. Green , Z. A. Fayad , and S. Tsimikas. 2011. Targeted iron oxide particles for in vivo magnetic resonance detection of atherosclerotic lesions with antibodies directed to oxidation-specific epitopes. Journal of the American College of Cardiology. 57: 337 – 347.

5. Briley-Saebo , K. C. , T. H. Nguyen , A. M. Saeboe , Y. S. Cho , S. K. Ryu , E. R. Volkova , S. Dickson , G. Leibundgut , P. Wiesner , S. Green , *et al*. 2012. In vivo detection of oxidation-specific epitopes in atherosclerotic lesions using biocompatible manganese molecular magnetic imaging probes. Journal of the American College of Cardiology. 59: 616 – 626.

6. Aikawa , M. , S. Sugiyama , C. C. Hill , S. J. Voglic , E. Rabkin , Y. Fukumoto , F. J. Schoen , J. L. Witztum , and P. Libby. 2002. Lipid lowering reduces oxidative stress and endothelial cell activation in rabbit atheroma. Circulation. 106: 1390 – 1396.
7. Tsimikas , S. , M. Aikawa , F. J. Miller , Jr., E. R. Miller , M. Torzewski, S. R. Lentz , C. Bergmark , D. D. Heistad , P. Libby , and J. L. Witztum. 2007. Increased plasma oxidized phospholipid: apolipoprotein B-100 ratio with concomitant depletion of oxidized phospholipids from atherosclerotic lesions after dietary lipid-lowering: a potential biomarker of early atherosclerosis regression. Arteriosclerosis, Thrombosis, and Vascular Biology. 27: 175 – 181.

8. Torzewski , M. , P. X. Shaw , K. R. Han , B. Shortal , K. J. Lackner , J. L. Witztum , W. Palinski , and S. Tsimikas. 2004. Reduced in vivo aortic uptake of radiolabeled oxidation-specific antibodies reflects changes in plaque composition consistent with plaque stabilization. Arteriosclerosis, Thrombosis, and Vascular Biology. 24: 2307 – 2312.

9. Tsimikas , S. , A. Miyanohara , K. Hartvigsen , E. Merki , P. X. Shaw , M. Y. Chou , J. Pattison , M. Torzewski , J. Sollors , T. Friedmann , *et al*. 2011. Human oxidation-specific antibodies reduce foam cell formation and atherosclerosis progression. Journal of the American College of Cardiology. 58: 1715 – 1727.

10. Taleb , A. , J. L. Witztum , and S. Tsimikas. 2011. Oxidized phospholipids on apolipoprotein B-100 (OxPL/apoB) containing lipoproteins: a biomarker predicting cardiovascular disease and cardiovascular events. Biomarkers in Medicine. 5: 673 – 694.

11. Schiopu , A. , J. Bengtsson , I. Soderberg , S. Janciauskiene , S. Lindgren , M. P. S. Ares , P. K. Shah , R. Carlsson , J. Nilsson , and G. N. Fredrikson. 2004. Recombinant human antibodies against aldehyde modified apolipoprotein B-100 peptide sequences inhibit atherosclerosis. Circulation. 110: 2047 – 2052.

12. Caligiuri , G. , J. Khallou-Laschet , M. Vandaele , A. T. Gaston , S. Delignat , C. Mandet , H. V. Kohler , S. V. Kaveri , and A. Nicoletti. 2007. Phosphorylcholine-targeting immunization reduces atherosclerosis. Journal of the American College of Cardiology. 50: 540 – 546.

13. Kramer , M. C. , S. Z. Rittersma , R. J. de Winter , E. R. Ladich , D. R. Fowler , Y. H. Liang , R. Kutys , N. Carter-Monroe , F. D. Kolodgie , A. C. van der Wal , *et al*. 2010. Relationship of thrombus healing to underlying plaque morphology in sudden coronary death. Journal of the American College of Cardiology. 55: 122 – 132.

14. Farb , A. , D. K. Weber , F. D. Kolodgie , A. P. Burke , and R. Virmani. 2002. Morphological predictors of restenosis after coronary stenting in humans. Circulation. 105: 2974 – 2980.

15. Kolodgie , F. D. , J. Narula , A. P. Burke , N. Haider , A. Farb , Y. Hui-Liang , J. Smialek , and R. Virmani. 2000. Localization of apoptotic macrophages at the site of plaque rupture in sudden coronary death. American Journal of Pathology. 157: 1259 – 1268.

16. Virmani , R. , F. D. Kolodgie , A. P. Burke , A. Farb , and S. M. Schwartz. 2000. Lessons from sudden coronary death: a comprehensive morphological classification scheme for atherosclerotic lesions. Arteriosclerosis, Thrombosis, and Vascular Biology. 20: 1262 – 1275.

17. Kolodgie , F. D. , H. K. Gold , A. P. Burke , D. R. Fowler , H. S. Kruth , D. K. Weber , A. Farb , L. J. Guerrero , M. Hayase , R. Kutys , *et al*. 2003. Intraplaque hemorrhage and progression of coronary atheroma. The New England Journal of Medicine. 349: 2316 – 2325.

18. Young , S. G. , J. L. Witztum , D. C. Casal , L. K. Curtiss , and S. Bernstein. 1986. Conservation of the low density lipoprotein receptor-binding domain of apoprotein B. Demonstration by a new monoclonal antibody, MB47. Arteriosclerosis. 6: 178 – 188.

19. Boullier , A. , P. Friedman , R. Harkewicz , K. Hartvigsen , S. R. Green , F. Almazan , E. A. Dennis , D. Steinberg , J. L. Witztum , and O. Quehenberger. 2005. Phosphocholine as a pattern recognition ligand for CD36. The Journal of Lipid Research. 46: 969 – 976.

20. Friedman , P. , S. Horkko , D. Steinberg , J. L. Witztum , and E. A. Dennis. 2002. Correlation of antiphospholipid antibody recognition with the structure of synthetic oxidized phospholipids. Importance of Schiff base formation and aldol condensation. The Journal of Biological Chemistry. 277: 7010 – 7020.

21. Tsimikas , S. , W. Palinski , S. E. Halpern , D. W. Yeung , L. K. Curtiss , and J. L. Witztum. 1999. Radiolabeled MDA2, an oxidation-specific, monoclonal antibody, identifies native atherosclerotic lesions in vivo. Journal of Nuclear Cardiology. 6: 41 – 53.

22. Shaw , P. X. , S. Horkko , S. Tsimikas , M. K. Chang , W. Palinski , G. J. Silverman , P. P. Chen , and J. L. Witztum. 2001. Human-derived anti-oxidized LDL autoantibody blocks uptake of oxidized LDL by macrophages and localizes to atherosclerotic lesions in vivo. Arteriosclerosis, Thrombosis, and Vascular Biology. 21: 1333 – 1339.

23. Tsimikas , S. , H. K. Lau , K. R. Han , B. Shortal , E. R. Miller , A. Segev , L. K. Curtiss , J. L. Witztum , and B. H. Strauss. 2004. Percutaneous coronary intervention results in acute increases in oxidized phospholipids and lipoprotein(a): short-term and long-term immunologic responses to oxidized low-density lipoprotein. Circulation. 109: 3164 – 3170.

24. Seimon , T. A. , M. J. Nadolski , X. Liao , J. Magallon , M. Nguyen , N. T. Feric , M. L. Koschinsky , R. Harkewicz , J. L. Witztum , S. Tsimikas , *et al*. 2010. Atherogenic lipids and lipoproteins trigger CD36–TLR2-dependent apoptosis in macrophages undergoing endoplasmic reticulum stress. Cell Metabolism. 12: 467 – 482.

25. Berliner , J. A. , N. Leitinger , and S. Tsimikas. 2009. The role of oxidized phospholipids in atherosclerosis. The Journal of Lipid Research. 50 (Suppl): S207 – S212.

26. Podrez , E. A. , E. Poliakov , Z. Shen , R. Zhang , Y. Deng , M. Sun , P. J. Finton , L. Shan , M. Febbraio , D. P. Hajjar , *et al*. 2002. A novel family of atherogenic oxidized phospholipids promotes macrophage foam cell formation via the scavenger receptor CD36 and is enriched in atherosclerotic lesions. The Journal of Biological Chemistry. 277: 38517 – 38523.

27. Shaw , P. X. , S. Horkko , M. K. Chang , L. K. Curtiss , W. Palinski , G. J. Silverman , and J. L. Witztum. 2000. Natural antibodies with the 15 idiotype may act in atherosclerosis, apoptotic clearance, and protective immunity. Journal of Clinical Investigation. 105: 1731 – 1740.

28. Tsimikas , S. , B. P. Shortal , J. L. Witztum , and W. Palinski. 2000. In vivo uptake of radiolabeled MDA2, an oxidation-specific monoclonal antibody, provides an accurate measure of atherosclerotic lesions rich in oxidized LDL and is highly sensitive to their regression. Arteriosclerosis, Thrombosis, and Vascular Biology. Biol. 20: 689 – 697.

29. Shao , B. , S. Pennathur , I. Pagani , M. N. Oda , J. L. Witztum , J. F. Oram , and J. W. Heinecke. 2010. Modifying apolipoprotein A-I by malondialdehyde, but not by an array of other reactive carbonyls, blocks cholesterol effl ux by the ABCA1 pathway. Journal of Biological Chemistry. 285: 18473 – 18484.

30. Tsimikas , S. , Z. Mallat , P. J. Talmud , J. J. Kastelein , N. J. Wareham , M. S. Sandhu , E. R. Miller , J. Benessiano , A. Tedgui , J. L. Witztum , *et al*. 2010. Oxidation-specific biomarkers, lipoprotein(a), and risk of fatal and nonfatal coronary events. Journal of the American College of Cardiology. 56: 946 – 955.

31. Kiechl , S. , J. Willeit , M. Mayr , B. Viehweider , M. Oberhollenzer , F. Kronenberg , C. J. Wiedermann , S. Oberthaler , Q. Xu , J. L. Witztum , *et al*. 2007. Oxidized phospholipids, lipoprotein(a), lipoprotein-associated phospholipase A2 activity, and 10-year cardiovascular outcomes: prospective results from the Bruneck study. Arteriosclerosis, Thrombosis, and Vascular Biology. 27: 1788 – 1795.

32. Bergmark , C. , A. Dewan , A. Orsoni , E. Merki , E. R. Miller , M. J. Shin , C. J. Binder , S. Horkko , R. M. Krauss , M. J. Chapman , *et al*. 2008. A novel function of lipoprotein [a] as a preferential carrier of oxidized phospholipids in human plasma. Journal of Lipid Research. 49: 2230 – 2239.

33. Rosenfeld , M. E. , W. Palinski , S. Yla-Herttuala , S. Butler , and J. L. Witztum. 1990. Distribution of oxidation specific lipid-protein adducts and apolipoprotein B in atherosclerotic lesions of varying severity from WHHL rabbits. Arteriosclerosis. 10: 336 – 349.

34. Scanlon , C. E. O. , B. Berger , G. Malcom , and R. W. Wissler. 1996. Evidence for more extensive deposits of epitopes of oxidized low density lipoprotein in aortas of young people with elevated serum thiocyanate levels. Atherosclerosis. 121: 23 – 33.

35. Weismann , D. , K. Hartvigsen , N. Lauer , K. L. Bennett , H. P. Scholl , P. Charbel Issa , M. Cano , H. Brandstatter , S. Tsimikas , C. Skerka , *et al*. 2011. Complement factor H binds malondialdehyde epitopes and protects from oxidative stress. Nature. 478: 76 – 81.

36. Ravandi , A. , S. M. Boekholdt , Z. Mallat , P. J. Talmud , J. J. Kastelein , N. J. Wareham , E. R. Miller , J. Benessiano , A. Tedgui , J. L. Witztum , *et al*. 2011. Relationship of IgG and IgM autoantibodies and immune complexes to oxidized LDL with markers of oxidation and inflammation and cardiovascular events: results from the EPIC-Norfolk Study. Journal of Lipid Research. 52: 1829 – 1836.

37. Tabas , I. , K. J. Williams , and J. Boren. 2007. Subendothelial lipoprotein retention as the initiating process in atherosclerosis: up-date and therapeutic implications. Circulation. 116: 1832 – 1844.

38. Lundstam , U. , E. Hurt-Camejo , G. Olsson , P. Sartipy , G. Camejo , and O. Wiklund. 1999. Proteoglycans contribution to association of Lp(a) and LDL with smooth muscle cell extracellular matrix. Arteriosclerosis, Thrombosis, and Vascular Biology. 19: 1162 – 1167.

39. Dangas , G. , J. A. Ambrose , D. J. D'Agate , J. H. Shao , S. Chockalingham , D. Levine , and D. A. Smith. 1999. Correlation of serum lipoprotein(a) with the angiographic and clinical presentation of coronary artery disease. American Journal of Cardiology. 83: 583 – 585 , A7.

40. Clarke , R. , J. F. Peden , J. C. Hopewell , T. Kyriakou , A. Goel , S. C. Heath , S. Parish , S. Barlera , M. G. Franzosi , S. Rust , *et al*. 2009. Genetic variants associated with Lp(a) lipoprotein level and coronary disease. New England Journal of Medicine. 361: 2518 – 2528.

41. Kamstrup , P. R. , A. Tybjaerg-Hansen , R. Steffensen , and B. G. Nordestgaard. 2009. Genetically elevated lipoprotein(a) and increased risk of myocardial infarction. JAMA. 301: 2331 – 2339.

42. Merki , E. , M. J. Graham , A. E. Mullick , E. R. Miller , R. M. Crooke , R. E. Pitas , J. L. Witztum , and S. Tsimikas. 2008. Antisense oligonucleotide directed to human apolipoprotein B-100 reduces lipoprotein(a) levels and oxidized phospholipids on human apolipoprotein B-100 particles in lipoprotein(a) transgenic mice. Circulation. 118: 743 – 753.

43. Cannon , C. P. , S. Shah , H. M. Dansky , M. Davidson , E. A. Brinton , A. M. Gotto , M. Stepanavage , S. X. Liu , P. Gibbons , T. B. Ashraf , *et al*. 2010. Safety of anacetrapib in patients with or at high risk for coronary heart disease. New England Journal of Medicine. 363: 2406 – 2415.

44. Raal , F. J. , R. D. Santos , D. J. Blom , A. D. Marais , M. J. Charng , W. C. Cromwell , R. H. Lachmann , D. Gaudet , J. L. Tan , S. Chasan-Taber , *et al*. 2010. Mipomersen, an apolipoprotein B synthesis inhibitor, for lowering of LDL cholesterol concentrations in patients with homozygous familial hypercholesterolaemia: a randomised, double-blind, placebo-controlled trial. Lancet. 375: 998 – 1006.

CHAPTER 6

A systematic evaluation of the cellular innate immune response during the process of human atherosclerosis

R.A. van Dijk
K. Rijs
A. Wezel
J.F. Hamming
F.D. Kolodgie
R.Virmani
A.F. Schaapherder
J.H.N. Lindeman

Journal of the American Heart Association 2016

ABSTRACT

Background: The concept of innate immunity is well recognized within the spectrum of atherosclerosis, which is primarily dictated by macrophages. Although current insights to this process are largely based on murine models, there are fundamental differences in the atherosclerotic microenvironment and associated inflammatory response relative to the humans. In this light, we characterized the cellular aspects of the innate immune response in normal, non-progressive, and progressive human atherosclerotic plaques.

Material and methods: A systematic analysis of the innate immune response was performed on 110 well-characterized human peri-renal aortic plaques with immunostaining for specific macrophage subtypes (M1 and M2-lineage) and their activation markers neopterin and HLA-DR together with dendritic cells, NK cells, mast cells, neutrophils, and eosinophils.

Results: Normal aortae were devoid of LDL, macrophages, dendritic cells, NK cells, mast cells, eosinophils and neutrophils. Early, atherosclerotic lesions exhibited heterogeneous populations of (CD68+) macrophages whereby 25% were double positive "M1" (CD68+/ iNOS+/CD163-), 13% "M2" double positive (CD68+/iNOS-/CD163+) and 17% triple-positive for (M1) iNOS (M2)/ CD163 and CD68 with the remaining (~40%) only stained for CD68. Progressive fibroatheromatous lesions, including vulnerable plaques showed increasing numbers of NK cells and fascin positive cells mainly localized to the media and adventitia while the M1/M2 ratio and level of macrophage activation (HLA-DR and neopterin) remain unchanged. On the contrary, stabilized (fibrotic) plaques showed a marked reduction in macrophages and cell activation with a concomitant decrease in NK cells, dendritic cells, and neutrophils.

Conclusion: Macrophage "M1" and "M2" subsets together with fascin-positive dendritic cells are strongly associated with progressive and vulnerable atherosclerotic disease of human aorta. The observations here support a more complex theory of macrophage heterogeneity than the existing paradigm predicated on murine data and further indicate the involvement of (poorly-defined) macrophage subtypes or greater dynamic range of macrophage plasticity than previously considered.

INTRODUCTION

Macrophages and possibly other cellular components of the innate immune system are paramount in the initiation, progression and complications of atherosclerosis[1,2,3]. At the same token, data from animal studies shows that these cells orchestrate atherosclerosis regression and plaque stabilization, underlining the central role of these cell types in the atherosclerotic process[4,5,6].

It is now recognized that macrophages constitute a highly heterogeneous and dynamic cell population that were initially labeled as pro-inflammatory M1 macrophages and tissue regenerative M2 macrophages, although more elaborative classifications have been brought forward and some even pointed out that macrophage differentiation is a continuum[7]. Experimental studies mainly involving mice implies a major shift in macrophage identity during the atherosclerotic process with pro-inflammatory processes (classically activated M1 macrophages) involved in the initiation and progression of the disease, and alternatively activated M2 macrophages) linked to resolution and repair[8]. Much of the theory in this area has been driven by *in vitro* studies exploring gene/protein expression patterns and functional attributes of monocytes or macrophages subjected to various treatments[9,10].

Knowledge on the innate immune system in the atherosclerotic process essentially relies on observations from rodent models[11]. Yet, there are fundamental immunological and inflammatory differences between rodents and humans[12,13,14]. Moreover, lesions in established murine atherosclerosis models fail to progress to advanced vulnerable plaques complicated by rupture hence inflammatory responses in advanced stages of the disease cannot be characterized in these models[15]. Consequently, it's becoming recognized that observations from animal models may not necessarily translate to the human atherosclerotic process, particularly when considering the inflammatory milieu[16,17,18].

In this regard we considered a systematic evaluation of the cellular components of the innate immune system (macrophages and their subtypes, dendritic cells, mast cells, natural killer cells, neutrophils and eosinophils) throughout the process of human atherosclerosis, particularly in relation to complicated plaques, relevant to symptomatic disease. To that end, we performed a systematic histological evaluation of these components using a unique collection of biobanked human arterial tissues that covers the full spectrum of lesion progression.

Results from this study confirm an extensive and dynamic inflammatory process involving specific cellular components of the innate immune system occurring throughout disease progression. Furthermore, it was concluded that a simple dichotomous classification system for macrophage differentiation falls short in the biological context.

MATERIAL AND METHODS

Patients and tissue sampling

Tissue sections were selected from a large tissue bank containing over 400 individual abdominal aortic wall patches (AAWPs) that were obtained during liver, kidney or pancreas transplantation (*viz.* all material was from cadaveric donors). Details of this bank have been described previously by van Dijk *et al*.[19]. All patches were harvested from grafts that were eligible for transplantation (*i.e.* all donors met the criteria set by The Eurotransplant Foundation) and due to national regulations, only transplantation relevant data for donation is available. Sample collection and handling was performed in accordance with the guidelines of the Medical and Ethical Committee in Leiden, Netherlands and the code of conduct of the Dutch Federation of Biomedical Scientific Societies (http://www.federa.org /?s=1&m=82&p=0&v=4#827).

Histologic sections of AAWPs were stained by haematoxylin and eosin (H&E) and Movat pentachrome for classification of the lesions (in accordance with the modified AHA classification as proposed by Virmani *et al.*[20, 21]*).* Classification was performed by two independent observers without knowledge of the character of the aortic tissue[19, 20]. In all cases, the aortic tissue block showing the most advanced plaque from each patient was used for further analysis. The lesion types included in this classification are described below. In order to obtain a balanced and representative study group, 10 to 12 samples were randomly selected from representative lesion morphologies. A total of 110 samples were used for further immunohistochemistry staining and analysis.

Characterization of the lesions and histological definitions

A detailed description of plaque characterization, morphological analysis is provided in reference 19. Plaque morphologies included adaptive intimal thickening (AIT), intimal xanthoma (IX), pathological intimal thickening (PIT), early (EFA) and late fibroatheroma (LFA), thin cap fibroatheroma (TCFA), acute plaque rupture (PR), healed plaque rupture (HR) and fibrotic calcific plaque (FCP).

Immunohistochemistry

Single immunostaining for visualizing macrophages, dendritic cells (DC), mast cells, and neutrophils.

Histologic sections of formalin-fixed paraffin embedded aortic tissues decalcified in Kristensen fluid were immunostained using antibodies directed against the macrophage activation marker neopterin, HLA-DR (cell activation marker), fascin (dendritic cells), tryptase (mast cells), myeloperoxidase (MPO) and matrix metallopeptidase 8 (MMP8; neutrophils) and EG2 (eosinophils). The details and antibodies used for immunohistochemical staining are listed in Table I. Antigen

retrieval was heat-induced using either citrate (pH 6) or TRIS-EDTA (pH 9.2) buffers or proteolytic digestion with trypsin, when necessary. Antibody binding was visualized by a polymer-based HRP substrate (EnVision®, Dako, A/S, Glostrup, Denmark) with diaminobenzidine (DAB) as the chromogen and Gill's hematoxylin as counterstain. Tissue sections from human tonsils and abdominal aortic aneurysms were used for positive controls while negative controls were performed by omitting the primary antibody.

Double-labeling immunohistochemistry for visualizing Natural Killer (NK) cells and Low Density Lipoprotein (LDL) with elastin.

NK cells (T-bet$^+$/CD4$^-$) were identified by double labelling against T-bet (NK cells and T-helper1 cells) and CD4 (T-helper cells) with DAB and Vina Green chromogens, respectively, as described previously[22]. Dual staining for LDL and elastin was performed with an antibody directed against apolipoprotein B100 with DAB and counterstained by fuchsin.

Triple-labeling immunohistochemistry for M1 and M2 macrophage subpopulations

Details of all antibodies are listed in Table 1. Primary markers included CD68 (pan-MΦ macrophage marker with iNOS (inducible nitric oxide synthase, M1) and CD163 (macrophage scavenger receptor, M2). Macrophage phenotype was further validated with IL6 (M1) and dectin-1 (M2, major β-glucan receptor on macrophages). Antibody reactions were detected using an EnVision® + System – horseradish peroxidase (HRP) labeled polymer anti-mouse/anti-rabbit functioned as the secondary antibody (DAKO) and positive reactions were visualized with DAB and Vina Green chromogen or 4plus Biotinylated Universal Goat link kit (Biocare Medical, Concord, CA) in combination with 4plus streptavidin AP label for Ferangi Blue and Warp Red visualizations. For triple stainings a second heat induced citrate antigen retrieval was used following incubation with denature solution (Biocare Medical) to inactivate the preceding labels.

Quantification of the immunostained cells

Aortic lesion area was defined as the region between the lumen and first elastic lamina over a circumferential width of 1mm. For fibroathermatous plaques, the lateral distance was expanded to include flanking regions of the necrotic core incorporating shoulder regions. Regions of interest (ROI) were selected from the central region of the plaque and lateral shoulder regions with corresponding areas of underlying media and the adventitia (Figure 1). Three representative areas within separate ROIs involving the intima, media and adventitia were imaged at 200x magnification (Axiovision 4.6.3). A total of 9 images per atherosclerotic lesion, which were each analyzed.

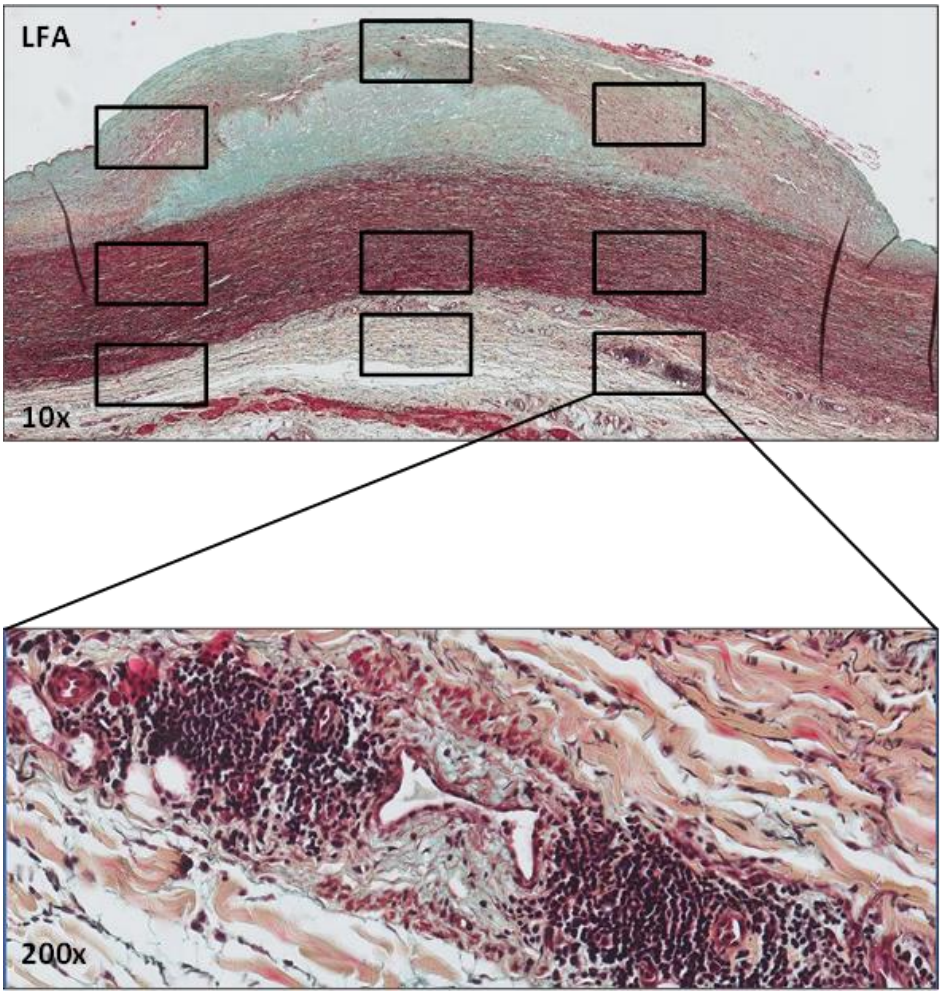

Figure 1. Defining the 9 regions of interest (ROI) within atherosclerotic lesions. Early aortic fibroatheroma stained by Movat pentachrome with regions of interest (ROIs, boxed areas) selected within the fibrous cap, flanking shoulders and underlying media and the adventitia. Immunostaining for select inflammatory markers within ROIs was quantitatively assessed with an image processing program (Image J; plug-in Cellcounter). An additional high resolution image of an adventitial inflammatory infiltrate at 200x magnification is shown to illustrate the cellular detail.

Positive staining for mast cells (tryptase), NK cells (T-bet^{+}/CD4^{-}), dendritic cells (fascin) and neutrophils (myeloperoxidase and MMP8) was quantified using Image J Colour Deconvolution. Tissue sections stained for macrophages (CD68), neopterin and HLA-DR were quantified and presented as a percentage of plaque area. Triple immunostains for macrophage subtypes were analyzed using the Nuance multispectral imaging system FX[23] based on unmixed colour spectra from DAB, Warp Red and Vina Green or Ferangi Blue.

Table 1. Antibodies used in the present study

Antibody, clone	Host isotype; subclass	Specificity	Pretreatment		Dilution	Reference/source
Apolipoprotein B	Goat (polyclonal), IgG	apoLipoprotein B	Tris/EDTA	pH 9.2	1:4000	Abcam
CD4	Rabbit (polyclonal)	T-helper cells	Citrate	pH 6.0	1:200	Abcam
CD68, KP1	Mouse (monoclonal), IgG1	Pan Macrophage	Tris/EDTA	pH 9.2	1:7000	DAKO Cytomation
CD163,10d6	Mouse (monoclonal) IgG1	"M2" Macrophages (triple stains)	Tris/EDTA	pH 9.2	1:200	Thermo scientific/neomarkers
Dectin-1, NBP2-13845	Rabbit (polyclonal)	"M2" Macrophages (triple stains)	Tris/EDTA	pH 9.2	1:50	Novus Biologicals
EG2	Mouse	Activated eosinophils	Trypsin	-	1:600	Pharmacia Diagnostics
Fascin, 55k-2	Mouse (monoclonal), IgG1	Dendritic Cells	Citrate	pH 6.0	1:800	DAKO Cytomation
HLA-DR, TAL.1B5	Mouse (monoclonal), IgG1	antigen presenting cells (APC)	Citrate	pH 6.0	1:200	DAKO Cytomation
IL-6, NYRhIL6	Mouse (monoclonal), IgG2	"M1" Macrophages (triple stains)	Citrate	pH 6.0	1:400	Santa Cruz
iNOS	Rabbit (polyclonal), IgG	"M1" Macrophages (triple stains)	Tris/EDTA	pH 6.0	1:400	Abcam
Myeloperoxidase	Rabbit (polyclonal)	Neutrophils	-	-	1:5000	Dako Cytomation
MMP8, MAB9081	Mouse (monoclonal) IgG2a	Neutrophils	Trypsin	-	1:1000	R&D systems
Neopterin	Rabbit (polyclonal)	Activated macrophages	Citrate	pH 6.0	1:500	Biogenesis
T-bet	Rabbit (polyclonal)	NK cells / T helper1-cells	Tris/EDTA	pH 9.2	1:200	Santa Cruz
Tryptase, AA1	Mouse (monoclonal), IgG1	Mast cells	Citrate	pH 6.0	1:3000	Dako Cytomation

Total numbers of M1 macrophages ($CD68^+/iNOS^+$ or $CD68^+/IL6^+$) and M2 macrophages ($CD68^+/CD163^+$ or CD68+/$Dectin\text{-}1^+$) were expressed as a percentage of co-localized CD68 as well as the percentage of the triple positive immunostaining (IL6/Dectin-1/CD68 or iNOS/CD163/CD68) in addition to the percentage of CD68 without any co-localization.

Statistical analysis

Data are presented as means ± SEM. The means of cellular distribution were compared using One-way ANOVA. The relationship between the amount of positive cells in aortic layers (intima, media and adventitia) within a particular lesion types was analyzed by Spearman's correlation and compared with other lesion morphologies (SPSS 20.0; Chicago, IL). The Wilcoxon-Mann-Whitney test was used to analyze the non-normally distributed data of the mean total number of cells within each atherosclerotic phase and the Kruskal Wallis test was used to control for a type 1 error. A value of $p<0.05$ was considered statistically significant.

RESULTS

Study population

The male/female ratio among donors was 54.5% male and the mean age was ~47 years. There was a strong relationship between donor age and the stage of atherosclerosis[19] morphology whereby normal aortic wall samples had a mean age of 17 years, while those with end-stage fibrocalcific plaques were 60 years of age. Cardiovascular risk factors of smoking were known in 34%, hypertension in 15% while two donors received statin therapy (Table 2).

Cellular aspects of the innate immune response

Normal and non-progressive lesions

The intima and media of the normal aortic wall are devoid of LDL, macrophages, dendritic cells, NK cells, mast cells, and neutrophils. Early, non-progressive atherosclerotic lesions inclusive of adaptive intimal thickening (AIT) and intimal xanthoma (IX)) showed traces of LDL (apolipoprotein B100) within the intima (Figure 2). By definition IX lesions showed extensive infiltration of ($CD68^+$) macrophage foam cells (Figure 3), which was also heterogeneous, as shown by additional markers for M1 and M2 macrophages. Spectral imaging analysis of macrophage subtypes showed a predominance of "M1" ($CD68^+$/ $iNOS^+/CD163^-$) over "M2" ($CD68^+/iNOS^-/CD163^+$) macrophages (25% and 13%, respectively) (Figure 4) with approximately 17% of the macrophages co-expressing both (M1) iNOS and CD163 (M2) markers, with the remaining only positive for CD68.

Table 2. Demographic data of the 110 studied aortic samples

	Male		**Female**	
N	60		50	
Mean age (years) [SD]	46.9	[19.8]	47.0	[15.7]
Mean length (cm) [SD]	178.9	[11.7]	165.6	[11.9]
Mean weight (kg) [SD]	80.0	[16.2]	63.9	[14.5]
Mean BMI (kg/m2) [SD]	24.9	[3.0]	22.5	[4.3]
Patients with known history of nicotine abuse [percentage]	21	[35%]	17	[34%]
Patients with known history of hypertension* [percentage]	13	[21.7%]	10	[20%]
Patients with known diabetes [percentage]	0	[0.0%]	1	[2%]
Cause of Death [n, percentage]				
Severe head trauma	11	[18.3%]	7	[14.0%]
Cerebral vascular accident (CVA)	8	[13.3%]	10	[20.0%]
Subarachnoid bleeding (SAB)	15	[25%]	14	[28.0%]
Cardiac arrest	7	[11.6%]	0	[0.0%]
Trauma	1	[1.6%]	1	[2.0%]
Other	6	[10%]	3	[6.0%]
Unknown	16	[26.6%]	15	[30%]
Medication [n, percentage]				
Anti-hypertensives	11	[18.3%]	6	[12.0%]
Statins	1	[1.6%]	1	[2.0%]
Anti-coagulants	1	[1.6%]	2	[4.0%]
Other	5	[8.3%]	8	[16.0%]
None	31	[51.7%]	22	[44.0%]
Unknown	11	[18.3%]	9	[18.0%]

*Known antihypertensive medication / systolic blood pressure >140mmHg and diastolic >90mm Hg in the period preceding death. Abbreviations: SD = Standard Deviation.

Comparable results were obtained with a second set of validation markers IL6 (M1) and dectin-1 (M2) (Figure 4B).

Intimal xanthomas were further assessed for the general cellular activation marker HLA-DR and macrophage-specific marker neopterin (Figure 5 and 6). The profuse macrophage infiltration seen in IX is paralleled by increased expression of HLA-DR and neopterin in this early stage of the atherosclerotic process.

Mast cells (Figure 7) are also reported to express CD68 and may thus (partly) account for the CD68 double negative population. Tryptase/CD68 double staining indeed showed strong CD68 reactivity on mast cells although given the sparse number of mast cells in the intimal layer the overall effects are likely minimal unlike the interpretation of the macrophage data for the media and adventitia where mast cells populations are more prominent (Figure 7E). NK cells (Figure 8), dendritic cells (Figure 9) and neutrophils (Figure 10) are not identified in the intimal layer of normal aorta and non-progressive lesions. Moreover, the NK cells and dendritic cells that are seen in the media are located at the medial-adventitial border. No eosinophils ($EG2^+$) were identified in the normal and non-progressive lesions.

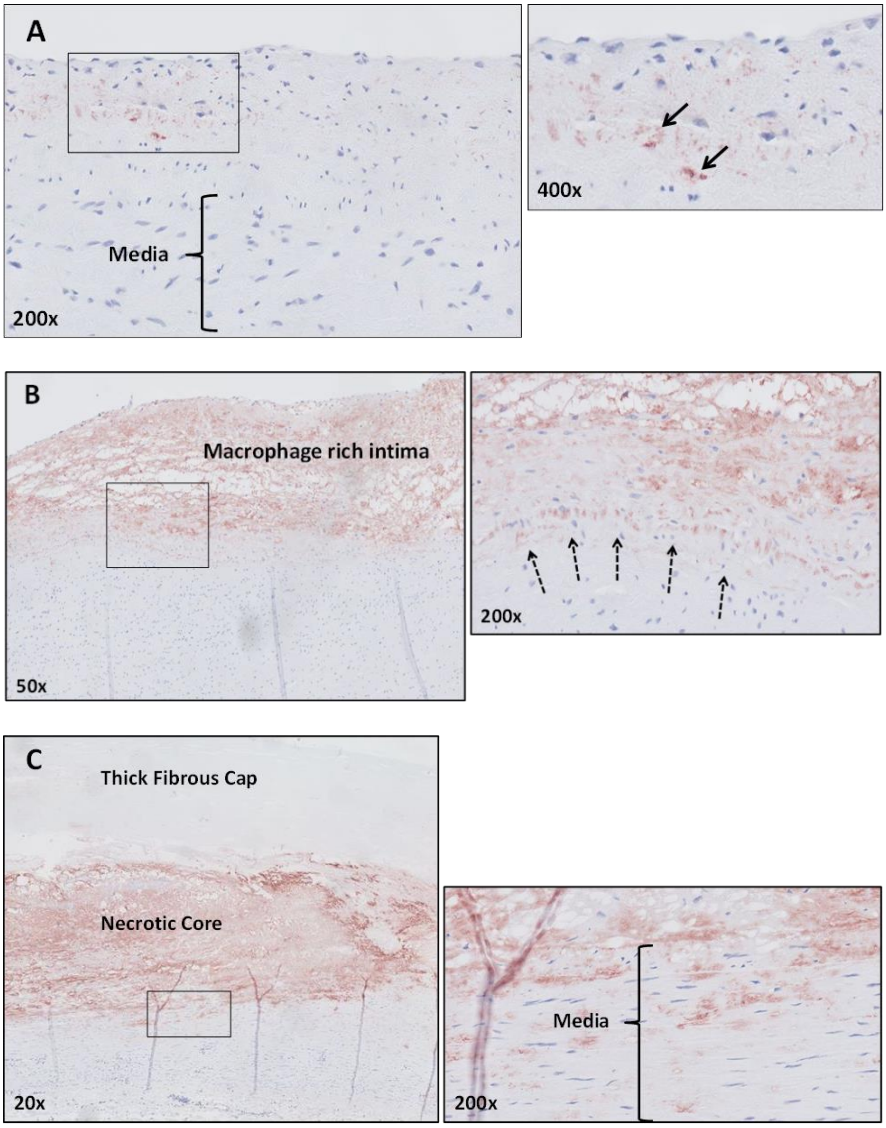

Figure 2. Apolipoprotein B100 (LDL) deposition.A. Representative image (200x) of an aorta with adaptive intimal thickening stained for ApolipoproteinB100 with a high resolution image at a 400x magnification. ApolipoproteinB100 accumulation is confined to the intima (black arrow).B. Representative image (50x) of an intimal xanthoma (IX) stained for ApolipoproteinB100 with a high resolution image at a 200x magnification. Increase in intimal ApoB100 deposition within the intima. Accumulation of ApoB100 is restricted to the intima (dotted arrows represent the internal elastic lamina).C. Representative image (20x) of a late fibroatheroma (LFA) stained for ApolipoproteinB100 with a high resolution image at a 200x magnification at the intimal-medial border. This stage of atherosclerosis is characterized by accumulation of ApoB100 within the media, coinciding loss of integrity of the internal elastic lamina. All ApoB100 samples were visualized with DAB and counterstained with haematoxylin.

Progressive atherosclerotic lesions

Progressive lesions of pathological intima thickening (PIT), early fibroatheroma (EFA) and late fibroatheroma (LFA) are characterized by loss of integrity of the intimal medial border zone as hallmarked by increasing apolipoprotein B100 infiltration in the inner media layer (Figure 2C) along with a major increase in the macrophage content both in the intima and adjacent media (Figure 3 and 4). In parallel, we observe increased levels of macrophage activation, as indicated by HLA-DR and neopterin expression. The percentage of M1 macrophages increases in late fibroatheroma (~27%) and slightly decreases, as the lesions progress towards a vulnerable thin cap fibroatheroma or plaque rupture. On the other hand, M2 macrophages slightly increase as early and late fibroatheromas (~13%) progress towards a thin cap fibroatheroma (~17%) while the number of monocytes and macrophages double positive for the M1 and M2 marker remains stable (Figure 4A and B). $CD68^+$ cells negative for M1 and M2 markers slightly tend to increase in number as lesions progress towards plaque rupture, an observation that may (partly) reflect a major increase in the number of mast cells within the adventitia (Figure 7).

Progressive numbers of NK cells are found within the media and adventitia of these more advanced lesions (Figure 8). Fascin positive cells significantly increase in number in the intima and media (*$P<0.0004$ and ‡$p<0.0001$) and remain stable within the adventitia.

Only 1 or 2 neutrophils are present in the intima (~8% of total) and the neutrophils identified in the media are located intravascular in the infiltrating *vasa vasorum* (Figure 10B and C).

Vulnerable atherosclerotic lesions

Thin cap fibroatheromas and plaque ruptures are characterized by a further increase in macrophage content in the intima and media, but the M1/M2 ratio and the level of macrophage activation (HLA-DR and neopterin) remain unchanged when compared to stable lesions (figure 4). Increased numbers of mast cells and NK cells, and fascin positive cells are found in all the vascular layers. Increasing numbers of intravascular neutrophils are observed in the media, and absent within the neointima and areas outside vessels. Overall, eosinophils are absent in the progressive and vulnerable stages.

Healed and stabilized lesions

Healed ruptures (HR) and fibrocalcific plaques (FCP) associated with vessel stabilization showed a marked reduction in the number of macrophages and decrease in cell activation, as indicated by reduced HLA-DR positivity and intimal neopterin expression. M1 macrophages increase in number whereas the M2 lineage remains stable. NK cells, dendritic cells, and neutrophils significantly decrease in number as lesions stabilize. Eosinophils remain absent.

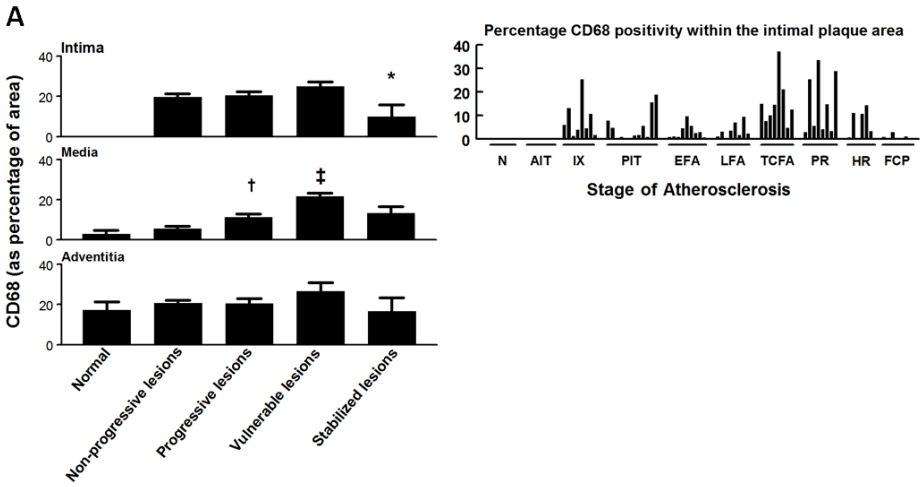

Figure 3. Macrophage (CD68+) distribution in normal, non-progressive, progressive, vulnerable, and stable atherosclerotic plaques. **A.** The mean percentage of CD68 positive area within various regions of interest (intima, media and adventitia) plotted by lesion morphology (±SEM). An additional plot of the intima illustrates the percentage of CD68 positivity for individual plaque stratified by the stage of atherosclerosis. CD68 is seen from the stage of intimal xanthoma. CD68 positivity increases during disease progression and is maximal for vulnerable plaques, followed by a significant decrease when the lesions stabilize (* $p<0.005$). CD68 positivity in the media increases with progressive atherosclerotic lesions and vulnerable lesions († $p < 0.004$, ‡ $p< 0.001$) in contrary to the adventitia, which remained relatively constant except for a slight decrease for stabilizing lesions. **B.** Representative images of intimal xanthoma (IX), late fibroatheroma (LFA) and a thin cap fibroatheroma (TCFA) stained by Movat pentachrome with corresponding immunostain for macrophages (CD68; KP-1). Macrophages and macrophage foam cells essentially form the IX. The necrotic core in LFA stains highly positive for CD68, representing accumulation of macrophage remnants and is therefore was excluded during morphometric analysis. While the thick fibrous cap of the LFA is mainly negative for CD68, the shoulder regions show infiltration by macrophages and macrophage foam cells (see the 50x magnification) in addition to a notable presence within the media (see the 100x magnification). More advanced TCFAs demonstrate increased macrophage accumulation in the cap. Total number of cases in figure A: 85 (normal 9, non-progressive lesions 18 (*viz.* AIT (10) and IX (8)), progressive lesions 29 (*viz.* PIT (12), EFA (9) and LFA (8)), vulnerable lesions 16 (*viz.* TCFA (8) and PR (8)) and stabilized lesions 13 (*viz.* HR (7) and FCP (6)). Abbreviations: N: normal, AIT: adaptive intimal thickening, IX: Intimal xanthoma, PIT: Pathological intimal thickening, EFA: early fibroatheroma, LFA: late fibroatheroma, TCFA: thin cap fibroatheroma, PR: plaque rupture, HR: healed rupture and FCP: fibrotic calcified plaque. For a detailed description concerning the classification see Material & Methods section.

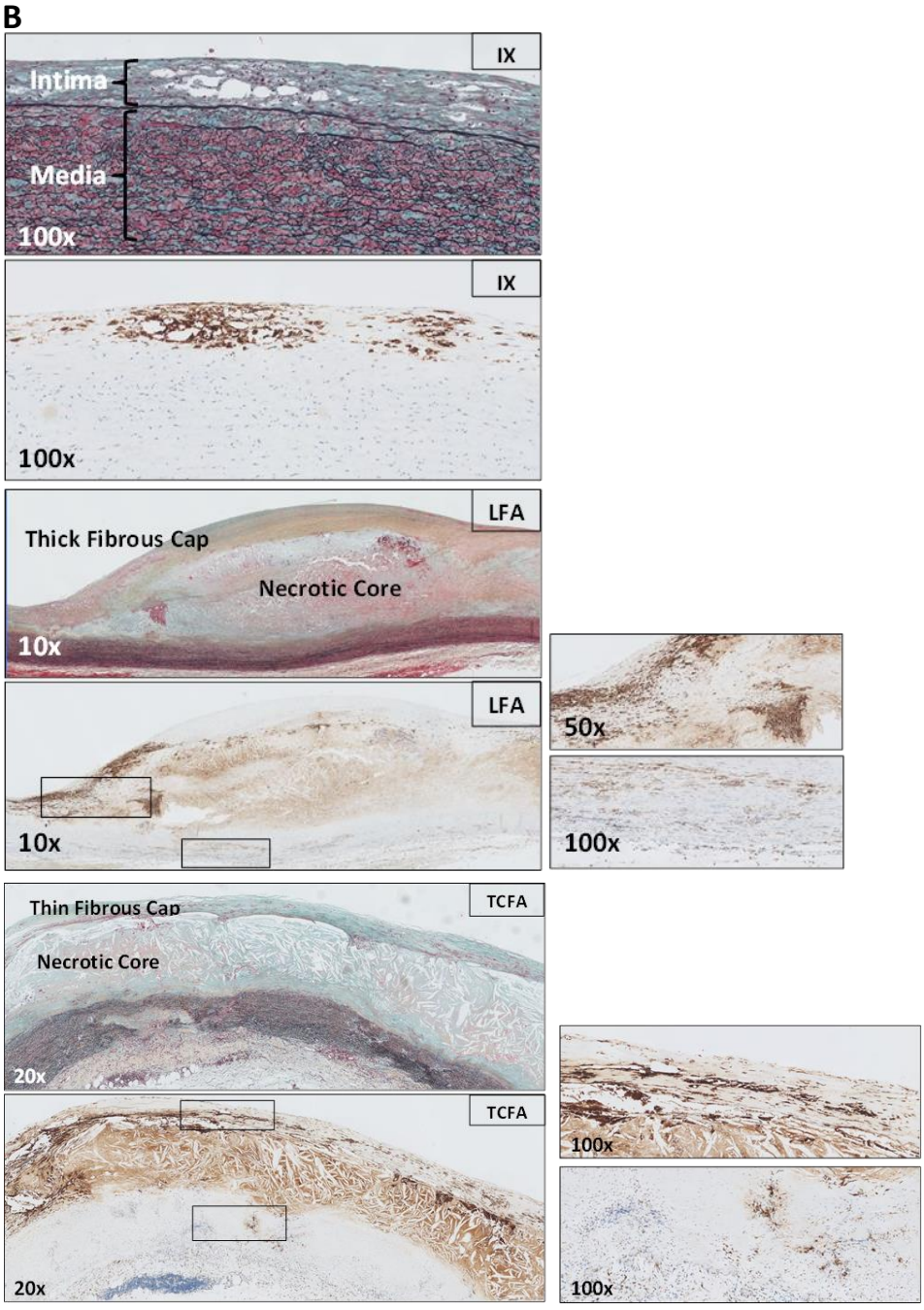

Figure 3. Continued.

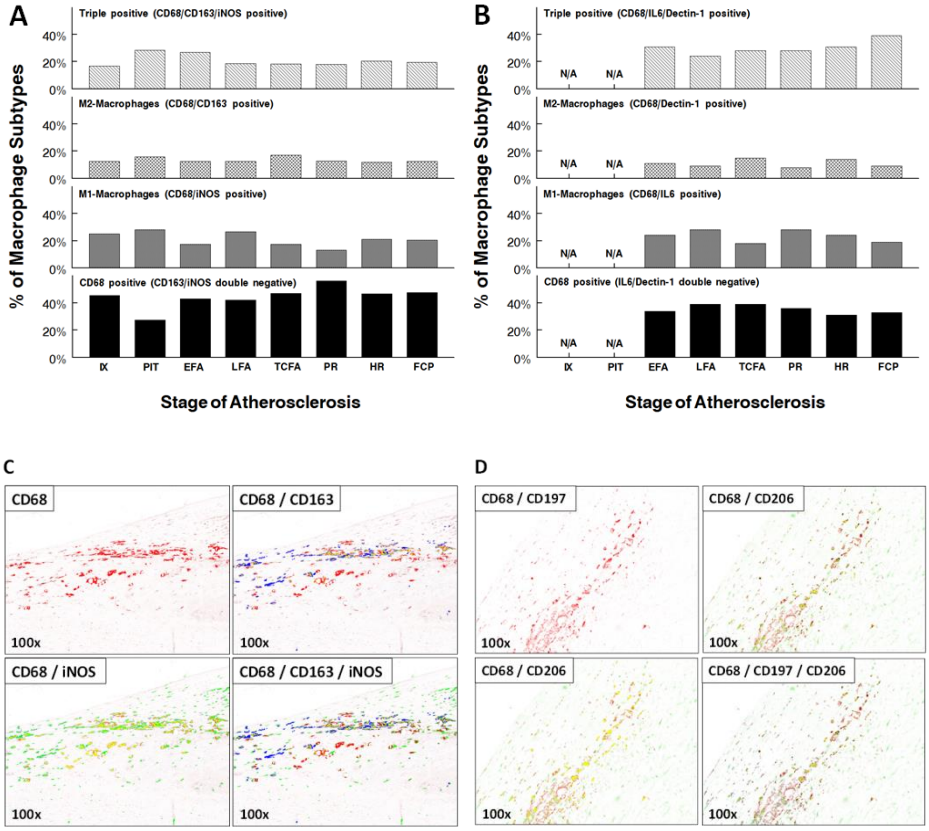

Figure 4. Macrophage subclass distribution (intima) during aortic atherosclerosis. **A.** Lesional macrophages were identified by the pan macrophage marker CD68, and respective subclasses identified based on the expression of iNOS (M1) and CD163 (M2). Various macrophage subtypes are plotted as a relative percentage of the total amount of CD68 cells for each atherosclerotic stage. As lesions progress towards a vulnerable phase (*i.e.* TCFA and PR) there is a slight decreases in the extent of M1 macrophages whereas the M2 lineage increases, resulting in a 1:1 ratio. Within healed and stabilized FCP the M1:M2 ration is ~2:1. About 20-30% of the macrophages stain positive for both iNOS and CD163 and over 40% of the macrophages are double negative for the selective markers. **B.** Confirmation of M1 (iNOS) and M2 (CD163) expressing macrophages within various progressive, vulnerable lesions, and stable aortic lesions substituting IL6 and Dectin-1 as respective "M1" and "M2" markers. Nearly the same percentages and distribution of M1 and M2 macrophages was observed when compared with lesions triple-stained for iNOS and CD163 where ~ 20-30 percent of the macrophages express both IL6 and Dectin-1 and nearly 40% of the macrophages are double negative for both markers. **C.** Representative images of a shoulder region at a 10x magnification triple stained with CD68 (pan macrophage marker, Warp Red chromogen; Spectral image colour red), iNOS (inducible nitric oxide synthase; M1-macrophages, DAB; Spectral image colour green) and CD163 (macrophage scavenger receptor; M2-macrophages, Ferangi Blue; Spectral image colour blue). Yellow indicates the amount of co-localization between the various macrophage markers. **D.** Representative images of a shoulder region at a 9100 magnification triple stained with CD68 (pan macrophage marker, Vina Green chromogen; spectral image color red), CD197 (M1 macrophages, Vulcan Red; spectral image color green) and CD206 (M2 macrophages, Ferangi Blue; spectral image color blue). Yellow indicates the amount of colocalization between the various macrophage markers. EFA indicates early fibroatheroma; FCP, fibrotic calcified plaque; HR, healed rupture; IX, intimal xanthoma; LFA, late fibroatheroma; N/A, not applicable; PIT, pathological intimal thickening; PR, plaque rupture; TCFA, thin-cap fibroatheroma.

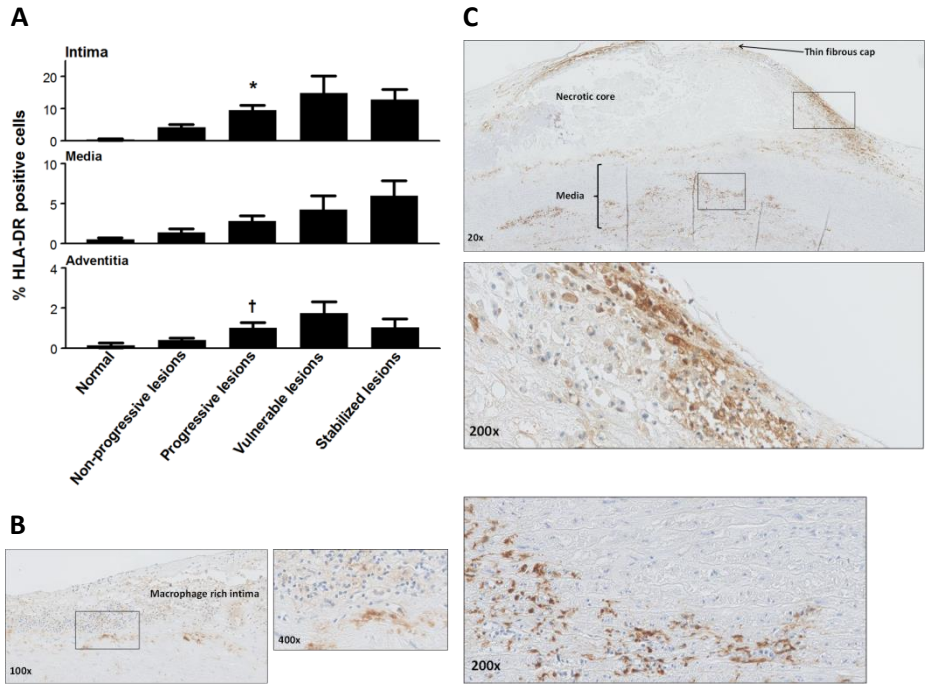

Figure 5. HLA-DR expression during aortic atherosclerosis. **A.** The mean percentage of HLA-DR expression (intima, media and adventitia) based on lesion morphology. HLA-DR expression increases within all the vascular layers (significant within the intima and the adventitia with progressive atherosclerosis (* $p<0.002$; † $p<0.01$)) and tend to decrease in the stabilized phase. **B.** Representative image of an intimal xanthoma (IX) stained for HLA-DR at 100x magnification with a high-resolution image at a 400x magnification. HLA-DR staining is clearly seen in macrophage rich areas located in the intima. **C.** Representative image of a thin cap fibroatheroma (TCFA) stained for HLA-DR at 20x magnification with a more detailed (200x magnification) of the macrophage foam cell rich shoulder region and media. Expression of HLA-DR is more extensive in advanced and vulnerable stages of atherosclerosis. Total number of cases in figure A: 89 (normal 8, non-progressive lesions 24, progressive lesions 34, vulnerable lesions 14 and stabilized lesions 9. The large solid bars in figure A represent the mean percentage of HLA-DR within the aortic wall section per atherosclerotic phase ± SEM. All sections were developed with DAB and counterstained with Mayer's haematoxylin.

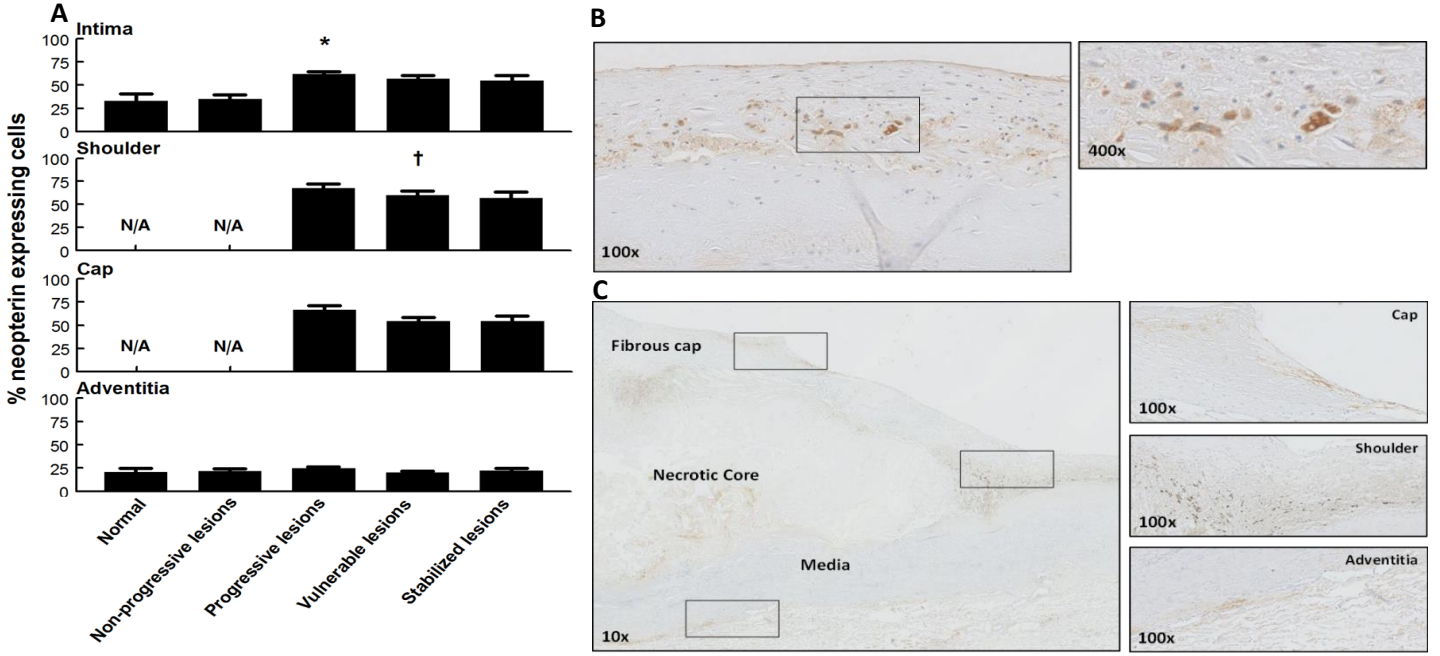

Figure 6. Neopterin expression during aortic atherosclerosis. **A.** The mean percentage of neopterin (intima, media and adventitia) based on lesion morphology. Neopterin expression is minimal in early atherosclerosis, but increases during progressive disease (*p<0.0007) afterwards, remains relatively unchanged for stable healed plaque ruptures and fibrocalcific plaques. There is a small, but significant decrease in neopterin expression within the shoulder regions of vulnerable plaques († p<0.043). Adventitial neopterin staining is relatively minimal and stable throughout all lesion morphologies. **B.** Representative image of an intimal xanthoma (IX) stained for neopterin with a high resolution image at a 400x magnification. The neopterin expression is seen in areas containing macrophage foam cells. **C.** Representative image of a healed rupture (HR) stained for neopterin with high resolution details of the cap, shoulder and adventitia at a 100x magnification. Neopterin expression is present within the various areas of the atherosclerotic lesion. Total number of cases in figure A: 102 (normal 7, non-progressive lesions 23, progressive lesions 35, vulnerable lesions 22 and stabilized lesions 15. The large solid bars in figure A represent the mean percentage of neopterin expression within the aortic wall section per atherosclerotic phase ± SEM. All sections were developed with DAB and counterstained with Mayer's haematoxylin.

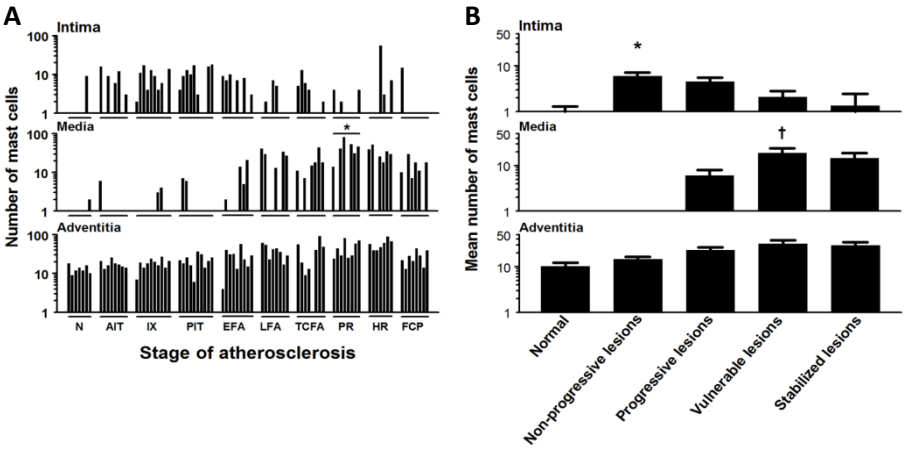

Figure 7. Mast cell (tryptase+) distribution during aortic atherosclerosis. **A.** Mast cells are constitutively present in the intima and adventitia in the aortic wall. The media practically remains devoid of mast cells until the progressive lesions. A significant increase in mast cells is seen in the media of ruptured plaques (* $p<0.01$). **B.** The highest number of mast cells within the intima is present in the non-progressive phase ($p<0.01$) while showing a gradual decrease with lesion progression achieving a minimum for stable fibrocalcific plaques. The media remains almost devoid of mast cells in the normal aorta's and in the non-progressive lesions but significantly increases in vulnerable plaques († $P<0.0001$) in contrast to adventitial mast cells, which remain relatively stable throughout the atherosclerotic process. **C.** Representative image of a normal aorta stained for tryptase with high-resolution images of the intima (400x magnification) and adventitia (200x magnification), as indicated by the black arrows. Note the adventitial mast cells are scattered and mainly located near *vasa vasorum*. **D.** Representative image of a late fibroatheroma with a large necrotic core stained for Tryptase at 20x magnification with high-resolution images of media and adventitia at a 400x magnification. Mast cells are relatively more and remain in close proximity to the *vasa vasorum*. **E.** Representative image of the adventitia of an intimal xanthoma double stained for CD68 (Vina Green) and tryptase (Warp Red). CD68 positive mast cells are identified (arrows) and using the Nuance multispectral imaging system FX the co-localization can be separately analyzed. Total number of cases in figure A and B: 83 (normal 7, non-progressive lesions 18 (*viz.* AIT (8) and IX (10)), progressive lesions 27 (*viz.* PIT (10), EFA (9) and LFA (8)), vulnerable lesions 16 (*viz.* TCFA (8) and PR (8)) and stabilized lesions 15 (*viz.* HR (7) and FCP (8)). In figure A, the vertical axis of the intima, media and adventitia is presented as a log-scale. Each solid bar in figure A represents the number of positively stained mast cells within the intima, media and adventitia of one aortic plaque. The large solid bars in figure B represent the mean total number of mast cells within the entire aortic wall per atherosclerotic phase ± SEM. For abbreviations and a detailed description concerning the classification see Material & Methods section. All sections were developed with DAB and counterstained with Mayer's haematoxylin.

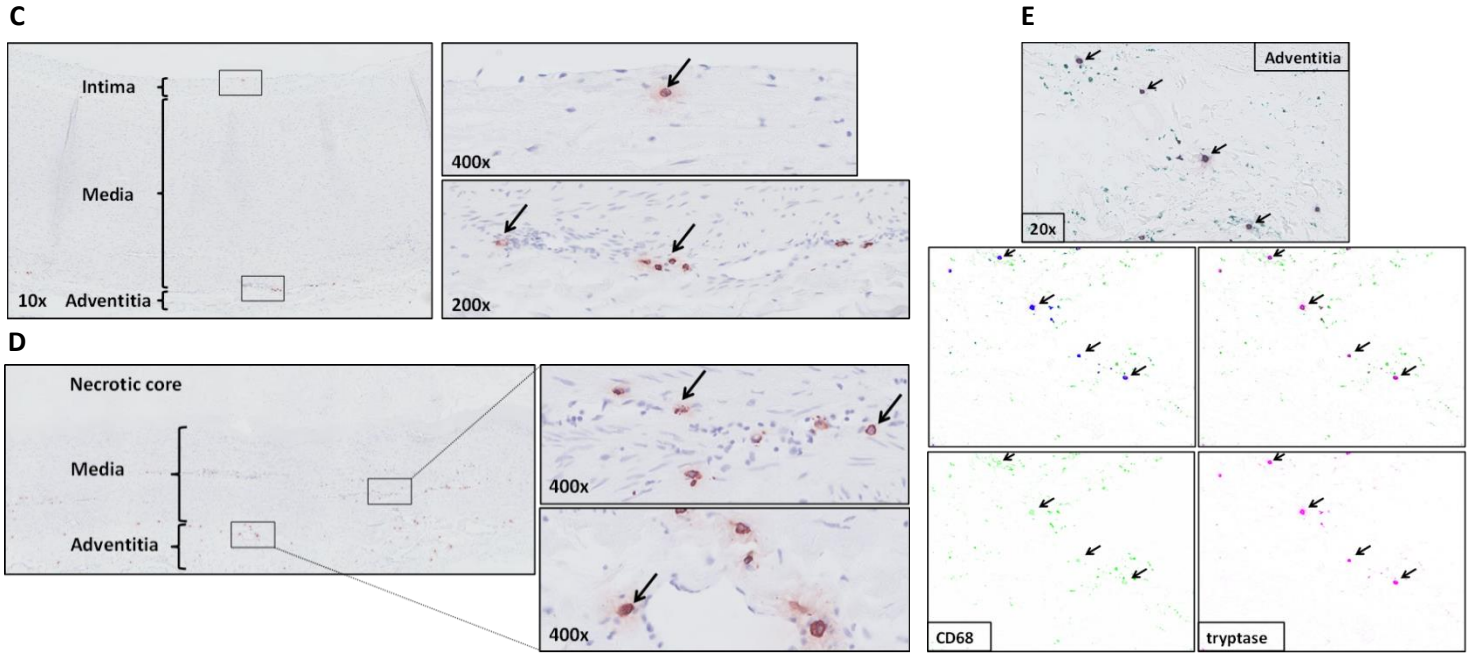

Figure 7. Continued.

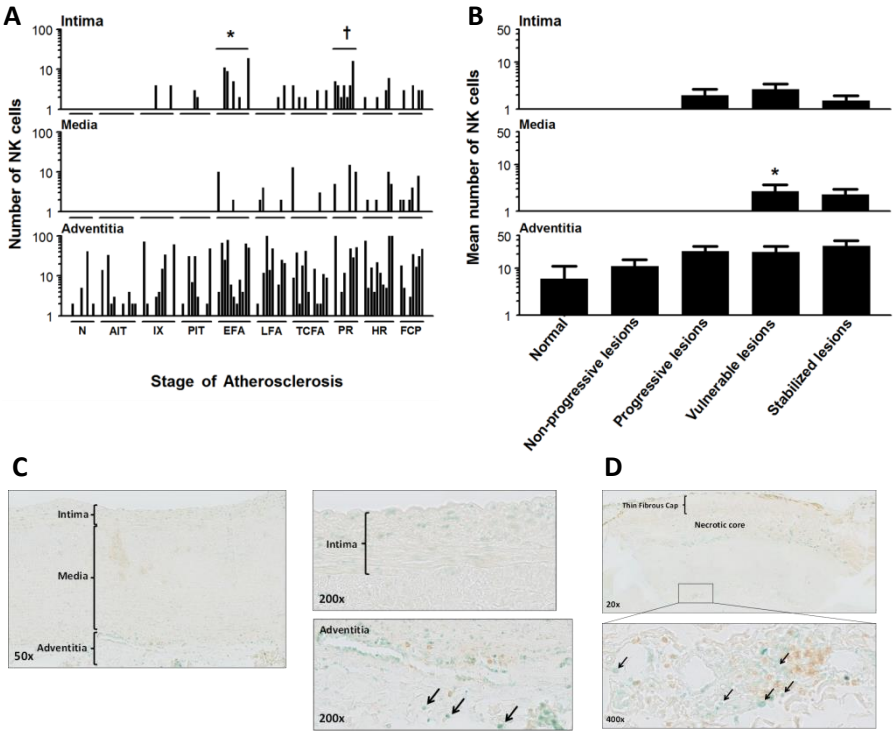

Figure 8. NK cell (T-bet+/CD4-) distribution during aortic atherosclerosis. **A.** A significant increase in NK cells is seen in the intima in EFA (* $p<0.01$) and in ruptured plaques († $p<0.011$). The media practically remains devoid of NK cells in progressive atherosclerosis. NK cells are constitutively and similarly present in the adventitia throughout the disease process. **B.** NK cells are minimally present in the aortic intima and media. NK cells are largely confined to the adventitia and the medial-adventitial border zone and the number of NK cells increases during the atherosclerotic process. A small but significant increase in NK cells in the media is seen in the vulnerable phase (*viz.* TCFA and PR). (* $p<0.001$). **C.** Illustrative images of an non progressive lesion (AIT) showing T-Bet+/CD4- cells (methylgreen; black arrows). Note T-helper cells (CD4+ single positive) cells in the adventitia (brown; diaminobenzidine chromogen) and the Thelper1 cells (CD4 and T-bet double positive cells). **D.** Representative low power image of a TCFA dual immunostained for CD4/T-bet with a high resolution image of the adventitia at 20x magnification. Note the predominant adventitial location of NK cells (Vinagreen; black arrows). The lesion is a consecutive slide from the Movat and CD68 shown in Figure 3B. Total number of cases in figure A and B: 100 (normal 8, non-progressive lesions 23 (*viz.* AIT (12) and IX (11)), progressive lesions 31 (*viz.* PIT (10), EFA (11) and LFA (10)), vulnerable lesions 20 (*viz.* TCFA (12) and PR (8)) and stabilized lesions 18 (*viz.* HR (10) and FCP (8)). Each solid bar in figure A represents the number of positively stained NK cells within the intima, media and adventitia of a single lesion while the large solid bars in figure B represent the mean total number of NK cells within the aortic wall section per atherosclerotic phase ± SEM. For abbreviations and a detailed description concerning the classification see Material & Methods section. All sections were developed with Vina green and DAB and counterstained with Mayer's haematoxylin.

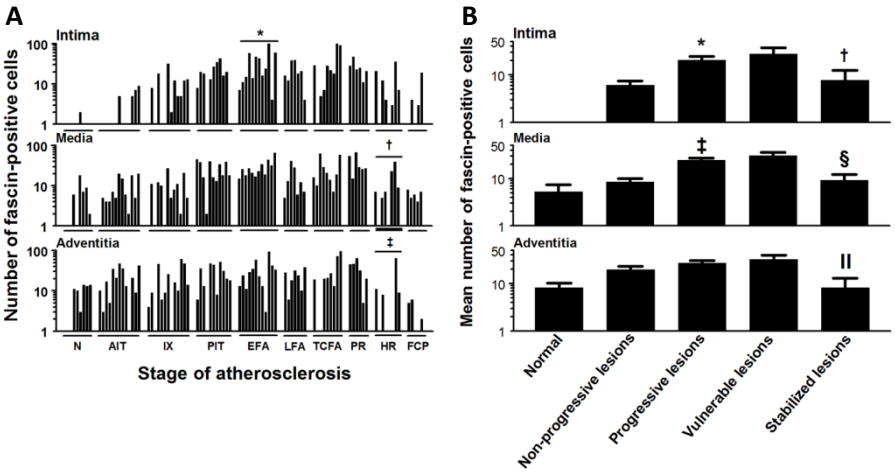

Figure 9. Dendritic cell (fascin+) distribution during aortic atherosclerosis. **A.** Dendritic cells (DCs) are mainly localized to the adventitia near the medial border and gradually increase in number with lesion progression such that DC's are minimally present in the normal intima and intima of non-progressive lesions while significantly increased in progressive atherosclerotic plaque (* $p<0.046$). On the contrary, a significantly decrease in dendritic cells is seen in stabilizing lesions († $p<0.001$ and ‡ $p<0.029$). **B.** The amount of dendritic cells in the intima and media increases significantly in the progressive phase (* $P<0.0004$, ‡ $p<0.0001$). In post ruptured stabilized atherosclerotic lesions the number of fascin-positive cells decrease in all the vascular layers († $p<0.015$, § $p<0.0004$ and ‖ $p<0.002$). **C.** Representative image (100x) of a non-progressive lesion (IX) stained for fascin. Only a few dendritic cells are identified in the deeper intima. **D.** Representative image (10x) of TCFA stained for fascin. This example of a TCFA is from a consecutive slide as the example seen in figure 6C. Note the abundance of fascin-positive cells in the intima, media and adventitia. **E.** Illustrative image (10x) of a FCP stained for fascin with a high-resolution image of the adventitia (200x) showing a relative decrease in fascin-positive cells in all vascular layers. Total number of cases in Figure A and B: 92 (normal 8, non-progressive lesions 26 (*viz.* AIT (13) and IX (13)), progressive lesions 30 (*viz.* PIT (11), EFA (12) and LFA (7)), vulnerable lesions 15 (*viz.* TCFA (9) and PR (6)) and stabilized lesions 13 (*viz.* HR (8) and FCP (5)). The vertical axis of the intima, media and adventitia in figure A and B is presented as a log-scale. Each solid bar in figure A represents the number of fascin-positive cells within the intima, media and adventitia of one aortic plaque. The large solid bars in figure B represent the mean total number of fascin-positive cells within the aortic wall section per atherosclerotic phase ± SEM. For abbreviations and a detailed description concerning the classification see Material & Methods section. All sections were developed with DAB and counterstained with Mayer's haematoxylin.

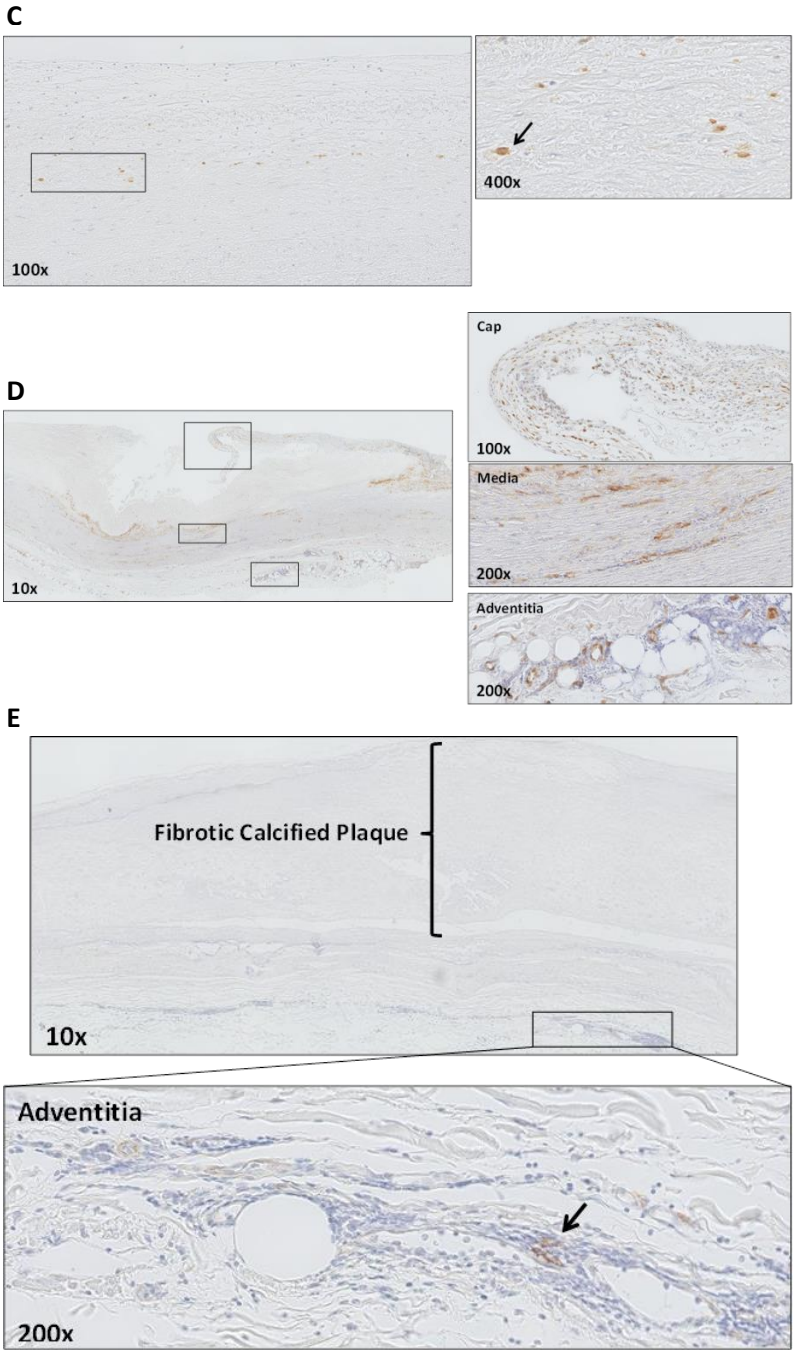

Figure 9. Continued.

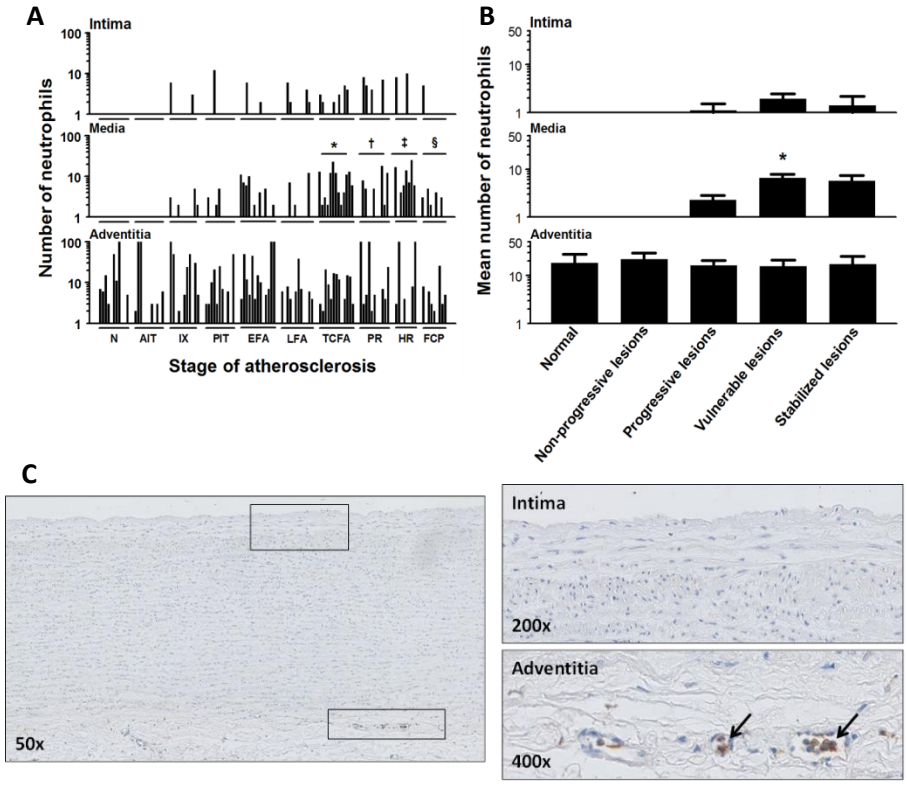

Figure 10. Neutrophil (myeloperoxidase+) distribution during aortic atherosclerosis. **A.** Minimal presence of intimal neutrophils during the atherosclerotic process. Medial neutrophils significantly increase in TCFA and PR (* $p<0.0002$, † $p<0.033$) and healing ruptures (‡ $p<0.007$) and decrease in FCP (§ $p<0.0002$). **B.** Overall the mean amount of neutrophils within the media significantly increase in vulnerable lesions (* $p<0.0005$). **C.** Illustrative image (50x) of a normal aorta stained for MPO with high resolution images of the intima (200x) and the adventitia (400x). The identified neutrophils are all intravascular located in the vaso vasorum (black arrows). This example of a TCFA is again a consecutive section of the Movat and CD68 provided in Figure 3B and 8D. Neutrophils in the media and adventitia are located within the infiltrating vaso vasorum (black arrows). Total number of cases in figure A and B: 108 (normal 11, non-progressive lesions 22 (*viz.* AIT (11) and IX (11)), progressive lesions 35 (*viz.* PIT (11), EFA (13) and LFA (11)), vulnerable lesions 24 (*viz.* TCFA (13) and PR (11)) and stabilized lesions 16 (*viz.* HR (7) and FCP (9)). The vertical axis of the intima, media and adventitia in figure A and B is presented as a log-scale. Each solid bar in figure A represents the number of neutrophils within the intima, media and adventitia of one aortic plaque. The large solid bars in figure B represent the mean total number of neutrophils within the aortic wall section per atherosclerotic phase ± SEM. For abbreviations and a detailed description concerning the classification see Material & Methods section. All sections were developed with DAB and counterstained with Mayer's haematoxylin.

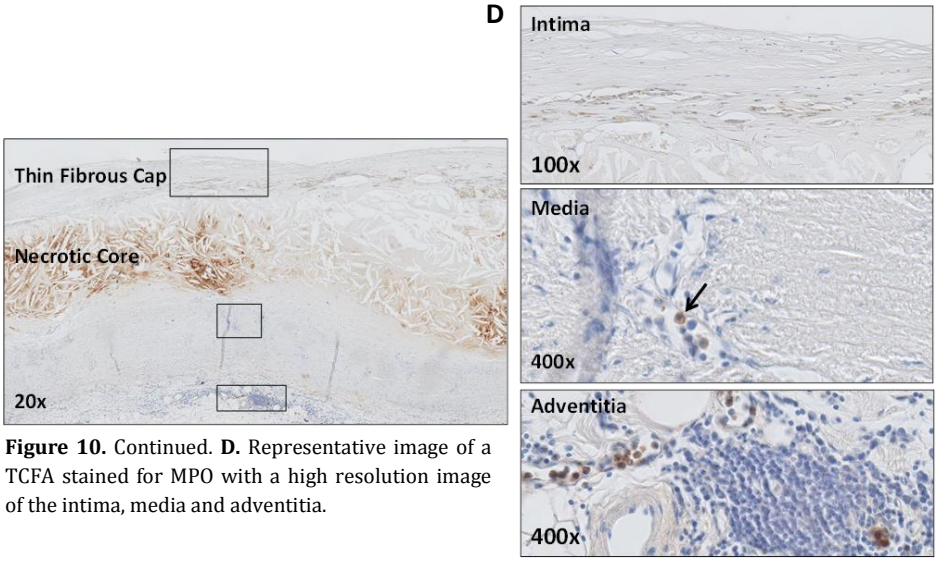

Figure 10. Continued. **D.** Representative image of a TCFA stained for MPO with a high resolution image of the intima, media and adventitia.

DISCUSSION

To a large extent, murine studies have emphasized the pivotal role of the innate immune system in the development and progression of atherosclerosis[11] although there are fundamental metabolic, inflammatory and immunologic differences that exist between various mouse strains, and more importantly between mouse and man. As such, definitive evidence on how observations of lipoprotein oxidation, inflammation and immunity translate to human atherosclerotic disease is still lacking[24]. Consequently, it has been pointed out that studies in the human atherosclerotic process are essential to ensure the data obtained from experimental murine atherosclerosis models is relevant[17,25]. This explorative study is based on histological observations from a unique biobank of human aorta, which allows evaluation of the full spectrum of atherosclerotic disease.

Our findings confirm a predominance of macrophages. Multiplex staining for M1/M2 macrophages failed to show a significant predominance in M1 macrophages in the foam cell rich areas, which is inconsistent with a dichotomous classification system for macrophage phenotype differentiation[26] as been described for murine models were M2 macrophages dominate the later stages of atherosclerotic disease. Moreover, quantitative findings for mast cells, NK cells, eosinophils and neutrophils do not imply these cell types as critical contributors to plaque destabilization.

LDL and innate immunity in lesion progression

Accumulation of LDL fragments is the primary trigger for the atherosclerotic process and is directly linked to activation and perpetuation of the innate immune response[27]. In the present study, Apo B100 was used to visualize pro-atherogenic lipoprotein particles mainly consistent with low-density lipoprotein (LDL) accumulation although antibody staining is not specific for oxidation products. In an earlier study we extensively reported on oxidation specific epitopes, apolipoprotein B100 and apo(a) in a wide range of human coronary and carotid atherosclerotic lesions and demonstrated that plaques in early atherosclerotic lesions are enriched in apolipoprotein B100[28].

Apolipoprotein B100 expression was limited to the intimal layer in aortic wall samples classified as normal, adaptive intimal thickening and intimal xanthoma. On the contrary, transition to pathological intimal thickening, the earliest form of progressive atherosclerosis, is characterized by the accumulation of apolipoprotein B100 within the medial wall, which in fact is much earlier than previously reported[29]. Demonstration that the transition to irreversible atherosclerosis is associated with a loss of internal elastic lamina integrity hallmarks the beginning of medial and adventitial involvement in atherosclerosis, a phenomenon that warrants further investigation[30, 31].

Macrophage subtypes

Macrophages play a critical role in innate and acquired immunity, and are in varying degrees involved in all phases of atherosclerotic lesion development particularly in regards to lipid core formation, lesion remodeling, and degradation of the fibrous cap, as seen in advanced symptomatic disease[32]. Macrophage accumulation in the intimal layer of the vessel wall is observed in early, non-progressive atherosclerotic lesions and is thought to be essentially driven by the accumulation of oxidized LDL[33, 34]. In the present study, the overall number of CD68-positive macrophages increased with advancing disease, in concordance with previous studies. Among the various lesion types, macrophage infiltration was most prominent in TCFAs particularly in regions of the fibrous cap, and least for healing ruptures and fibrocalcific plaques[19]. It is generally assumed that macrophages, through release of matrix metalloproteinases directly contribute to plaque destabilization [7, 32]. The overall amount of lesional macrophages as recognized in the present study however is less pronounced compared with murine atherosclerosis[7] and affords a different perspective on the complexity of human plaques[19] particularly in reference to animal models.

Contrary to murine atherosclerosis, we found no evidence of a macrophage subclass shift during initiation, progression, rupture and ultimate stabilization of human atherosclerotic lesions. Overall, approximately 20-30% of macrophages in

early to advanced plaques are double positive for both M1 and M2 markers challenging the paradigm of a clear M1-M2 dichotomy. This finding was further confirmed using alternative M1 and M2 markers (IL-6/Dectin-1), respectively in combination with CD68 to exclude the possibility that the iNOS/CD163/CD68 combination was inadequate in identifying all M1/M2 macrophages. Moreover, ~40% of the intimal macrophages were double negative for iNOS/CD163 or alternatively, IL-6/Dectin-1. CD68 was equally expressed in tryptase positive mast cells, which may partially contribute to macrophages double negative for M1 or M2 markers.

Taken together, a simple dichotomous classification scheme as proposed for macrophage differentiation in mice falls short in the biological context and complexity of human disease. Clearly, more than 2 subtypes of macrophages with presumably functionally different roles might be involved in human atherosclerosis[8]. As mentioned, the current immunostaining techniques likely fall short in identifying known and unknown macrophage subsets in human disease for lack of specificity. Single-cell analyses could provide invaluable insights into studying macrophage heterogeneity, but is technically challenging and beyond the scope of this paper. Along these same lines, a functional equivalence to murine macrophages remains unclear where caution is warranted with directly extrapolation of findings from mouse to humans or *vice versa*.

Dendritic Cells

Dendritic cells are professional antigen-presenting cells and constitute a uniquely interface between innate and adaptive immune system[35]. The identification of dendritic cells in human and mouse vascular wall has stimulated interest in the role of these cells in the pathogenesis of several acute and chronic vascular disorders, including atherosclerosis[36]. How dendritic cells influence the initiation and progression of atherosclerosis remains unclear. On basis of their pivotal role in antigen presentation, activating T cells, and secreting cytokines, and perhaps also their ability to become foam cells, it has been suggested that dendritic cells are critically involved in the pathogenesis of atherosclerosis[37,38].

Unfortunately, attempts to visualize dendritic cell subtype markers (CD80, CD86, DC lamp, DC sign) failed on formalin-fixed paraffin embedded (FFPE) material, as demonstrated in a previous study[39]. As such, dendritic cells could only be recognized by the general DC-marker fascin, which has been showed to correlate with DC maturation into antigen presenting cells[40]

There was a strong positive relationship between progressive disease and fascin positive dendritic cells in all vascular layers. The accumulation of dendritic cells within atherosclerosis-prone areas of normal aorta further supports the involvement of immune mechanisms from very early stages of the disease[41].

Dendritic cells residing in the media and adventitia were mainly located near the infiltrating *vaso vasorum* and adventitial infiltrates of T cells. Dendritic cells are known to patrol this region of the plaque sampling antigens and presenting them to T lymphocytes. Our previous study regarding the adaptive immune response in human atherosclerosis identified such organized tertiary lymphoid structures in the adventitia[22].

The current observations indicate a prominent role of dendritic cells in human atherosclerosis. However, different roles for dendritic cells in atherogenesis or plaque progression have been identified in mouse models while a clear attribution to dendritic cells and the exact molecular mechanisms engaged remain unresolved. The identification of human homologs of mouse dendritic cell subsets and further work in this area will aid to promote translational approaches of single cell studies.

Mast cells

Abundance of mast cells in the shoulder region of human coronary atheromas spurred interest in a possible role of these cells in the atherosclerotic process[42]. Although a role for mast cells is supported by a rodent studies, a role in human atherosclerosis remains unclear with the current knowledge[43,44].

Mast cells were most prominent in the media and adventitial layers and were independent of the phase of atherosclerosis. Similarly, intimal mast cell infiltration constitutes an early event in the atherosclerotic process, which subsequently plateaus. Specifically, our data do not imply an association between mast cell content and plaque destabilization and on the contrary, suggest an apparent decrease in progressive and vulnerable atherosclerotic lesions. Moreover, we did not find extracellular mast cell granules associated with fibrous cap thinning in contrary to the proposed active participation in substantial degradation of the extracellular matrix and local weakening of inflamed atherosclerotic lesions, a situation well documented in diseases affecting the connective tissue[45, 46, 47]. Altogether, these findings fail to point to a direct relationship between intimal mast cell content and cap destabilization.

Considering medial and adventitial mast cells were typically located within or in close proximity to the infiltrating *vaso vasorum* it's conceivable that these cells are involved in plaque neovascularization in advancing and vulnerable atherosclerotic lesions. Yet an alternative explanation would be that mast cells enter through and home in the proximity of the infiltrating *vaso vasorum*[26,36]. The accumulation of mast cells in shoulder regions of human coronary atheromas may be similarly secondary to the neovascularization. Overall, these observational data neither support nor refute a role for mast cell in the progression and complications of atherosclerosis. Such a role can only be assessed in clinical studies. Although aggressive immunosuppression for abdominal aortic aneurysms appeared to have

no effect on resident mast cells, including macrophages and SMCs, a similar study on atherosclerosis related end-points is urgently missing[48].

Natural killer (NK) cells

Natural killer cells are cytotoxic lymphocytes that are part of the innate immune system. Apart from their cytotoxic action, they are an important early source of interferon-γ (IFNγ) and tumor-necrosis factor (TNF) in response to acute injury and infections. NK cells can prime macrophages to secrete pro-inflammatory cytokines and play a key role in viral defense, tumor surveillance and tolerance during pregnancy[49]. In the context of atherosclerosis, it is demonstrated *in vitro* that NK cells infiltrate the vessel wall and promote atherosclerotic lesion development in murine models of the disease[50]. Along these lines, deficiency of functional NK cells has been found to reduce lesion size[51]. At this point a role of NK cells in clinical atherosclerosis remains still unclear.

We tested several classical NK cell markers (CD56, NKp30 and the PEN5 epitope) in order to visualize NK cells, y*et al*l these markers failed on FFPE material and therefore selected an alternative strategy of applied double staining for the Th1/NK cell specific transcription factor T-bet in combination with CD4 staining. $CD4^-$/$T\text{-}bet^+$ cells classified as "NK cells" were abundant in abdominal aortic aneurysm tissue, but minimal in atherosclerotic samples. The few NK cells present in the intima were most common to advanced and vulnerable stages of atherosclerosis. While CD56 immunostaining clearly identified aortic ganglia (and NK cells in tumor tissue), samples of aortic atherosclerosis were negative. In essence, NK cells failed to present as a major local factor contributing to human atherosclerotic disease despite previous indications suggesting marginally decreased systemic NK cell activity in advanced atherosclerosis in the elderly[52].

Neutrophils

Neutrophils are emerging as a potential new player in the atherosclerotic process primarily based on murine studies suggesting their involvement in the initiation of the atherosclerotic process, as well as plaque angiogenesis in later stages of the disease[53, 54]. Moreover, neutrophil infiltration at the level of a disrupted plaque could potentially contribute to plaque progression due to release high amounts of reactive oxygen species and the pro-oxidant enzyme myeloperoxidase[55,]. Yet, a role for neutrophils in human atherogenesis, atheroprogression, and atherosclerotic plaque destabilization is still unclear based on available data[56].

Selective immunostaining suggested that neutrophils were mainly present in the *vasa vasorum*, or in the post-hemorrhagic hematoma due to surgical manipulation where the specific neutrophil markers MPO or MMP8 failed to identified tissue-infiltrating neutrophils with no association of atherosclerotic progression or

plaque vulnerability. The failure to detect neutrophil infiltrates within atherosclerotic tissue however, may be related to the short half-life of these cells although our earlier protein-based studies showed negligible MMP8 and CXCL8 expression thus indicating an absence of neutrophil remnants within the atherosclerotic aorta wall[57,58]. To summarize, these observational data do not support a primary role of neutrophils in human atherosclerosis, but rather indicates that neutrophil presence is related to surgical manipulation of the aorta during removal[59].

Eosinophils

Were fully absent during the entire process of human atherosclerosis.

Limitations

Numerous inflammatory cell phenotypes identified within well- defined morphological stages of atherosclerosis emphasize the complexity of the innate immune response and atherosclerotic disease. This study was performed on aortic sections of deceased individuals, where continuous data represents incidental findings from a large series of patients and therefore may not necessarily reflect longitudinal data. Another limitation of the study is the fact the all findings are based on IHC using paraffin-embedded tissue sections, which precludes use of other relevant and confirmatory markers, particularly those for dendritic cells. Although IHC has the advantage of showing the spatial relationships, multiple staining is challenging, and allows only limited marker sets. Consequently, findings in this study should be considered in this context. Moreover, differences in plaque inflammation may also exist among various vascular beds, although our previous work clearly shows that aortic atherosclerosis follow a similar pattern of disease progression as for coronary tissue[19, 20, 21].

In conclusion, the presence of various macrophage subsets and fascin-positive dendritic cells are strongly associated with atherosclerotic disease of human aorta, particularly for progressive and vulnerable fibroatheromatous plaques. A less prominent role however, is suggested for mast cells and NK cells, while a direct relation with neutrophils and eosinophils was not established. More interestingly, macrophage heterogeneity is far more complex than the current paradigm predicated on murine data and supports the involvement of additional (poorly-defined) macrophage subtypes or perhaps a greater dynamic range of macrophage plasticity. Clearly, there is a divergence in observational data between murine models of atherosclerosis from our human atherosclerosis studies, which point to a limited translational aspect of animal findings.

REFERENCES

1 Fernández-Velasco M, González-Ramos S, Boscá L. Involvement of monocytes/macrophages as key factors in the development and progression of cardiovascular diseases. Biochemical Journal. 2014; 458(2):187-193.

2 Douaiher J, Succar J, Lancerotto L, Gurish MF, Orgill DP, Hamilton MJ, Krilis SA, Stevens RL. Development of mast cells and importance of their tryptase and chymase serine proteases in inflammation and wound healing. Advances in Immunology. 2014;122:211-252.

3 Ma Y, Yabluchanskiy A, Lindsey ML. Neutrophil roles in left ventricular remodeling following myocardial infarction. Fibrogenesis Tissue Repair. 2013;6(1):11.

4 Hansson GK, Libby P, Schönbeck U, Yan ZQ. Innate and adaptive immunity in the pathogenesis of atherosclerosis. Circulation Research. 2002;91(4):281-291.

5 Peled M, Fisher EA. Dynamic Aspects of Macrophage Polarization during Atherosclerosis Progression and Regression. Frontiers in Immunology. 2014;5:579.

6 Wang XP, Zhang W, Liu XQ, Wang WK, Yan F, Dong WQ, Zhang Y, Zhang MX. Arginase I enhances atherosclerotic plaque stabilization by inhibiting inflammation and promoting smooth muscle cell proliferation. European Heart Journal. 2014 Apr;35(14):911-919.

7 Moore KJ, Tabas I. Macrophages in the pathogenesis of atherosclerosis. Cell. 2011;145(3):341-355.

8 Chinetti-Gbaguidi G, Colin S, Staels B. Macrophage subsets in atherosclerosis. Nature Reviews Cardiology. 2015;12(1):10-17.

9 Kadl, A., Meher AK, Sharma PR, Lee MY, Doran AC, Johnstone SR, Elliott MR, Gruber F, Han J, Chen W, Kensler T, Ravichandran KS, Isakson BE, Wamhoff BR, Leitinger N. Identification of a novel macrophage phenotype that develops in response to atherogenic phospholipids via Nrf2. Circulation Research. 2010;107:737–746.

10 Johnson, J.L., and Newby, A.C. Macrophage heterogeneity in atherosclerotic plaques. Current Opinion in Lipidology. 2009;20:370–378

11 Libby P, Ridker PM, Hansson GK. Progress and challenges in translating the biology of atherosclerosis. Nature. 2011;473(7347):317-325.

12 Martinez FO, Helming L, Milde R, Varin A, Melgert BN, Draijer C, Thomas B, Fabbri M, Crawshaw A, Ho LP, Ten Hacken NH, Cobos Jiménez V, Kootstra NA, Hamann J, Greaves DR, Locati M, Mantovani A, Gordon S. Genetic programs expressed in resting and IL-4 alternatively activated mouse and human macrophages: similarities and differences. Blood. 2013;121(9):e57-69.

13 Bryant CE, Monie TP. Mice, men and the relatives: cross-species studies underpin innate immunity. Open Biology. 2012;2(4):120015.

14 Colucci F, Di Santo JP, Leibson PJ. Natural killer cell activation in mice and men: different triggers for similar weapons? Nature Immunology. 2002;3(9):807-813.

15 Ylä-Herttuala S, Bentzon JF, Daemen M, Falk E, Garcia-Garcia HM, Herrmann J, Hoefer I, Jukema JW, Krams R, Kwak BR, Marx N, Naruszewicz M, Newby A, Pasterkamp G, Serruys PW, Waltenberger J, Weber C, Tokgözoglu L. Stabilisation of atherosclerotic plaques. Position paper of the European Society of Cardiology (ESC) Working Group on Atherosclerosis and vascular biology. Thrombosis and Haemostasis. 2011;106(1):1-19.

16 Seok J, Warren HS, Cuenca AG, Mindrinos MN, Baker HV, Xu W, Richards DR, McDonald-Smith GP, Gao H, Hennessy L, Finnerty CC, López CM, Honari S, Moore EE, Minei JP, Cuschieri J, Bankey PE, Johnson JL, Sperry J, Nathens AB, Billiar TR, West MA, Jeschke MG, Klein MB, Gamelli RL, Gibran NS, Brownstein BH, Miller-Graziano C, Calvano SE, Mason PH, Cobb JP, Rahme LG, Lowry SF, Maier RV, Moldawer LL, Herndon DN, Davis RW, Xiao W, Tompkins RG. Genomic responses in mouse models poorly mimic human inflammatory diseases. Proceedings of the National Academy of Sciences U S A. 2013;110(9):3507-3512.

17 Mestas J, Hughes CC. Of mice and not men: differences between mouse and human immunology. Journal of Immunology. 2004;172(5):2731-2738

18 Jiang X, Shen C, Yu H, Karunakaran KP, Brunham RC. Differences in innate immune responses correlate with differences in murine susceptibility to Chlamydia muridarum pulmonary infection. Immunology. 2010;129:556-566

19 van Dijk RA, Virmani R, von der Thüsen JH, Schaapherder AF, Lindeman JH. The natural history of aortic atherosclerosis: a systematic histopathological evaluation of the peri-renal region. Atherosclerosis. 2010;210(1):100-106.

20 Virmani R, Kolodgie FD, Burke AP, Farb A, Schwartz SM. Lessons from sudden coronary death: a comprehensive morphological classification scheme for atherosclerotic lesions. Arteriosclerosis, thrombosis, and vascular biology. 2000;10(5):1262-1275.

21 K. Yahagi, F.D. Kolodgie, F. Otsuka, A. V. Finn, H. R. Davis, M.Joner, R.Virmani. Pathophysiology of native coronary, vein graft, and in-stent atherosclerosis. Nature Reviews Cardiology.2015; ahead of publication.

22 van Dijk RA, Duinisveld AJ, Schaapherder AF, Mulder-Stapel A, Hamming JF, Kuiper J, de Boer OJ, van der Wal AC, Kolodgie FD, Virmani R, Lindeman JH. A change in inflammatory footprint precedes plaque instability: a systematic evaluation of cellular aspects of the adaptive immune response in human atherosclerosis. Journal of American Heart Association. 2015;4(4).

23 van der Loos C.M. Multiple immunoenzyme staining: methods and visualizations for the observation with spectral imaging. Journal of Histochemistry & Cytochemistry. 2008;56: 313-328.

24 Chen YC, Peter K. Determining the characteristics of human atherosclerosis: A difficult but indispensable task providing the direction and proof of concept for pioneering atherosclerosis research in animal models, Atherosclerosis. 2015.

25 Watanabe H, Numata K, Ito T, Takagi K, Matsukawa A. Innate immune response in Th1- and Th2-dominant mouse strains. Shock. 2004;22:460-466

26 David MM, Justin PE. Exploring the full spectrum of macrophage activation. Nature Reviews Immunology. 2008;8(12): 958–969.

27 Yan ZQ, Hansson GK. Innate immunity, macrophage activation, and atherosclerosis. Immunology Reviews. 2007;219:187-203.

28 van Dijk RA, Kolodgie F, Ravandi A, Leibundgut G, Hu PP, Prasad A, Mahmud E, Dennis E, Curtiss LK, Witztum JL, Wasserman BA, Otsuka F, Virmani R, Tsimikas S. Differential expression of oxidation-specific epitopes and apolipoprotein(a) in progressing and ruptured human coronary and carotid atherosclerotic lesions. Journal of Lipid Research. 2012;53(12):2773-2790.

29 Moreno PR, Purushothaman KR, Fuster V, O'Connor WN. Intimomedial interface damage and adventitial inflammation is increased beneath disrupted atherosclerosis in the aorta: implications for plaque vulnerability. Circulation. 2002;105(21):2504-2511.

30 Libby P, Hansson GK. Inflammation and immunity in diseases of the arterial tree: players and layers. Circulation Research. 2015;116(2):307-311.

31 Otsuka F, Kramer MCA, Woudstra P, Yahagi K, Ladich E, Finn AV, de Winter RJ, Kolodgie FD, Wight TN, Davis HR, Joner M, Virmani R. Natural progression of atherosclerosis from pathologic intima thickening to late fibroatheroma in human coronary arteries: A pathology study. Atherosclerosis. 2015;241(2):772-782.

32 Virmani R, Burke AP, Farb A, Kolodgie FD. Pathology of the vulnerable plaque. Journal of American College of Cardiology. 2006;47:C13–C18.

33 Ross R. Atherosclerosis—an inflammatory disease. The New England Journal of Medicine. 1999;340(2):115–126.

34 Glass CK,Witztum JL. Atherosclerosis the road ahead. Cell. 2001;104:503–516.

35 Bobryshev YV. Dendritic cells in atherosclerosis: current status of the problem and clinical relevance. European Heart Journal. 2005;26(17):1700-1704.

36 Choi JH, Do Y, Cheong C, Koh H, Boscardin SB, Oh YS, Bozzacco L, Trumpfheller C, Park CG, Steinman RM. Identification of antigen-presenting dendritic cells in mouse aorta and cardiac valves. Journal of Experimental Medicine. 2009;206:497–505.

37 Hansson GK, Libby P. The immune response in atherosclerosis: a double-edged sword. Nature Reviews Immunology. 2006;6(7):508-519.

38 Gordon S, Taylor PR. Monocyte and macrophage heterogeneity. Nature Reviews Immunology. 2005;5:953-964.

39 Van Vré EA, Bosmans JM, Van Brussel I, Maris M, De Meyer GR, Van Schil PE, Vrints CJ, Bult H. Immunohistochemical characterisation of dendritic cells in human atherosclerotic lesions: possible pitfalls. Pathology. 2011;43(3):239-247.

40 Al-Alwan MM, Rowden G, Lee TD, West KA. Fascin is involved in the antigen presentation activity of mature dendritic cells. Journal of Immunology 2001; 166: 338-45.

41 Zernecke A. Dendritic cells in atherosclerosis: evidence in mice and humans. Arteriosclerosis, thrombosis, and vascular biology. 2015;35(4):763-770.

42 Holmes DR Jr, Savage M, LaBlanche JM, Grip L, Serruys PW, Fitzgerald P, Fischman D, Goldberg S, Brinker JA, Zeiher AM, Shapiro LM, Willerson J, Davis BR, Ferguson JJ, Popma J, King SB 3rd, Lincoff AM, Tcheng JE, Chan R, Granett JR, Poland M. Results of Prevention of REStenosis with Tranilast and its Outcomes (PRESTO) trial. Circulation. 2002;106: 1243-1250.

43 Spinas E, Kritas SK, Saggini A, Mobili A, Caraffa A, Antinolfi P, Pantalone A, Tei M, Speziali A, Saggini R, Conti P. Role of mast cells in atherosclerosis: a classical inflammatory disease. International Journal of Immunopathology and Pharmacology. 2014;27(4):517-521.

44 Kaartinen M, Penttilä A, Kovanen PT. Accumulation of activated mast cells in the shoulder region of human coronary atheroma, the predilection site of atheromatous rupture. Circulation. 1994;90:1669-1678.

45 Bromley M, Fisher WD, Woolley DE. Mast cells at site of cartilage erosion in the rheumatoid joint. Annals of the Rheumatic Diseases. 1984;43:76-79.

46 Loke P, Gallagher I, Nair MG, Zang X, Brombacher F, Mohrs M, Allison JP, Allen JE. Alternative activation is an innate response to injury that requires CD4+ T cells to be sustained during chronic infection. Journal of Immunology. 2007;179:3926–3936.

47 Coussens, L.M. Raymond WW, Bergers G, Laig-Webster M, Behrendtsen O, Werb Z, Caughey GH, Hanahan D. Inflammatory mast cells up-regulate angiogenesis during squamous epithelial carcinogenesis. Genes & Development. 1999;13:1382-1397.

48 Lindeman JH1, Rabelink TJ, van Bockel JH. Immunosuppression and the abdominal aortic aneurysm: Doctor Jekyll or Mister Hyde? Circulation. 2011;124(18):e463-e465.

49 O'Shea JJ, Murray PJ. Cytokine signaling modules in inflammatory responses. Immunity. 2008;28:477–487.

50 Stöger JL, Gijbels MJ, van der Velden S, Manca M, van der Loos CM, Biessen EA, Daemen MJ, Lutgens E, de Winther MP. Distribution of macrophage polarization markers in human atherosclerosis. Atherosclerosis. 2012 Dec;225:461-468.

51 Whitman SC, Rateri DL, Szilvassy SJ, Yokoyama W, Daugherty A. Depletion of natural killer cell function decreases atherosclerosis in low-density lipoprotein receptor null mice. Arteriosclerosis, thrombosis, and vascular biology. 2004;24(6):1049-1054.

52 Bruunsgaard H, Pedersen AN, Schroll M, Skinhøj P, Pedersen BK. Decreased natural killer cell activity is associated with atherosclerosis in elderly humans. Experimental Gerontology. 2001;37(1):127-136.

53 Weber C, Zernecke A, Libby P. The multifaceted contributions of leukocyte subsets to atherosclerosis: lessons from mouse models. Nature Reviews Immunology. 2008; 8:802–815.

54 Soehnlein O. Multiple roles for neutrophils in atherosclerosis. Circulation Research. 2012;110(6):875-888.

55 Drechsler M, Megens RT, van Zandvoort M, Weber C, Soehnlein O. Hyperlipidemia-triggered neutrophilia promotes early atherosclerosis. Circulation. 2010;122:1837–1845.

56 Döring Y, Drechsler M, Soehnlein O, Weber C. Neutrophils in atherosclerosis: from mice to man. Arteriosclerosis, thrombosis, and vascular biology. 2015;35(2):288-295.

57 Lindeman JH, Abdul-Hussien H, Schaapherder AF, Van Bockel JH, Von der Thüsen JH, Roelen DL, Kleemann R. Enhanced expression and activation of pro-inflammatory transcription factors distinguish aneurysmal from atherosclerotic aorta: IL-6- and IL-8-dominated inflammatory responses prevail in the human aneurysm. Clinical Science. 2008; 114: 687-697.

58 Abdul-Hussien H, Soekhoe RG, Weber E, von der Thüsen JH, Kleemann R, Mulder A, van Bockel JH, Hanemaaijer R, Lindeman JH. Collagen degradation in the abdominal aneurysm: a conspiracy of matrix metalloproteinase and cysteine collagenases. American Journal of Pathology. 2007;170: 809-817.

59 Libby P, Lichtman AH, Hansson GK. Immune effector mechanisms implicated in atherosclerosis: from mice to humans. Immunity. 2013;38:1092–1104.

CHAPTER 7

A change in inflammatory foot print precedes plaque instability: A systematic evaluation of cellular aspects of the adaptive immune response in human atherosclerosis

R.A. van Dijk
A.J.F. Duinisveld
A.F. Schaapherder
A. Mulder-Stapel
J.F. Hamming
J. Kuiper
O.J. de Boer
A.C. van der Wal
F.D. Kolodgie
R.Virmani
J.H.N. Lindeman

Journal of the American Heart Association 2015

ABSTRACT

Background: Experimental studies characterize adaptive immune response as a critical factor in the progression and complications of atherosclerosis. Yet, it is unclear whether these observations translate to the human situation. This study systematically evaluates cellular components of the adaptive immune response in a biobank of human aortas covering the full spectrum of atherosclerotic disease.

Material and methods: A systematic analysis was performed on 114 well-characterized peri-renal aortic specimens with immunostaining for T-cell subsets (CD3/4/8/45RA/45RO/FoxP3) and the Th1/non-Th1/Th17 ratio (CD4+T-bet+/CD4+T-bet–/CD4+/IL-17+ double staining). CD20 and CD138 were used to identify B-cells and plasma cells, while B-cell maturation was evaluated by AID/CD21 staining and expression of lymphoid homeostatic CXCL13.

Results: Scattered CD4 and CD8 cells with a T memory subtype were found in normal aorta and early, non-progressive lesions. The total number of T-cells increases in progressive atherosclerotic lesions (~1:5 CD4/CD8 T-cell ratio). A further increase in medial and adventitial T-cells is found upon progression to vulnerable lesions. This critical stage is further hallmarked by de-novo formation of adventitial lymphoid-like structures containing B-cells and plasma cells, a process accompanied by transient expression of CXCL13. A dramatic reduction of T-cell subsets, disappearance of lymphoid structures, and loss of CXCL13 expression characterize post-ruptured lesions. FoxP3 and Th17 T-cells were minimally present throughout the atherosclerotic process.

Conclusion: Transient CXCL13 expression, restricted presence of B-cells in human atherosclerosis, along with formation of non-functional extranodal lymphoid structures in the phase preceding plaque rupture, indicates a “critical” change in the inflammatory footprint before and during plaque destabilization

INTRODUCTION

Atherosclerosis is a highly dynamic[1,2] metabolic disease with a strong inflammatory component [3,4,5.] Compelling evidence, largely based on data derived from murine models of atherosclerotic disease, implies extensive involvement of the adaptive immune response in the initiation, progression and complications of atherosclerotic disease[6]. As a consequence, the adaptive immune response is considered a potential target for medical interventions.

An open question is how these observations translate to the human situation. There are fundamental immunological and inflammatory differences between mice and men[7,8,9.] Moreover, murine models of accelerated atherosclerotic disease require an immunologic background with exaggerated Th1-cell responsiveness in order for atherosclerosis to develop[8,9]. Hence, observations from mouse models may be skewed towards Th1 response. Extrapolation of the murine data is further complicated by absence of vulnerable lesion formation in the current models of atherosclerotic disease. As a result, data on a possible involvement of the adaptive immune response in the advanced stages of atherosclerotic disease is missing.

Available human data on the other hand largely relies on surgical specimens. Yet, it is important to note that this material generally represents the final stages of the disease process[10,11]. As such, data from these human studies is not representative for the earlier and intermediate phases of atherosclerotic disease; hence knowledge on the nature of the adaptive immune response in the human atherosclerotic process is limited.

Given the above considerations, we regarded an evaluation of the adaptive immune response within the process of atherosclerotic lesion formation, progression and stabilization relevant. To that end, we performed comprehensive and systematic histological assessment of cellular aspects of the adaptive immune response in tissue samples from a biobank of arterial tissue that covers the full spectrum of human atherosclerotic disease. Results from this explorative study confirm extensive and dynamic presence of cellular components of the adaptive immunity in the human atherosclerotic process, and reveal profound changes in the inflammatory foot print immediately prior to and during the process of plaque destabilization.

MATERIAL AND METHODS

Patients and tissue sampling

Tissue sections were selected from a tissue bank of aortic wall patches that were obtained during liver, kidney and pancreas transplantation with grafts derived from cadaveric donors. Details of this bank have been described previously by van

Dijk *et al* [12]. All patches were from grafts that were eligible for transplantation (*i.e.* all donors met the criteria set by The Eurotransplant Foundation). Due to national regulations, only transplantation relevant data for donation is available, as such background information on the specimens is limited. Sample collection and handling was performed in accordance with the guidelines of the Medical and Ethical Committee in Leiden, Netherlands and the code of conduct of the Dutch Federation of Biomedical Scientific Societies (http://www.federa.org/?s=1&m=82&p=0&v=4#827).

Each tissue block in the bank was Movat and H&E stained and classified according to the modified American Heart Association (AHA) classification as proposed by Virmani *et al* by two independent observers with no knowledge of the characteristics of the aortic patch [12,13]. The tissue block showing the most advanced plaque was used for further studies. In order to obtain balanced and representative study groups, we selected the first 100 aortic wall samples from the tissue bank. Due to the fact the vulnerable lesions (*i.e.* thin cap fibroatheroma and plaque ruptures) were under-represented we randomly selected several aortic wall samples classified as vulnerable lesions from the remaining 250 patches in order to obtain approximately 10-12 samples from each atherosclerotic stage. A total of 114 cases were selected for further examination. Demographic data and the causes of death are summarized in Table I.

Characterization of the lesions and histological definitions

Aortic samples not showing any signs of intimal thickening and intimal inflammation where classified as normal. The other samples were classified based on the most advanced lesion type present in the section. Lesions were defined as adaptive intimal thickening (AIT), intimal xanthoma (IX), pathological intimal thickening (PIT), early fibroatheroma (EFA), late fibroatheroma (LFA), thin cap fibroatheroma (TCFA), acute plaque rupture (PR), healed plaque rupture (HR) and fibrotic calcified plaque (FCP). For detailed descriptions concerning a complete overview on plaque processing, morphological analysis and additional information concerning the studied population are provided in reference 12.

Immunohistochemistry

All specimens used for immunohistochemistry were washed in phosphate-buffered saline (PBS), formalin fixed and decalcified (Kristensens solution) and paraffin embedded using standard procedures. The details of the antibodies used for immunohistochemistry are listed in Table II. Conjugated biotinylated horse anti-mouse (1:400 dilution; Vector laboratories, Amsterdam, The Netherlands) or Envision® + System – HorseRadish Peroxidase (HRP) labeled polymer anti mouse/anti rabbit (prediluted; Dako, Heverlee, Belgium) functioned as secondary antibodies. Sections were developed with Nova Red® or DAB and counterstained

with Mayer's haematoxylin or methylgreen. Positive and negative controls were always included and performed by adding or omitting the primary antibody on 3-Aminopropyltriethoxysilane (APES)-slides containing human tonsils.

The Foxp3/CD3 and IL-17/CD3 double staining was performed to identify Regulatory T cells and Th17cells, respectively (Table I). Conjugated polymer anti mouse/ anti rabbit (Immunologic®) functioned as secondary antibodies. After the goat-derived anti-IL17 incubation, a rabbit anti-goat secondary antibody (Southern Biotech, Birmingham, AL, USA) served as a bridge reagent for the next step with alkaline phosphatase (AP) anti-rabbit polymer (Immunologic®, Duiven, The Netherlands). All immunohistochemical stainings were performed as previously described[14]. Despite many attempts and various techniques, we did not succeed to use GATA-3 as the T-helper 2 marker. We therefor had to turn to double staining for CD4/Tbet to identify the T-helper lineage (Lineage: Th1= $CD4^+/Tbet^+$ and non-Th1= $CD4^+/Tbet^-$) having regard to the provision that non-Th1 may also include Th0, Th17 and Th22 populations.

Table 1. Demographic data of the 114 studied aortic samples

	Male		**Female**	
N	64		50	
Mean age (years) [SD]	49.4	[14.3]	43,8	[17.3]
Mean length (cm) [SD]	179.9	[11.9]	166.6	[12.1]
Mean weight (kg) [SD]	80.1	[16.3]	64.9	[15.3]
Mean BMI (kg/m2) [SD]	24.8	[3.1]	22.9	[4.4]
Patients with known history of nicotine abuse [percentage]	21	[36.8%]	17	[39.5%]
Patients with known history of hypertension* [percentage]	13	[22.8%]	10	[23.3%]
Patients with known diabetes [percentage]	0	[0.0%]	1	[2.3%]
Cause of Death [n, percentage]				
Severe head trauma	11	[17.1%]	7	[14.0%]
Cerebral vascular accident (CVA)	8	[12.5%]	10	[20.0%]
Subarachnoid bleeding (SAB)	15	[23.4%]	14	[28.0%]
Cardiac arrest	7	[10.9%]	0	[0.0%]
Trauma	1	[1.5%]	1	[2.0%]
Other	6	[9.3%]	3	[6.0%]
Unknown	16	[25.0%]	15	[30%]
Medication [n, percentage]				
Anti-hypertensives	11	[19.3%]	6	[14.0%]
Statins	1	[1.7%]	1	[2.3%]
Anti-coagulants	1	[1.7%]	2	[4.7%]
Other	5	[8.8%]	8	[18.6%]
None	31	[54.4%]	22	[51.2%]
Unknown	11	[19.3%]	9	[20.9%]

*Known antihypertensive medication / systolic blood pressure >140mmHg and diastolic >90mm Hg in the period preceding death. Abbreviations: SD = Standard Deviation.

Table 2. Antibodies used in the present study

Antibody, clone	Host isotype; subclass	Specificity	Pretreatment		Dilution	Reference/source
CD3, polyclonal	Rabbit	Pan T cells	10x Tris/EDTA	pH 9,2	1:200	DAKO
CD4, 4B12	Mouse, IgG1-κ	T helper-cells	10x Tris/EDTA	pH 9,2	1:200	DAKO
CD8, C8/144B	Mouse, IgG1-κ	Cytotoxic T-ells	10x Tris/EDTA	pH 9,2	1:200	DAKO
CD45RA, HI100	Mouse, IgG2b-κ	Naive T cells	Citrate	pH 6,0	1:2000	BioLegend
CD45RO, UCHL1	Mouse, IgG2a-κ	Memory T cells	Citrate	pH 6,0	1:1000	BioLegend
CD20, L26	Mouse	Pan B cells	Citrate	pH 6,0	1:1000	DAKO
CD21, IF8(4)	Mouse, IgG1-κ	Follicular Dendritic Cells, mature B cells	Citrate	pH 6,0	1:400	DAKO
CD138, MI15	Mouse	Plasma cells	10x Tris/EDTA	pH 9,2	1:1000	DAKO
CCR7, ab191575	Rabbit, polyclonal	Activated T-lymphocytes	Citrate	pH 9,2	1:200	Abcam
Tbet, polyclonal	Rabbit, sc-21003	T helper1-cells	10x Tris/EDTA	pH 9,2	1:800	Santa Cruz
IL-17, polyclonal	Goat	Th-17 cells	-	pH 9.0	1:50	R&D
FoxP3, clone 236A/E7	Mouse	Regulatory T cells	-	pH 9.0	1:50	Abcam
CXCL13, cat no AF801	Goat	Lymphorganogenic chemokine	Citrate	pH 6,0	1:100	R&D
anti-AID, EK2 5G9	Rat	Activation-induced cytidine deaminase	Citrate	pH 6,0	1:16.000	Cell Signalling

Table 3. Histological classification of aortic tissue according to the modified AHA classification proposed by Virmani *et al*

Morphological description	Abbreviation	Male			Female			Total
		N	Mean age	[SD]	N	Mean age	[SD]	N
Normal aorta	N	7	23.8	[18.9]	5	10.0	[3.7]	12
Non-progressive intimal lesions								
Adaptive intimal thickening	AIT	5	40.5	[10.0]	5	30.4	[9.0]	10
Intimal xanthoma	IX	7	37.3	[10.0]	5	34.2	[14.8]	12
Progressive atherosclerotic lesions								
Pathological intimal thickening	PIT	5	46.0	[8.9]	7	55.4	[11.5]	12
Early fibroatheroma	EFA	7	50.9	[5.9]	5	46.0	[3.5]	12
Late fibroatheroma	LFA	5	55.0	[3.6]	7	51.1	[11.6]	12
Vulnerable atherosclerotic lesions								
Thin cap fibroatheroma	TCFA	7	57.2	[5.2]	4	60.3	[5.7]	11
Plaque rupture	PR	7	56.9	[2.6]	3	45.0	[13.1]	10
Stabilizing lesions								
Healing rupture	HR	8	58.1	[11.1]	4	57.0	[0]	12
Fibrotic calcified plaque	FCP	6	62.7	[6.8]	5	53.0	[11.4]	11
		64	49.4	[14.3]	50	43.8	[17.3]	114

*Abbreviations: SD = Standard Deviation.

Assessment of immunolocalization of T cells (and T cell subset), B cells and plasma cells

The tissue block showing the most advanced plaque was used for further studies. When the aortic sample contained more than one lesion, the most advanced lesion on the slide was used. The lesion was defined as the area between the endothelium and the first elastic lamina over a distance of 1mm. In the presence of a necrotic core the distance was expanded with another 500µm on both sides of the necrotic core to include the adjacent shoulder region[12]. The regions of interest (ROI) were the intima (and in the presence of an early or late necrotic core the intima was divided in a cap and both shoulder regions), the media and the adventitia (figure 1). Within the ROIs (*i.e.* intima, media and adventitia), three representative adjacent images were made at a 200x magnification. A total of 9 images per atherosclerotic lesion were separately analyzed from the lesion. Immunostaining intensity was quantitatively assessed with an image processing program (Image J; plug-in Cell counter). Representative examples of the immunological stainings are provided in figure 2.

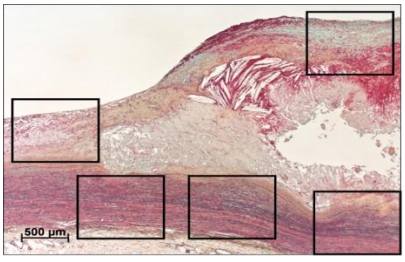

Figure 1. Example of the regions of interest as used for the assessment of immunolocalization of T cells (and T cell subset), B cells and plasma cells in a healed rupture. The regions of interest are drawn in the fibrous cap, in one of the shoulders and three times in the media in this particular example. For every lesion (normal of ruptured) a total of nine images were made (3 in the intima, 3 in the media and 3 in the adventitia) and the immunostaining was quantitatively assessed with an image processing program (Image J; plug-in Cellcounter).

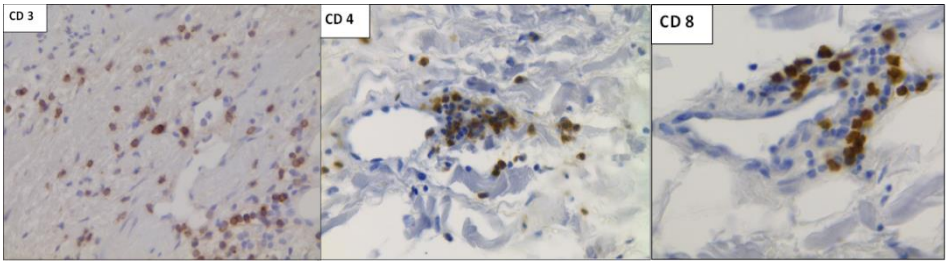

Figure 2. High resolution examples of the immunohistochemical staining for CD3, CD4 and CD8 cells. The high resolution images are examples of the quality of the immunohistochemical staining for CD3, CD4 and CD8. All images were taken at a 400x magnification at the medial adventitial border. Within all the images one can see the clear positively stained Tcells mainly located near the *vasa vasorum*. All sections were developed with DAB and counterstained with Mayer's haematoxylin.

Statistical analysis

Data in figures are presented as mean ± SEM. Spearman's correlation was used to demonstrate the relationship between the amount of positive cells in the intima, media and adventitia within one phase of the atherosclerotic disease and compared with the previous and/or next phase in atherosclerosis (SPSS 20.0; Chicago, IL). The study population consisted of 114 individuals. However during the staining process some tissue samples were lost. Therefor the total number of samples for each staining may be less than 114. The Wilcoxon-Mann-Witney test was used to analyze the non-normally distributed data of the mean total number of cells within each atherosclerotic phase and the Kruskal Wallis test was used to control for a type 1 error. A value of $p < 0.05$ was considered statistically significant.

RESULTS

Study population

Characteristics of the studied population are provided in Table I. The male/female ratio was evenly distributed (57% male), as was the mean age for each sex (~49-years). There was a strong correlation between donor age and atherosclerosis progression[12] (Table 3). The mean donor age for the aortic wall samples classified as normal was 23-years, whereas the mean age for aortas with fibrotic calcified plaques, representing the final stage of the disease, was 62-years. Nearly 40% of patients had a known history of smoking and 2 patients received statin therapy. Twenty-three patients had a known history of hypertension; 17 of these patients received anti-hypertensive medication.

Normal aorta and non-progressive atherosclerotic lesions

The intima and media layers of the normal (non-atherosclerotic) aortic wall are devoid of $CD3^+$ T cells. Scattered T cells found at the medial-adventitial border are mainly $CD45RO^+$ (memory) T cells. The $CD4^+$ (Thelper) to $CD8^+$ (cytotoxic) T cell ratio is approximately 1:2 (figure 3A). Th_1 cells) and non-Th1 cells were also expressed in a 1:2 ratio (Figure 3B).

Naïve T cells ($CD45RA^+$), Regulatory T cells ($CD3^+/FoxP3^+$), Th17 cells ($CD3^+/IL17A^+$), B cells ($CD20^+$) and plasma cells ($CD138^+$) are all absent in aorta's classified as normal.

Isolated T cells in the thickened intima, and progressive numbers of T cells in the medial/adventitial border characterize so-called non-progressive lesions (*i.e.* adaptive intimal thickening and intimal xanthomas). Memory T cells remain the dominant phenotype, and the subset ratios remains unchanged ($CD4^+/8^+$; Th1/TH2). Regulatory T cells, Th17 cells, naïve T cells, B cells and plasma cells are absent in these early lesions (figure 4).

Progressive atherosclerotic lesions

A significant increase is seen in intimal $CD3^+$ T cells ($p<0.0001$) in progressive lesions (early fibroatheroma and late fibroatheroma) with beginning infiltration of the medial wall as well. The predominance of cytotoxic T cells persists ($CD4^+$: $CD8^+$ T cell ratio 1:5) in the early fibroatheroma, and T helper cells are dominated by the Th_1 lineage at a 1:3 ratio. Transition from an early to late fibroatheroma stage is accompanied by the accumulation of T cells in the intima shoulder regions of the lesion, and the $CD4^+/CD8^+$ T cell ratio shifts from 1:5 in early fibroatheroma to ~1.5:1 in late fibroatheroma.

Memory T cells remain the dominant phenotype in advanced lesions, yet scattered naïve T cells ($CD45RA^+$) start to appear within the medial-adventitial border in lesions classified as EFA. A further increase in naïve T cells and T memory cells is seen in late fibroatheroma with a notable accumulation of T cells alongside infiltrating *vasa vasorum* in the outer layers of the media underlying the necrotic core. In general, B cells and plasma cells are absent, although present in a minority of individuals (Figure 9). Regulatory T cells and Th17 cells are not identified in the progressive lesions.

The vulnerable lesions

Thin cap fibroatheromas and ruptures are hallmarked by a peak in T cell infiltration in the adventitia underneath to the culprit lesion. The thin cap remains devoid of T cells and the number of T helper cells decreases resulting in an approximate 1:1 CD4/CD8 cell ratio. Non-Th1 cells remain the dominant T-helper lineage in the vulnerable phase, due to doubling of the number of non-Th1 cells (Figure 6). Dispersed memory T cells and naïve T cells are abundantly present in the media and adventitia near the *vasa vasorum*. Absence of CD45RO/CCR7 double positive cells indicates that all CD45RO+ T cells within the lesion and infiltrates are effector memory T cell and the only few central memory T cells are identified in the aortic wall located within the *vasa vasorum* of the adventitia (figure 10).

A unique finding in the vulnerable lesions is the appearance of B-cells and occasional plasma cells in tertiary follicle-like structures. Staining for CXCL13, a homeostatic, lymphorganogenic chemokine that is critical for organization follicle-like structures, shows CXCL13 expression exclusively in vulnerable lesions, (*viz.* no CXCL13 staining was found in the other stages of the disease) and reveals a particular staining pattern of a dendritic network with extension from the follicles (Figure 9). Additional staining for mature B cells (CD2) and Activation-induced cytidine deaminase (AID) was mainly negative; indicating the lack of B cell maturation. Scattered $FoxP3^+$ T cells are found within the intima and underlying adventitia in 2 of 9 aortic sections of thin cap fibroatheroma (figure 6). On the other hand, Th17 cells are absent in vulnerable lesions.

Stabilized lesions

Healing plaque ruptures exhibit a dramatic decrease in T cells (P<0.001), naïve T cells, and disappearance of B cells and plasma cells. The decline in T cells is more outspoken for the CD4+ cells than for the CD8+ cells for all vascular layers. Within the TCFA,non-Th1 cells dominate over Th1 with a five-fold-increase and in stable lesions the Th1/non-Th1 cell ratio returns to 1:2 as seen in normal aorta's (figure 3B). The decline in memory T cells predominantly reflects a reduction localized to the intima (P<0.01). The overall number of memory T cells in the media and adventitia remains stable. Native T cell numbers are highly variable. The follicles-like structures vanish and CXCL13 disappeared from the arterial wall. No regulatory T cells or Th17 cells are detected in the stabilized lesions.

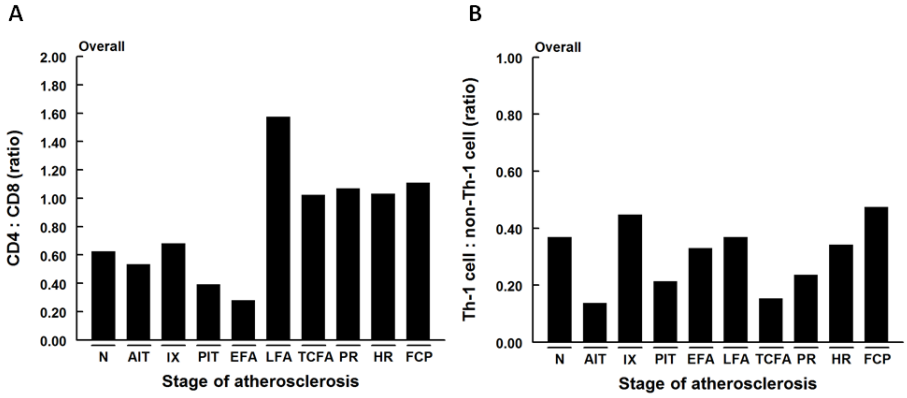

Figure 3. The CD4/CD8 and Th1/non-Th1 ratio per stage of atherosclerosis. **A.** The number of CD8 cells dominate the overall T cell count in normal aorta's and in the early stages of atherosclerosis up until the early fibroatheroma. In late fibroatheroma, vulnerable atherosclerosis (*i.e.* thin cap fibroatheroma and plaque ruptures) and post-ruptured plaques the total number of CD4 and CD8 cells are practically in balance. **B.** Non-Th1 cells dominate the Thelper lineage not only in normal aorta's but also during the entire development of atherosclerotic lesions. Within thin cap fibroatheroma the non-Th1 cells dominate the Th1 cells with a factor 5 and as the lesion stabilizes the Th1/non-Th1 cell ratio returns to 0.4-0.5 as seen in normal aorta's. The solid bars represent the mean number of CD4 (Figure A) or Th1 (Figure B) cells per stage of atherosclerosis divided by the mean number of CD8 (Figure A) or non-Th1 (Figure B) cells per stage of atherosclerosis.

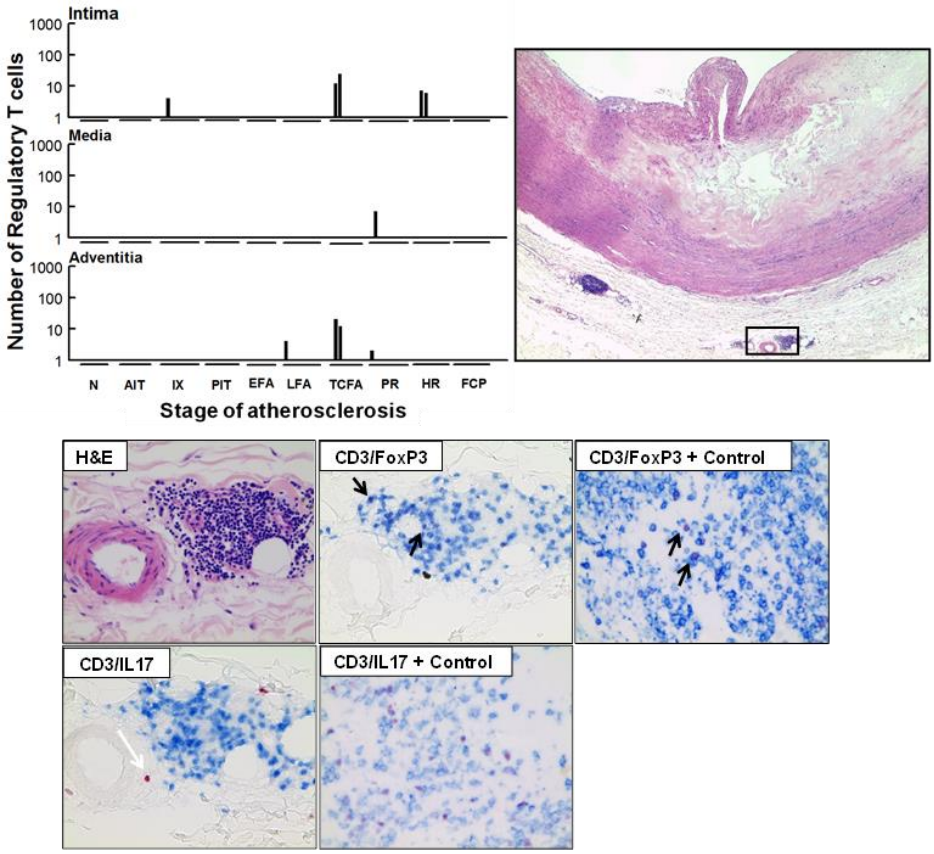

Figure 4. Number of regulatory T cells within the various layers of the aortic wall per stage of atherosclerosis. Only one aortic sample with an intimal xanthoma stained positive for FoxP3+ T cells (4 scattered cells). Within the aortic samples classified as a thin cap fibroatheroma two lesions showed 12 and 24 FoxP3+ T cells in the intima with respectively 20 and 12 FoxP3+ T cells in the adjacent adventitia. A few scattered FoxP3+ T cells were seen in the intima of two healed ruptured plaques. The additional figures show an H&E stained adventitial follicle in a thin cap fibroatheroma with the consecutive sections stained for regulatory T cells (CD3+/FoxP3+) and Th17 cells (CD3+/IL17+). There are a limited number of regulatory T cells (black arrow) in the vulnerable phase and Th17 cells were not identified. A few scattered CD3-/IL17+ cells (white arrow) were seen in the adventitia that, as previous studies showed, can be addressed to macrophages15. A human tonsil (not associated with the aortic biobank) functioned as a positive control for the CD3/IL17 staining and showed numerous Th17 cells. Ferangi blue was used to develop CD3 and alkaline phosphatase (AP) for FoxP3 and IL17. The solid bars represent the number of FoxP3+ T cells within the various layers of the aorta per stage of atherosclerosis. Total number of cases: 95 (N (9), AIT (9), IX (11), PIT (11), EFA (10), LFA (9), TCFA (9), PR (10), HR (8) and FCP (11)). For abbreviations and a detailed description concerning the classification see Material & Methods section. All images were taken at a 400x magnification.

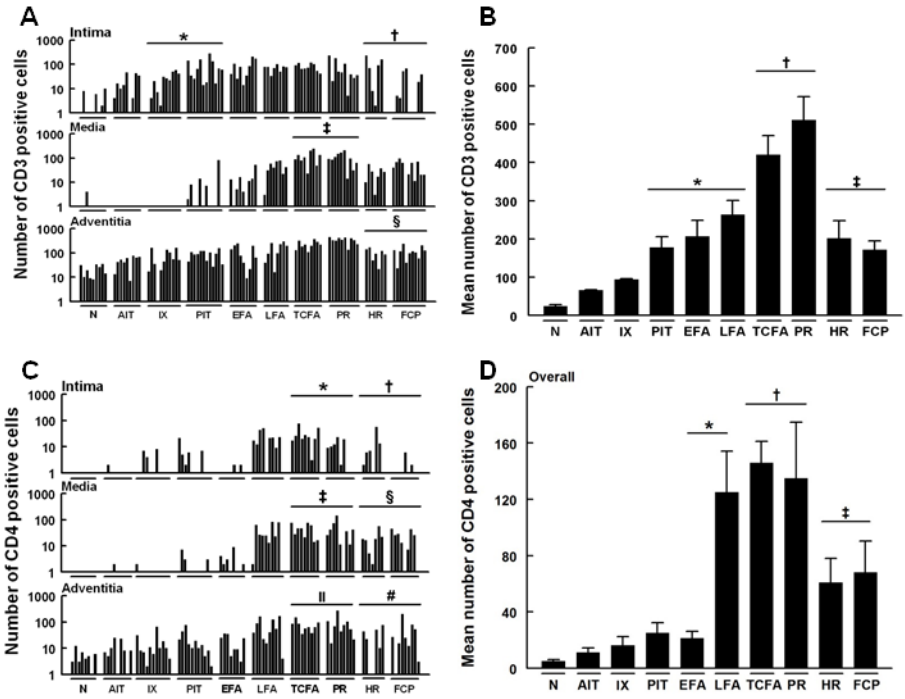

Figure 5. Number of CD3+, CD4+ and CD8+ T cells within the various layers of the aortic wall. **A.** Intimal CD3+ T cells are present in all stages of atherosclerosis. There is a significant influx of CD3+ T cells in intimal xanthomas and pathological intimal thickening when compared to normal aortic wall samples (* P<0.009). The number stabilizes as the lesion becomes vulnerable (*viz.* TCFA and PR). A significant decrease († P<0.014) is seen in the stabilizing lesions (*viz.* HR and FCP) compared to vulnerable lesions (*viz.* TCFA and PR). The media remains clear of CD3+ T cells until pathological intimal thickening and shows a remarkable increase in CD3+ expressing T cells (‡ P<0.0001) in vulnerable lesions. There are an increasing number of CD3+ T cells in the adventitia with advancing atherosclerosis. Stabilized plaques are hallmarked by a significant decrease in adventitial CD3+ T cells (§ P<0.0001) when compared to the vulnerable lesions. **B.** The total number of CD3+ T cells in all vascular layers increases with advancing atherosclerosis. Progressive atherosclerotic lesions (*viz.* PIT, EFA and LFA) show significantly more CD3+ T cells compared to non-progressive lesions (AIT and IX; * P<0.0001). A further increase is seen in vulnerable lesions († P<0.0001) whereas lesion stabilization is hallmarked by a dramatic decrease (‡ P<0.0001). Total number of cases in figures A and B: 95 (N (9), AIT (9), IX (11), PIT (12), EFA (9), LFA (8), TCFA (9), PR (10), HR (7) and FCP (11)). **C.** The intima remains practically devoid of CD4+ T cells up until late fibroatheroma. There is a significant increase of T-helper cells in vulnerable lesions compared to PIT, EFA and LFA followed by a significant decrease in stabilizing lesions (*P 0.008: †P<0.004). Similar patterns are seen within the media and adventitia (‡ P<0.0001; § p<0.003; וו P<0.002 and # P<0.008). **D.** T-helper cells significantly increase in progressive and vulnerable lesions in comparison to PIT, EFA and LFA followed by a decrease in stabilized lesions (* P<0.021; † P<0.0001 and ‡ P<0.001). Total number of cases in figures C and D: 91 (N (8), AIT (9), IX (11), PIT (11), EFA (8), LFA (10), TCFA (9), PR (9), HR (7) and FCP (9)).

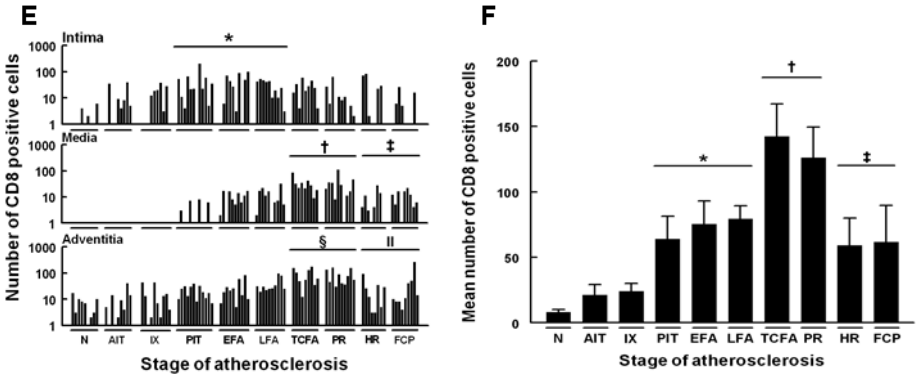

Figure 5 Continued. **E.** Cytotoxic T cells are more abundantly present in the intima in the progressive stages of atherosclerosis (* P<0.001) when compared to normal, AIT and IX. The media and adventitia show an increasing number of cytotoxic T cells within progressive atherosclerotic lesions (PIT, EFA en LFA) compared to the prior phases followed by significant rise within the vulnerable plaques and a significant decrease as the lesions stabilize († P<0.0001; ‡ P<0.0001; § P<0.0001 and וו P<0.0001). F. The total number of cytotoxic T cells follows a similar pattern as the T-helper lineage in figure B; a significant increase within progressive and vulnerable lesions followed by a decrease in stabilized lesions (* P<0.002; † P<0.0001 and ‡ P<0.0001). Total number of cases in figures E and F: 96 (N (9), AIT (9), IX (10), PIT (12), EFA (10), LFA (10), TCFA (9), PR (10), HR (8) and FCP (9)). The vertical axis of figures A, C and E is presented as a log-scale. Each solid bar in figure A, C and E represents the number of positively stained T cells within the intima, media and adventitia of one aortic plaque. The solid bars in figures B, D and F represent the mean total number of cells within the entire aortic wall per stage of atherosclerosis ± SEM. Abbreviations: N: normal, AIT: adaptive intimal thickening, IX: Intimal xanthoma, PIT: Pathological intimal thickening, EFA: early fibroatheroma, LFA: late fibroatheroma, TCFA: thin cap fibroatheroma, PR: plaque rupture, HR: healed rupture and FCP: fibrotic calcified plaque. For a detailed description concerning the classification see Material & Methods section.

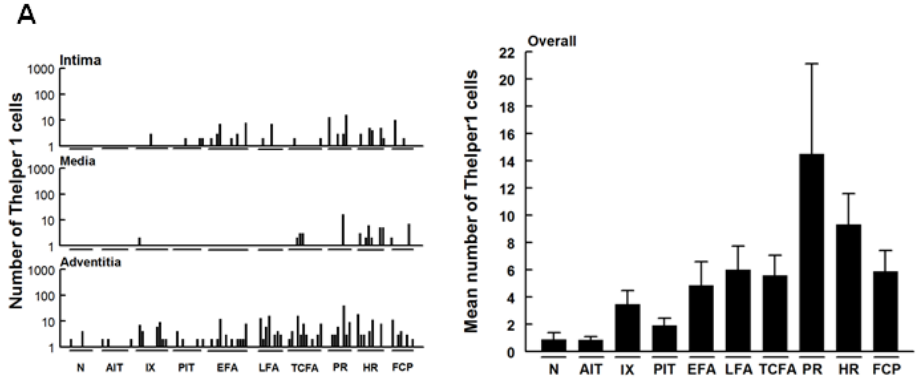

Figure 6. Number of Thelper1 and non-Thelper1 cells within the various layers of the aortic wall. **A.** There is a gradual increase in Thelper1 cells in the intima and adventitia with advancing atherosclerotic lesions. An increase is seen in the amount of Thelper1 cells within ruptured plaques; note the fact that these cells are mainly located in the adventitia. Total number of cases in figure A: 97 (N (9), AIT (9), IX (11), PIT (11), EFA (12), LFA (8), TCFA (12), PR (8), HR (9) and FCP (8)).

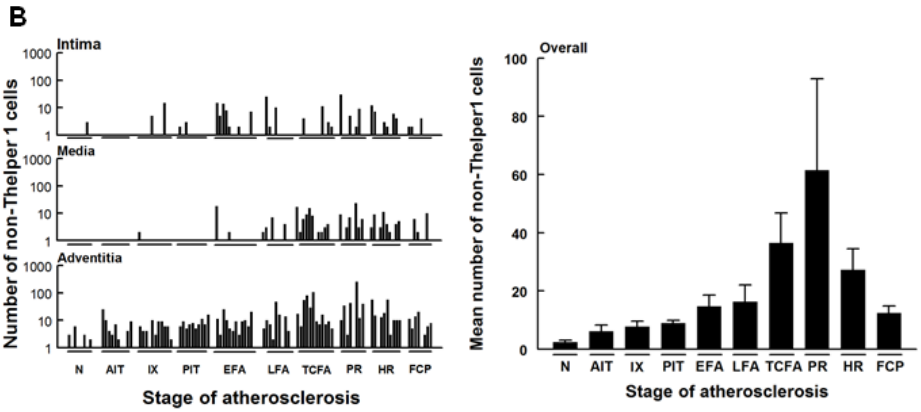

Figure 6. Continued. **B.** There are far more non-Thelper1 cells within the aortic wall compared to the number of Thelper1 cells. However, the same gradual increase is seen in number as the atherosclerotic lesions progress towards the vulnerable thin cap fibroatheroma. Again, an increase is seen within ruptured plaques. Total number of cases in figures B: 98 (N (8), AIT (10), IX (11), PIT (10), EFA (12), LFA (9), TCFA (12), PR (8), HR (10) and FCP (8)).

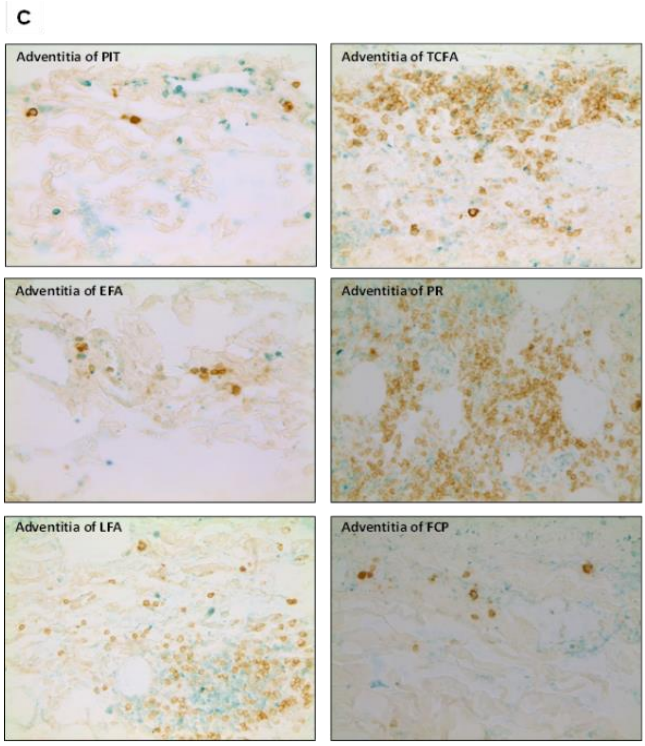

C. Illustrative images of the adventitia adjacent to the intimal plaque in the various stages of the atherosclerotic process with CD4/Tbet double-staining corresponding with the presented graphs A and B. Thelper1 cells are identified by staining positive for CD4 (brown; diamino-benzidine chromogen) and Tbet (methylgreen). Non-Thelper1 cells are CD4 positive and Tbet negative. Note that there are numerous cells that only stain Tbet positive. The vertical axis of the figures with the intima, media and adventitia separated is presented as a log-scale and the solid bars represent the number of Thelper1 or non-Thelper1 cells within the various layers of one aortic plaque. The solid bars in the adjacent figures represent the mean total number of Th1 cells or non-Th1 cells within the entire aortic wall ± SEM.

For abbreviations and a detailed description concerning the classification see Material & Methods section. All images were taken at a 400x magnification.

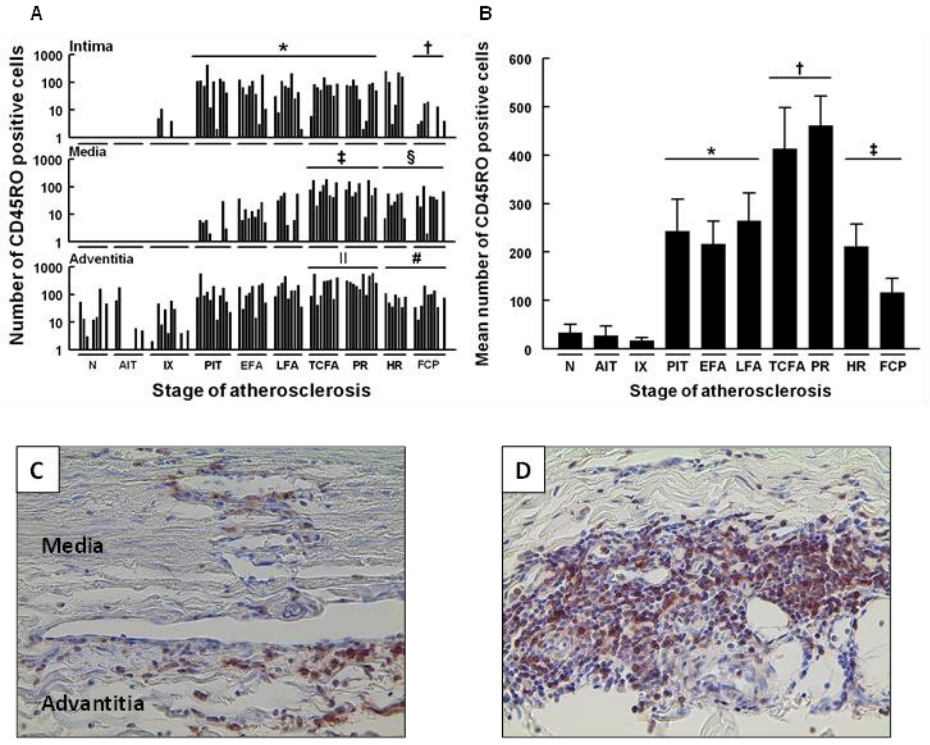

Figure 7. Number of memory T cells within the various layers of the aortic wall. **A.** Progressive atherosclerotic lesions and vulnerable plaques represent a high amount of CD45RO+ T cells in the intima (* P<0.011). Only fibrotic calcified lesions show a significant decrease compared to vulnerable lesions († P<0.001). In comparison with normal, AIT and IX the media and adventitia show an increasing number of memory T cells within progressive atherosclerotic lesions followed by significant rise within the vulnerable plaques and a significant decrease as the lesions stabilize († P<0.0001; ‡ P<0.0001; § P<0.0001 and וו P<0.0001). **B.** Memory T cells significantly increase in number within progressive and vulnerable lesions followed by a decrease in stabilized lesions (* P<0.0001; † P<0.0001 and ‡ P<0.0001). **C. D.** Are illustrative images of the CD45RO staining of respectively the adventitia of a LFA and the adventitia of a TCFA corresponding with the presented graphs. All sections were developed with DAB and counterstained with Mayer's haematoxylin. The vertical axis of figure A is presented as a log-scale. The solid bars in figure A represent the number of CD45RO+ T cells within the various layers of one aortic plaque. The solid bars in figures B represent the mean number of CD45RO+ T cells within the entire aortic wall of one aortic plaque ± SEM. Total number of cases in figures A and B: 95 (N (9), AIT (9), IX (12), PIT (11), EFA (9), LFA (9), TCFA (9), PR (10), HR (7) and FCP (10)). For abbreviations and a detailed description concerning the classification see Material & Methods section. All images were taken at a 400x magnification.

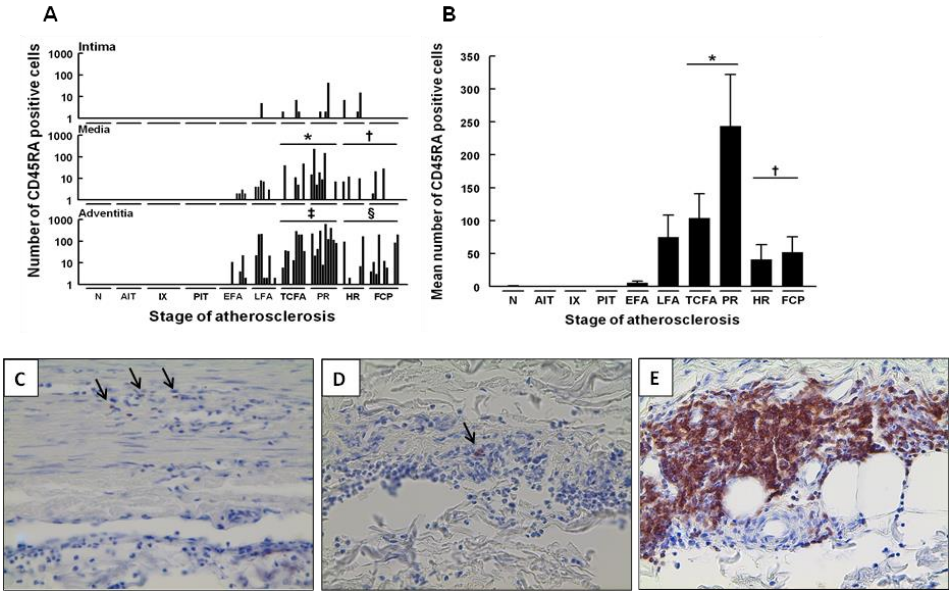

Figure 8. Number of naïve T cells within the various layers of the aortic wall. **A.** Limited numbers of CD45RA+ T cells are detected in the intima of vulnerable lesions. However, the media and adventitia contain a significant increase in naïve T cells within the vulnerable lesions compared to the progressive lesions (EFA and LFA) followed by a decrease in stabilized lesions (* P<0.001; † P<0.006; ‡ P<0.0001 and § P<0.0001). **B.** Naïve T cells increase significantly in number in vulnerable plaques (* P<0.0001) and decrease dramatically in number when the lesions stabilize († P<0.0001). The vertical axis of figure A is presented as a log-scale. The solid bars in figure A represent the number of CD45RA+ T cells within the various layers of one aortic plaque. Notice the significant increase of adventitial naïve T cells in the vulnerable lesions (**D** and **E**) compared to the progressive lesions (**C**) and the naive T cells alongside the *vasa vasorum* (black arrows). All sections were developed with DAB and counterstained with Mayer's haematoxylin. The solid bars in figures B represent the mean number of CD45RA+ T cells within the entire aortic wall of one aortic plaque ± SEM. Total number of cases in figures A and B: 97 (N (9), AIT (9), IX (11), PIT (11), EFA (10), LFA (9), TCFA (9), PR (10), HR (8) and FCP (11)). For abbreviations and a detailed description concerning the classification see Material & Methods section. All images were taken at a 400x magnification.

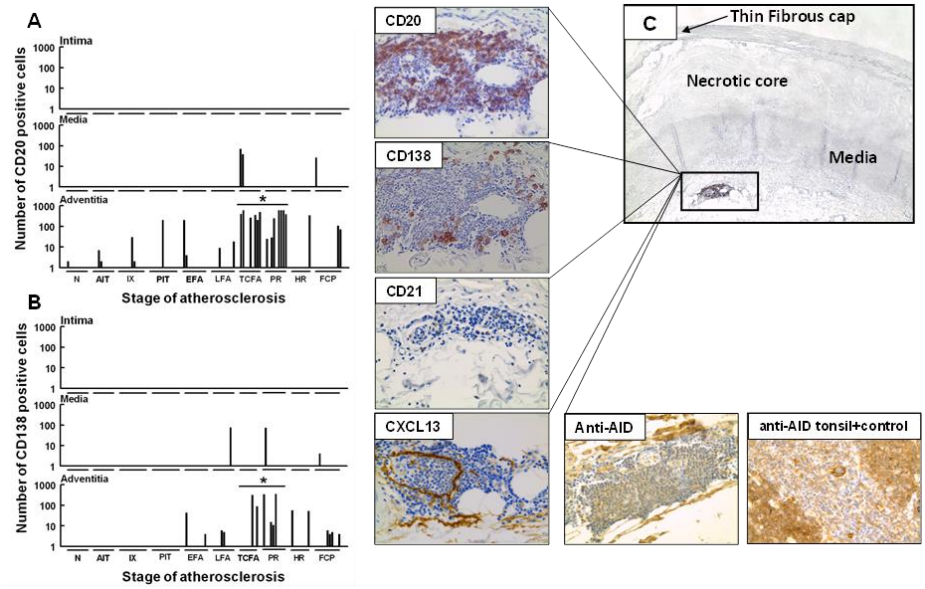

Figure 9. Number of CD20+ B cells and CD138+ plasma cells in the various layers of the aortic wall. The intima and media of the aortic wall remain largely deprived of CD20+ B cells and CD138+ plasma cells (resp. figure **A** and **B**), although incidental B cells are found in the adventitia. There is a significant increase in the amount of B cells and plasma cells in the adventitia in close proximity to the intimal plaque in the vulnerable lesions compared to the prior phase (* $P<0.0001$ and * $P<0.003$). Total number of cases: 91 (N (9), AIT (9), IX (11), PIT (11), EFA (10), LFA (9), TCFA (9), PR (10), HR (8) and FCP (11)). Figure **C** shows an adventitial follicle in a thin cap fibroatheroma consecutively stained for CD20, CD21 and CXCL13. Notice the abundance of (CD21 negative) B cells clustered around the CXCL13 positive radiating pattern of tube-like structures. Anti-AID stained negative within the adventitial infiltrates. Due to the disturbing amount of background staining, a high resolution image of a positive control for the anit-AID staining in a human tonsil is provided to illustrate the mature B-cell. All images were taken at a 400x magnification. All sections were developed with DAB and counterstained with Mayer's haematoxylin. The vertical axis is presented as a log-scale. The solid bars represent the number of CD20+ B cells or CD138+ plasma cells within the various layers of one aortic plaque. For abbreviations and a detailed description concerning the classification see Material & Methods section.

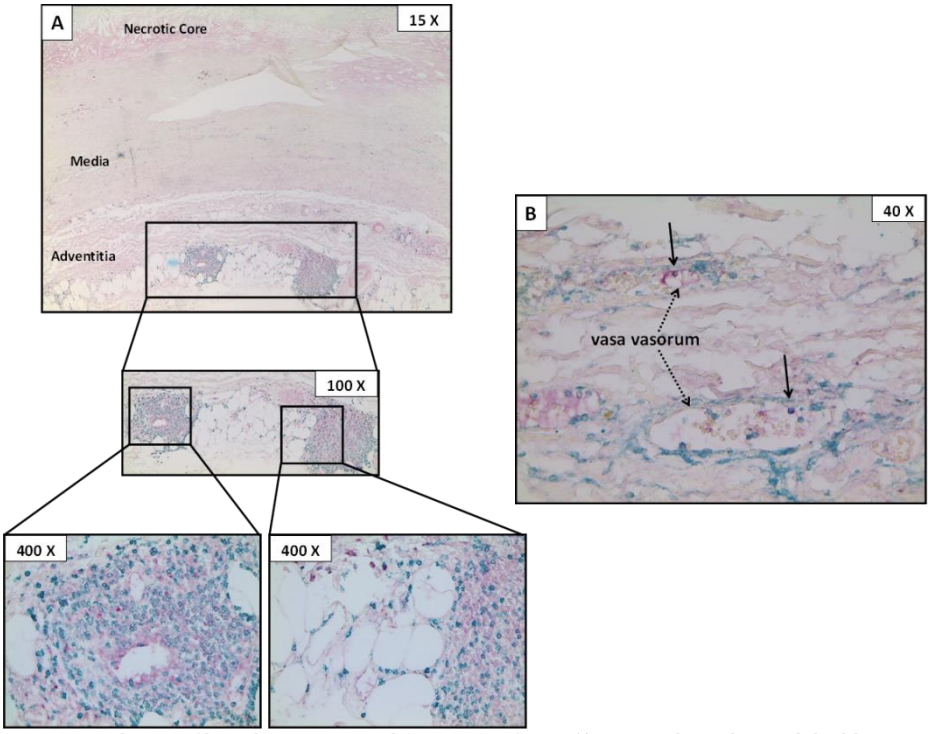

Figure 10. Thin cap fibroatheroma stained for CD45R0/CCR7 [16]. Immunohistochemical double staining for CCR7/CD45R0 was done to differentiate between effector memory T cells (CCR7-) and central memory T cells (CCR7+). **A.** The adventitia of the aortic wall containing a thin cap fibroatheroma consists of numerous T cells in follicle-like structures. All the CD45R0+ T cells (chromogen Ferangi blue) within the lesion and infiltrates are effector memory T cell (CCR7-; otherwise warp red (klinipath, Duiven, Netherlands)). Only a few cells stain positive for CCR7 but negative for CD45R0. **B.** The only few central memory Tcells (CD45R0+/CCR7+) identified in the aortic wall are located within the *vasa vasorum* of the adventitia. The image was taken at a 400x magnification.

DISCUSSION

A wealth of preclinical evidence supports a critical role of the adaptive immunity in the initiation and progression of atherosclerosis[17,18]. This study, based on histological observations in human aorta sections, confirms extensive and progressive involvement of cellular components of the adaptive immune response in atherosclerosis[19]. Findings point to profound changes in the nature of the response in the lead up to plaque destabilization and show extinguishing of inflammatory processes upon plaque stabilization. This study reveals fundamental differences between the human atherosclerotic disease *and* mouse models of the disease; particularly with respect to a very limited presence of regulatory T cells, absence of Th17 cells throughout the atherosclerotic process, and lack of B-cells in the early-, intermediate-, and final stages of the process.

Insight in the atherosclerotic process highly depends on observations from murine models of the disease[20]. Indeed, genetically modified mouse models have been critical for understanding the atherosclerotic process. Yet, by virtue of the metabolic adaptations in the lipoprotein metabolism, necessary to induce atherosclerotic lesion formation, the process in these animals is essentially lipid driven; a situation that may not fully mimic the human situation[21,22]. Translation of rodent findings is further obscured by critical dependence on genetic backgrounds with Th1 dominated immune responses in order for atherosclerosis to develop; by the fundamental and intrinsic differences in inflammatory and immune responses between mice and men and by failure of the experimental lesions to progress to culprit lesions (vulnerable plaque) formation[23,24,25.] Consequently, information provided by these models may be biased, and is incomplete at least with respect to vulnerable lesions. As result the preclinical observations may not directly translate to the human situation[8,9].

Data on human atherosclerosis is also limited, a situation largely reflecting the fact that most observations are made on material obtained during surgical procedures (e.g. endarterectomy). This material typically represents the final stage(s) of the disease and, in the case of an endarterectomy material, will not provide information on the outer media and the adventitia, both major interphases in vessel wall inflammation. With this in mind, we set up a biobank of aortic wall samples from organ grafts designated for transplantation. Material from this bank almost covers the full life span (5-80 years) and shows a nearly equal sex distribution. The relatively healthy pre-mortal status of the donors is reflected by minimal use of statins and antihypertensive drugs. Classification was done for all individual tissue sections in the bank, *viz.* each individual tissue block was Movat and haematoxylin stained, and histologically staged using an established adapted version of the AHA classification system[12,13]. Modifications in the adapted classification system highlight specific critical morphological events in the final stages of the disease process. This allows for a more precise interpretation of processes occurring during plaque destabilization and subsequent healing. An earlier systematic evaluation of material in the biobank showed that the bank covers the full spectrum of atherosclerotic disease[12]. Exact morphologic descriptions and examples of the different lesions have been published and discussed previously[12].

Immunohistochemical staining for CD3, CD4 and CD8 shows progressive T-cell accumulation during the atherosclerotic process. The earlier phases are dominated by diffuse cytotoxic T cell infiltration but progressive quantities of T helper cells are found during progression of the disease resulting in an increase in the $CD4^+/CD8^+$ T cell ratio during disease progression. These observations are in line with an earlier report on renal artery atherosclerosis, and with observations from

other progressive inflammatory disorders[26,27]. Due to inherent limitations of paraffin embedded tissue, we were unable to test whether these shifts reflect an (auto)immune phenomenon as has been proposed in the context of advanced atherosclerotic disease[28,29].

CD4/T-Bet double staining was used to identify Th1 cells. T-bet is the lineage defining transcription factor for Th1 cells [30]. In the absence of Th17 and with minimal regulatory T cells throughout the atherosclerotic spectrum we defined the CD4+/T-bet negative cells as non-Th1 cells. Quantification of the Th1/non-Th1 ratio on basis of the CD4/T-Bet double staining did not confirm Th1 dominance in human atherosclerotic process. This may indicate that the presumed Th1 dominance in atherosclerosis reflects an artificial phenomenon related to the requirement of Th1 dominated backgrounds in mouse models in order for atherosclerosis to develop. Yet, alternative explanations are that identification based on T-Bet positivity underestimates the number of Th1 cells or, vice versa, that identification based on cytokine profiles overestimates the number of Th1 cells[31].

Findings for the CD45RO (T-memory cells) and CD45RA (naïve T-cells) largely follow observations for other solid organs (predominance of T-memory cells) and extend those made in rodent models of atherosclerotic disease showing increasing T-cell infiltration during disease progression, with a clear maximum during plaque destabilization followed by a rapid decline during plaque stabilization (plaque healing)[32]. A remarkable and novel observation is the change in the inflammatory foot print that accompanies plaque destabilization, and that fully resolves during plaque stabilization. This change appears to precede plaque destabilization, is confined to the area adjacent to the culprit lesion. On the cellular level this change is characterized by a sharp increase in the number of T-helper cells, emergence of naïve T-cells, and the appearance of B-cells and occasional plasma cells in tertiary follicle-like structures. B-cells in the follicles are largely Activation-induced cytidine deaminase (AID) and CD21 negative indicating gross absence of B-cell maturation[33,34]. These observations suggest that signals promoting B-cell homing and follicle assembly accompany (and may even precede) plaque destabilization, but that essential signals critical for maturation of B-cells are missing.

The chemokine CXCL13 is a pivotal homeostatic signal for follicle formation[35,36]. As of the appearance of follicle-like structures we performed immunostaining for CXCL-13 and observed CXCL-13 expression exclusively in association with the follicle-like structures in the vulnerable lesions, *viz.* CXCL-13 was not detected in the other stages of the disease. CXCL13 distribution shows a remarkable radiating pattern of tube-like structures that may reflect expression in dendritic cells [37].

In the light of the remarkable association between CXCL13 and plaque instability, we tested an association between plasma CXCL13 levels and acute cardiovascular

events (acute myocardial infarction) in plasma samples of the Mission study[37]. CXCL13 was largely undetectable and no association was found between CXCL-13 and cardiovascular events (results not shown). Absence of such an observation may reflect the highly localized character of CXCL13 expression in the vulnerable lesion.

B-cells are considered critical players in the atherosclerotic process, albeit their role (protective, detrimental) is still under debate[38,39]. Our findings of a very restricted presence of B-cells in human atherosclerosis follow observations from Frostegård *et al*[40]. Hence, these findings and gross absence of signs of B cell maturation in the infiltrating B cells, exclude an autocrine or paracrine role of B-cells in the human atherosclerotic process. Yet, humoral factors released by B-cells in para vascular lymph nodes or more distant locations may well be involved in the disease process.

Regulatory T cells were incidentally found in a subset of the vulnerable lesions, whereas Th17 cells were fully absent in the aortic sections. This latter observation follows results of a comprehensive analysis of cytokines in atherosclerotic wall samples that failed to detect IL-17 in all samples tested (detection threshold of the assay <1 pg/L)[41]. Although these observations do not exclude a distant role for these cell populations, they seem to contradict observations from murine models implying these cells as local key-players in the atherosclerotic process.

Limitations: this study was performed on aortic sections of deceased individuals, as such seemingly the continuous data in this study is composed of incidental findings from a large series of patients and the data may therefore not necessarily reflect longitudinal data. Another limitation of the study is the fact the all findings are based on IHC using paraffin-embedded tissue sections. Although IHC has the advantage of showing the spatial relationships, multiple stainings are elaborative, and only allow for a very limited marker sets. Consequently, findings in this study should be considered at a global level. *I.e.* the apparent mismatch between the total number of CD3 count and the sum of CD4 and CD8 may reflect abundance of other CD3 expressing populations such as NK and NK-T cells but also reflect technical limitations of IHC with different epitope availabilities and antibody efficacies. Yet, it is likely that the latter phenomena would equally apply to all tissue sections, and it is thus unlikely that this would influence the conclusions of the study.

In conclusion, this study shows clear changes in the cellular components of adaptive immune system in anticipation of and during plaque destabilization. Observations that suggest that changes in the inflammatory foot print precede and accompany plaque instability. It is tempting to speculate that delineation of this chain of events may provide clues for early culprit lesion detection and plaque stabilization.

REFERENCES

1 Hansson GK. Inflammation, atherosclerosis, and coronary artery disease. New England Journal of Medicine. 2005; 1685.

2 Hansson GK, Libby P. The immune response in atherosclerosis: a double-edged sword. Nature Reviews Immunology. 2006; 508-519.

3 Mallat Z, Taleb S, Ait-Oufella H, Tedgui A. The role of adaptive T cell immunity in atherosclerosis. Journal of lipid research. 2009; S364.

4 Libby P, Ridker PM, Hansson GrK. Inflammation in Atherosclerosis: From Pathophysiology to Practice. Journal of the American College of Cardiology. 2009; 2129-2138.

5 Seok J, Warren HS, Cuenca AG, Mindrinos MN, Baker HV, Xu W, Richards DR, McDonald-Smith GP, Gao H, Hennessy L, Finnerty CC, López CM, Honari S, Moore EE, Minei JP, Cuschieri J, Bankey PE, Johnson JL, Sperry J, Nathens AB, Billiar TR, West MA, Jeschke MG, Klein MB, Gamelli RL, Gibran NS, Brownstein BH, Miller-Graziano C, Calvano SE, Mason PH, Cobb JP, Rahme LG, Lowry SF, Maier RV, Moldawer LL, Herndon DN, Davis RW, Xiao W, Tompkins RG. Genomic responses in mouse models poorly mimic human inflammatory diseases. Proceedings of the National Academy of Sciences. 2013; 3507-3512.

6 Weber C, Zernecke A, Libby P. The multifaceted contributions of leukocyte subsets to atherosclerosis: lessons from mouse models. Nature Reviews Immunology. 2008; 802-815.

7 Mestas J, Hughes CCW. Of mice and not men: differences between mouse and human immunology. The Journal of Immunology. 2004; 2731.

8 Schulte S, Sukhova GK, Libby P. Genetically programmed biases in Th1 and Th2 immune responses modulate atherogenesis. American Journal of Pathology. 2008; 1500-1508.

9 Dansky HM, Charlton SA, Sikes JL, Heath SC, Simantov R, Levin LF, Shu P, Moore, KJ, Breslow JL, Smith JD. Genetic background determines the extent of atherosclerosis in ApoE-deficient mice. Arteriosclerosis, Thrombosis and Vascular Biology. 1999; 1960-1968.

10 De Boer OJ, Van Der Meer JJ, Teeling P, Van Der Loos CM, Van Der Wal AC. Low numbers of FOXP3 positive regulatory T cells are present in all developmental stages of human atherosclerotic lesions. Public Library of Science one. 2007; 779.

11 Tavora F, Kutys R, Li L, Ripple M, Fowler D, Burke A. Adventitial lymphocytic inflammation in human coronary arteries with intimal atherosclerosis. Cardiovascular pathology. 2009; 61-68.

12 van Dijk RA, Virmani R, von der Thüsen JH, Schaapherder AF, Lindeman JHN. The natural history of aortic atherosclerosis: a systematic histopathological evaluation of the peri-renal region. Atherosclerosis. 2010; 100-106.

13 Virmani R, Kolodgie FD, Burke AP, Farb A, Schwartz SM. Lessons from sudden coronary death: a comprehensive morphological classification scheme for atherosclerotic lesions. Arteriosclerosis, thrombosis, and vascular biology. 2000; 1262.

14 de Boer OJ, Li X, Teeling P, Mackaay C, Ploegmakers HJ, van der Loos CM, Daemen MJ, de Winter RJ, van der Wal AC. Neutrophils, neutrophil extracellular traps and interleukin-17 associate with the organisation of thrombi in acute myocardial infarction. Thrombosis and Haemostasis. 2013; 290-297

15 Chen L, Bea F, Wangler S, Celik S, e, Wang Y, Böckler D, e, Dengler TJ. Inhibition of IL-17A attenuates atherosclerotic lesion development in apoE-deficient mice. Journal of Immunology. 2009; 8167-8175.

16 Mackay C.R. Dual personality of memory T cells. Nature. 1999; 659-660

17 Swirski FK, Nahrendorf M. Leukocyte behavior in atherosclerosis, myocardial infarction, and heart failure. Science. 2013; 161-166.

18 Wigren M, Nilsson J, Kolbus D. Lymphocytes in atherosclerosis. Clinica Chimica Acta. 2012; 1562-1568.

19 Libby P, Ridker PM, Hansson GK. Progress and challenges in translating the biology of atherosclerosis. Nature. 2011; 317-325.

20 Kleemann R, Zadelaar S, Kooistra T. Cytokines and atherosclerosis: a comprehensive review of studies in mice. Cardiovascular Research. 2008; 360-376.

21 Emerging Risk Factors Collaboration, Di Angelantonio E, Sarwar N, Perry P, Kaptoge S, Ray KK, Thompson A, Wood AM, Lewington S, Sattar N, Packard CJ, Collins R, Thompson SG, Danesh J. Major lipids, apolipoproteins, and risk of vascular disease. Journal of the American Medical Association. 2009; 1993-2000.

22 Lichtman AH. Adaptive immunity and atherosclerosis: mouse tales in the AJP. American Journal of Pathology. 2013; 5-9.

23 Huber SA, Sakkinen P, David C, Newell MK, Tracy RP. T helper-cell phenotype regulates atherosclerosis in mice under conditions of mild hypercholesterolemia. Circulation. 2001; 2610-2616

24 Mestas J1, Hughes CC. Of mice and not men: differences between mouse and human immunology. Journal of Immunology. 2004; 2731-2738.

25 Ni M, Chen WQ, Zhang Y. Animal models and potential mechanisms of plaque destabilisation and disruption. Heart. 2009; 1393-1398.

26 Kotliar C, Juncos L, Inserra F, de Cavanagh EM, Chuluyan E, Aquino JB, Hita A, Navari C, Sánchez R. Local and systemic cellular immunity in early renal artery atherosclerosis. Clinical Journal of American Society of Nephrology. 2012; 224-230.

27 Aoshiba K, Koinuma M, Yokohori N, Nagai A; Respiratory Failure Research Group in Japan. Differences in the distribution of CD4+ and CD8+ T cells in emphysematous lungs. Respiration. 2004; 184-190.

28 Artemiadis AK, Anagnostouli MC: Apoptosis of oligodendrocytes and post-translational modifications of myelin basic protein in multiple sclerosis: possible role for the early stages of multiple sclerosis. European Neurology 2010; 65–72

29 Hussein MR, Hassan HI, Hofny ER, Elkholy M, Fatehy NA, Abd Elmoniem AE, Ezz El-Din AM, Afifi OA, Rashed HG. Alterations of mononuclear inflammatory cells, CD4/CD8+ T cells, interleukin 1beta, and tumour necrosis factor alpha in the bronchoalveolar lavage fluid, peripheral blood, and skin of patients with systemic sclerosis. Journal of Clinical Pathology. 2005; 178-184.

30 Oestreich KJ, Weinmann AS. T-bet employs diverse regulatory mechanisms to repress transcription. Trends in Immunology. 2012; 78-83

31 de Boer OJ, van der Wal AC, Verhagen CE, Becker AE. Cytokine secretion profiles of cloned T cells from human aortic atherosclerotic plaques. Journal of Pathology. 1999; 174-179.

32 Alberts-Grill N, Rezvan A, Son DJ, Qiu H, Kim CW, Kemp ML, Weyand CM, Jo H.Dynamic immune cell accumulation during flow-induced atherogenesis in mouse carotid artery: an expanded flow cytometry method. Arteriosclerosis, Thrombosis and Vascular Biology. 2012; 623-632.

33 Houtkamp MA, de Boer OJ, van der Loos CM, van der Wal AC, Becker AE. Adventitial infiltrates associated with advanced atherosclerotic plaques: structural organization suggests generation of local humoral immune responses. Journal of Pathology. 2001; 263-269.

34 Hu Y1, Ericsson I2, Doseth B3, Liabakk NB4, Krokan HE5, Kavli B6. Activation-induced cytidine deaminase (AID) is localized to subnuclear domains enriched in splicing factors. Experimental Cell Research. 2014; 178-192.

35 Smedbakken LM, Halvorsen B, Daissormont I, Ranheim T, Michelsen AE, Skjelland M, Sagen EL, Folkersen L, Krohg-Sørensen K, Russell D, Holm S, Ueland T, Fevang B, Hedin U, Yndestad A, Gullestad L, Hansson GK, Biessen EA, Aukrust P. Increased levels of the homeostatic chemokine CXCL13 in human atherosclerosis - Potential role in plaque stabilization. Atherosclerosis. 2012; 266-273.

36 I Daissormont, M Lipp, EAL Biessen. The CXCL13-CXCR5 axis contributes to atherosclerosis development in LDLr−/− mice by regulating lymphocyte migration to perivascular lymph organs. Cardiovascular Research. 2010: S43-S44.

37 Liem SS, van der Hoeven BL, Oemrawsingh PV, Bax JJ, van der Bom JG, Bosch J,Viergever EP, van Rees C, Padmos I, Sedney MI, van Exel HJ, Verwey HF, Atsma DE, van der Velde ET, Jukema JW, van der Wall EE, Schalij MJ. MISSION!: optimization of acute and chronic care for patients with acute myocardial infarction. American Heart Journal. 2007; e1-11.

38 Ait-Oufella H, Herbin O, Bouaziz JD, Binder CJ, Uyttenhove C, Laurans L, Taleb S, Van Vré E, Esposito B, Vilar J, Sirvent J, Van Snick J, Tedgui A, Tedder TF, Mallat Z. B cell depletion reduces the development of atherosclerosis in mice. Journal of Experimental Medicine. 2010; 1579-1587

39 Caligiuri G, Nicoletti A, Poirier B, Hansson GK. Protective immunity against atherosclerosis carried by B cells of hypercholesterolemic mice. Journal of Clinical Investigation. 2002; 745-753.

40 Frostegård J, Ulfgren A-K, Nyberg P, *et al*.. Cytokine expression in advanced human atherosclerotic plaques: dominance of pro-inflammatory (Th1) and macrophage-stimulating cytokines. Atherosclerosis. 1999; 33-43.

41 Lindeman JH, Abdul-Hussien H, Schaapherder AF, Van Bockel JH, Von der Thüsen JH, Roelen DL, Kleemann R. Enhanced expression and activation of pro-inflammatory transcription factors distinguish aneurysmal from atherosclerotic aorta: IL-6 and IL-8 dominated inflammatory responses prevail in the human aneurysm. Clinical Science. 2008; 687-697..

CHAPTER 8

Activator protein-1 (AP-1) signalling in human atherosclerosis: results of a systematic evaluation and intervention study

C.A. Meijer
P.A.A. Le Haen
R.A. van Dijk
M. Hira
J.F. Hamming
J.H. van Bockel
J.H.N. Lindeman

Clinical Science 2012

ABSTRACT

Background: Animal studies implicate the AP-1 (activator protein-1) pro-inflammatory pathway as a promising target in the treatment of atherosclerotic disease. It is, however, unclear whether these observations apply to human atherosclerosis. Therefore we evaluated the profile of AP-1 activation through histological analysis and tested the potential benefit of AP-1 inhibition in a clinical trial.

Material and methods: AP-1 activation was quantified by phospho-c-Jun nuclear translocation (immunohistochemistry) on a biobank of aortic wall samples from organ donors. The effect of AP-1 inhibition on vascular parameters was tested through a double blind placebo-controlled cross-over study of 28 days doxycycline or placebo in patients with symptomatic peripheral artery disease. Vascular function was assessed by brachial dilation as well as by plasma samples analysed for hs-CRP (high-sensitivity C-reactive protein), IL-6 (interleukin-6), IL-8, ICAM-1 (intercellular adhesion molecule-1), vWF (von Willebrand factor), MCP-1 (monocyte chemoattractant protein-1), PAI-1 (plasminogen activator inhibitor-1) and fibrinogen.

Results: Histological evaluation of human atherosclerosis showed minimal AP-1 activation in non-diseased arterial wall (*i.e.* vessel wall without any signs of atherosclerotic disease). A gradual increase of AP-1 activation was found in non-progressive and progressive phases of atherosclerosis respectively ($P<0.044$). No significant difference was found between progressive and vulnerable lesions. The expression of phospho-c-Jun diminished as the lesion stabilized ($P<0.016$) and does not significantly differ from the normal aortic wall ($P<0.33$). Evaluation of the doxycycline intervention only revealed a borderline-significant reduction of circulating hs-CRP levels (−0.51 μg/ml, $P=0.05$) and did not affect any of the other markers of systemic inflammation and vascular function.

Conclusion: Our studies do not characterize AP-1 as a therapeutic target for progressive human atherosclerotic disease.

INTRODUCTION

Atherosclerosis is a lipid-driven disorder with a strong inflammatory component. The efficacy of lipid-lowering interventions to reduce incident atherosclerotic disease has been firmly established, yet its success rate remains limited to an approximate 30% reduction in clinical events[1]. Hence, the need for complementary strategies beyond that of lipid lowering is widely acknowledged.

Inflammation is a key factor in the progression and complications of atherosclerotic disease. Consequently, strategies aimed at the 'central hub' of inflammation have been brought forward as a reasonable target in limiting vascular inflammation[2]. In vitro and animal studies implicate the common inflammatory transcription factor AP-1 (activator protein-1) as a critical correlate in the initiation and progression of vascular dysfunction, and atherogenesis. Hence, AP-1 inhibition has been proposed as an attractive target to prevent progression of atherosclerosis[3,4,5,6].

However, as the available literature on the role of the AP-1 pathways in human atherosclerosis is limited, we decided to explore the possible role of AP-1 in atherosclerotic disease. To that end, we first performed a systematic histological evaluation of AP-1 activation in the successive stages of atherosclerotic disease. This evaluation showed abundant AP-1 activation throughout all stages of atherosclerosis. We next performed a clinical study to test whether quenching of AP-1 activation improves vascular function. The tetracycline analogue doxycycline has been shown to have a direct inhibitory effect on the activation of JNK1 (c-Jun N-terminal kinase 1) and JNK2, two key members of the AP-1 pathway[7]. These in vitro findings were corroborated in a clinical study that showed that a 2-week doxycycline intervention in patients with an AAA (abdominal aortic aneurysm) quenches aortic wall AP-1 activation[8].

Hence it was reasoned that doxycycline provides a means of evaluating a possible role of AP-1 in human atherosclerosis. We therefore tested whether doxycycline improves vascular function in high-risk patients (patients with peripheral artery disease) in a double-blind placebo controlled cross-over trial.

MATERIAL AND METHODS

AP-1 activation

All sample collection and handling were performed in accordance with the guidelines of the Medical and Ethical Committee in Leiden, The Netherlands and the code of conduct of the Dutch Federation of Biomedical Scientific Societies (http://www.federa.org/? s=1&m=82&p=0&v=4#827).

A systematic analysis of AP-1 activation (phospho-c- Jun) was performed on material from a large biobank of aortic patches that were removed along with the kidney during kidney explanation from heart-beating, brain-dead multiple organ donors. All donors met the criteria set by The Eurotransplant Foundation. The patches were divided into 5 μm paraffin-embedded sections. The stage of atherosclerosis for each section was classified according to the modified classification of the American Heart Association proposed by Virmani *et al*.[9] (Table 1). All analyses were performed on the dominant lesion in the tissue section, *i.e.* the section showing the most advanced grade of atherosclerosis. Details of the first 260 cases in this bank have been published previously[12].

In order to achieve balanced study groups, we consecutively selected pre-classified samples for each stage (Table 1) from the tissue bank. The sections were stained for the identification of activatedAP-1 (phospho-c-Jun, nuclear translocation using the anti-phospho-c-Jun clone KM-1; Cell Signaling, 1:800 overnight). Conjugated biotinylated anti-mouse IgG was used as a secondary antibody. Sections were developed with Nova Red (Vector Laboratories). Corroboration with the downstream marker PAI-1 (plasminogen activator inhibitor-1) was performed with an in-house rabbit polyclonal antibody that recognizes both the free and complex form[10,11]. Conjugated biotinylated anti-rabbit anti-IgG (1:1000 dilution, Amersham Biosciences) was used as secondary antibody. Sections were counterstained with Mayer's haematoxylin. Stained sections were histologically analysed for positive nuclear signalling and classified according to intensity. The degree of AP-1 activity was assessed semi-quantitatively within the atherosclerotic lesion: − (absent), +/− (<10% of component area stained positively), + (10–50%) and ++ (>50%). Intimal, medial and adventitial layers were analysed separately. Particular interest was paid to the various cell types present in the atherosclerotic lesion *i.e.* endothelial cells, monocytes/macrophages and SMCs (smooth muscle cells).

An atherosclerotic lesion was defined as the area between the endothelium and internal elastic lamina over a distance of 1 mm. In the presence of a necrotic core, the distance was expanded by another 500μm on both sides of the necrotic core to include the adjacent shoulder region[12].

Intervention study

An open crossover double-blind placebo-controlled trial was used to evaluate the effect of doxycycline therapy on vascular functioning (Dutch Trial Registry NTR1389 http://www.trialregister.nl/trialreg/admin/rctview.asp? TC=1389). As current medical strategies focus on high-risk patients, we recruited patients with symptomatic PAD (peripheral arterial disease) from the outpatient department of vascular surgery. PAD patients were chosen for their condition, which is associated

with a high risk for CVD (cardiovascular disease)[13,14]. PAD was confirmed by a history of intermittent claudication and an ankle-brachial pressure index <0.9. Patients with a history of lower extremity revascularization or endarterectomy, with diabetes mellitus or known hypersensitivity for tetracycline derivates, or treated with antibiotics or immunosuppressive agents were excluded from participation in the study. In order to exclude potential effects of different kinds or doses of cholesterol-lowering agents all subjects were switched to, or started with, simvastatin (40 mg/day) at least 4 weeks prior to the start of study medication. All subjects participated in two sessions and both received treatments of 28 days of doxycycline (100 mg/day) (t 12=15–23 h) or placebo in a cross-over design. Dosing was separated by a washout period of 28 days.

Informed consent was obtained from each patient. Randomization was performed by the Leiden University Medical Center pharmacy.

Brachial flow-mediated dilation

Endothelial function was evaluated through flow-mediated vasodilation of the brachial artery, an established test that assesses the vasodilatory response to transient ischaemia. Endothelium independent vasodilation of the brachial artery was assessed through the artery's vasodilatory response to NTG (nitroglycerine)[15]. Flow- and NTG-mediated vasodilations were measured on each visit.

After overnight fasting, patients were examined in the supine position after 15 min of rest in a quiet room at room temperature. Patients refrained from vasoactive drugs, coffee and tea for at least 8 h prior to testing. The right brachial artery was visualized in longitudinal sections above the elbow, by high-resolution ultrasound using a 10 MHz linear probe on an Aloka 5500 SSD machine. Reactive hyperaemia was triggered by inflating a pneumatic tourniquet distal to the brachial artery to 50 mmHg above the systolic pressure for 5 min and dilation of the vessel was evaluated 1 min after releasing the tourniquet. The diameter of the brachial artery was measured in triplicate at the R-wave of the ECG, at the interface of the intima and media of the anterior and posterior wall. The brachial artery was allowed to return to its resting state for at least 15 min. Endothelium-independent vasodilation was studied by brachial artery diameter changes 4 min after administering 400 μg of NTG sublingual. The inter- and intra-observer variability for the measurement of the diameter of brachial artery was <0.1 mm. Flow-mediated vasodilation and NTG-mediated vasodilation were defined as the percentage increase in artery diameter during dilation.

Endothelium and inflammation

Fasting blood samples were taken from the patients' left arm(non-study arm) just after evaluating vascular reactivity. Samples were centrifuged at 2000 g at 4°C for 20 min and the obtained plasma was removed and subsequently recentrifuged at 12 000 g for 10 min. Plasma was stored at −80°C until analysis. Glucose, insulin, hs-CRP (high-sensitivity C-reactive protein), TAG (triacylglycerol), HDL (high-density lipoprotein)-cholesterol and total cholesterol concentrations were determined in one batch at the certified clinical laboratory of the Leiden University Medical Center. The plasma concentration of LDL (low-density lipoprotein)-cholesterol was obtained using Friedewald estimation. The plasma concentration of vWF (von Willebrand factor), ICAM-1 (intercellular adhesion molecule-1), PAI-1, MCP-1 (monocyte chemoattractant protein-1), IL (interleukin)-6, IL-8, hs-CRP and fibrinogen were obtained using ELISA an in-house ELISA using a rabbit anti-human vWF (A0082; Dako) and an HRP (horseradish peroxidase)-conjugated rabbit anti-human VWF antibody (P0226; Dako), an R&D Systems human ICAM-1 ELISA(DY720), an in-house ELISA using a PAI-1 coating monoclonal antibody 3-3b conjugate, an R&D Systems human MCP-1 ELISA (DY279), a Sanquin PeliKine-compact human IL-6 ELISA (M1916),a Sanquin PeliKine-compact human IL-8 ELISA(M1918) and an in-house ELISA using a fibrinogen coating α-XDP conjugate. hs-CRP was measured on a cobas c system (04628918; Roche Diagnostics). vWF was calibrated against a pool of human plasma (available from Sanquin). All other calibrating solutions were supplied within the kit. Samples were diluted to maintain plasma concentration well within the accuracy boundaries of the kits. All samples were analysed in duplicate. The reproducibility and accuracy of the ELISA tests were within the limits of the standard kit.

Statistical analysis

Mean levels of AP-1 expression in the immunohistochemical analysis were compared with the one-way ANOVA. Differences between the groups were assessed by Fisher's LSD (least significant difference) analysis. $P<0.05$ was considered statistically significant. Power calculation for the crossover study was based on published data[7,14]. A group size of 12 patients allowed for a discriminating power of more than 95% for a 20% difference in arterial dilation[17] and reduction of pro-inflammatory cytokines 8 between placebo and therapeutic treatment. The normality of different variables was tested. Wilcoxon signed ranks test was used if normal distribution of the data was not applicable (see Table 3). Statistical significance was defined as a two-sided $P<0.05$.Data in the Figures are presented as means (S.D.) in Table 2 or as medians (25th and 75th percentiles) in Table 3). All statistical analyses were performed using SPSS for Windows, version 17.0.

RESULTS

Immunohistochemistry

AP-1 activation (phospho-c-Jun nuclear translocation) was evaluated in 98 human aortic wall samples that cover the full spectrum of atherosclerotic disease (Table 1). Minimum activation of AP-1 was found in the normal aortic wall. In these samples, nuclear staining was mainly limited to the endothelial cells (Table 1 and Figure 1). A gradual increase of AP-1 activation was found in non-progressive and progressive phases of atherosclerosis respectively ($P<0.33$ and $P<0.044$ respectively; Figure 2), with involvement of macrophages and SMCs (Table 1 and Figure 1). No further significant increase was found in the vulnerable lesion types ($P<0.48$; Figure 2). In advanced lesions (*i.e.* progressive and vulnerable phases), activated cells were distributed throughout the vascular wall with a particular strong nuclear staining of macrophages and SMCs (Table 1 and Figure 1). A notable sharp reduction in AP-1 activation was found in the stabilized lesion types, *i.e.* healed ruptures and fibrotic calcified plaques ($P=0.016$; Figures 1 and 2). AP-1-regulated PAI-1 gene expression showed a distribution parallel to the activated AP-1 expression, with a significant increase in the progressive lesions ($P<0.002$; Figure 3).

Doxycycline intervention

A total of 15 patients were enrolled in the study. One patient experienced photosensitivity reaction and withdrew from the study. No other adverse events occurred. Two subjects were lost to follow up for reasons that were not study related. The mean age of the participants was 67+ −8 years and 82% were male. All characteristics were assessed just prior to the start of the study (Table 2). Evaluation of systemic markers of inflammation (hs-CRP, IL-6, IL-8 and fibrinogen) only revealed a borderline significant decrease in plasma hs-CRP concentration after doxycycline treatment (−0.51μg/ml, $P=0.050$; Table 3).

Endothelial cell activation markers (ICAM, vWF and PAI-1) were not influenced by the treatment (Table 3). In addition to the circulating inflammatory and endothelial cell activation markers, we also assessed flow-mediated vasodilation as a functional test of endothelial function. Flow-mediated vasodilation (baseline value, 13.2%) and NTG-mediated vasodilation (baseline value, 11.3%) were not influenced by doxycycline treatment −5.9%(−14.9 to 3.9), $P=0.10$; and −5.4% (−16.4 to 0.7), $P=0.18$; values are medians (25th to 75th percentiles) (Table 3).

Table 1. Qualitative Phospho-c-Jun expression in endothelial cells SMC's, and monocytes/macrophages within the various atherosclerotic lesions

			Phospho-c-Jun expression		
Morphological description	n	Cell Type	Endothelial cells	Smooth muscle cells*	Monocytes/Macrophages**
Normal aorta	10		+/-	+/-	-
Non-atherosclerotic lesions					
Adaptive intimal thickening	10		+/-	+	-
Intimal xanthoma	10		+/-	+	+
Progressive atherosclerotic lesions					
Pathological intimal thickening	10		+/-	++	+
Early fibroatheroma	10		+	+	+/-
Late fibroatheroma	10		+	+	+/-
Vulnerable atherosclerotic lesions					
Thin cap fibroatheroma	10		+	++	+
Plaque rupture	8		+	+	+
Stabilized atherosclerotic lesions					
Healed ruptures	10		+/-	+	+
Fibrotic calcified plaque	10		+/-	+	+/-

Lesions are classified according the modified American Heart Association classification by Virmani *et al.* [8]. * P <0.041 and ** P <0.009 between the groups, as determined by ANOVA. –, no expression of phospho-c-Jun; +/–,0–10%; +, 10–50 %; ++, >50 %.

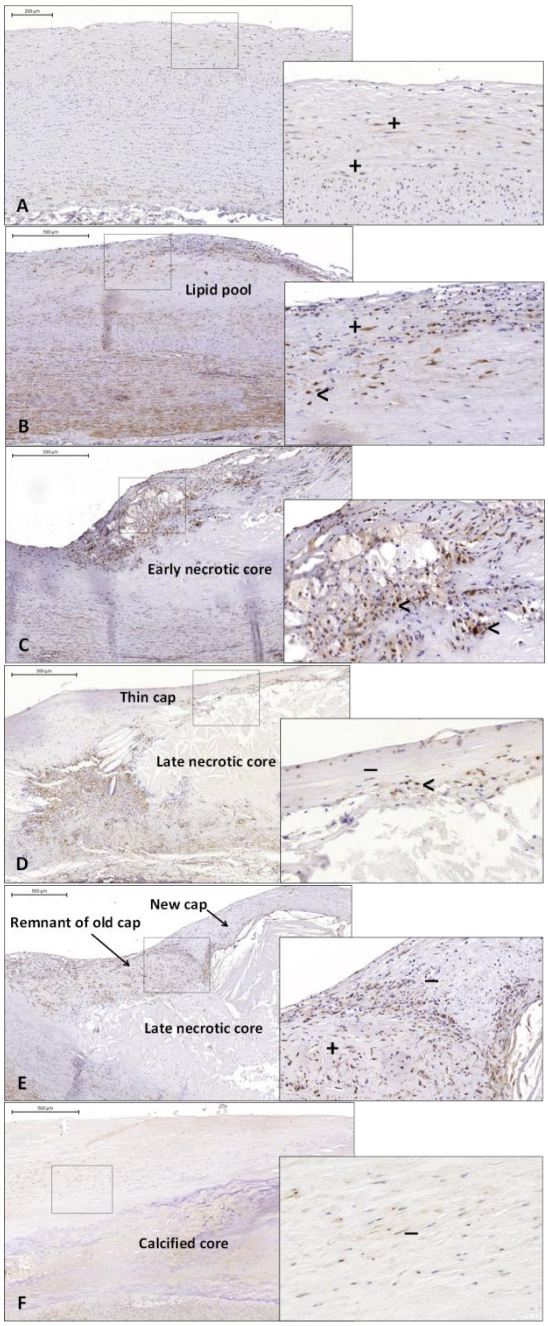

Figure 1. Phospho-c-Jun expression during the evolution of human atherosclerosis. The intima within the normal aortic wall and in aortas containing adaptive intimal thickening showed minimal expression of phospho-c-Jun in the nuclei of the vascular SMC (A). There was a higher amount of phospho-c-Jun expression in the infiltrating SMCs and monocytes surrounding the lipid pools in pathological intimal thickening (B). In early fibroatheromata almost 50 % of the monocytes and macrophages stained positive for phospho-c-Jun (C). In the thin cap fibroatheroma, the vulnerable phase in atherosclerosis, the very few SMCs that were found within the fibrous cap lacked phospho-c-Jun expression (D). In the fibrous cap of healed atherosclerotic ruptures was a remarkable difference in phospho-c-Jun expression between the SMCs in the remnants of the old cap and the newly formed cap (E). Fibrotic calcified lesions were mostly acellular and minimally expressed phospho-c-Jun (F). +, phospho-c-Jun-positive SMC; –, phospho-c-Jun-negative SMC; <, phospho-c-Jun-positive monocyte or macrophage.

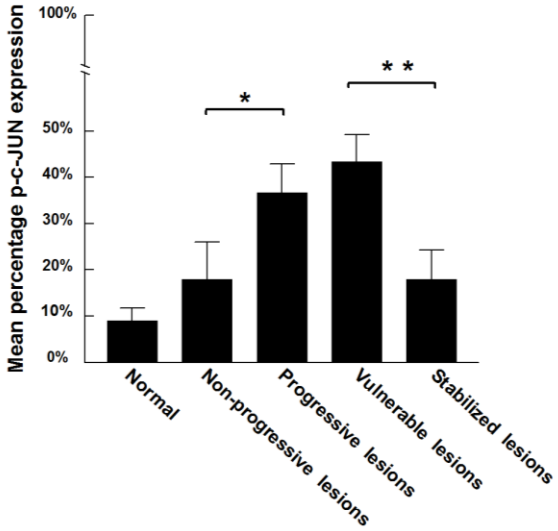

Figure 2. Phospho-c-Jun expression within the various atherosclerotic lesions. There was minimal phospho-c-Jun (p-c-JUN) expression within the endothelial cells and SMCs of the normal aortic wall. This expression increased gradually during the development of atherosclerosis. Activation of phospho-c-Jun increased significantly from non-progressive to progressive lesions (∗ P <0.044). No significant difference was found between progressive and vulnerable lesions (P <0.48). The expression of phospho-c-Jun diminished as the lesion stabilized (∗∗ P <0.016) and did not significantly differ from the normal aortic wall (P <0.33). Values are means+ −S.E.M. For the detailed qualification scale, see the aterials and methods section.

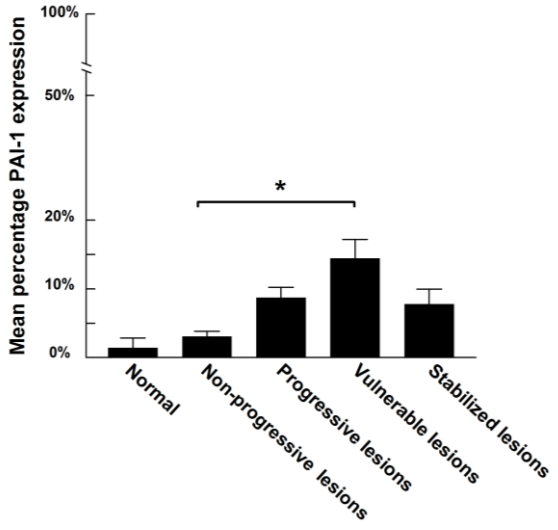

Figure 3. PAI expression within the observed lesion in relation to the atherosclerotic stage. There is a significant increase in PAI expression when atherosclerosis evolves from a non-progressive lesion into a vulnerable lesion (∗P <0.002). Values are means ± S.E.M. For the detailed qualification scale and an overview of the various atherosclerotic clusters, see the Materials and methods section.

Table 2. Patient characteristics

Characteristic	
Age (years)	67 (8)
Male gender	82%
BMI (kg/m2)	25.0 (5.0)
Smoking (%)	100
DM (%)	0.0
Total cholesterol (mmol/l)	4.37 (0.85)
TAG (mmol/l)	1.62 (1.62)
HDL (mmol/l)	1.26 (0.50)
Glucose (mmol/l)	5.95 (0.54)
Brachial artery diameter (mm)	3.8 (0.6)

Values are means (S.D.), n =12. BMI, body mass index; DM, diabetes mellitus; TAG, triacylglycerol.

Table 3. Markers of inflammation and vascular function

Parameter	Baseline	Doxycycline–placebo	P
Circulating markers			
hs-CRP (μg/ml)	2.21 (1.28–5.20)	−0.51 (−6.46 to 0.04)*	0.05
Fibrinogen (mg/ml)	5.38 (3.89–6.23)	−1.12 (−0.53 to 3.00)	0.18
IL-6 (pg/ml)	1.80 (0.92–2.03)	−0.11 (−1.38 to 2.54)*	0.33
IL-8 (pg/ml)	4.28 (3.24–7.74)	0.68 (−1.38 to 2.54)	0.53
MCP-1 (pg/ml)	ND	–	–
ICAM-1 (102 ng/ml)	1.88 (1.37–2.17)	−0.13 (−0.36 to 0.34)	0.35
vWF (% HPP)	149.6 (114.3–164.5)	−16.8 (−58.9 to 27.6)	0.58
PAI-1 (ng/ml)	34.4 (26.2–49.7)	4.6 (−20.5 to 46.1)	0.58
Dilation			
Flow-mediated (%)	13.2 (6.9–16.4)	−5.9 (−14.1 to 3.9)	0.10
NTG-mediated (%)	11.3 (8.8–25.1)	−5.4 (−16.4 to 0.7)	0.18

Values are medians (25th–75th percentile), n =12. Doxycycline–placebo represents the difference between the doxycycline treatment and the placebo treatment. P <0.05 for doxycycline–placebo. ND, non-detectable; concentration below the detection limit of the assay (<20 pg/ml). *Exclusion of a patient in the placebo arm with elevated levels of hs-CRP and IL-6 due to infection.

DISCUSSION

Modulation of chronic vascular inflammation is now considered the most promising complementary strategy for the prevention of incident CVD. Typically, this strategy will focus on patients with clinical or subclinical atherosclerosis, *i.e.* those with progressive atherosclerotic lesions. On the basis of animal studies, the AP-1 pro-inflammatory pathway has been implicated in the initiation and progression of atherosclerotic disease. Upregulation of AP-1 in rabbits increased with age-related vascular SMC proliferation[18,19] and in rats AP-1 mediated AngII (angiotensin II)-induced inflammation[20]. Additionally, it has been shown that AP-1 deficiency protects against the development of atherosclerosis in hypercholesterolaemic mice 5. In humans, AP-1 was activated in progressive and

unstable atherosclerotic plaques and proposed as a switch for inflammatory tissue response and repair[21,22].

Consequently, these studies imply AP-1 as a reasonable target for complementary therapeutic strategies, but its potential role in human atherosclerosis remains unclear. Our histological analysis shows a gradual increase in the activation of the AP-1 system during the development of atherosclerotic disease, from normal up to progressive atherosclerotic lesions. Remarkably, further transition from progressive to vulnerable lesion types is not associated with significant increase of AP-1 activation. This 'plateau phase' of activation clearly diminishes in the fibrotic calcified stabilized plaques. The extent of activation of the AP-1 system is paralleled by a shift in activated cell types, from mainly endothelial cells in normal tissue to predominantly vascular SMCs in advanced atherosclerotic lesions. Accordingly, these observations suggest that AP-1 activation is an early event in human atherosclerotic disease and that it is not prominently involved in further progression of the disease (advanced atherosclerosis and its complications). In order to further test or refute a possible role of AP-1 activation in the perpetuation of advanced atherosclerosis, we performed an intervention study with doxycycline in a group of patients with PAD. The presence of PAD identifies patients with systemic atherosclerosis at a high risk of cardiovascular events, as reflected by general endothelial dysfunction and a high incidence of myocardial infarction and stroke[13,14]. This endothelial impairment is related to the severity of the circulatory failure in the affected limb and with increased plasma markers of inflammation [23], and is a potentially reversible manifestation of progressive vascular disease[24,25]. Flow- and NTG- mediated vasodilation of the brachial artery are especially suitable to detect changes in endothelial functioning and have been reported as a widely used research tool and a marker of cardiovascular atherosclerosis[13,26,27].

Independent of their antibiotic properties, doxycycline and other members of the tetracycline family of antibiotics have been recognized as potent anti-inflammatory and immunomodulating agents[28,29,30,31]. Sub-antimicrobial doses of doxycycline are now registered for the treatment of active periodontitis and rosacae[32,33]. In vitro studies have shown that the effects are (in part) related to an effect on the AP-1 inflammatory pathway. In fact, doxycycline appeared equally effective as the established AP-1 inhibitor SP600125[7].

Doxycycline is safe and has an excellent tissue penetration[34,35], making it a suitable candidate for clinical studies. We previously studied the effects of 2 weeks of perioperative doxycycline treatment on vascular inflammation in AAA, and found that doxycycline has a profound but selective effect on vascular inflammation, as indicated by a clear reduction in aortic wall IL-6 and IL-8 levels, and a respective 75% and 96% reduction in aortic wall neutrophil and cytotoxic T-

cell content. Further evaluation showed that this effect is mediated by a selective reduction in AP-1 activation (measured by phospho-c-Jun)[8]. Baseline AP-1 (non-phosphorylated c-Jun) levels were not influenced by doxycycline treatment. As such these clinical findings corroborate the in vitro findings of Kim *et al*.[7], and we thus hypothesized that doxycycline provides a means of modulating AP-1 activation in atherosclerosis.

Despite the clear effects in aneurysmal disease, we did not observe any effect on each of the markers studied in the atherosclerotic patients. It is unlikely that failure of the intervention reflects a pharmacokinetic limitation. Our studies in AAA show that a brief period of 2 weeks (*i.e.* one half of the treatment period in this study) suffices for a profound effect. In these studies, we also observed that the effect was already maximal at doses as low as 50 mg. A more likely explanation for the failure of doxycycline in our patients are the profound differences in the inflammatory footprint between aneurysmal disease and atherosclerotic disease, with AP-1 being prominently involved in aneurysmal disease, but to a much lesser extend in advanced atherosclerotic disease[36].We cannot fully exclude that the negative findings are based on a type II statistical error; however, the study was powered on results from a previous positive study[8]. As of the consistent negative findings for all markers studied and the cross-over design, it is in our opinion unlikely that a larger study would have significantly different results. The study does not support a major role for AP-1 in the initiation and progression of atherosclerosis.

Our results do not exclude that AP-1 inhibition has a beneficial effects in the earliest phases (initiation phase) of the disease. However, given the fact that manifest atherosclerotic disease is present in more than 75% of male population between 20 and 30 years of age 37, such a treatment should typically be initiated before the age of 20 years, and be maintained throughout the rest of life. We consider such a strategy unrealistic. Our findings do not exclude a role of AP-1 in complications of atherosclerotic disease such as plaque rupture. It has been suggested before that doxycycline decreases the risk of acute coronary syndromes[38]. Thrombo-occlusive events usually occur in the vulnerable stages of the atherosclerotic process, including plaque rupture and erosion. Plaque rupture is an acute event with inflammatory characteristics distinctive from progressive lesions. Given the presumably acute nature of this process, this will be typically missed in our cross- sectional sample collection.

In conclusion, the response to inhibition of the activated AP-1 system is largely missing in the advanced stages of human atherosclerosis. The results of our intervention seemingly contrast with animal studies, in which AP-1 deficiency in hypercholesterolaemic mice ultimately prevented atherosclerosis. These results, however, apply to the initiation of the atherosclerotic process, whereas human atherosclerotic disease reflects the advanced (*i.e.* progressive and vulnerable) stages. This is in line with our systematic evaluation of AP-1 activation in the successive atherosclerotic stages showing that AP-1 activation occurs early in the process and is not related to advanced atherosclerosis and complications. The mere presence of AP-1 in progressive human atherosclerotic tissue is not an indication of the extent of the disease process.

REFERENCES

1 Ford, I., Murray, H., Packard, C. J., Shepherd, J., Macfarlane, P.W. and Cobbe, S. M. (2007) Long-term follow-up of the West of Scotland Coronary Prevention Study. N. Engl. J. Med. 357, 1477–1486

2 De Caterina, R., Massaro, M., Scoditti, E. and Annunziata Carluccio, M. (2010) Pharmacological modulation of vascular inflammation in atherothrombosis. Ann. N.Y. Acad. Sci. 1207, 23–31

3 Wang, J., An, F. S., Zhang, W., Gong, L., Wei, S. J., Qin, W. D., Wang, X. P., Zhao, Y. X., Zhang, Y., Zhang, C. and Zhang, M. X. (2011) Inhibition of c-Jun N-terminal kinase attenuates low shear stress-induced atherogenesis in apolipoprotein E-deficient mice. Mol. Med. 17, 990–999

4 Muslin, A. J. (2008) MAPK signalling in cardiovascular health and disease: molecular mechanisms and therapeutic targets. Clin. Sci. 115, 203–218

5 Osto, E., Matter, C. M., Kouroedov, A., Malinski, T., Bachschmid, M., Camici, G. G., Kilic, U., Stallmach, T., Boren, J., Iliceto, S. *et al*. (2008) c-Jun N-terminal kinase 2 deficiency protects against hypercholesterolemia-induced endothelial dysfunction and oxidative stress. Circulation 118, 2073–2080

6 Manning, M. W., Cassis, L. A. and Daugherty, A. (2003) Differential effects of doxycycline, a broad-spectrum matrix metalloproteinase inhibitor, on angiotensin II-induced atherosclerosis and abdominal aortic aneurysms. Arterioscler. Thromb. Vasc. Biol. 23, 483–488

7 Kim, H. S., Luo, L., Pflugfelder, S. C. and Li, D. Q. (2005) Doxycycline inhibits TGF-β1-induced MMP-9 via Smad and MAPK pathways in human corneal epithelial cells. Invest. Ophthalmol. Visual Sci. 46, 840–848

8 Lindeman, J. H., Abdul-Hussien, H., van Bockel, J. H., Wolterbeek, R. and Kleemann, R. (2009) Clinical trial of doxycycline for matrix metalloproteinase-9 inhibition in patients with an abdominal aneurysm: doxycycline selectively depletes aortic wall neutrophils and cytotoxic T cells. Circulation 119, 2209–2216

9 Virmani, R., Kolodgie, F. D., Burke, A. P., Farb, A. and Schwartz, S. M. (2000) Lessons from sudden coronary death: a comprehensive morphological classification scheme for atherosclerotic lesions. Arterioscler. Thromb. Vasc. Biol. 20, 1262–1275

10 Keeton, M. R., Curriden, S. A., van Zonneveld, A. J. and Loskutoff, D. J. (1991) Identification of regulatory sequences in the type 1 plasminogen activator inhibitor gene responsive to transforming growth factor β.J.Biol. Chem 266, 23048–23052

11 Lindeman, J. H. N., Pijl, H., Toet, K., Eilers, P. H. C., van Ramshorst, B. and Buijs, M. M. (2007) Human visceral adipose tissue and the plasminogen activator inhibitor type 1. Int. J. Obes. 31, 1671–1679

12 van Dijk, R. A., Virmani, R., von der Thusen, J. H., Schaapherder, A. F. and Lindeman, J. H. (2010) The natural history of aortic atherosclerosis: a systematic histopathological evaluation of the peri-renal region. Atherosclerosis 210, 100–106

13 Criqui, M. H., Langer, R. D., Fronek, A., Feigelson, H. S., Klauber, M. R., McCann, T. J. and Browner, D. (1992) Mortality over a period of 10 years in patients with peripheral arterial disease. N. Engl. J. Med. 326, 381–386

14 Gokce, N., Keaney, Jr, J. F., Hunter, L. M., Watkins, M. T., Nedeljkovic, Z. S., Menzoian, J. O. and Vita, J. A. (2003) Predictive value of noninvasively determined endothelial dysfunction for long-term cardiovascular events in patients with peripheral vascular disease. J. Am. Coll. Cardiol. 41, 1769–1775

15 Akamatsu, D., Sato, A., Goto, H., Watanabe, T., Hashimoto, M., Shimizu, T., Sugawara, H., Sato, H., Nakano, Y., Miura, T. *et al*. (2010) Nitroglycerin-mediated vasodilation of the brachial artery may predict long-term cardiovascular events irrespective of the presence of atherosclerotic disease. J. Atheroscler. Thromb. 17, 1266–1274

16 Hukshorn, C. J., Lindeman, J. H., Toet, K. H., Saris,W. H., Eilers, P. H., Westerterp-Plantenga, M. S. and Kooistra, T. (2004) Leptin and the proinflammatory state associated with human obesity. J. Clin. Endocrinol. Metab. 89, 1773–1778

17 Cheetham, C., O'Driscoll, G., Stanton, K., Taylor, R. and Green, D. (2001) Losartan, an angiotensin type I receptor antagonist, improves conduit vessel endothelial function in Type II diabetes. Clin. Sci. 100, 13–17

18 Metzler, B., Hu, Y., Dietrich, H. and Xu, Q. (2000) Increased expression and activation of stress-activated protein kinases/c-Jun NH2-terminal protein kinases in atherosclerotic lesions coincide with p53. Am. J. Pathol. 165, 1875–1886

19 Rivard, A., Principe, N. and Andres, V. (2000) Age-dependent increase in c-fos activity and cyclin A expression in vascular smooth muscle cells. A potential link between aging, smooth muscle cell proliferation and atherosclerosis. Cardiovasc. Res. 45, 1026–1034

20 Chen, Y. and Currie, R. W. (2005) Heat shock treatment suppresses angiotensin II-induced SP-1 and AP-1 and stimulates Oct-1 DNA-binding activity in heart. Inflamm. Res. 54, 338–343

21 Chen, F., Eriksson, P., Hansson, G. K., Herzfeld, I., Klein, M., Hansson, L. O. and Valen, G. (2005) Expression of matrix metalloproteinase 9 and its regulators in the unstable coronary atherosclerotic plaque. Int. J. Mol. Med. 15, 57–65

22 Hansson, G. K. and Hermansson, A. (2011) The immune system in atherosclerosis. Nat. Immunol. 12, 204–212

23 Brevetti, G., Silvestro, A., Di Giacomo, S., Bucur, R., Di Donato, A., Schiano, V. and Scopacasa, F. (2003) Endothelial dysfunction in peripheral arterial disease is related to increase in plasma markers of inflammation and severity of peripheral circulatory impairment but not to classic risk factors and atherosclerotic burden. J. Vasc. Surg. 38, 374–379

24 Arcaro, G., Zenere, B. M., Saggiani, F., Zenti, M. G., Monauni, T., Lechi, A., Muggeo, M. and Bonadonna, R. C. (1999) ACE inhibitors improve endothelial function in type 1 diabetic patients with normal arterial pressure and microalbuminuria. Diabetes Care 22, 1536–1542

25 Taneva, E., Borucki, K., Wiens, L., Makarova, R., Schmidt-Lucke, C., Luley, C. andWestphal, S. (2006) Early effects on endothelial function of atorvastatin 40 mg twice daily and its withdrawal. Am. J. Cardiol. 97, 1002–1006

26 Barth, J. D. (2002) An update on carotid ultrasound measurements of intima-media thickness. Am. J. Cardiol. 89, 32B–39B

27 Faulx, M. D., Wright, A. T. and Hoit, B. D. (2003) Detection of endothelial dysfunction with brachial artery ultrasound scanning. Am. Heart J. 145, 943–951

28 Ryan, M. E., Ramamurthy, S. and Golub, L. M. (1996) Matrix metalloproteinases and their inhibition in periodontal treatment. Curr. Opin. Periodontol. 3, 85–96

29 Bendeck, M. P., Conte, M., Zhang, M., Nili, N., Strauss, B. H. and Farwell, S. M. (2002) Doxycycline modulates smooth muscle cell growth, migration, and matrix remodeling after arterial injury. Am. J. Pathol. 160, 1089–1095

30 Soory, M. (2007) Periodontal diseases and rheumatoid arthritis: a coincident model for therapeutic intervention? Curr. Drug Metab. 8, 750–757

31 Sapadin, A. N. and Fleischmajer, R. (2006) Tetracyclines: nonantibiotic properties and their clinical implications. J. Am. Acad. Dermatol. 54, 258–265

32 Caton, J. and Ryan, M. E. (2011) Clinical studies on the management of periodontal diseases utilizing subantimicrobial dose doxycycline (SDD). Pharmacol. Res. 63, 114–120

33 McKeage, K. and Deeks, E. D. (2010) Doxycycline 40 mg capsules (30 mg immediate-release/10 mg delayed-release beads): anti-inflammatory dose in rosacea. Am. J. Clin. Dermatol. 11, 217–222

34 Smith, K. and Leyden, J. J. (2005) Safety of doxycycline and minocycline: a systematic review. Clin. Ther. 27, 1329–1342

35 Axisa, B., Loftus, I. M., Naylor, A. R., Goodall, S., Jones, L., Bell, P. R. and Thompson, M. M. (2002) Prospective, randomized, double-blind trial investigating the effect of doxycycline on matrix metalloproteinase expression within atherosclerotic carotid plaques. Stroke 33, 2858–2864

36 indeman, J. H., Abdul-Hussien, H., Schaapherder, A. F., Van Bockel, J. H., Von der Th¨ usen, J. H., Roelen, D. L. and Kleemann, R. (2008) Enhanced expression and activation of pro-inflammatory transcription factors distinguish aneurysmal from atherosclerotic aorta: IL-6- and IL-8-dominated inflammatory responses prevail in the human aneurysm. Clin. Sci. 114, 687–697

37 Joseph, A., Ackerman, D., Talley, J. D., Johnstone, J. and Kupersmith, J. (1993) Manifestations of coronary atherosclerosis in young trauma victims. An autopsy study. J. Am. Coll. Cardiol. 22, 459–467

38 Kardara, M., Papazafiropoulou, A., Katsakiori, P., Petropoulos, C. and Jelastopulu, E. (2006) Protective effect of doxycycline use on coronary artery disease? J. Infect. 52, 243–246

CHAPTER 9

Visualizing TGF-β and BMP signaling in human atherosclerosis: a histological evaluation based on Smad activation

R.A. van Dijk
C.C. Engels
A.F. Schaapherder
A. Mulder-Stapel
P. ten Dijke
J.F. Hamming
J.H.N. Lindeman

Histology and Histopathology 2012

ABSTRACT

Background: The TGF-β superfamily members Transforming Growth Factor-β (TGF-β/Activin) and Bone Morphogenetic Proteins (BMP) have been implicated in the pathogenesis of atherosclerosis. However, their role in human disease remains controversial. In this study we used Smad phosphorylation as a read out for TGF-β and BMP signaling during the initiation, progression and (de)stabilization of human atherosclerotic disease.

Material and methods: A systematic analysis was performed in 114 peri-renal aortic patches (stained with Movat Pentachrome, H&E, pSmad2, pSmad1,5,8 and PAI-1) covering the entire atherosclerotic spectrum (Atherosclerosis: 2010). Immunostaining against T-cells (CD3) and monocytes and macrophages (CD68) was used to explore a putative association between TGF-β and BMP signaling and vascular inflammation.

Results: Smad phosphorylation was present within the normal arterial wall in approximately 10% of the endothelial cells and intimal smooth muscle cells. A significant increase in pSmad2 and pSmad1,5,8 positivity was found in non-progressive lesions (> 50% positivity). No further increase or decrease was found in the progressive atherosclerotic lesions, vulnerable and stabilized lesions. No association was found between TGF-β and BMP signaling and CD3 and CD68 expression, nor cap thickness.

Conclusion: Activation of the TGF-β and BMP pathways is an early event in atherosclerotic lesion formation. No significant relationships were found between Smad phosphorylation and vessel wall inflammation or plaque vulnerability.

INTRODUCTION

Atherosclerotic disease is a metabolic disorder with a strong inflammatory component[1]. Early phases of the disease are characterized by progressive lipid accumulation in the intima, followed by formation of an atherosclerotic lesion that is identified by a necrotic core and an overlying collagenous cap. This cap shields the highly prothrombotic contents of the core from the blood stream. Increased inflammation, protease activity and impaired matrix turn-over in the cap area results in destabilization of the cap[2,3], which may ultimately result in exposure of the necrotic core followed by acute thrombosis and (partial) occlusion of the vessel[4].

The Transforming Growth Factor-Beta (TGF-β) super family of ligands (TGF-β, Activin and Bone Morphogenetic Proteins (BMP)) is a group of widely expressed growth factors/cytokines that have broad activities on matrix homeostasis and inflammatory systems[2,3,5,6]. TGF-β family members exhibit comprehensive anti-inflammatory effects on a wide range of cells, including endothelial cells, macrophages and T-cells, as well as fibroblasts and smooth muscle cells[7,8].

Because of their comprehensive effects on inflammation and matrix homeostasis, members of the TGF-β superfamily have been proposed as critical regulators of the atherosclerotic process[9;10]. However, the exact relationship between TGF-β/BMP signaling and atherosclerosis is far from clear. Animal studies consistently show a negative association between TGF-β concentration and the extent of atherosclerosis. Human studies on the other hand indicate a positive correlation between circulating plasma TGF-β and atherosclerosis progression[2,8,11,12,13]. The basis for this apparent contrast is unclear. Possible explanations are that it reflects differences between the animal models of atherosclerosis and the actual disease and/or the fact that most human studies have been performed in patients with advanced atherosclerotic disease. A further caveat is that most human studies rely on circulating TGF-β levels, which may not necessarily reflect TGF-β local levels or activities[11]. Regulation of the TGF-β and BMP signalling pathways is complex, involving extensive regulation of bioavailability of ligands and receptors, as well as tightly controlled intracellular signalling pathways[7,12,14,15,16].

The canonical TGF-β family signalling is via type I and type II cell surface receptors that exhibit serine/threonine kinase activity. Upon induction of heteromeric complex by the ligand, the type I receptor is phosphorylated by type II receptor. This in turn results in phosphorylation of the C-terminus of receptor regulated Smads (R-Smads) that are responsible for the intracellular signaling. Whereas Smad2 is phosphorylated by TGF-β type I receptor, Smad1,-5 and -8 are phosphorylated by BMP type I receptors[14]. As a consequence the involvement of

TGF-β activity and BMP signaling pathways in human atherosclerosis is still unclear[6,12].

We performed a systematic histological evaluation of receptor phosphorylated Smad2 (pSMAD2) and -1,5,8 (pSmad1,5,8) as read out for the canonical TGF-β and BMP signaling pathways throughout the complete spectrum of human atherosclerotic disease. As well as phosphorylated Smad expression we evaluated the expression of Human Plasminogen Activator Inhibitor type-1 (PAI-1)[17,18]. Expression of PAI-1 is under strict control of Smads (Smad3) and considered one of the classical targets of the TGF-β receptor pathway[19,20].

The results of this study demonstrate that activation of the TGF-β and BMP pathways occurs in the earliest phases of human atherosclerotic disease. This activation level remains stable during further progression of the disease. No significant relationships were found between Smad2 or Smad1,5,8 phosphorylation, and vessel wall inflammation or plaque vulnerability.

MATERIAL AND METHODS

Patients and tissue sampling

All sections in the study were selected from a tissue bank of aortic wall patches that were obtained during kidney transplantation with donor kidneys from cadaveric donors. Details of this bank have been described previously by van Dijk *et al*[21]. All patches were derived from grafts that were eligible for transplantation (*i.e.* all donors met the criteria set by The Eurotransplant Foundation). Due to national regulations, only transplantation relevant data from donation is available. Sample collection and handling was performed in accordance with the guidelines of the Medical and Ethical Committee in Leiden, Netherlands and the code of conduct of the Dutch Federation of Biomedical Scientific Societies (http://www.federa.org/?s=1&m=82&p=0&v=4#827).

All sections in the bank are Movat stained and classified by two independent observers with no knowledge of the characteristics of the aortic patch[4,21].

Characterization of the lesions and histological definitions

Allocation to the different groups was based on the most advanced lesion in the section. Classification was done according to the modified AHA classification as proposed by Virmani *et al*[4]: *viz.* adaptive intimal thickening (AIT), intimal xanthoma (IX) (*i.e.* non-progressive lesions); pathological intimal thickening (PIT), early fibroatheroma (EFA), late fibroatheroma (LFA) (*i.e.* progressive atherosclerotic lesions); thin cap fibroatheroma (TCFA), acute plaque rupture (PR)

(*i.e.* vulnerable plaques); healed plaque rupture (PR) and fibrotic calcified plaque (FCP) (*i.e.* stable atherosclerotic lesions).

Normal lesions were defined as aortic wall samples consisting merely of subendothelial proteoglycan rich layers that were devoid of infiltrating smooth muscle cells and/or macrophages[22]. In order to obtain balanced and representative study groups we randomly selected 10-12 samples from each stage. A total of 114 cases were selected.

Immunohistochemistry

Immunohistochemical single stains were performed on 4 μm thick sections prepared from formalin fixed, paraffin embedded tissue, as described previously[21]. The following antibodies were used as read-out for TGF-β and BMP signaling: rabbit polyclonal phosphorylated Smad2 (cat#3108, 1:100, Cellsignaling; Leiden, the Netherlands), rabbit polyclonal phosphorylated Smad1,5,8 (AB-246-NA, 1:50, R&D Systems, Abingdon), and PAI-1 staining was performed with an in-house rabbit polyclonal antibody that recognizes both the free and complexed form[18]. Conjugated biotinylated anti-rabbit anti-IgG (1:1000, Amersham Biosciences, Buckinghamshire, UK) was used as secondary antibody. Sections were counterstained with Mayer's Haematoxylin.

Quantification of inflammation was performed by staining for macrophages with mouse monoclonal CD68 (KP-1, isotype IgG1-kappa, Dako, Denmark: diluted at 1:400 overnight) and T- lymphocytes with rabbit polyclonal CD3 (AB828, Abcam, Cambridge, UK; diluted at 1:200 overnight).

Assessment of immunolocalization of the intermediate TGF-β pathway, macrophage and T-cell markers

The lesion was defined as the area between the endothelium and internal elastic lamina over a distance of 1mm. In the presence of a necrotic core the distance was expanded another 500μm on both sides of the necrotic core to include the adjacent shoulder region. The regions of interest (ROI) are the intima (in the presence of a (early) necrotic core the intima was divided into a cap and both shoulder regions), media and adventitia. Particular interest was taken in the various cell types present in the atherosclerotic lesion (*i.e.* monocytes/macrophages, lymphocytes and smooth muscle cells).

The degree of pSmad2, pSmad1,5,8, PAI-1, CD3 and CD68 intensity was assessed semi-qualitatively on a scale of 0 – 4 by two observers: 0 (absent/no positive staining in ROI); 1 (<10% of cells in ROI stained positively) ; 2 (10-50% of cells in ROI stained positively); 3 (50 > 75% of cells in ROI stained positively) and 4 (>75% of cells in ROI stained positively).

Statistical analysis

Data in figures are presented as mean ± SEM. Mean variables between the various lesions were compared with the one-way analysis of variance (ANOVA; SPSS 17.0; Chicago, IL), followed by post-hoc Fisher's LSD test. A value of $p < 0.05$ was considered statistically significant.

RESULTS

Studied population

Data were obtained from 114 consecutive peri-renal aortic samples from organ donors aged from 5 to 76 years (Table 1). The male/female ratio was evenly distributed between the clusters (Table 2). There was a strong relationship between donor age and the stage of atherosclerosis[21]. Normal aortic wall samples had a mean age of ~18-years, whereas the mean age for aortas with fibrotic calcified plaques was ~58-years.

Table 1. Demographic data of the 114 studied patients.

	Male		**Female**	
N	64		50	
Mean age (years) [SD]	49.4	[44-58]	43,8	[38-47]
Mean length (cm) [SD]	179.9	[175.0-185.8]	166.6	[160.0-175.0]
Mean weight (kg) [SD]	80.1	[75.3-85.0]	64.9	[57.0-75.0]
Mean BMI (kg/m2) [SD]	24.8	[23.0-26.0]	22.9	[21.0-26.0]
Patients with known history of nicotine abuse	21		17	
Patients with known history of hypertension	13		10	
Patients with known diabetes	0		1	
Cause of Death				
Severe head trauma	11		7	
Cerebral vascular accident (CVA)	8		10	
Subarachnoid bleeding (SAB)	15		14	
Cardiac arrest	7		0	
Trauma	1		1	
Other	6		3	
Unknown	12		19	
Medication				
Anti-hypertensives	11		6	
Statins	1		1	
Anti-coagulants	1		2	

TGF-β signaling: Smad2 phosphorylation

About 10% of the smooth muscle cells (SMCs) and endothelial cells in normal aortas stain positive for phosphorylated Smad2 (Figure 1a and 2a). There is an immediate increase in pSMAD2 positivity (> 50% positivity ($p < 0.029$) Figure 2a) in the earliest phases of atherosclerotic disease (non-progressive lesions). No further increase in pSMAD2 positivity is observed in the more advanced stages of the disease (*i.e.* progressive atherosclerotic lesions, vulnerable and stabilized lesions).

Smad2 activation is similar in the different layers of the vessel wall (intima, media or adventitia). We did not observe a shift in pSmad2 positivity over the individual cell types (monocytes/lymphocytes and SMCs) throughout all stages of atherosclerosis (data not shown). No relationship was found between pSmad2 positivity and cap thickness.

Table 2. Histological classifications of the aortic tissue.

Atherosclerotic cluster	Virmani classification	Male		Female	
		N	Mean age in years [range]	N	Mean age in years [range]
Normal aorta	Normal aorta	4	23.8 [11-40]	3	10.0 [6-13]
Nonprogressive lesions	Adaptive intimal thickening	9	40.5 [31-46]	12	30.4 [21-40]
	Intimal xanthoma	10	37.3 [33-48]	8	34.2 [19-45]
Progressive atherosclerotic lesions	Pathological intimal thickening	5	46.0 [38-55]	7	55.4 [44-67]
	Early fibroatheroma	7	50.9 [44-55]	6	46.0 [42-48]
	Late fibroatheroma	6	55.0 [51-58]	10	51.1 [43-57]
Vulnerable lesions	Thin cap fibroatheroma	6	56.5 [54-59]	3	60.3 [57-67]
	Plaque rupture	7	56.9 [56-59]	2	45.0 [30-54]
Stabilized lesions	Healing rupture	4	58.1 [57-67]	1	57.0 [57-57]
	Fibrotic calcified plaque	2	62.7 [56-67]	2	53.0 [45-63]

Phosphorylated Smad2 and vascular inflammation

The mean expression of lesional monocytes/macrophages and T cells (CD3) increased with advancing atherosclerosis in all layers of the aortic wall (figure 3). No relation was found between Smad2 phosphorylation and the amount of CD3 positive cells (Figure 4a). Healing of a ruptured lesion (*i.e.* healed ruptures and fibrotic calcified plaques) was associated with a significant reduction in CD3 positive cells ($p < 0.0001$).

Most Smad2 phosphorylation was seen in the lesions containing minimal CD68 expressing cells ($p < 0.038$; figure 5a). The degree of Smad2 phosphorylation did not significantly change when the amount of CD68 expressing cells in the lesions increased.

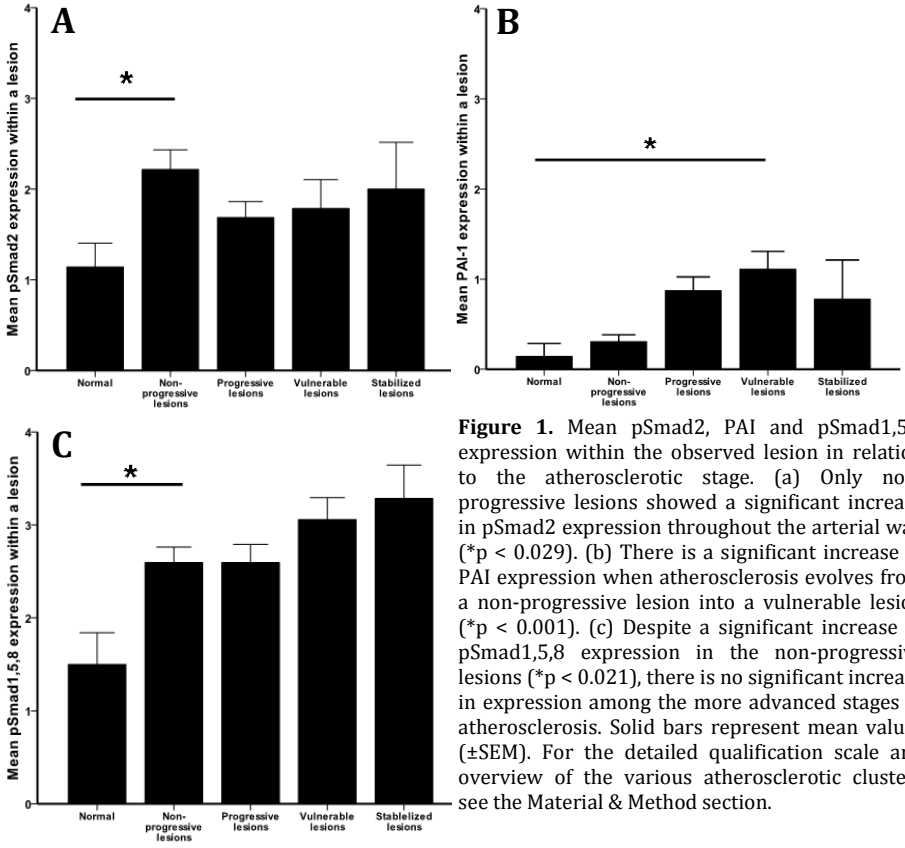

Figure 1. Mean pSmad2, PAI and pSmad1,5,8 expression within the observed lesion in relation to the atherosclerotic stage. (a) Only non-progressive lesions showed a significant increase in pSmad2 expression throughout the arterial wall (*$p < 0.029$). (b) There is a significant increase in PAI expression when atherosclerosis evolves from a non-progressive lesion into a vulnerable lesion (*$p < 0.001$). (c) Despite a significant increase in pSmad1,5,8 expression in the non-progressive lesions (*$p < 0.021$), there is no significant increase in expression among the more advanced stages of atherosclerosis. Solid bars represent mean values (±SEM). For the detailed qualification scale and overview of the various atherosclerotic clusters see the Material & Method section.

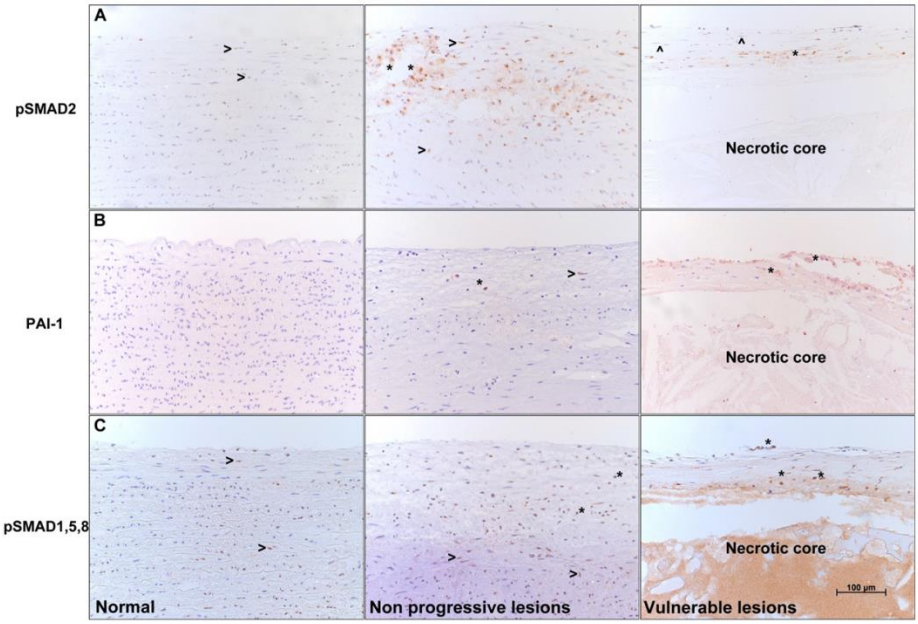

Figure 2. Expression of pSmad2, PAI-1 and pSmad1,5,8 in the human aorta. (a) Within the normal aortic wall only few SMCs stain positively for pSmad2. Macrophages and SMCs expressing pSmad2 are abundantly present within the intima and media of non-progressive lesions. The SMCs resident in the thinning cap of the vulnerable lesions remain devoid of Smad2 activation. (b) Minimal PAI-1 expression was found in the intimal layer of normal aortic tissue. In the vulnerable lesions the thin fibrous cap lacks PAI-1 positive SMCs, whereas almost all macrophages stained positive for PAI-1. (c) Early non-progressive lesions are characterized by a significant increase in Smad1,5,8 positivity. The vulnerable thin cap mainly consists of pSmad1,5,8 expressing monocytes and/or macrophages. All images were taken at 20x magnification and correspond with the indicated 100µm scalebar. (>: Intimal or medial positively stained SMCs; *: Positively stained monocytes or macrophages; ^: Intimal SMCs devoid of Smad2 activation).

PAI-1 expression

Minimal PAI-1 expression was observed in the intimal layer of normal aortic tissue (figure 1b and 2b). PAI-1 positivity was found in 10% of the SMCs (predominantly in the infiltrating SMCs) in pathological intimal thickening (*i.e.* progressive lesions). A further increase in PAI-1 expressing SMCs was found with advancing atherosclerosis (non-progressive vs. vulnerable lesions $p<0.001$; figure 1b and 2b). In the vulnerable lesions the thin fibrous cap was devoid of PAI-1 positive SMCs, whereas almost all macrophages stained positive for PAI-1.

No association was found between PAI-1 positivity and Smad2 phosphorylation ($p=0.407$). Similarly, no relationship was observed between PAI-1 positivity and the amount of inflammatory cells (CD3 or CD68 expressing monocytes ($p<0.804$ and $p<0.557$ resp., figure 4b and 5b)).

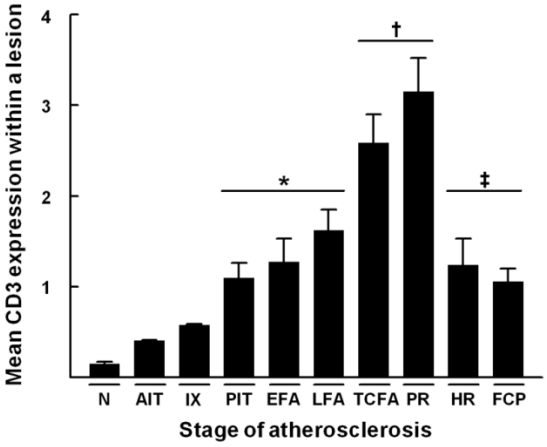

Figure 3. Mean number of CD3 positive cells per lesion plotted against the stage of atherosclerosis. There is no significant increase in CD3 positive cells until the stage of pathological intimal thickening (PIT). As the degree of atherosclerosis advances up to plaque rupture (PR), the amount of CD3 positive cells increases significantly (*/†$p < 0.000$). Within stabilized lesions (*i.e.* HR and FCP) the CD3 positive cells decrease significantly (‡$p < 0.000$). Solid bars represent mean values (±SEM). (Abbreviations; see material and methods section)

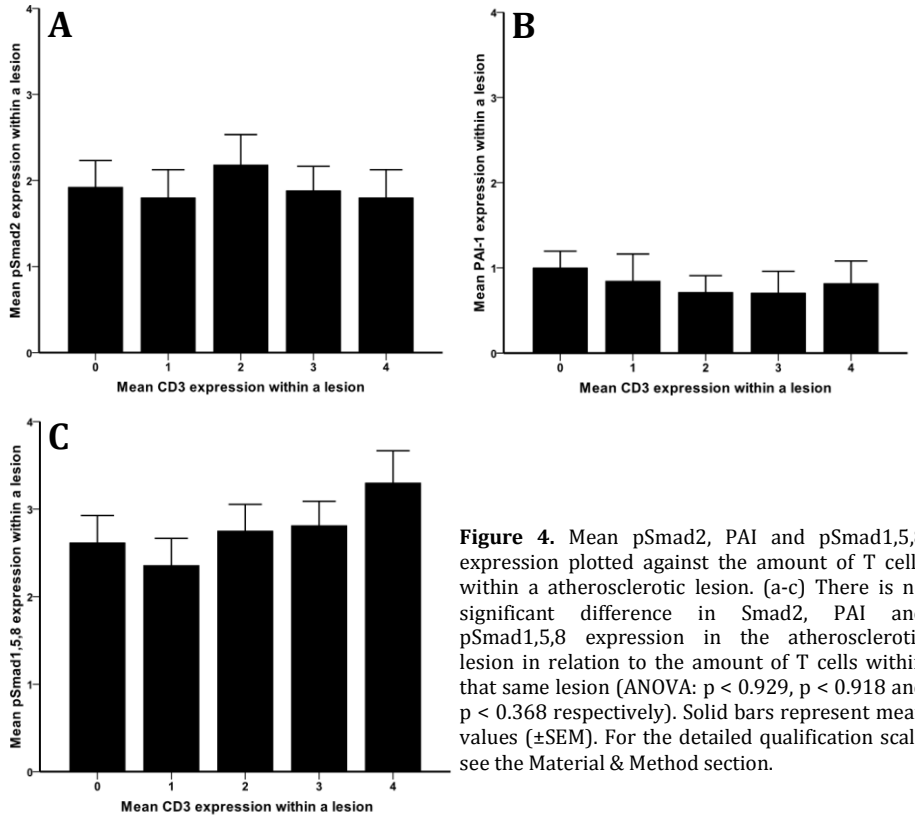

Figure 4. Mean pSmad2, PAI and pSmad1,5,8 expression plotted against the amount of T cells within a atherosclerotic lesion. (a-c) There is no significant difference in Smad2, PAI and pSmad1,5,8 expression in the atherosclerotic lesion in relation to the amount of T cells within that same lesion (ANOVA: $p < 0.929$, $p < 0.918$ and $p < 0.368$ respectively). Solid bars represent mean values (±SEM). For the detailed qualification scale see the Material & Method section.

BMP signaling: Smad1,5,8 phosphorylation

Approximately 10% of the endothelial and intimal SMCs within normal aortic tissue were positive for pSmad1,5,8. Early non-progressive lesions were characterized by a significant increase in pSmad1,5,8 positivity ($p < 0.02$; Figure 1c and 2c). No further increase was found in the progressive phases of the atherosclerotic process (*i.e.* progressive atherosclerotic lesions, vulnerable and stabilized lesions).

No relationship was found between Smad1,5,8 phosphorylation and plaque stability (*i.e.* cap thickness; data not shown).

pSmad1,5,8 and vascular inflammation

We did not observe a relation between Smad1,5,8 phosphorylation and the CD68 intensity or the amount of CD3 positive cells (Figure 4c and 5c).

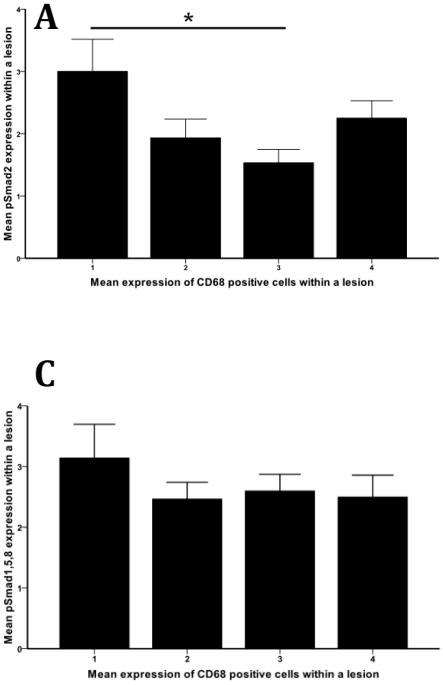

Figure 5. Mean pSmad2, PAI and pSmad1,5,8 expression plotted against the intensity of KP-1 positive staining within the same lesion. (a) Smad2 activation is maximum when the atherosclerotic lesion is absent in CD68 positive cells (~75%). When the intensity of CD68 positive staining increases (0 > 25-50%) a significant decrease is found in Smad2 expressing cells throughout the entire lesion (*$p < 0.038$). (b) PAI-1 expression remains minimal with increasing CD68. No significant relation was found between PAI-1 positivity and the increasing amount of CD68 expressing monocytes/macrophages. (c) Smad1,5,8 activation remains stable with increasing CD68 intensity. Solid bars represent mean values (±SEM). For the detailed qualification scale see the Material & Method section.

DISCUSSION

Despite a wealth of animal data, there is limited data available on a putative role of the TGF-β superfamily in human atherosclerosis[16]. In the present observational study we focussed on Smad phosphorylation at the C-terminus (the receptor phosphorylated site) to evaluate the activation of the canonical TGF-β and BMP signaling pathways during progression and (de)stabilization of human atherosclerotic disease[14]. We have established a unique database of vascular tissue containing aortic samples that originate from the peri-renal region, a recognized lesion prone location[21,22,23]. The results of this study show an immediate activation of TGF-β and BMP pathways upon initiation of the atherosclerotic process. No further activation was observed during further progression of the disease. No associations were found between Smad phosphorylation and indices of vascular inflammation or plaque stability.

A large number of animal studies imply members of TGF-β family as key regulators of the atherosclerotic process. It was demonstrated that interference with TGF-β signaling results in an increased tendency to form lipid lesions, as well as progression towards a more vulnerable plaque phenotype[8,9,12]. Based on these animal data it was postulated that the TGF-β superfamily members are critically involved in the atherosclerotic process. Data from human studies on the other hand are less consistent and are difficult to interpret, as they are based on studies on isolated endothelial cells[13], surgical material representing the final stages of atherosclerotic disease[24,25] or TGF-β plasma levels[11,26]. Studies on the other superfamily members (Activin and BMP) are currently missing[14,16]. Signaling of these factors occurs through both Smad-dependent (Smad2 for TGF-β and Activin; Smad1,5,8 for BMP) and Smad-independent pathways[14,27]. They play a key role in the regulation of cellular proliferation, differentiation, adhesion, apoptosis and production of extracellular matrix components. With respect to inflammation, these factors are generally considered anti-inflammatory[5,6,28].

Our results for Smad activation show that TGF-β family members affect all vascular associated cell types, in all three layers of the arterial wall throughout all stages of human atherosclerosis[29]. Within the normal aortic wall approximately 10-15% of the endothelial cells and intimal SMCs express pSmad2 and/or pSmad1,5,8. These findings correspond with previous *in vitro* studies implicating a baseline level of 'naturally' active shear stress induced TGF-β[5,11,24,25].

Our study shows an increase in expression of pSmad2 and pSmad1,5,8 in intimal SMCs and macrophages during the transition from normal aortic tissue to early atherosclerotic lesions. These lesions are characterized by adaptive intimal thickening due to infiltrating SMCs, increased extra cellular matrix production and macrophage foamcell formation in response to accumulation of LDL cholesterol[1,4].

The immediate increase in Smad phosphorylation in these early stages may reflect induction of TGF-β or Activin expression by oxidized LDL[30]. TGF-β and Activin are both involved in macrophage biology but their exact role remains unclear. They both enhance the differentiation of monocytic cells into macrophages. TGF-β stimulates leukocyte and SMC chemotaxis and as such it may contribute to early macrophage migration and lipid accumulation, whereas Activin-A has been reported to inhibit foamcell formation[5,16,31].

A remarkable observation in our study was the dominance of pSmad2 positive macrophages over pSmad2 negative macrophages. The Smad2 positive macrophages are often referred to as M2-subtype macrophages, suggesting dominance of the anti-inflammatory class of macrophages in atherosclerotic disease[32,22]. This notion is supported by dominance of CD163 positive macrophages in human atherosclerosis (unpublished data by van Dijk *et al*.). Although the M2-type of macrophage is generally considered tissue protective, our findings may indicate that, in the context of atherosclerosis, M2-type macrophages can promote lesion formation.

The TGF-β super family of ligands has also broad activities on endothelial cells and matrix homeostasis[2,3,6]. Inhibition of TGF-β signaling in atherosclerosis-prone mice significantly accelerates lesion development. This suggests an important protective role of endogenous TGF-β activity against the development of atherosclerosis[9]. Our findings however show that progression of atherosclerotic lesions into more complicated plaques (*viz.* progressive atherosclerotic lesions, vulnerable lesions and stabilized lesions) is not paralleled by changes in Smad phosphorylation. These findings are not necessarily in conflict with the animal derived data and may suggest that TGF-β is involved in the (prevention of) initiation of atherosclerosis.

Destabilization of the fibrous cap is a key event in the development of vulnerable atherosclerotic lesions[4]. Thinning of the fibrous cap is associated with a decreasing SMC/macrophages ratio[21]. We did not observe a change in the overall expression in pSmad 2 and pSmad 1,5,8 phosphorylation during the transition from stable to vulnerable lesions. As such our findings do not support animal observations suggesting that impaired TGF-β signaling underlies formation of an unstable plaque phenotype[8,9,10]. However, it should be noted that TGF-β is a potent stimulus of connective tissue accumulation, and is implicated in the pathogenesis of fibrotic disorders with Smad3 as a key intracellular signal transducer[34]. Human Plasminogen Activator Inhibitor -1 (PAI-1) is a gene that is potently induced by TGF-β and specifically binds the TGF-β/activin pathway-restricted Smad3 protein[17]. Our results show a significant increase in PAI-1 expression with progression towards vulnerable lesions, indicating that TGF-β is involved in the more advanced stages of the atherosclerotic disease. Without a valid pSmad3

antibody available for paraffin embedded tissue we cannot firmly conclude whether or not TGF-β is highly relevant as regards to cap thickness.

Mallat *et al* highlight the specific involvement of TGF-β in the regulation of T-cell biology and postulated disruption of TGF-β signaling as an explanation for the increased number of T-cells in atherosclerosis[19,35]. Our results show a remarkable increase in T-cell content during the evolution of the atherosclerotic lesion towards a vulnerable plaque. Such a mechanism is not supported by observations from this study, in which no association between TGF-β and BMP signaling and T-cell content was observed.

Although our findings are highly consistent and show a distinctive pattern throughout the entire atherosclerotic spectrum, a potential limitation of the present study arises from the fact that we were restricted to paraffin embedded aortic tissue. Moreover, although the immunohistochemical staining procedures used for the detection of phosphorylated Smads allow for a spatial evaluation, they are semi-quantitative and do not allow direct conclusions with respect to the TGF-β or Activin signaling[14]. As such, it should be noted that we cannot exclude that the Activin or TGF-β pathway are activated simultaneously during the atherosclerotic process.

CONCLUSION

All in all, our findings in this unique database covering the entire spectrum of human atherosclerotic disease do not specifically characterize TGF-β and BMP signaling as key regulators in the progression and complications of atherosclerosis. Our material does not rule out a role for TGF-β and BMP in the initiation of the earliest atherosclerotic lesions. As this paper focuses on Smad phosphorylation as read-out for TGF-β and BMP signaling, it cannot be excluded that the signaling through different pathways also mediate the activity of TGF-β and BMP in atherosclerotic disease. No relationship was found between Smad2, or Smad1,5,8 phosphorylation and plaque growth, cap destabilization or plaque stabilization.

REFERENCES

1 Hansson G.K. (2001). Immune mechanisms in atherosclerosis. A.T.V.B. 21, 1876-1890.

2 Redondo S., Santos-Gallego C.G. and Tejerina T. (2006). TGF-β1: a novel target for cardiovascular pharmacology. Cytokine & Growth Factor Reviews. 18, 279-286.

3. Mehta J.L. and Attramadal H. (2007). The TGF superfamily in cardiovascular biology. Cardiovascular Research. 74, 181-183.

4. Virmani R., Kolodgie F.D., Burke A.P., Farb A. and Schwartz SM. (2000). Lessons from sudden coronary death: a comprehensive morphological classification scheme for atherosclerotic lesions. A.T.V.B. 20, 1262-1275.

5. Engelse M.A., Neele J.M., van Achterberg T.A.E., van Aken B.E., van Schaik R.H.N., Pannekoek H. and de Vries C.J. (1999). Human activin-A is expressed in the atherosclerotic lesion and promotes the contractile phenotype of smooth muscle cells. Circulation Research. 85, 931-939

6. Singh N.N. and Ramji D.P. (2006). The role of transforming growth factor-β in atherosclerosis. Cytokine & Growth Factor Reviews. 17, 487-499.

7. Grainger D.J. (2004). Transforming growth factor β and atherosclerosis: so far, so good for the protective cytokine hypothesis. A.T.V.B. 24, 399-404.

8. Frutkin A.D., Otsuka G., Stempien-Otero A., Sesti C., Du L., Jaffe M., Dichek H.L., Pennington C.J., Edwards D.R., Nieves-Cintrón M., Minter D., Preusch M., Hu J.H., Marie J.C. and Dichek D.A. (2009). TGF-β 1 Limits Plaque Growth, Stabilizes Plaque Structure, and Prevents Aortic Dilation in Apolipoprotein E-Null Mice. A.T.V.B. 29, 1251-1257.

9. Mallat Z., Gojova A., Marchiol-Fournigault C., Esposito B., Kamate C., Merval R., Fradelizi D. and Tedgui A. (2001). Inhibition of transforming growth factor-β signaling accelerates atherosclerosis and induces an unstable plaque phenotype in mice. Circulation Research. 89, 930-934.

10. Lutgens E., Gijbels M., Smook M., Heeringa P., Gotwals P., Koteliansky V.E. and Daemen E.J. (2002). Transforming growth factor-β mediates balance between inflammation and fibrosis during plaque progression. A.T.V.B. 22, 975-982.

11. Wang X.L., Liu S.X. and Wilcken D.E.L. (1997). Circulating transforming growth factor 1 and coronary artery disease. Cardiovascular Research. 34, 404-410.

12. Grainger D.J. (2007). TGF-β and atherosclerosis in man. Cardiovascular Research. 74, 213-222.

13. Volger O.L., Fledderus J.O., Kisters N., Fontijn R.D., Moerland P.D., Kuiper J., van Berkel T.J., Bijnens A.P., Daemen M.J., Pannekoek H. and Horrevoets A.J. (2007). Distinctive Expression of Chemokines and Transforming Growth Factor-{ β} Signaling in Human Arterial Endothelium during Atherosclerosis. American Journal of Pathology. 171, 326-337.

14. Heldin C.H., Miyazono K. and ten Dijke P. (1997). TGF-β signalling from cell membrane to nucleus through SMAD proteins. Nature. 390, 465-471.

15 Kalinina N., Agrotis A., Antropova Y., Ilyinskaya O., Smirnov V., Tararak E. and Bobik A. Signaling in Smooth Muscle Cells of Fibrofatty Lesions. A.T.V.B. 24, 1391-1396.

16. Bobik A. (2006). Transforming growth factor- βs and vascular disorders. A.T.V.B. 26, 1712-1720

17. Dennler S., Itoh S., Vivien D., ten Dijke P., Huet S. and Gauthier J.M. (1998). Direct binding of Smad3 and Smad4 to critical TGF beta-inducible elements in the promoter of human plasminogen activator inhibitor-type 1 gene. The EMBO Journal. 17, 3091-3100.

18. Lindeman J.H.N., Pijl H., Toet K., Eilers P.H.C., van Ramshorst B. and Buijs M.M. (2007). Human visceral adipose tissue and the plasminogen activator inhibitor type 1. International Journal of Obesity. 31, 1671-1679.

19. Mallat Z. and Tedgui A. (2002). The role of transforming growth factor β in atherosclerosis: novel insights and future perspectives. Current Opinion in Lipidology. 13, 523-529.

20. Vaughan D.E. (2006). PAI-1 and TGF-β: Unmasking the Real Driver of TGF-β Induced Vascular Pathology. Arteriosclerosis, Thrombosis, and Vascular Biology. 26, 679-680.

21. van Dijk R.A., Virmani R., von der Thüsen J.H., Schaapherder A.F. and Lindeman J.H.N. (2010). The natural history of aortic atherosclerosis: a systematic histopathological evaluation of the peri-renal region. Atherosclerosis. 210,100-106.

22. Stary H.C., Blankenhorn D.H., Chandler A.B., Glagov S., Insull Jr W., Richardson M., Rosenfelt M.E., Schaffer S.A., Schwartz C.J., Wagner W.D. and Wissler R.W. (1992). A definition of the intima of human arteries and of its atherosclerosis-prone regions. A report from the Committee on Vascular Lesions of the Council on Arteriosclerosis, American Heart Association. A.T.V.B. 12, 120-134.

23. Negishi M., Lu D., Zhang Y.Q., Sawada Y., Sasaki T., Kayo T., Ando J., Izumi T., Kurabayashi M., Kojima I., Masuda H. and Takeuchi T. (2001). Upregulatory Expression of Furin and Transforming Growth Factor-β by Fluid Shear Stress in Vascular Endothelial Cells. A.T.V.B. 21, 785-790.

24. Grainger D.J., Kemp P.R., Metcalfe J.C., Liu A.C., Lawn R.M., Williams N.R., Grace A.A., Schofield P.M. and Chauhan A. (1995). The serum concentration of active transforming growth factor- is severely depressed in advanced atherosclerosis. Nature Medicine. 1, 74-79.

25. Grainger D.J., Wakefield L., Bethell H.W., Farndale R.W. and Metcalfe J.C. (1995). Release and activation of platelet latent TGF-β in blood clots during dissolution with plasmin. Nature Medicine. 1, 932-937.

26. Bot PTG, Hoefer *I.E.*, Sluijter J.P.G., van Vliet P., Smits A.M., Lebrin F., Moll F., de Vries J.P., Doevendans P., Piek J.J., Pasterkamp G. and Goumans M.J. (2009). Increased Expression of the Transforming Growth Factor-β Signaling Pathway, Endoglin, and Early Growth Response-1 in Stable Plaques. Stroke. 40, 439-447.

27. Persson U., Izumi H., Souchelnytskyi S., Itoh S., Grimsby S., Engström U., Heldin C.H., Funa K. and ten Dijke P. (1998). The L45 loop in type I receptors for TGF-beta family members is a critical determinant in specifying Smad isoform activation. FEBS Letters. 434, 83-87.

28. Smith C., Yndestad A., Halvorsen B., Ueland T., Waehre T., Otterdal K., Scholz H., Endresen K., Gullestad L., Frøland S.S., Damås J.K. and Aukrust P. (2004). Potential anti-inflammatory role of activin A in acute coronary syndromes. J.A.C.C. 44, 369-375.

29. de Sousa Lopes S.M., Carvalho R.L., van den Driesche S., Goumans M.J., ten Dijke P. and Mummery C.L. (2003). Distribution of phosphorylated Smad2 identifies target tissues of TGF beta ligands in mouse development. Gene Expressions Patterns. 3, 355-360.

30. Leonarduzzi G., Sevanian A., Sottero B., Arkan M.C., Biasi F., Chiarpotto E., Basaga H. and Poli G. (2001). Up-regulation of the fibrogenic cytokine TGF-β 1 by oxysterols: a mechanistic link between cholesterol and atherosclerosis. The FASEB Journal.15, 1619-1621.

31. Yamada R., Suzuki T., Hashimoto M., Eto Y., Shiokawa K. and Muramatsu M. (1992). Induction of differentiation of the human promyelocytic cell line HL-60 by activin/EDF. Biochemical and Biophysical Research Communications. 187, 79-85.

32. Shimada K. (2009). Immune System and Atherosclerotic Disease: heterogeneity of leukocyte subsets participating in the pathogenesis of atherosclerosis. Circulation Journal. 73, 994-1001.

33. Spencer M., Yao-Borengasser A., Unal R., Rasouli N., Gurley C.M., Zhu B., Peterson C.A. and Kern P.A. (2010). Adipose tissue macrophages in insulin resistant subjects are associated with collagen VI, fibrosis and demonstrate alternative activation. American Journal of Physiology- Endocrinology And Metabolism. 299, 1016-1027

34. Lakos G., Takagawa S., Chen S.J., Ferreira A.M., Han G., Masuda K., Wang X.J., DiPietro L.A and, Varga J. (2004). Targeted disruption of TGF-beta/Smad3 signaling modulates skin fibrosis in a mouse model of scleroderma. American Journal of Pathology. 165, 203-217.

35. Gojova A., Brun V., Esposito B., Cottrez F., Gourdy P., Ardouin P., Tedgui A., Mallat Z. and Groux H. (2003). Specific abrogation of transforming growth factor-β signaling in T cells alters atherosclerotic lesion size and composition in mice. Blood. 102, 4052-4058.

CHAPTER 10

SUMMARY AND FUTURE PERSPECTIVES.

Summary

Atherosclerosis is the leading cause of death worldwide[1]. A wealth of preclinical research performed over the past decades has led to many compelling hypotheses about the biological, pathophysiological and immunological bases of atherosclerotic lesion formation, and its complications such as myocardial infarction and stroke[2]. Despite this progress, the leap from experimental animal findings to human atherosclerosis and clinical application presents many challenges[3,4]. Essential gaps remain in translating experimental findings on how processes such as lipoprotein oxidation, inflammation and immunity contribute to human atherosclerotic disease and its complications. Bridging these gaps is required to achieve the full promise of scientific advances in atherosclerosis[2].

In an attempt to bridge the existing gaps we systematically evaluated the course of the human atherosclerotic process using a unique biobank containing over 500 individual peri-renal abdominal aortic wall patches, that were obtained during liver, kidney or pancreas transplantation, and over 600 coronary artery segments of the left coronary artery that were collected from healthy human hearts retrieved from Dutch post-mortem donors within 24 hours after circulatory stop and brought to the National Heart Valve for heart valve donation. These biobanks allowed us to use tissue from a group of apparently healthy individuals with an equal age and sex distribution, thereby avoiding potential bias introduced by the use of autopsy material from coronary death victims (mostly either young or old patients) or by the use of material from patients undergoing vascular surgery (generally end-stage atherosclerotic disease). Altogether the studies in this thesis systematically describe the critical morphological, pathophysiological and immunological characteristics of the human atherosclerotic process from initial non-progressive lesions to advanced unstable culprit lesions that underlie the clinical manifestations of human atherosclerosis.

Morphological aspects of the atherosclerotic process

Qualitative characterization of the atherosclerotic process fully relies on morphological classification based on histological plaque characteristics. Based on their observations from coronary death victims, Virmani *et al*. refined the AHA consensus classification in order to better reflect the heterogeneity of the advanced stages of atherosclerotic disease[5,6]. It is unclear whether and how this human classification system based on the coronary artery can be applied to other vascular beds. In **Chapter 2** we describe and validate the coronary artery-based Virmani classification for the human peri-renal aorta. Aortic atherosclerotic lesions follow a similar pattern of progression as seen in coronary tissue, but grow far

beyond the size of coronary atherosclerotic lesions. Macrophages and foam cells play a large, contributing role in the evolution of the necrotic core, plaque progression and destabilization in aortic atherosclerosis. It is generally assumed that macrophages, through release of matrix metalloproteinases directly contribute to destabilization. The association between thinning of the fibrous cap and macrophage infiltration, and a significant decrease in macrophage content in healing ruptures underpins this assumption.

Carotid intimal media thickness (IMT) and coronary calcium scores emerged as epidemiological measures of atherosclerotic burden[7]. Yet, these measures are also progressively advocated as individual risk prediction tools, and changes in carotid IMT are now used as surrogate endpoints in clinical trials aimed at stabilizing or reversing the atherosclerotic disease[8]. **Chapter 3** tests the validity of IMT as a surrogate of the degree of atherosclerosis.

Results confirm an association between tissue IMT and plaque progression, but also show plateauing and even reductions in tissue IMT readings in the vulnerable and particularly stabilized lesions. Findings also show a large variability in tissue IMT, thereby resulting in wide confidence intervals around the trend.

As for calcium scores, calcium deposits reflect the later stages of the disease, and are particularly prominent in the so called stabilized lesions. Calcium scores should be considered a retrospective marker, identifying patients with manifest atherosclerotic disease, whereas a negative calcium score does not rule out presence of atherosclerotic disease.

Remarkably, while the majority of data on disease initiation and progression is based on information from mouse models of atherosclerosis, an unequivocal descriptive classification for murine atherosclerosis is however missing. In **Chapter 4** we show that the established "Virmani Classification" for coronary atherosclerosis can be universally applied for aortic and murine atherosclerosis, allowing a one to one comparison of murine and human atherosclerosis and a means of positioning preclinical findings in the human context.

The early stages of atherosclerosis in mice are comparable to the early stages of atherosclerosis as seen in their human counterpart. Based on the histological characteristics, it is concluded that the lesions in mice do not progress beyond an early fibroatheroma, and consequently that aspects of advanced and vulnerable lesion formation, and successive healing are missing in these models.

In direct comparison with their human counterparts we clearly see that the advanced lesions in mice are significantly smaller in size and lack an adventitial vaso vasorum. Due to the relatively small lesions in mice, an ischemic trigger is missing since the entire atherosclerotic process can still be sustained through

diffusion. Consequently, critical aspects such as ischemia and neovascularization are missing.

Molecular and cellular aspects of human atherosclerosis

A primordial event in atherogenesis is LDL accumulation in intimal layer of the vessel wall[9]. Extensive experimental data defines the role for oxidized LDL cholesterol in both progression and regression of atherosclerosis. **Chapter 5** systematically describes the relationship between the various oxidation-specific LDL epitopes (OSE), such as malondialdehyde-lysine (MDA2), E06, and IK17, and lipoprotein (a) (Lp(a)) in early and clinically relevant advanced human atherosclerotic plaques.

As lesions progress they become progressively enriched in apo(a), oxidized phospholipid (OxPL), and MDA related epitopes (IK17). Specifically the apo(a) epitopes were present in most of the early and advanced lesions, whereas OxPL, and IK17 epitopes were highly prevalent in foamy macrophages in thin fibrous caps, necrotic cores, and ruptured plaques suggesting that they are more closely associate with advancing and unstable plaques. The observed differences in immunoreactivity patterns presented among the different antibodies provide a framework for understanding the relationship between OSE and lipoproteins and the progression and destabilization of human atherosclerotic lesions. Specific epitopes are generated and/or enriched during different pathophysiological stages of lesion development, progression, and destabilization.

A crucial role for the cellular components of the innate immune system (in particular macrophages) is well accepted[10,11]. It is now recognized that macrophages constitute a highly heterogeneous and dynamic cell population. Experimental studies mainly involving mice imply a major shift in macrophage identity during the atherosclerotic process with pro-inflammatory processes (classically activated M1 macrophages) dominating the initiation and progression phases of the disease, and alternatively activated M2 macrophages being the dominate phenotype in plaque resolution and repair[12].

Cellular components of the innate immune system are discussed in **Chapter 6** and were systematically evaluated throughout the process of human atherosclerosis, particularly in relation to complicated plaques, relevant to symptomatic disease.

A notable finding was that transition to pathological intimal thickening, the earliest form of progressive and irreversible atherosclerosis, is characterized by the accumulation of apolipoprotein B100 within the medial wall. This transition is

associated with a loss of internal elastic lamina integrity hallmarks the beginning of medial and adventitial involvement in atherosclerosis, a phenomenon that warrants further investigation.

Macrophages play a critical role in innate and acquired immunity. They are involved in all phases of atherosclerotic lesion development particularly in regards to lipid core formation, lesion remodeling, and degradation of the fibrous cap through release of matrix metalloproteinases, as seen in advanced symptomatic disease. Contrary to murine atherosclerosis, we found no evidence of a macrophage subclass shift during initiation, progression, rupture and ultimate stabilization of human atherosclerotic lesions. More interestingly, we identified a dominant class of macrophages that are double positive for both M1 and M2 markers challenging the paradigm of a clear M1-M2 dichotomy. Macrophage heterogeneity is far more complex than the current paradigm predicated on murine data and supports the involvement of additional (poorly-defined) macrophage subtypes or perhaps a greater dynamic range of macrophage plasticity.

Results show a strong positive relationship between progressive disease and fascin positive dendritic cells in all vascular layers. However, different roles have been identified for dendritic cells in atherogenesis and/or plaque progression in mouse models while a clear attribution to dendritic cells and the exact molecular mechanisms engaged remain unresolved.

Findings in human atherosclerotic lesions challenge claims based on murine models of the disease. Contrary to mice, mast cells are not associated with progression of human atherosclerotic lesions. Natural killer cells, abundantly present

in mice, are minimally present in human lesions. Murine studies imply a role for neutrophils in the initiation of the atherosclerotic process and plaque angiogenesis in later stages of the disease; our observational data in humans does not support a primary role of neutrophils. Neutrophil presence appears principally related to surgical manipulation of the aorta during removal.

Clearly, this divergence in observational data between murine models of atherosclerosis from our human atherosclerosis studies points to a limited translational aspect of animal findings.

The cellular components of the adaptive immune response are discussed in **Chapter 7** and were systematically evaluated throughout the process of atherosclerotic lesion formation, progression, destabilization and stabilization. Findings point to profound changes in the nature of the response in the lead up to plaque destabilization and show extinguishing of inflammatory processes upon plaque stabilization.

Fundamental differences exist between the human atherosclerotic disease and mouse models of the disease; particularly with respect to a very limited presence of regulatory T cells, absence of Th17 cells throughout the atherosclerotic process, and lack of B-cells in the early-, intermediate-, and final stages of the process. The earlier phases are dominated by diffuse cytotoxic T cell infiltration but progressive quantities of T helper cells are found during progression of the disease. Unlike findings in mice, we did not confirm Th1 dominance in human atherosclerotic process.

A remarkable and novel observation is the change in the inflammatory footprint that accompanies plaque destabilization and that fully resolves during plaque stabilization. On the cellular level this change is characterized by a sharp increase in the number of T-helper cells, emergence of naïve T-cells, and the appearance of B-cells and occasional plasma cells in tertiary follicle-like structures. CXCL-13 expression (a pivotal homeostatic signal for follicle formation) was exclusively observed in association with the follicle-like structures in the vulnerable lesions. Note; CXCL-13 was not detected in the other stages of the disease.

Our findings of a very restricted presence of B-cells in human atherosclerosis and gross absence of signs of B cell maturation in the infiltrating B cells exclude an autocrine or paracrine role of B-cells in the human atherosclerotic process. All in all, this study shows clear changes in the cellular components of adaptive immune system in anticipation of and during plaque destabilization. It is tempting to speculate that delineation of this chain of events may provide clues for early culprit lesion detection and plaque stabilization.

On the basis of animal studies, the AP-1 pro-inflammatory pathway has been implicated in the initiation and progression of atherosclerotic disease[13,14]. As such AP-1 signaling has been brought forward as a critical correlate in the initiation and progression of vascular dysfunction and atherogenesis, and AP-1 inhibition has been proposed as an attractive target to prevent progression of atherosclerosis. In **Chapter 8** we demonstrate that in the early and later stages of human atherosclerosis, active AP-1 is indeed present in the aortic wall. In order to test for a possible role of AP-1 activation in the perpetuation of advanced atherosclerosis we quenched AP-1 activation by administering doxycycline to patients with peripheral vascular disease in a double-blind cross-over study. The absence of an effect of doxycycline administration on all activation markers investigated led to the conclusion that although AP-1 (and thus AP-1 inhibition) may be involved in the development of early atherosclerosis, it has no significant role in the later, clinically apparent stages of atherosclerosis.

Acute manifestations of atherosclerosis are thought to essentially reflect destabilization and rupture of a pre-existing vulnerable thin cap fibroatheroma5. Because of their comprehensive effects on inflammation and matrix homeostasis, members of the Transforming Growth Factor-Beta (TGF-β) super family of ligands (TGF-β, Activin and Bone Morphogenetic Proteins (BMP)) have been proposed as critical regulators of the atherosclerotic process in a large number of animal studies[15,16]. The role of TGF-β and BMP signaling pathways throughout the complete spectrum of human atherosclerotic is evaluated In **Chapter 9**. TGF-β family members exhibit comprehensive anti-inflammatory effects on a wide range of cells, including endothelial cells, macrophages and T-cells, as well as fibroblasts and smooth muscle cells. Effects are all mediated by the classical signalling Smad phosphorylation pathways. Our results show that TGF-β family members affect all vascular associated cell types, in all three layers of the arterial wall throughout all stages of human atherosclerosis. Progression of atherosclerotic lesions into more complicated plaques (*viz.* progressive atherosclerotic lesions, vulnerable lesions and stabilized lesions) is not paralleled by changes in Smad phosphorylation.

All in all, our findings do not specifically characterize TGF-β and BMP signaling as key regulators in the progression and complications of atherosclerosis.

FUTURE PERSPECTIVES

Work in this thesis shows remarkable morphological parallels between disease progression in commonly used atherosclerotic mouse models and the human pathology. Despite these clear similarities, gross differences exist between advanced atherosclerosis in mice and men. In particular all aspects associated with cap maturation and plaque destabilization are missing in the murine models. These essential gaps hinder the translation of experimental findings to the clinical context in which plaque destabilization is thought to underlie all acute manifestations of atherosclerotic disease. Addressing the translational difficulties and gaps is a major challenge for future atherosclerosis research. Future research would benefit from the development of a more authentic human-like model; one that particularly incorporates aspects of the cap biology such as fibrosis and neovascularization in advanced lesions.

In this respect there have been several promising advances in porcine models of atherosclerosis that could prove essential for exploring the processes in late atherosclerosis[17]. Pig models have a more human-like size cardiovascular anatomy and are of closer physiologic and genetic resemblance to humans than rodents. Progressive atherosclerotic lesions in pigs exhibit overall morphology and several specific histopathological features that are shared with human lesions but not seen

in mice and include plaque neovascularization, intraplaque haemorrhages and solid calcifications similar to different stages of calcification in human lesions[18]. It is however important to note that also in porcine models, thrombotic complications due to atherosclerosis and advanced calcified plaques are rare, showing that even in this model critical aspects of human atherosclerosis are missing.

A remarkable observation in our vascular biobank material is the dominance of fibrotic calcified plaques (FCP) in middle aged individuals. According to the Virmani classification FCP represent the end-stage of atherosclerotic disease with plaque consolidation following rupture and healing[5,6]. The high prevalence of (multiple) FCPs samples in our biobank implies that all these patients experienced plaque rupture(s) with subsequent healing without any apparent clinical symptoms. On a morphological level the majority of FCP are almost entirely acellular and contain condensed calcified remnants of the necrotic core. On this basis referring to these lesions as a fibrotic calcified scar (FCS) rather than a calcified plaque (FCP) seems more appropriate.

The studies in this thesis confirm the postulated differences in inflammatory involvement in human and murine atherosclerosis[19]. Whilst NK cells, regulatory T cells and Th17 cells are established factors in murine atherosclerosis, they are virtually absent in human atherosclerosis challenging a role for these cells in human atherosclerosis. Our data on human atherosclerosis also point to a considerable macrophage heterogeneity and diversity that is far more complex than the simple dichotomous classification scheme as proposed for macrophage differentiation in mice. Standard histological methods fall short to explore this variability. Although technically challenging, single-cell analyses could provide invaluable insights into further studying macrophage heterogeneity.

Atherosclerosis in mice critically depends on an immunological background of Th1-cells[20]. Cytotoxic T-cells and T-memory cells are continuously abundantly present in human atherosclerosis whereas naïve T-cells and B-cells are almost exclusively present in the vulnerable phase. The absence of B-cell maturation suggests that this solely reflects a change in homing signals rather than an antigen driven response. B-cells are considered critical players in the atherosclerotic process; albeit their role, being either protective or detrimental, is still under debate and requires special attention in future research.

In rodents anti-inflammatory treatment almost indiscriminately results in plaque regression. Although anti-inflammatory treatment is widely considered a valid target in humans, it is important to point out that this optimism is not supported by clinical data. Potent anti-inflammatory actions have been firmly established for statins and ACE-inhibiters on the vascular wall[21]. However, this does not translate

in a clinical superiority to other forms of cholesterol respectively blood pressure lowering treatment[22, 23, 24]. One might argue that the pleiotropic anti-inflammatory effects of statins and ACE-inhibitors are too weak to achieve the desired clinical effect. In this context it is important to note that systemic inhibition of IL-1β also failed to show a positive effect on the function and structure of the arterial wall in aortic and carotid atherosclerosis[25]. This challenges the commonly assumed canonical role of inflammation in atherosclerosis, and might suggest that the inflammatory component in atherosclerosis is merely an epiphenomenon rather than causative. This last notion is further supported by our interventional study where quenching AP-1 activation had no significant role in the later, clinically apparent stages of atherosclerosis. Considering the central role of Inflammation in general is a significant contributing and indispensable factor in wound healing and tissue repair. There might even be a possibility that advanced atherosclerotic lesions are beyond repair.

The patient centered studies in this thesis clearly show that we must reach beyond the available tools in the laboratory to probe the pathophysiology of atherosclerosis, and more urgently strive to bridge the gap to human disease[26]. Special attention should go out to advanced atherosclerosis since this essential phase is missing in current models. Given the high prevalence of FCP in middle aged and elderly individuals, a relevant model would be one with neo-atherosclerotic plaque formation on an existing fibrotic calcified plaque. This type of lesion seems to develop without direct communication with the underlying adventitia and vaso vasorum and should therefore be considered a unique entity in the atherosclerotic process.

REFERENCES

1 http://www.who.int/mediacentre/factsheets/fs310/en/index1.html

2 Libby, P., Ridker, P. M., & Hansson, G. K. (2011). Progress and challenges in translating the biology of atherosclerosis. Nature, 473(7347), 317-325.

3 Zadelaar, S., Kleemann, R., Verschuren, L., de Vries-Van der Weij, J., van der Hoorn, J., Princen, H. M., & Kooistra, T. (2007). Mouse models for atherosclerosis and pharmaceutical modifiers. Arteriosclerosis, thrombosis, and vascular biology, 27(8), 1706-1721.

4 Daugherty, A. Mouse models of atherosclerosis. The American journal of the medical sciences, 2002, 323.1: 3.

5 Virmani, R., Kolodgie, F. D., Burke, A. P., Farb, A., & Schwartz, S. M. (2000). Lessons from sudden coronary death a comprehensive morphological classification scheme for atherosclerotic lesions. Arteriosclerosis, thrombosis, and vascular biology, 20(5), 1262-1275.

6 Yahagi, K., Kolodgie, F. D., Otsuka, F., Finn, A. V., Davis, H. R., Joner, M., & Virmani, R. (2015). Pathophysiology of native coronary, vein graft, and in-stent atherosclerosis. Nature Reviews Cardiology.

7 Greenland P, Alpert JS, Beller GA, *et al*. American College of Cardiology Foundation; American Heart Association. 2010 ACCF/AHA guideline for assessment of cardiovascular risk in asymptomatic adults: a report of the American College of Cardiology Foundation/American Heart Association Task Force on Practice Guidelines. Journal of the American College of Cardiology. 2010; 56 :e50-103.

8 Costanzo P, Cleland JG, Atkin SL, Vassallo E, Perrone-Filardi P. Use of Carotid Intima-Media Thickness Regression to Guide Therapy and Management of Cardiac Risks. Current Treatment Options in Cardiovascular Medicine. 2012; 14: 50-56.

9 Ross R. Atherosclerosis—an inflammatory disease. The New England Journal of Medicine. 1999;340(2):115–126.

10 Fernández-Velasco M, González-Ramos S, Boscá L. Involvement of monocytes/macrophages as key factors in the development and progression of cardiovascular diseases. Biochemical Journal. 2014; 458(2):187-193.

11 Hansson GK, Libby P, Schönbeck U, Yan ZQ. Innate and adaptive immunity in the pathogenesis of atherosclerosis. Circulation Research. 2002;91(4):281-291.

12 Chinetti-Gbaguidi G, Colin S, Staels B. Macrophage subsets in atherosclerosis. Nature Reviews Cardiology. 2015;12(1):10-17.

13 Wang, J., An, F. S., Zhang, W., Gong, L., Wei, S. J., Qin, W. D., Wang, X. P., Zhao, Y. X., Zhang, Y., Zhang, C. and Zhang, M. X. (2011) Inhibition of c-Jun N-terminal kinase attenuates low shear stress-induced atherogenesis in apolipoprotein E-deficient mice. Molecular Medicine 17, 990–999

14 Osto, E., Matter, C. M., Kouroedov, A., Malinski, T., Bachschmid, M., Camici, G. G., Kilic, U., Stallmach, T., Boren, J., Iliceto, S. *et al*. (2008) c-Jun N-terminal kinase 2 deficiency protects against hypercholesterolemia-induced endothelial dysfunction and oxidative stress. Circulation 118, 2073–2080

15 Engelse M.A., Neele J.M., van Achterberg T.A.E., van Aken B.E., van Schaik R.H.N., Pannekoek H. and de Vries C.J. (1999). Human activin-A is expressed in the atherosclerotic lesion and promotes the contractile phenotype of smooth muscle cells. Circulation Research. 85, 931-939.

16 Singh N.N. and Ramji D.P. (2006). The role of transforming growth factor-β in atherosclerosis. Cytokine & Growth Factor Reviews. 17, 487-499.

17 Shim J1, Al-Mashhadi RH1, Sørensen CB1, Bentzon JF. Large animal models of atherosclerosis--new tools for persistent problems in cardiovascular medicine..Journal of Pathology. 2016 Jan;238(2):257-66.

18 Hamamdzic D, Wilensky RL. Porcine models of accelerated coronary atherosclerosis: role of diabetes mellitus and hypercholesterolemia. Journal of Diabetes Research. 2013.

19 Lichtman AH. Adaptive immunity and atherosclerosis: mouse tales in the AJP. American Journal of Pathology. 2013; 5-9.

20 Schulte S, Sukhova GK, Libby P. Genetically programmed biases in Th1 and Th2 immune responses modulate atherogenesis. American Journal of Pathology. 2008; 1500-1508.

21 Kortekaas KE, Meijer CA, Hinnen JW, Dalman RL, Xu B, Hamming JF, Lindeman JH. ACE inhibitors potently reduce vascular inflammation, results of an open proof-of-concept study in the abdominal aortic aneurysm. PloS one. 2014 Dec 4;9(12):e111952.

22 Ridker PM. Residual inflammatory risk: addressing the obverse side of the atherosclerosis prevention coin. European heart journal. 2016 Jun 7;37(22):1720-1722.

23 Robinson JG. Models for describing relations among the various statin drugs, low-density lipoprotein cholesterol lowering, pleiotropic effects, and cardiovascular risk. American Journal of Cardiology. 2008 Apr 1;101(7):1009-1015.

24 Law MR, Morris JK, Wald NJ. Use of blood pressure lowering drugs in the prevention of cardiovascular disease: meta-analysis of 147 randomised trials in the context of expectations from prospective epidemiological studies. British Medical Journal. 2009;338.

25 Choudhury RP, Birks JS, Mani V, Biasiolli L, Robson MD, L'Allier PL, Gingras MA, Alie N, McLaughlin MA, Basson CT, Schecter AD. Arterial effects of canakinumab in patients with atherosclerosis and type 2 diabetes or glucose intolerance. Journal of the American College of Cardiology. 2016 Oct 18;68(16):1769-1780.

26 Libby P, Ridker PM, Hansson GK. Progress and challenges in translating the biology of atherosclerosis. Nature. 2011; 317-325.

Appendices

Nederlandse samenvatting

Dankwoord

List of Publications

Curriculum Vitae

Samenvatting

Atherosclerose is wereldwijd de voornaamste ziekte- en doodsoorzaak[1]. Een overvloed aan preklinisch onderzoek heeft de afgelopen decennia geleid tot vele overtuigende hypothesen over de biologische, pathofysiologische en immunologische grondslagen van het atherosclerotische proces en de bijkomende complicaties zoals een myocard- en herseninfarct[2]. Ondanks alle vooruitgang blijft het op vele vlakken een uitdaging om de experimentele successen van proefdieronderzoek op het gebied van atherosclerose te vertalen naar de mens[3,4].. Het invullen van deze kennislacunes is een vereiste om uiteindelijk volledige wetenschappelijke vooruitgang te kunnen boeken in atherosclerotisch onderzoek[2].

In een poging deze vertaalslag te realiseren hebben we systematisch het humane atherosclerotische proces geëvalueerd aan de hand van een unieke biobank van ruim 500 individuele secties van de peri-renale aorta en ruim 600 segmenten van de linker coronair arterie; verkregen tijdens lever-, nier- of pancreastransplantatie (aorta) en van weefseldonoren die hun aortaklep doneerden (coronairen). Deze biobanken stelden ons in de gelegenheid om vaatweefsel met een gelijke distributie van leeftijd en geslacht te analyseren van een grote groep relatief gezonde (overleden) individuen. Dientengevolge konden potentiele bias vermeden worden welke wel geïntroduceerd worden bij het gebruik van primair autopsie materiaal van slachtoffers van hart- en vaatziekten (voornamelijk jonge of oude patiënten) of van patiënten die een vasculaire ingreep ondergaan (voornamelijk eindstadium atherosclerotisch vaatlijden). Tezamen geven de studies in dit proefschrift een overzicht van de morfologische, pathofysiologische en immunologische karakteristieken van het humane atherosclerotische proces vanaf de vroege niet progressieve laesies tot aan de vergevorderde, instabiele plaques, die ten grondslag liggen aan de klinische manifestaties van humane atherosclerose.

Morfologische aspecten van het atherosclerotische proces

Kwalitatieve karakterisering van het atherosclerotische proces is volledig gebaseerd op een morfologische classificatie op basis van histologische kenmerken van de plaque. Op basis van de observaties van atherosclerotische plaques in de coronairen van slachtoffers van een myocard infarct hebben Virmani *et al.* de bestaande AHA classificatie verfijnd, met als doel een betere en meer chronologische afspiegeling te creëren van de heterogeniteit van de vergevorderde stadia van atherosclerose[5,6]. Het is vooralsnog onduidelijk hoe en of deze menselijke indeling op basis van de coronair arterie kan worden toegepast op de andere vasculaire structuren. In **Hoofdstuk 2** beschrijven en valideren we de op de coronaire gebaseerde Virmani classificatie voor de humane peri-renale aorta.

Atherosclerotische laesies in de aorta volgen een vergelijkbaar patroon van ontwikkeling in vergelijking met de coronair arterie, maar zijn aanzienlijk groter in omvang. Bij atherosclerose van de aorta spelen macrofagen en schuimcellen een aanzienlijke bijdragende rol in de evolutie van de necrotische kern, plaque progressie en plaque destabilisatie. Het wordt verondersteld dat macrofagen, door afgifte van matrix metalloproteinasen, bijdragen aan plaque destabilisatie. De directe associatie tussen het verdunnen van de fibrotische cap en de focale infiltratie van macrofagen, en de significante daling van het gehalte aan macrofagen in stabiliserende, geruptureerde plaques ondersteunen deze veronderstelling, ook voor de aorta.

De intima media dikte (IMT) van de carotis en de calciumscore in de coronairen zijn ontwikkeld als epidemiologische meetinstrumenten voor de mate van atherosclerose[7]. Gesuggereerd wordt dat deze instrumenten ook gebruikt kunnen worden voor individuele risico-inventarisatie en dat veranderingen van de IMT gebruikt kunnen worden als surrogaat eindpunt in klinische studies gericht op het stabiliseren en/of omkeren van het atherosclerotische proces[8]. **Hoofdstuk 3** test de validiteit van IMT metingen en calciumscores als surrogaat voor de mate van atherosclerose.

De resultaten bevestigen een associatie tussen de IMT en het stadium van atherosclerose, maar tonen tevens een afvlakking en zelfs een afname van de IMT in de instabiele plaques en voornamelijk de gestabiliseerde plaques. De bevindingen tonen een aanzienlijke variabiliteit in IMT, resulterend in een zeer ruim betrouwbaarheidsinterval rond de trend.

Voor wat betreft de calciumscore; deposities van calcium reflecteren de latere stadia van atherosclerose en zijn voornamelijk prominent in de zogenaamde gestabiliseerde fase. De calciumscore moet beschouwd worden als een retrospectieve marker welke hoofdzakelijk patiënten kan identificeren met manifest atherosclerotisch vaatlijden. Daarentegen sluit een negatieve calciumscore de aanwezigheid van atherosclerose plaques zeker niet uit.

Hoewel de kennis over de initiatie en de progressie van atherosclerotische plaques grotendeels is gebaseerd op informatie afkomstig van muismodellen van atherosclerose is het een opmerkelijk gegeven dat een eenduidige en consistente classificatie van atherosclerose in de muis nog ontbreekt. In **Hoofdstuk 4** tonen we aan dat de op de coronair arterie gebaseerde “Virmani classificatie” kan worden toegepast op de atherosclerose in de muis op het niveau van de aortaklep. Dit betekent dat het mogelijk is om plakstadia van mens en muis 1 op 1 te vergelijken. Het is hiermee mogelijk om de preklinische bevindingen te plaatsen in een humane context.

De vroege stadia van atherosclerose in de muis zijn vergelijkbaar met de vroege stadia van humane atherosclerose. Op basis van de histologische karakteristieken kan geconcludeerd worden dat de atherosclerotische laesies in muizen zich niet verder ontwikkelen dan een 'early fibroatheroma' en dat dientengevolge de aspecten van de instabiele, geruptureerde plaques met opeenvolgende genezing in deze modellen ontbreken.

In vergelijking met humane atherosclerose zien we dat plaques in muizen significant kleiner zijn en dat de *vaso vasorum* in de adventitia ontbreken. Door de beperkte omvang van de laesies in muizen ontbreekt een ischemische trigger en kan de vitaliteit van het atherosclerotisch weefsel worden onderhouden door middel van diffusie. Een consequentie hiervan is dat kritieke aspecten van humane atherosclerose zoals ischemie en neovascularisatie ontbreken.

Moleculaire en cellulaire aspecten van humane atherosclerose

Een fundamentele, cruciale stap in het atherosclerotische proces is accumulatie van LDL in de intima van de vaatwand[9]. Een overvloed aan experimentele data definieert een centrale rol voor geoxideerd LDL cholesterol in de progressie van atherosclerose. In **Hoofdstuk 5** wordt systematisch de relatie beschreven tussen de verschillende oxidatie-specifieke LDL epitopen (OSE); *i.e.* malondialdehyde-lysine (MDA2), E06, en IK17, and lipoproteïne (a) (Lp(a)) in vroege stadia en de klinisch relevante geavanceerde humane atherosclerotische plaques.

Parallel aan het vorderen van het atherosclerotisch proces treedt in de laesies een verrijking op van apo(a), geoxideerde fosfolipide (OxPL), en MDA gerelateerde epitopen (IK17). In zowel de vroege stadia en de meer gevorderde laesies zijn in het bijzonder de apo(a) epitopen aanwezig. De epitopen van OxPL en IK17 epitopen zijn zeer dominant aanwezig in de macrofagen schuimcellen in de dunne fibrotische cap, de necrotische kern en de geruptureerde plaque. Dit suggereert dat deze gerelateerd zijn aan de vergevorderde en instabiele plaques. De geobserveerde patroonvariatie van immunoreactiviteit tussen de verschillende antilichamen vormen een kader voor het begrijpen van de relaties tussen OSE en lipoproteïnen en de progressie en stabilisatie van humane atherosclerotisch plaques. Specifieke epitopen kunnen worden gegenereerd of accumuleren tijdens de verschillende pathofysiologische stadia van plaque ontwikkeling, progressie en destabilisatie.

Het is alom geaccepteerd dat er in het atherosclerotische proces een cruciale rol is weggelegd voor de cellulaire componenten van het aangeboren immuunsysteem (en in het bijzonder de macrofagen)[10,11]. Macrofagen vormen een zeer heterogene en dynamische celpopulatie. Verondersteld wordt dat de pro-inflammatoire

processen (klassieke geactiveerde M1 macrofagen) de initiatie en progressieve fase van de ziekte domineren en de alternatieve geactiveerde M2 macrofagen het dominante fenotype zijn in plaque resolutie en herstel[12]. Voornamelijk experimentele muisstudies impliceren een belangrijke verschuiving in het macrofaag fenotype tijdens atherosclerose.

Hoofdstuk 6 beschrijft de cellulaire componenten van het aangeboren immuunsysteem en dan in het bijzonder de relatie tot de gecompliceerde plaques die ten grondslag liggen aan symptomatisch vaatlijden.

Een opmerkelijke bevinding was dat de transitie naar een pathologische verdikking van de intima (PIT), de eerste vorm van progressieve en irreversibele atherosclerose, wordt gekarakteriseerd door accumulatie van apolipoproteine B100 in de media. Deze transitie is geassocieerd met het verlies van integriteit van de *lamina elastica interna* en kenmerkt het begin van de betrokkenheid van de media en adventitia in atherosclerose, een fenomeen dat nader onderzoek verdient.

Macrofagen vertolken een cruciale rol in het aangeboren en verworven immuunsysteem. Ze zijn betrokken in alle fases van de ontwikkeling van de atherosclerotische plaque en in het bijzonder in relatie tot de ontwikkeling van de lipide kern, re-modellering van de plaque en degradatie van de fibrotische cap door afgifte van matrix metalloproteinasen zoals gezien wordt in symptomatisch vaatlijden. In tegenstelling tot de bevindingen in atherosclerotische muismodellen vonden wij geen bewijs voor een verschuiving in fenotypering van de macrofaag tijdens initiatie, progressie, ruptuur of stabilisatie van humane atherosclerotische plaques. Een nog interessanter feit is dat we een dominant fenotype van macrofagen hebben geïdentificeerd die dubbel positief is voor zowel de M1 als M2 marker. Dit betwist het huidige paradigma van een eenduidige M1-M2 dichotomie. De heterogeniteit van macrofagen is complexer dan de huidige op muismodellen gebaseerde theorie momenteel beschrijft. Ons onderzoek ondersteunt de betrokkenheid van additionele (slecht gedifferentieerde) subtypen macrofagen en suggereert zelfs een groter dynamisch bereik van de plasticiteit van macrofagen.

De resultaten laten verder een sterke positieve relatie zien tussen progressieve ziekte en fascine positieve dendritische cellen in zowel de intima, de media en de adventitia. Er zijn echter verschillende rollen geïdentificeerd voor dendritische cellen in de atherogenese en/of progressie van de atherosclerotische plaque in muismodellen. Een specifieke bijdrage van de dendritische cellen en de exacte moleculaire mechanismen zijn tot op heden nog niet helder.

Onze bevindingen in de humane atherosclerotische laesies betwisten claims die zijn gebaseerd op muismodellen van atherosclerose. In tegenstelling tot bevindingen in muismodellen zijn mestcellen niet geassocieerd met de progressie

van humane atherosclerotische laesies. Natural Killer T-cellen, in overvloed aanwezig in de atherosclerotische laesies in de muis, zijn minimaal aanwezig in de humane laesies. Verder impliceren muisstudies een rol voor neutrofielen gedurende de initiatie van het atherosclerotische proces en plaque angiogenese in de latere fase van het de ziekte; onze observationele data in de mens ondersteunen deze primaire rol voor neutrofielen niet. De aanwezigheid van neutrofielen lijkt principieel primair gerelateerd te zijn aan de chirurgische manipulatie tijdens het verwijderen van de aorta.

Het is duidelijk dat de verschillen in waarnemingen tussen muismodellen van atherosclerose en onze humane atherosclerose studies duidt op een beperkt translationeel aspect van dierlijke bevindingen.

De cellulaire componenten van het verworven immuunsysteem zijn systematisch geëvalueerd gedurende de initiatie en ontwikkeling van de atherosclerotische plaque, de progressie, destabilisatie en stabilisatie en komen uitgebreid ter discussie in **Hoofdstuk 7**. De bevindingen wijzen op diepgaande veranderingen in de aard van de reactie in aanloop naar plaquedestabilisatie en laten zien dat het inflammatoire proces uitdooft bij stabilisatie van de plaque.

Ons onderzoek toont fundamentele verschillen aan tussen humane atherosclerose en de muismodellen van atherosclerose; in het bijzonder met betrekking tot het zeer beperkte aantal regulatoire T-cellen, de afwezigheid van Th17 cellen gedurende het gehele atherosclerotische proces en het gebrek aan B-cellen in de vroege, intermediaire en latere stabiele stadia van de ziekte. Diffuse infiltratie van cytotoxische T-cellen domineren de vroege fase, echter gedurende progressie van de ziekte worden er in toenemende hoeveelheid T-helper cellen geïdentificeerd in de atherosclerotische plaques. In tegenstelling tot de bevindingen in muizen konden wij een Th1 dominantie niet bevestigen in het humane atherosclerotische proces.

Een zeer opmerkelijke en niet eerder beschreven observatie is een karakteristiek inflammatiepatroon in de adventitia van de vaatwand die de destabilisatie van de plaque lijkt te begeleiden en weer volledig uitdooft in de stabiliserende fase. Op cellulair niveau wordt deze verandering gekarakteriseerd door een forse toename van T-helper cellen, een exodus van natieve T-cellen en de opkomst van B-cellen met een enkele plasma cel in een follikel-achtige structuur in de adventitia. De expressie van CXCL-13 (een centraal homeostatisch migratie-signaal voor follikelformatie) wordt exclusief geobserveerd in associatie met de follikel-achtige structuren in de instabiele laesies. N.B. CXCL-13 wordt niet gedetecteerd in alle andere stadia van atherosclerose.

Onze bevindingen van een zeer beperkte aanwezigheid van B-cellen in het humane atherosclerotische proces en de complete afwezigheid van B-cel maturatie

in de infiltrerende B-cellen sluiten een autocriene of paracriene rol voor B-cellen gedurende humane atherosclerose uit. Samenvattend toont deze studie illustratieve veranderingen aan in de cellulaire componenten van het aangeboren immuunsysteem voorafgaand en gedurende destabilisatie van de atherosclerotische plaque. Het is verleidelijk om te speculeren dat het visualiseren van deze keten van gebeurtenissen kan bijdragen aan een vroegtijdige detectie van de symptomatische plaque en plaque stabilisatie.

Op basis van experimentele dierstudies is de activiteit van transcriptiefactor Activator protein-1 (AP-1) in verband gebracht met de initiatie en progressie van atherosclerose[13,14]. Hierop is gesuggereerd dat AP-1 gereguleerde inflammatie een centrale rol speelt in de initiatie en progressie van vasculaire dysfunctie en atherogenese met de inhibitie van AP-1 als mogelijk aangrijpingspunt ter preventie van progressie van atherosclerose. In **Hoofdstuk 8** demonstreren we dat er inderdaad sprake is van geactiveerde AP-1 in de wand van de aorta in de vroege en latere fase van humane atherosclerose. Vervolgens werd in een dubbel-blind gecontroleerde cross-over studie doxycycline toegediend aan patiënten met perifeer vaatlijden om zodoende de AP-1 activatie te onderdrukken en de mogelijke rol van AP-1 activatie gedurende vergevorderde atherosclerose te testen. De afwezigheid van een effect bij alle onderzochte activatie-markers leidde tot de conclusie dat AP-1 (en dus AP-1 inhibitie) mogelijk wel betrokken is bij het ontstaan van atherosclerose, maar geen rol van betekenis heeft in de latere, symptomatische atherosclerose.

De algemene gedachte is dat de acute manifestaties van atherosclerose het gevolg zijn van de destabilisatie en het ruptureren van een pre-existente kwetsbare 'thin cap fibroatheroma'[5]. Naar aanleiding van een groot aantal dierstudies zijn de leden van de Transforming Growth Factor-Beta (TGF-β) super familie (*i.e.* TGF-β, Activin en de Bone Morphogenetic Proteins (BMP)), vanwege hun uitgebreide effecten op inflammatie en matrix homeostase, voorgesteld als zijnde kritische regulatoren van het atherosclerotische proces[15,16]. De rol van de TGF-β en BMP signaleringsroute gedurende het complete spectrum van humane atherosclerose is geëvalueerd in **Hoofdstuk 9**. De TGF-β familieleden vertonen uitgebreide anti-inflammatoire effecten op een groot aantal cellen, inclusief endotheel cellen, macrofagen, T-cellen, fibroblasten en gladde spiercellen. De effecten worden allemaal gemedieerd door de klassieke signaleringsroute van Smad fosforylatie. Onze resultaten laten zien dat de TGF-β familieleden effect hebben op alle vasculaire geassocieerde celtypes in alle lagen van de vaatwand en gedurende alle stadia van humane atherosclerose. De progressie van atherosclerotische laesies naar de meer gecompliceerde plaques (*i.e.* progressive

atherosclerotic lesions, vulnerable lesions en stabilized lesions) gaat niet gepaard met veranderingen in Smad fosforylatie.

Concluderend worden de TGF-β en BMP signaleringsroutes niet gekarakteriseerd als essentiële regulatoren van de progressie van atherosclerotische laesies en/of de complicaties van atherosclerose.

Toekomstperspectief

De studies in dit proefschrift tonen opmerkelijke morfologische parallellen tussen progressie van de ziekte in veelgebruikte muismodellen van atherosclerose en de humane pathologie. Ondanks deze overduidelijke overeenkomsten bestaan er grove verschillen tussen geavanceerde atherosclerose in muis en mens. Hierbij wordt in het bijzonder gedacht aan aspecten die geassocieerd zijn met de maturatie van de fibrotische kap en destabilisatie van de plaque welke allen ontbreken in de muismodellen. Deze essentiële verschillen belemmeren de vertaling van de experimentele bevindingen naar de klinische context waarin plaque destabilisatie en plaqueruptuur wordt toegeschreven aan nagenoeg alle acute manifestaties die aan atherosclerose ten grondslag liggen. Het aanpakken van de beperkingen in de vertaalslag en kennislacunes is een grote uitdaging voor toekomstig atherosclerotisch onderzoek. Dit onderzoek zou baat hebben bij de ontwikkeling van een authentiek mensachtig model; één die in het bijzonder de biologie van de cap omvat zoals fibrose en plaque-neovascularisatie in de vergevorderde laesies.

In dit opzicht zijn er al verschillende veelbelovende vooruitgangen geboekt in varkensmodellen van atherosclerose die essentieel zouden kunnen blijken voor het verder exploreren van de processen aangaande de latere fases van atherosclerose[17]. De atherosclerotische laesies in de varkensmodellen komen qua grootte, cardiovasculaire anatomie, fysiologie en op genetisch vlak meer overeen met de mens dan met de muis. De progressievere atherosclerotische laesies in varkens hebben een algemenere morfologie en vertonen een aantal specifieke histopathologische kenmerken die ook worden gezien in de mens, zoals plaque neovascularisatie, intraplaque bloedingen en solide verkalkingen vergelijkbaar met de verschillende stadia van verkalking in de humane laesies[18]. Deze kenmerken worden niet primair gezien bij muizen. Het is echter belangrijk te realiseren dat ook in de varkens modellen trombotische complicaties als gevolg van atherosclerose en geavanceerde verkalkte plaques zeldzaam zijn en dat ook in dit model enkele kritische aspecten van humane atherosclerose ontbreken.

Onze vasculaire databank toont een overvloed aan fibrotische gecalcificeerde plaques (FCP) in patiënten van middelbare leeftijd. In de Virmani classificatie is de

FCP het eindstadium van humane atherosclerose waarbij de initiële plaque na een ruptuur (of rupturen) en heling nagenoeg volledig geconsolideerd is[5,6]. De hoge prevalentie van (meerdere) FCPs in onze biobank betekent dat al deze patiënten een plaqueruptuur (of rupturen) hebben gehad zonder verdere klinische symptomen of consequenties. Op morfologisch niveau is de meerderheid van de FCPs bijna volledig acellulair en bevatten gecondenseerde verkalkte restanten van de necrotische kern. Op basis hiervan lijkt het geschikter om deze laesies te benaderen als een fibrotische gecalcificeerd litteken in plaats van een plaque.

De studies in dit proefschrift bevestigen de gepostuleerde verschillen in de betrokkenheid van de inflammatoire componenten tussen atherosclerose in de mens en in de muis[19]. Terwijl NK-cellen, regulatoire T-cellen en Th17 cellen gevestigde factoren zijn in de muismodellen van atherosclerose, zijn ze vrijwel afwezig in het humane atherosclerotische proces. Derhalve wordt de toegeschreven rol van deze cellen uit muisstudies in humane atherosclerose betwist. Verder tonen onze gegevens over humane atherosclerose een aanzienlijke heterogeniteit en diversiteit onder macrofagen, één die veel complexer is dan het eenvoudigere dichotome classificatieschema zoals die wordt voorgesteld voor de differentiatie van macrofagen bij muizen. Standaard histologische onderzoeksmethoden schieten te kort om deze variabiliteit nader te verkennen. Hoewel technisch uitdagend, zou 'single-cell analyses' waardevolle inzichten kunnen verschaffen in de verdere studie naar de heterogeniteit van macrofagen.

In tegenstelling tot de mens kan in muismodellen atherosclerotische proces pas geschieden na genetische modificatie en op een immunologische achtergrond van Th1-cellen[20]. In humane atherosclerose zijn cytotoxische T-cellen en T-memory cellen continu en in overvloed aanwezig, terwijl natieve T-cellen en B-cellen vrijwel uitsluitend aanwezig zijn in de instabiele fase. B-cellen worden beschouwd als kritische spelers in het atherosclerotische proces; hoewel hun rol, hetzij beschermend of schadelijk, nog steeds ter discussie staat en dat nader onderzoek verdient.

Bij muizen resulteert een anti-inflammatoire therapie bijna altijd in plaque regressie. Hoewel een anti-inflammatoire behandeling algemeen beschouwd wordt als een valide therapie bij de mens is het belangrijk erop te wijzen dat dit optimisme niet wordt ondersteund door klinisch onderzoek. De potente anti-inflammatoire werking van bijvoorbeeld statines en ACE-remmers op de vaatwand zijn herhaaldelijk aangetoond[21]. Dit betekent echter niet dat deze therapievormen klinisch superieur zijn aan andere vormen van cholesterol- of bloeddrukverlagende behandeling[22, 23, 24]. Men zou kunnen betogen dat de pleiotrope anti-inflammatoire effecten van statines en ACE-remmers te zwak zijn om het gewenste klinische effect te bereiken. In dit verband is het tevens

belangrijk om op te merken dat systemische remming van IL-1β evenmin een positief effect heeft op de functie en structuur van de vaatwand bij atherosclerose in de aorta en de carotiden[25]. Dit gegeven betwist in zekere zin de algemeen aangenomen sleutelrol van inflammatie in atherosclerose en zou kunnen suggereren dat de inflammatoire componenten in atherosclerose slechts een randverschijnsel zijn in plaats van een oorzakelijke factor. Dit laatste denkbeeld wordt ondersteund door onze interventie studie waarbij het onderdrukken van de AP-1 activatie geen significante rol bleek te hebben in de latere, klinisch manifeste stadia van atherosclerose. Gezien de centrale rol van ontsteking een belangrijke bijdragende en onmisbare factor is in wondgenezing en weefselherstel bestaat er zelfs de mogelijkheid dat geavanceerde atherosclerotische laesies zijn niet meer te repareren zijn.

De studies in dit proefschrift, waarbij de mens centraal staat, laten duidelijk zien dat we verder moeten reiken dan de bestaande en beschikbare experimentele modellen van atherosclerose om uiteindelijk de pathofysiologie van atherosclerose in de mens te ontrafelen[26]. Er zal bijzondere aandacht uit moeten gaan naar vergevorderde atherosclerotische plaques gezien het feit dat deze essentiële fases ontbreken in de huidige toegepaste diermodellen. Mede gezien de hoge prevalentie van FCPs in mensen van middelbare en oudere leeftijd, zou een relevant model er één zijn van neo-atherosclerotische plaquevorming op al bestaande fibrotische verkalkte plaques. Dit type plaque lijkt zich namelijk te ontwikkelen zonder directe communicatie met de onderliggende adventitia en *vasa vasorum* en zou beschouwd kunnen worden als een unieke, symptomatische fase in het atherosclerotische proces.

REFERENCES

1 http://www.who.int/mediacentre/factsheets/fs310/en/index1.html

2 Libby, P., Ridker, P. M., & Hansson, G. K. (2011). Progress and challenges in translating the biology of atherosclerosis. Nature, 473(7347), 317-325.

3 Zadelaar, S., Kleemann, R., Verschuren, L., de Vries-Van der Weij, J., van der Hoorn, J., Princen, H. M., & Kooistra, T. (2007). Mouse models for atherosclerosis and pharmaceutical modifiers. Arteriosclerosis, thrombosis, and vascular biology, 27(8), 1706-1721.

4 Daugherty, A. Mouse models of atherosclerosis. The American journal of the medical sciences, 2002, 323.1: 3.

5 Virmani, R., Kolodgie, F. D., Burke, A. P., Farb, A., & Schwartz, S. M. (2000). Lessons from sudden coronary death a comprehensive morphological classification scheme for atherosclerotic lesions. Arteriosclerosis, thrombosis, and vascular biology, 20(5), 1262-1275.

6 Yahagi, K., Kolodgie, F. D., Otsuka, F., Finn, A. V., Davis, H. R., Joner, M., & Virmani, R. (2015). Pathophysiology of native coronary, vein graft, and in-stent atherosclerosis. Nature Reviews Cardiology.

7 Greenland P, Alpert JS, Beller GA, et al. American College of Cardiology Foundation; American Heart Association. 2010 ACCF/AHA guideline for assessment of cardiovascular risk in asymptomatic adults: a report of the American College of Cardiology Foundation/American Heart Association Task Force on Practice Guidelines. Journal of the American College of Cardiology. 2010; 56 :e50-103.

8 Costanzo P, Cleland JG, Atkin SL, Vassallo E, Perrone-Filardi P. Use of Carotid Intima-Media Thickness Regression to Guide Therapy and Management of Cardiac Risks. Current Treatment Options in Cardiovascular Medicine. 2012; 14: 50-56.

9 Ross R. Atherosclerosis—an inflammatory disease. The New England Journal of Medicine. 1999;340(2):115–126.

10 Fernández-Velasco M, González-Ramos S, Boscá L. Involvement of monocytes/macrophages as key factors in the development and progression of cardiovascular diseases. Biochemical Journal. 2014; 458(2):187-193.

11 Hansson GK, Libby P, Schönbeck U, Yan ZQ. Innate and adaptive immunity in the pathogenesis of atherosclerosis. Circulation Research. 2002;91(4):281-291.

12 Chinetti-Gbaguidi G, Colin S, Staels B. Macrophage subsets in atherosclerosis. Nature Reviews Cardiology. 2015;12(1):10-17.

13 Wang, J., An, F. S., Zhang, W., Gong, L., Wei, S. J., Qin, W. D., Wang, X. P., Zhao, Y. X., Zhang, Y., Zhang, C. and Zhang, M. X. (2011) Inhibition of c-Jun N-terminal kinase attenuates low shear stress-induced atherogenesis in apolipoprotein E-deficient mice. Molecular Medicine 17, 990–999

14 Osto, E., Matter, C. M., Kouroedov, A., Malinski, T., Bachschmid, M., Camici, G. G., Kilic, U., Stallmach, T., Boren, J., Iliceto, S. et al. (2008) c-Jun N-terminal kinase 2 deficiency protects against hypercholesterolemia-induced endothelial dysfunction and oxidative stress. Circulation 118, 2073–2080

15 Engelse M.A., Neele J.M., van Achterberg T.A.E., van Aken B.E., van Schaik R.H.N., Pannekoek H. and de Vries C.J. (1999). Human activin-A is expressed in the atherosclerotic lesion and promotes the contractile phenotype of smooth muscle cells. Circulation Research. 85, 931-939.

16 Singh N.N. and Ramji D.P. (2006). The role of transforming growth factor-β in atherosclerosis. Cytokine & Growth Factor Reviews. 17, 487-499.

17 Shim J1, Al-Mashhadi RH1, Sørensen CB1, Bentzon JF. Large animal models of atherosclerosis--new tools for persistent problems in cardiovascular medicine. .Journal of Pathology. 2016 Jan;238(2):257-66.

18 Hamamdzic D, Wilensky RL. Porcine models of accelerated coronary atherosclerosis: role of diabetes mellitus and hypercholesterolemia. Journal of Diabetes Research. 2013.

19 Lichtman AH. Adaptive immunity and atherosclerosis: mouse tales in the AJP. American Journal of Pathology. 2013; 5-9.

20 Schulte S, Sukhova GK, Libby P. Genetically programmed biases in Th1 and Th2 immune responses modulate atherogenesis. American Journal of Pathology. 2008; 1500-1508.

21 Kortekaas KE, Meijer CA, Hinnen JW, Dalman RL, Xu B, Hamming JF, Lindeman JH. ACE inhibitors potently reduce vascular inflammation, results of an open proof-of-concept study in the abdominal aortic aneurysm. PloS one. 2014 Dec 4;9(12):e111952.

22 Ridker PM. Residual inflammatory risk: addressing the obverse side of the atherosclerosis prevention coin. European heart journal. 2016 Jun 7;37(22):1720-1722.

23 Robinson JG. Models for describing relations among the various statin drugs, low-density lipoprotein cholesterol lowering, pleiotropic effects, and cardiovascular risk. American Journal of Cardiology. 2008 Apr 1;101(7):1009-1015.

24 Law MR, Morris JK, Wald NJ. Use of blood pressure lowering drugs in the prevention of cardiovascular disease: meta-analysis of 147 randomised trials in the context of expectations from prospective epidemiological studies. British Medical Journal. 2009;338.

25 Choudhury RP, Birks JS, Mani V, Biasiolli L, Robson MD, L'Allier PL, Gingras MA, Alie N, McLaughlin MA, Basson CT, Schecter AD. Arterial effects of canakinumab in patients with atherosclerosis and type 2 diabetes or glucose intolerance. Journal of the American College of Cardiology. 2016 Oct 18;68(16):1769-1780.

26 Libby P, Ridker PM, Hansson GK. Progress and challenges in translating the biology of atherosclerosis. Nature. 2011; 317-325.

Dankwoord

Tijd voor het meest bescheiden deel van het proefschrift. Laat het meer dan duidelijk zijn dat dit proefschrift niet zou hebben bestaan zonder de steun van een heleboel mensen. Ik zou willen beginnen met het uiten van mijn uiterste dank aan iedereen die heeft bijgedragen aan dit proefschrift en mij de afgelopen jaren in welke vorm dan ook heeft gesteund.

Dank aan mijn promotor prof. dr. J.f. Hamming. Beste Jaap, dank voor je steun voor dit project dat ik in 2007 ben gestart als onderzoeker binnen jouw afdeling. Dank voor je heldere, klinische en kritische visie op het hedendaagse onderzoek en dank voor je begeleiding door de jaren heen en de vele productieve discussies tijdens ons samenkomen.

Dr. J.H.N. Lindeman, mijn co-promotor en meest directe begeleider. Beste Jan, na vele jaren samen aan dit project te hebben gewerkt en de vele congressen die we met en zonder ski's hebben bezocht heb ik je leren kennen als een rasoptimist en een vooruitstrevend onderzoeker met een onconventionele en soms onnavolgbare benadering van hedendaagse vraagstukken. Zonder jou zou dit proefschrift er niet zijn geweest. Dank voor alles. Dank voor al je steun en adviezen gedurende de tijd die wij samen hebben meegemaakt op zowel professioneel als persoonlijk vlak.

Dr. A.F.M. Schaapherder, mijn co-promotor. Beste Sandro, zonder jouw inzet en hulp zou de vasculaire Biobank in zijn huidige vorm niet bestaan en daarmee ook dit proefschrift niet. Dank hiervoor en ook dank voor alle adviezen voor de series die ik zou moeten kijken (en ook gekeken heb) ter ontspanning.

Dr. R. Virmani. Dear Renu, your enthusiasm for cardiovascular research is inspiring for many researchers all over the world. It has been an honor for me to have had the opportunity to work with you in direct collaboration during my time CVPath Institute Inc. On the same note I would especially like to thank dr. F.D. Kolodgie and all employees at CVPath Inc. for their amazing input and help during my stay. Dear Frank, thank you for all your constructive work on the manuscripts that we have published together.

Adri Mulder. Lieve Adri, dank je wel voor al je directe begeleiding in het onderzoekslaboratorium op TNO en het LUMC. Jij bent zo niet het meest verantwoordelijk voor de hoge kwaliteit van de vaatbank zoals die er nu is.

Verder wil ik mijn collega onderzoekers Hazem, Arnoud en Charla bedanken voor alle gezellige momenten samen op het lab en tijdens onze periode met Jan samen.

Dr. A.D. Montauban van Swijndregt, mijn opleider Radiologie. Beste Alexander, dankzij jouw steun en de steun van alle Radiologen in het Onze Lieve Vrouwe Gasthuis heb ik mijn onderzoek kunnen continueren naast mijn klinische werkzaamheden als Radioloog in opleiding. Dank voor al het vertrouwen en de fantastische opleidingstijd.

Beste collega AIOS Radiologie uit het Onze Lieve Vrouwe Gasthuis in Amsterdam. Dank voor jullie geweldige samenwerking.

Lieve familie en schoonfamilie, bedankt voor al jullie liefde en steun de afgelopen jaren. Bedankt voor alle begrip op de momenten dat ik vanwege werk of onderzoek niet aanwezig kon zijn op feesten en verjaardagen.

Lieve pappa en mamma, bedankt voor al jullie steun de afgelopen jaren. Jullie hebben mij geleerd wat doorzettingsvermogen is en hoe belangrijk dat is in het leven. Het was een lang traject en er waren soms bemoedigende en liefdevolle woorden voor nodig om het focus te behouden. Dank voor jullie onvoorwaardelijke liefde. Lieve Johan en Marijke, broer en zus, jullie ook bedankt voor de steun en liefde door de jaren heen.

Sharon-Joy, mijn allerliefste vrouw, mijn alles. Vanaf dag één dat ik je leerde kennen heb jij mij onvoorwaardelijk gesteund in de keuzes die ik heb gemaakt. Samen zijn we verder gegaan in het leven en samen hebben we inmiddels een prachtig gezin opgebouwd met twee heerlijke zoons. Bedankt voor al je liefde en support. Zonder je interesse en begrip zou het niet zijn gelukt. Samen dit leven.

List of publications

A. Meershoek, **R.A. van Dijk**, S. Verhage, J.F. Hamming, A.J. van den Bogaerdt, A.J.Bogers, A.F. Schaapherder, J.H.N. Lindeman.
Histological evaluation disqualifies IMT and calcification scores as surrogates for grading coronary and aortic atherosclerosis.
International Journal of Cardiology. 2016 Dec;224:328-34.

M. Hoekstra, E.L. Zwerus, **R.A. van Dijk**, N.W. Willigenburg, D.J.F. Moojen, R.W.Poolman.
Does pain relief after intra-articular anaesthetic hip injection predict success of hip arthroplasty?
Submitted to *Clinical Orthopaedics and Related Research.*

R.A. van Dijk, K. Rijs, A. Wezel, J. F. Hamming, F. D. Kolodgie, R. Virmani, J.H.N.Lindeman.
Systematic Evaluation of the Cellular Innate Immune Response During the Process of Human Atherosclerosis.
Journal of the American Heart Association. 2016, 5(6), e002860.

R. A. van Dijk, A.J.F. Duinisveld, A.F. Schaapherder, A. Mulder-Stapel, J.F. Hamming, J. Kuiper, J.H.N. Lindeman.
A change in inflammatory footprint precedes plaque instability: a systematic evaluation of cellular aspects of the adaptive immune response in human atherosclerosis.
Journal of the American Heart Association. 2015, 4(4), e001403.

A. F. Albersen, **R. A. van Dijk,** E. J. T. Krul, E. A. Heldeweg, (2015).
Case report. Liposarcoom van het scrotum.
Tijdschrift voor Urologie. 2015, 5(2), 58-61.

P. le Haen, C.A. Meijer, **R.A.van Dijk**, M. Hira, J. Hajo van Bockel, J.H.N. Lindeman.
Activator Protein-1 (AP-1) signaling in Human Atherosclerosis. Results of a systematic evaluation and intervention study.
Clinical Science. 2012 May 1;122(9):421-428.

R.A.van Dijk, C.C. Engels, A.F. Schaapherder, A. Mulder-Stapel, J.H.N. Lindeman.
Visualizing TGF-β and BMP signaling in human atherosclerosis: a histological evaluation based on Smad activation.
Histology & Histopathology. 2012 Mar;27(3):387-96.

R.A.van Dijk, N. Cresswell, P.X. Shaw, F. Kolodgie, Cheng-Han Chen, J.L. Witztum, R. Virmani, Sotirios Tsimikas.
Differential Expression of Oxidation-Specific Epitopes and Lipoprotein (a) Reflect the Presence of Progressive and Ruptured Plaques in Human Coronary Arteries.
Journal of Lipid Research. 2012. 53, 2773-2790.

R.A.van Dijk, A.F. Schaapherder, J.H. von der Thüsen, R. Virmani, J.H.N. Lindeman.
The natural history of aortic atherosclerosis: a systemic histopathological evaluation of the peri-renal region.
Atherosclerosis. 2010 May 1;210(1):100-106.

CURRICULUM VITAE

Rogier Alexander van Dijk is geboren op 16 januari 1979 te Alphen a/d Rijn. Na het behalen van zijn VWO diploma aan het Coenecoop College in Waddinxveen heeft hij, na meerdere malen uitgeloot te zijn voor Geneeskunde, Biologie gestudeerd aan de Universiteit van Leiden. Na het behalen van zijn Bachelor of Science diploma in 2003 is hij datzelfde jaar via een zij-instroom procedure alsnog gestart met de opleiding Geneeskunde aan de Universiteit van Leiden. Tijdens de doctoraalfase is hij een onderzoekslijn gestart naar humane atherosclerose binnen de afdeling Vaatchirurgie in het Leids Universitair Medisch Centrum. Na het behalen van zijn Artsexamen eind 2007 heeft hij gewerkt als Arts Assistent Heelkunde in het Medisch Centrum Haaglanden te Den Haag. Gedurende deze periode heeft hij in 2009 de mogelijkheid gekregen om zijn onderzoek naar atherosclerose voort te zetten binnen het gerenommeerde cardiovasculaire onderzoeksinstituut CVPath Inc. in de Verenigde Staten onder leiding van Dr. Renu. Virmani. Zijn enthousiasme voor wetenschappelijk onderzoek was overduidelijk en bij terugkomst in Nederland in 2010 is het humane atherosclerose onderzoek uitgebreid naar een promotietraject onder leiding van prof. dr. J.F. Hamming. Het promotieonderzoek heeft volledig plaatsgevonden naast zijn fulltime werkzaamheden als arts en gedurende deze periode ontwikkelde hij een affiniteit met de technische aspecten van de moderne geneeskunde. In 2012 is hij begonnen met de opleiding Radiologie aan het Onze Lieve Vrouwe Gasthuis te Amsterdam onder leiding van dr. A.D. Montauban van Swijndregt. In mei 2017 heeft hij de opleiding tot Radioloog afgerond en is aansluitend gestart als Fellow Thorax Radiologie in het Meander Medisch Centrum te Amersfoort. Hij woont in Amsterdam met zijn vrouw Sharon-Joy en hun twee zoons Thijmen en Bob.